TUESDAY, JUNE 16, 1981

8:30-9:00 **Rotunda**

FORMAL OPENING

WELCOME AND CALL TO ORDER: L. Stephen Graham, Chairman, Local Arrangements Committee

WELCOME TO LAS VEGAS, NEVADA: The Honorable Robert List, Governor, State of Nevada

REMARKS: Alfred P. Wolf, Chairman, Scientific Program Committee

REMARKS: William R. Hendee, President, Society of Nuclear Medicine

REMARKS: Michael C. Cianci, President, Technologist Section-SNM

AWARDS: William H. Blahd, Chairman, Awards Committee, Paul C. Aebersold Award to Alfred P. Wolf

THE THIRD ANNUAL CHARLES DE HEVESY NUCLEAR MEDICINE PIONEER AWARD PRESENTATION honoring William G. Myers.

Henry N. Wagner, Jr., lecturer.

9:00-10:00 **Rotunda**

PLENARY SESSION

The Biological Effects of Low-Level Radiation: J. Martin Brown, Stanford University, Stanford, California

10:30-12:00 **ROOM A-1**

CARDIOVASCULAR I: RADIONUCLIDE STUDIES IN CONGENITAL AND VALVULAR HEART DISEASE

Moderator: Dan G. Pavel
Co-moderator: Sherman G. Sorenson

A NEW METHOD FOR THE DETECTION OF TRICUSPID INSUFFICIENCY. D.G. Pavel, B. Handler, W. Lam, C. Meyer-Pavel, E. Byrom, R. Pietras. University of Illinois Medical Center, Chicago.

The existence of tricuspid regurgitation (TR) can theoretically give a low value for the left/right (L/R) stroke volume ratio, called regurgitation index (RI), but this is non-specific and subject to false negative results. We have done a retrospective study to test the usefulness of detecting the retrograde pulsations generated by TR as a new means of diagnosis. Our routine LAO gated equilibrium studies on LFOV camera were used. A Fourier analysis algorithm of the whole field produced the amplitude (A) and phase (P) images. The latter was masked by the A image thresholded at 7% of the maximum amplitude in the field. The presence of clustered pixels, in phase with the atria, in the hepatic and splenic area on this P image was considered an indication of TR and called positive TR phase (TR-P). Three patients (pt) groups (G) were evaluated. G I: 12 pt with no cardiac disease. G II: 8 pt with TR (one of them had a surgically created TR and was evaluated before and after). G III: 9 pt without clinical evidence of TR but with enlarged R atrium and/or R ventricle with or without clinical evidence of R heart failure. Results: G I: none of the 12 pt showed evidence of positive TR-P; RI = 1.26 $\pm$ 0.05 (mean $\pm$ SEM). G II: 8/8 had a positive TR-P; RI = 0.63 $\pm$ 0.07 (2/8 had normal RI due to simultaneous L heart involvement). The pt who had the surgically created TR developed a positive TR-P only after surgery. G III: None had positive TR-P; RI = 0.89 $\pm$ 0.15. In conclusion: 1) The presence of positive TR-P over the liver and/or spleen area is seen in all TR pt. 2) In the absence of TR there is no evidence of positive TR-P even when there is R heart enlargement and/or failure. 3) A positive TR-P has 100% sensitivity and specificity for TR in this series.

THE EFFECT OF AORTIC VALVE REPLACEMENT ON LEFT VENTRICULAR FUNCTION AT REST AND DURING EXERCISE.
M. Hofmann, F. Schwarz, G. Schuler, H. Baumann, W. Kübler. Univ. of Heidelberg, Dept. of Cardiology, Heidelberg, Germ.

The extent of recovery of left ventricular dysfunction after aortic valve replacement (AVR) in patients with severe aortic valve disease (functional classes III and IV) is not yet quite clear.
Therefore we measured the ejection fraction (EF) six months after AVR in 26 patients with aortic stenosis (AS) and in 22 patients with aortic regurgitation (AR). EF was determined by means of the radionuclide angiography with the gated blood pool technique. The patients with AS and AR were further subdivided according to their preoperative EF into two subgroups: A with an EF<60% and B with an EF>60%. After AVR EF increased in patients with AS -subgroup A- from 44 to 70% and in patients with AR -subgroup A- from 51 to 65% (both values: p<.001). The EF in patients with AS -subgroup B- showed no significant change after AVR (from 69 to 70%; ns), as well as with AR -subgroup B- (from 66 to 68%; ns). Exercise testing increased EF to 83% in patients with AS -subgroup A- (p<.001), but did not increase EF in AR -subgroup A (68%). These results during exercise did not differ significantly from the respective values from subgroup B.
We conclude that AVR leads to an improvement of left ventricular dysfunction at rest in patients with AS and in patients with AR, both with preoperatively impaired left ventricular performance. Exercise after AVR, however, reveals normal left ventricular performance in patients with AS but not in patients with AR.

RADIONUCLIDE EVALUATION OF CARDIAC FUNCTION IN PATIENTS WITH CONGENITAL HEART DISEASE. J.M.K. Ceimo, D.S. Moodie, S.A. Cook, R.T. Go, C. Napoli, T. Hauser, W. McIntyre, and J. Gallagher. Cleveland Clinic Foundation, Cleveland, OH.

Nuclear imaging techniques and M-mode echocardiography have contributed to the evaluation of patients (pts) with congenital heart disease, but there have been few studies correlating non-invasive evaluation of ventricular function and cardiac physiology with angiography and catheterization calculations. In an attempt to evaluate the reliability of radionuclide imaging to define right and left ventricular function and estimate left to right shunts, 37 children and adults with congenital heart disease were studied. Radioisotopic determination of pulmonary flow systemic flow ratio (Qp/Qs), first pass right ventricular ejection fraction (RVEF), and gated left ventricular ejection fraction (LVEF) were compared with contrast ventriculography (right and left) and shunt determinations by oximetry. M-mode echocardiography with calculation of LVEF was also performed and correlated with nuclear and angiographic LVEF. Data obtained was compared for each of the following parameters: Qp/Qs, RVEF, and LVEF. The data showed an excellent correlation between catheterization and radionuclide estimations of Qp/Qs ($r = .92$, $p < .0001$) and angiographic and radionuclide estimates of LVEF ($r = .93$, $p < .0001$), and RVEF ($r = .82$, $p < .001$). Correlations between M-mode echocardiography and both radionuclide and angiographic LVEF were poor ($r = .35$, $r = .07$, respectively). Radionuclide imaging provides a reliable method for evaluation of right

and left ventricular function and shunt calculation in pts with congenital heart disease. Once the initial anatomic definition has been made at catheterization, these methods may obviate the need for repeated catheterizations.

CORONARY ARTERY TO PULMONARY ARTERY FISTULAS: THE SIGNIFICANCE OF ESTIMATION OF SHUNT FLOW TO LUNGS. M.H. Adatepe, O.M. Powell, G.H. Isaacs. Section of Nuclear Medicine, Allegheny General Hospital, Pittsburgh, PA.

A group of 6 adult patients (4 women, 2 men) with known coronary artery to pulmonary artery fistula were studied by injection of Tc-99m labeled MAA or microspheres into involved coronary artery following coronary arteriography. Main complaint was stable or unstable angina pectoris in 5, frequent PVC's in one patient. Physical examination was negative in all except one who had mitral stenosis in addition to fistula.

Coronary artery injection of one millicurie of Tc-99m labeled particles in 0.2 cc volume mixed with 10 cc of normal saline was established without any complication, symptom or sign in all patients.

Counts were obtained from lungs and myocardium utilizing a camera-computer system. Following formula is used to estimate shunt flow: % shunt flow = lung cpm X 100/myocardial cpm + lung cpm. In 6 patients shunt flow was calculated as 59%, 54%, 43%, 39%, 37% and 0%. Four of the patients with larger shunts were submitted to surgical correction procedure. Fifth patient is waiting for surgery. The patient with 0% shunt did not have surgery due to non-functioning fistula. The anginal chest pains in 3, PVC's in one patient have been relieved following the surgery.

Previously published methods such as oximetry, indicator dilution and inert gas inhalation have been inconsistent and generally unreproducible especially in cases involving small shunts.

The method we described above is helpful in determining the degree of relative shunt flow and decision for surgery.

CORRELATION OF SECOND HALF REGIONAL RIGHT VENTRICULAR EJECTION FRACTION WITH PULMONARY ARTERY SYSTOLIC PRESSURE. B.J. Friedman, B.L. Holman, J. Wynne, and J. Idoine. Brigham and Women's Hospital, Boston, MA.

The second half of regional right ventricular ejection fraction (2nd ½ RVEF) was correlated with the pulmonary artery systolic pressure (PASP) in 49 patients who had gated equilibrium radionuclide ventriculography and cardiac catheterization performed within 1-4 days of each other. Using a functional image of ejection fraction, a region of interest was drawn around the right ventricular free wall (RVFW). Patients with either discontinuities in the RVFW ejection shell, atrial fibrillation or clinical tricuspid regurgitation were excluded. The 2nd ½ RVEF was determined by first selecting the right ventricular end diastolic and end systolic frames. Right ventricular mid systole was then determined, and 2nd ½ RVEF defined by subtracting the end systolic counts from the mid systolic counts and dividing this difference by the background corrected end diastolic counts. There were 27 patients with normal PASP (range 18 to 30 mm Hg), and 22 patients with elevated PASP (range 31 to 73 mm Hg). The 2nd ½ RVEF for the group with normal PASP was mean = .38, sd = ± .08, range .30 to .54. The 2nd ½ RVEF for the patients with elevated PASP was mean = .22, sd = ± .06, range .13 to .32. The difference between the means was statistically significant ($p < .001$). A power curve fit($y = ax^b$, where $a = 10.91$ and $b = -0.87$) allowed accurate prediction of PASP ($r = 0.85$). Using a 2nd ½ RVEF of < 0.3 as the criterion of an elevated PASP resulted in a sensitivity of 0.86 and a specificity of 1.0 for the separation of patients with normal and increased PASP. We conclude the 2nd ½ portion of the RVEF may be used to estimate the pulmonary artery systolic pressure.

CHANGES IN LEFT VENTRICULAR VOLUMES DURING UPRIGHT EXERCISE IN PATIENTS WITH CHRONIC AORTIC REGURGITATION. A.S. Iskandrian, A.H. Hakki, B.L. Segal, M.N. Croll, and S.A. Kane. Cardiovascular Institute, Hahnemann Medical College and Hospital, Philadelphia, Pennsylvania.

The changes in left ventricular (LV) volumes during exercise (EX) in patients (pts) with aortic regurgitation (AR) are not well known. Twelve pts, (age 41 ± 12 years, mean ± SD) with moderate-to-severe AR (NYHC I or II) underwent symptom-limited upright EX on a bicycle ergometer. First-pass radionuclide angiograms using a multicrystal camera were obtained at rest (R) and peak EX. Twelve normal men (NL) served as a control. There was no difference between pts with AR compared to NL in the heart rate (beats/min at R (79 ± 11 vs 79 ± 12), and EX (157 ± 21 vs 150 ± 17), duration of EX (10.5 ± 2.7 vs 9.8 ± 3.6 minutes) and workload of EX (750 ± 220 vs 675 ± 245 KPM/min). Seven of the 12 pts with AR and all 12 NL responded by an increase of at least 5% in LV ejection fraction (EF) during EX.

	EDV (ml)		SV (ml)		EF	
	R	EX	R	EX	R	EX
AR	290±155	220±120	154±68	132±49	56±10	64±13
NL	153±25	174±37	95±14	120±34	62±6	75±4

{EDV, end-diastolic volume measured by the area-length method; SV, stroke volume}. During EX, there was slight (p:NS) increase in EDV in NL while the EDV decreased significantly ($p < 0.01$) in pts with AR. The SV increased ($p < 0.01$) in NL during EX while it decreased slightly in pts with AR (p:NS). We conclude: The LV-EDV decreases significantly during EX in pts with AR because of a decrease in regurgitation volume per beat (due to shortening of diastole or decrease in systemic resistance or both). Thus, the preload in AR is determined to a great extent by the regurgitant volume while in NL it is determined by venous return.

10:30-12:00 **ROOM D-1**

ENDOCRINE

Moderator: Stanley J. Goldsmith
Co-moderator: Alan D. Waxman

LOCALIZATION OF PHEOCHROMOCYTOMAS WITH I-131-M-IODOBENZYLGUANIDINE (I-131-MIBG). M. Gross, M. Frager, T. Valk, R. Kline, J. Sisson, D. Swanson, D. Wieland, N. Thompson, M. Tobes, W. Beierwaltes. The University of Michigan and the VA Medical Centers, Ann Arbor, MI.

Pheochromocytomas (PHEO) were localized with I-131-MIBG. Five hypertensive patients without PHEO served as controls. I-131-MIBG 0.5 mCi/1.73 sq m was given i.v. Images of areas of interest were made at 24, 48 and 72 hours post-injection. Adrenal uptake was estimated with a semioperator-independent computer algorithm.

Control subjects exhibited little or no scintigraphic image of their adrenal glands. All patients with sporadic PHEO gave clinical and hormonal evidence of their disease. Unilateral sporadic PHEOs were localized in 4 patients, and these findings were confirmed at operations. In one patient, recurrent PHEO could not be found by computerized tomography or ultrasonography, but the I-131-MIBG concentrated in 2 midline areas which at laparotomy were sites of the recurrent tumors. In patients with metastatic PHEOs: multiple areas of activity were seen in skull, chest and abdomen in one; in another, only ill-defined activity was seen. Calculated % uptake ranged from 0.14 to 2.6%/dose. I-131-MIBG tissue levels ranged from .007 to .049 dose/gm.

In 5 patients with multiple endocrine neoplasia 2a or 2b, images of the adrenal glands (none in 1, faint in 1, and distinct bilateral localizations in 3 patients) correlated with the degree of adrenal medulla function in each case (normal, borderline high, and high in 3). In one of these patients asymmetric bilateral PHEOs were removed; a cyst in a tumor was identified as a non-functioning area by I-131-MIBG but only as tumor by computerized tomography.

Adrenal medullary imaging with I-131-MIBG is a valuable, non-invasive method for the localization of PHEO.

PREOPERATIVE PARATHYROID LOCALIZATION USING RADIOACTIVE TOLUIDINE BLUE (RTB). S.T. Zwas, A. Czerniak, I. Avigad and I. Wolfstein. Ch. Sheba Medical Center, Tel Hashomer Israel.

The principal treatment of parathyroid adenoma or hyperplasia is surgical resection. It is known that the

biologic dye Toluidine Blue is concentrated in the parathyroid tissue and was used formerly for macroscopic localization of the parathyroids during surgery.

A method for the labelling of Toluidine Blue with radioiodine (I-131) was established and the radioiodinated T.B. was used for preoperative parathyroid imaging.

Following I.V. injection of 10 Ci/Kg RTB, parathyroid scintigraphy was performed for the first 20 min. followed immediately by thyroid imaging, using Tc-99m using Gamma Camera equipped with a pinehole collimator connected on line to a nuclear medicine computor.

Parathyroid and thyroid images were further processed and superimposed using the computor to deliniate the position of the parathyroids in relation to the thyroid gland.

We wish to summarize our results in the first 23 pts. with primary hyperparathyroidism studied and operated upon. RTB scintigraphy correctly localized 13 out of the 18 adenomas found in surgery. Of the 5 cases with hyperplasia 2 were fully localized and in each of the other 3 cases 2 or more hyperplastic glands were localized.

These preliminary results suggest good correlation with surgical findings but further experience is needed for complete evaluation of the proposed method.

COMPARATIVE STUDY OF TI-201 AND I-131 SCINTIGRAPHY IN POST-OPERATIVE METASTATIC THYROID CARCINOMA. V.M. Varma and R.C. Reba, George Washington University Hospital, Washington, DC

There have been recent reports that TI-201 is concentrated in primary and metastatic thyroid carcinoma. It is implied that TI-201 might be more suitable than I-131 for the evaluation of patients with metastatic thyroid carcinoma.

Ten patients with metastatic papillary and follicular carcinoma were scanned with TI-201 and I-131. All patients had prior near total thyroidectomy and 7 had received I-131 ablation therapy. The status of the patients at the time of the study was hypothyroid with documented endogenous TSH stimulation 8; euthyroid with functioning metastasis 1; euthyroid with small residual left lobe 1.

I-131 concentration was seen in 7 patients with cervical lymph node metastasis. Amongst these TI-201 concentration was present only in 4 patients with palpable cervical lymph nodes. In 1 patient with a cervical mass (metastatic well differentiated papillary cancer with anaplastic changes) TI-201 concentration was present with no I-131 concentration. In 3 patients with metastatic deposits seen on chest x-ray both I-131 and TI-201 concentration was present. Four patients with I-131 pulmonary concentration both chest x-ray and TI-201 scans were normal.

These observations are at variance with the published literature. In our series TI-201 concentration was seen only in patients with palpable metastatic lymph nodes or positive chest x-ray whereas I-131 concentration was present in all palpable as well as nonpalpable lymph node metastases and early lung metastases when chest x-ray is usually normal. Conclusion: TI-201 scintigraphy is useful only in patients with advanced metastatic thyroid carcinoma and does not replace I-131 scintigraphy in follow-up of these patients.

NON-DIAGNOSTIC ADRENAL IMAGING IN SUSPECTED PRIMARY ALDOSTERONISM (PA). B. Shapiro, M.D. Gross, J.E. Freitas, R.J. Grekin, J.H. Thrall, W.H. Beierwaltes. University of Michigan and VA Medical Center, Ann Arbor, MI.

To evaluate the causes for the reported variability of adrenal scintigraphy in PA a retrospective analysis of scintiscans performed for suspected PA revealed non-diagnostic imaging in 8 cases. All had hyperaldosteronism but further evaluation demonstrated elevated plasma renin activity (PRA) (secondary aldosteronism). Dexamethasone suppression (DS) 4 mg for 7 days was given prior to injection of 1 mCi I-131-6β-iodomethyl-19-norcholesterol (NP-59) and throughout the course of imaging. Scintiscans were obtained at 72, 96, and 120 hours using a gamma camera interfaced to a minicomputer. Normal DS adrenal imaging occurs at intervals greater than 5 days post injection. Activity visualized before 5 days is consistent with adenoma or hyperplasia. Early bilateral symmetric activity was noted in patients found later to have: renal artery stenosis (2 cases), Bartter's syndrome (1 case), use of oral contraceptives (2 cases) and diuretic therapy (1 case). Asymmetric bilateral early imaging (at 3 days) was observed in a patient with an aldosteronoma while on diuretic therapy for hypertension. Antecedent venography complicated by adrenal infarction with unilateral imaging was seen in 2 cases studied with Se-75-selenomethyl-19-norcholesterol in which adrenal hyperplasia was later demonstrated.

Factors associated with non-diagnostic adrenal scans are: 1) late imaging intervals on DS resulting in breakthrough of activity of the normal adrenal, 2) intrinsic or pharmacologic elevation of PRA, 3) unilateral lack of imaging due to adrenal infarction. Prior knowledge of the biochemical and drug status in addition to antecedent procedures is mandatory for precise adrenal scintiscan interpretation.

FACTORS INFLUENCING THE INCREASING INCIDENCE OF RADIOIODINE INDUCED HYPOTHYROIDISM IN GRAVES' DISEASE. A.J. Cunnien, I.D. Hay, C.A. Gorman, K. Offord, P.W. Scanlon, and D.S. Duick. Mayo Clinic and Foundation, Rochester, MN.

Von Hofe et al. (JNM 19:180, 1978) have reported that within 12 months of treatment with 10 mCi I-131 for Graves' disease (GD) 69% of their 48 patients treated in 1974-76 were hypothyroid, an incidence of hypothyroidism (HT) considered higher than would be expected from series reported in the 1950s and 1960s. To determine whether in the Mayo Clinic a similar trend was apparent, we estimated the early HT incidence for 191 patients treated with a mean dose of 9.8 mCi (range 7.5-12.5) in six calendar years during the past three decades (1950s: 1950/57, 1960s: 1962/67, 1970s: 1972/77). Three months after treatment the HT incidence during the three decades was 33, 55, and 67%. The incidence at one year increased from 48 and 60% in 1952 and 1957, through 81 and 82% in 1962 and 1967, to 78 and 80% in 1972 and 1977. In an attempt to explain these results we studied all patients treated with I-131 for GD during these six years and examined in each of 454 patients multiple variables known to influence the outcome of I-131 therapy.

Although the number of patients pretreated with thionamide drugs, the mean 24 hr I-131 uptake and the calculated dose of I-131 (μCi/estimated g thyroid tissue) showed no obvious trend across the decades, the initial administered dose steadily increased from a mean of 8.1 mCi in 1952 to 13.8 mCi in 1977. Concurrently, estimates of gland size increased from a mean of 26 g in 1952 to 43 g in 1977. If in GD patients thyroid size did not truly increase across the decades, the increasing incidence of early HT seen after I-131 in our institution may be explained by the conscious or unconscious decision to use larger doses through inflated estimates of thyroid gland weight.

HIGH DOSE I-131 TREATMENT OF PLUMMER'S DISEASE. N.D.Charkes Temple University Hospital, Philadelphia, PA.

In the past 18 years, the author has treated 33 patients with Plummer's disease with I-131, 25 of them with doses sufficient to deposit at least 14 mCi in the nodule(s) ("high dose" group), as recommended by Skillern (Arch.Int. Med. 110:888,1962). In 8 patients 1.5-9.0 mCi were deposited, as suggested by Eller (Ann. Int. Med. 52:976,1960)("low dose" group). Diagnosis was established scintigraphically by TSH stimulation of extranodular tissue after demonstration of non-suppressibility by l-T3, and effective half-life of thyroidal I-131 was measured ($T_{\frac{1}{2}e}$). Mean age of the entire group was 63.7 years, mean RAI uptake 36%, and mean $T_{\frac{1}{2}e}$ 5.7 days. Nodules were ablated in 18/25 of the high-dose group but in only 1/8 of the low dose group. When the response was correlated with estimated radiation dose, we found that the nodules were functionally ablated in 14/15 patients given >30,000 rads, 5/10 patients given 15,000-30,000 rads, and 0/8 patients given <15,000 rads. All successfully treated patients were relieved of hyperthyroidism, but only 3/8 low-dose patients became euthyroid. Low RAI uptake 3 months after therapy responded normally to TSH in 7/8 successfully treated patients, indicative of hypopituitary hypothyroidism, but 2 patients became permanently hypothyroid from thyroid failure. Conclusion: Successful treatment of Plummer's disease with I-131 (functional ablation of nodule(s))requires a radiation dose of 30,000 rads or more. Dose administration based on estimated individualized radiation dose, calculated from the tracer I-131 concentration and effective half-life, is preferable to giving a fixed I-131 dose.

10:30-12:00 **ROOM E-1**

GI I: HEPATOBILIARY FUNCTION

Moderator: Heidi S. Weissmann
Co-moderator: John E. Freitas

THE COMPARISON OF KINETICS AND IMAGE PATTERNS OF Tc-99mIDA DERIVATIVES IN NORMAL SUBJECTS. V.R. Bobba, G.T. Krishnamurthy, E. Kingston, P.H. Brown, M. Eklem, and F. Turner, VAMC and UOHSC, Portland, OR.

This investigation was undertaken to compare the kinetics and image patterns of four Tc-99m-IDA derivatives, HIDA, PIPIDA, EIDA and PBIDA in 35 normal subjects (NS). After an overnight fast, each NS received 5 mCi of Tc-99m-HIDA (N=10), Tc-99m-PIPIDA (N=10), Tc-99m-EIDA (N=7) and Tc-99m-PBIDA (N=7). The total blood clearance and urinary excretion were determined as percent of injected dose by collecting frequent blood and urine samples up to 24 hours. Serial hepatobiliary gamma camera images were obtained at 2 minute intervals for 60 minutes and at 3 and 24 hours. The data were simultaneously acquired on 64 x 64 computer matrix at 1 frame/min. The time of appearance of common bile duct (CBD), gallbladder (GB) and duodenum were noted for each agent on the images. The peak hepatic uptake time, the T 1/2 uptake and excretion times were determined from the unweighted non-linear least square curve generated from the region of interest over superolateral border of the right hepatic lobe.

The fastest blood clearance was noted with Tc-99m-EIDA followed by HIDA, PIPIDA and PBIDA. The 24 hours mean urine excretion was 15, 14, 12 and 5% of dose respectively for HIDA, PIPIDA, EIDA and PBIDA. Mean peak hepatic uptake time respectively was 20, 20, 14 and 26 min. T-1/2 uptake time ranged from 3.7 to 4.8 min. The mean hepatic excretion T-1/2 time was 48, 67, 37 and 153 min respectively. It is concluded that the time of appearance of major biliary structures with IDA derivatives is related to their hepatic excretion T-1/2 time.

THE NORMAL FASTING AND POSTPRANDIAL Tc-99m-DIISOPROPYL-IDA HEPATOBILIARY STUDY. W.C. Klingensmith III, V.M. Spitzer, A.R. Fritzberg, and C.C. Kuni. University of Colorado Health Sciences Center, Denver, CO.

Tc-99m-diisoprophyl-IDA hepatobiliary imaging studies were performed in eleven normal subjects in both the fasting (overnight) and postprandial (after breakfast) states. Analogue and digital images were acquired during the first sixty minutes following injection and urine was collected over the first three hours. In the five to sixty minute analogue images in both fasting and postprandial studies cardiac blood pool was almost never seen, renal pelvic radioactivity was commonly seen, the extrahepatic biliary tract was always seen, the left hepatic duct was almost always seen, and the left hepatic duct was always more prominent than the right hepatic duct. The biliary tract was visualized by ten minutes in nine of eleven fasting and ten of eleven postprandial studies. The gallbladder was visualized in all eleven fasting studies, but in only four postprandial studies ($p<0.05$). There was a trend for the liver to background ratio in 5 min images to be higher in postprandial studies ($p>0.05$). The parenchymal washout rate was faster in postprandial studies ($p<0.05$). The zero to sixty minute digital data indicated a greater hepatocyte clearance, an earlier time of peak parenchymal radioactivity, and a faster parenchymal washout in postprandial compared to fasting studies ($p<0.05$). Approximately nine percent of the injected dose was recovered in the urine during the first three hours in fasting and postprandial studies. The normal Tc-99m-diisopropyl-IDA study in the fasting and postprandial states is defined; significant differences between the two states exist.

Tc-99m IMINODIACETIC ACID CHOLESCINTIGRAPHIC EVALUATION OF ACALCULOUS CHOLECYSTITIS. H.S. Weissmann, D. Berkowitz, M. Fox, R. Rosenblatt, L.A. Sugarman and L.M. Freeman. Albert Einstein College of Medicine and Montefiore Hospital and Medical Center, Bronx, NY.

Tc-99m iminodiacetic acid (IDA) cholescintigraphy has an accuracy of 98% in the detection of acute cholecystitis. This study was undertaken to determine the accuracy of this technique in patients with acalculous cholecystitis.

The case records of all patients at MHMC with acalculous cholecystitis confirmed at surgery and pathologically were analyzed. Fifteen patients had pre-operative IDA studies performed during this study period (3/78-1179). The clinical presentations were as follows: Group I - admission diagnosis of cholecystitis (5), Group II - abdominal pain in whom the differential diagnosis of cholecystitis was considered (5), Group III - patients admitted with an unrelated diagnosis (5).

Other biliary tract studies performed included 1 normal intravenous cholangiogram and 1 nonvisualized cholecystogram. Of 9 sonograms, 4 were normal, 4 demonstrated "calculi" and 1 "sludge."

Of 10 patients with pathologically proven, acute acalculous cholecystitis, 7 had the typical cholescintigraphic pattern of acute cholecystitis (persistent nonvisualization of the gallbladder). Two patients had a pattern of CBD obstruction (cholangitis suspected clinically in both) and 1 had a normal pattern. In all 5 patients with chronic cholecystitis, the gallbladder (GB) visualized within 1 hour but in 4 the GB failed to contract in response to I.V. Sincalide. These results indicate that Tc-99m-IDA is a highly accurate method in the detection of acute acalculous cholecystitis, and though not diagnostic, is useful in suggesting GB disease in patients with chronic cholecystitis.

THE ROLE OF Tc-99m HIDA SCINTIGRAPHY IN THE SURGICAL MANAGEMENT OF ENTEROGASTRIC REFLUX. O.L. Manfredi, J. Schaumburg, P. Dayrit, P. Wickremesinghe. St. Vincent's Medical Center, Staten Island, N.Y.

The purpose of this paper is to demonstrate the value of Tc-99m HIDA scintigraphy in evaluating post surgical alkaline reflux gastritis. Fifteen patients referred from the GI Service complaining of upper abdominal pain, bilious vomiting, iron deficiency anemia and weight loss were studied. All had undergone gastric surgery (Bilroth II procedure) extending over a 4-15 year period. Diagnostic workup included Upper GI Series, G.B. Series and upper endoscopy with biopsy. All underwent Tc-99m HIDA enterogastric reflux scintigraphy which consisted of an I.V. injection of 5 mCi Tc-99m HIDA with sequential images obtained every 15 minutes for 1 hour. A standard fatty meal labelled with 250 uCi In-111 was then administered orally and serial images were acquired every 5 minutes for 1 hour. Images were stored on a computer and various regions of interest were defined over the biliary tree, duodenum, gastric remnant and background. The reflux indices were calculated utilizing the equation described by Tolin, Malmud, et al.

Of the 15 patients studied, 10 were recommended for surgery based on the symptomology and markedly increased Enterogastric Reflux Index. Reconstructive surgery (Roux-en-y procedure) was performed on 8 patients. At the end of 6 weeks, the patients were restudied post-operatively both by endoscopy and Tc-99m HIDA scintigraphy. All showed a marked reduction in the reflux index and resolution of all previous symptoms. It is concluded that Tc-99m HIDA enterogastric reflux scintigraphy is an important non-invasive modality not only in the diagnosis, but management of enterogastric reflux.

INTRASPLENIC BLOOD CELL KINETICS. A.M. Peters and J.P. Lavender. Hammersmith Hospital, London, England.

We have attempted to gain a better understanding of the intrasplenic kinetics of blood cells, specially platelets and heat damaged red cells (HDC). Gamma camera time activity curves over the spleen and peripheral blood clearance curves were constructed up to periods of one hour following I.V. injections of platelets labelled with In-111 and HDC labelled with Tc-99m. The uptake of platelets by the spleen was monoexponential with a time constant consistent with a closed 2 compartmental distribution between blood and spleen. The time constants of splenic uptake of platelets and HDC injected simultaneously were almost identical

up to 20 min following injection. Subsequently, slow accumulation in the spleen and clearance from the blood of HDC continued, whereas platelet levels became constant. We have confirmed that platelets, entering the spleen, pool there, rather than become irreversibly trapped, by showing that platelets injected into the splenic artery accumulate in peripheral blood with a time constant similar to that of the accumulation in the spleen of peripherally injected platelets. Comparative kinetics of HDC and platelets indicate that HDC pool in the spleen similarly to platelets and with a similar transit time. Platelet kinetic studies in a variety of clinical conditions suggested that platelet transit time was increased in polycythaemia and when splenic perfusion was reduced. Increased splenic perfusion resulted in only a small decrease in transit time. Any tendency, therefore, for cell pooling to decrease with lowered splenic blood flow would be opposed by increased transit time.

SCINTIGRAPHIC DETECTION OF CAVERNOUS HEMANGIOMAS. H.D. Royal, D. Front, O. Israel, J.A. Parker, G.M. Kolodny. Divisions of Nuclear Medicine, Beth Israel Hospital, Boston, MA and Rambam Hospital, Haifa, Israel.

The noninvasive diagnosis of cavernous hemangiomas is very desirable since biopsy of these lesions can be catastrophic. Previously reported results with ultrasound, computed tomography and scintigraphy have been inconclusive. Specifically, conventional hepatic flow studies (pertechnetate or sulfur colloid) have been misleading since cavernous hemangiomas appear "hypoperfused" due to the fact that incoming radioactivity is rapidly diluted in the hemangiomas' massive blood pool.

Over the past two years, we have studied 14 patients with cavernous hemangiomas using hepatic perfusion and delayed hepatic blood pool scintigraphy (in vivo labelled RBC's). In all 14 patients, decreased perfusion was noted on the initial flow studies whereas a markedly increased blood pool was noted on the delayed blood pool images (up to 2 hours after injection). 10/14 patients had normal liver function tests. In 11/14 patients the cavernous hemangiomas were discovered during a metastatic workup. Correct noninvasive diagnosis in these patients avoided the potential morbidity of a biopsy and had profound therapeutic and prognostic implications.

Hepatic perfusion and blood pool scintigraphy is a simple, safe, reliable means of detecting cavernous hemangiomas of the liver. Since these abnormalities of the liver are the most common vascular abnormality occurring in .4 to 7.0% of autopsied series and since their noninvasive diagnosis is critical, hepatic blood pool scintigraphy should replace conventional hepatic flow studies.

10:30-12:00 **ROOM B-1**

SYMPOSIUM: NUCLEAR MAGNETIC RESONANCE

Moderator: Paul C. Lauterbur
Co-moderator: Lawrence E. Crooks

(1) Paul C. Lauterbur, State University of New York, Stonybrook, NY. TRUE THREE DIMENSIONAL NMR ZEUGMATOGRAPHIC IMAGING WITH AND WITHOUT PARAMAGNETIC CONTRAST AGENTS.

(2) Larry E. Crooks and Peter L. Davis, University of California, San Francisco, CA. NMR IMAGES OF IN VIVO NORMAL AND ABNORMAL TISSUES.

(3) David G. Gadian, Oxford, England. HUMAN METABOLISM STUDIES BY PHOSPHOROUS NMR.

1:30-3:30 **ROOM B-1**

CARDIOVASCULAR II: MEASUREMENT OF VENTRICULAR FUNCTION

Moderator: Harvey J. Berger
Co-moderator: Ellinor B. Sokole

FIRST PASS RADIONUCLIDE ANGIOGRAPHY WITH ULTRASHORT LIVED IRIDIUM-191m. S.Treves, C.Cheng, A.Samuel, A.Fuji, R.M. Lambrecht. The Children's Hospital Medical Center, Harvard Medical School, Massachusetts Institute of Technology. Boston, MA. and Brookhaven National Laboratory. Upton, N.Y.

A new Os-191→Ir-191m radionuclide generator was used to obtain angiograms in 94 patients. Ir-191m has a physical half life of 4.96 sec. and decays to stable Ir emitting 65 and 129 keV photons in 60% and 30% abundance respectively. The generator has a 10% Ir-191m yield and a 3-5 x 10^{-3}% Os-191 breakthrough. It has a shelf life of a month.

The patients studied were from 4 days to 67 years of age (ave. 13 yr.). The referral diagnoses were: ventricular septal defect (47.4%), atrial septal defect (31.6%), patent ductus arteriosus (11.5%), and others (9.5%) including post operative transposition of the great arteries, superior vena caval obstruction, etc. In twelve patients who underwent Ir-191m angiography and cardiac catheterization simultaneously there was good correlation in the measurement of pulmonary to systemic flow ratio, Qp:Qs between these two methods (r = .90). Iridium-191m angiography was useful to diagnose and quantify left to right shunts. In 37 patients the Qp:Qs was 1.0-1.2; and in 49 patients 1.2->3.0. Preliminary results indicate that Ir-191m can also be used to measure right and left ventricular ejection fraction. Advantages of Ir-191m for angiography include: low radiation exposure to patients, high photon flux for rapid imaging, and the ability to obtain serial studies without background. Iridium-191m angiography is safe, accurate and reproducible.

A NEW METHOD FOR THE MEASUREMENT OF RIGHT VENTRICULAR FUNCTION USING AN ULTRA SHORT-LIVED ISOTOPE (KRYPTON- 81M) D.D.Sugrue, S.Kamal, A.Rozkovec, W.J.McKenna, C.M.Oakley, J.P.Lavender. Royal Postgraduate Medical School, London, UK.

Measurement of right ventricular ejection fraction (RVEF) using conventional, non-geometry dependent, count-based, first-pass radionuclide techniques and technetium labelled compounds ($t_{\frac{1}{2}}$ = 6 hours) carries the two disadvantages of unnecessary whole body radiation dose and the need for separate injections of isotope for repeated estimations. Krypton- 81M ($t_{\frac{1}{2}}$ = 13 secs), continuously eluted in 5% dextrose from a rubidium generator and infused through a peripheral vein, gives a high count density over the right ventricle at equilibrium. Radiation exposure can be minimised by turning the infusion pump on and off as required. The short $t_{\frac{1}{2}}$ and efficient exhalation of 81M KR ensures exceedingly low background counts. The high count density over the RV allows semi-automatic, computer-based detection of RV contours.

RVEF was measured in 10 normal volunteers and 8 patients with angiographically proven dilated cardiomyopathy. Determinations were made at rest and during stress by isometric exercise (1/3rd maximum x 3 minutes) and cold pressor test (3 minutes). Results (mean % ± S.D.) were as follows:-

	Normals (n=10) %	Cardiomyopathy (n=8) %
Rest	46.09 ± 9.54	28.87 ± 11.60
Isometric exercise	65.40 ± 7.50	36.83 ± 14.46
Cold pressor	65.0 ± 4.26	39.00 ± 12.42

It is concluded that this technique has considerable potential for serial study of right ventricular function.

SERIAL ASSESSMENT OF LEFT VENTRICULAR EJECTION FRACTION WITH THE MINIATURIZED CADMIUM TELLURIDE DETECTOR MODULE: POTENTIAL TECHNIQUE FOR CONTINUOUS MONITORING OF VENTRICULAR FUNCTION. H.J. Berger, P. B. Hoffer, J. Steidley, A. Gottschalk, B.L. Zaret, Yale Univ., New Haven, Ct.

Previous studies from this laboratory have described a miniaturized cadmium telluride (CdTe) semiconductor detector module that is affixed to the patient's (pt) chest and is suitable for assessment of left ventricular (LV) ejection fraction (EF). Using the Tc-99m labeled equilibrium blood pool, 1-minute ECG gated acquisitions are performed. The reproducibility of serial measurements and the effects of pt position, chest configuration, and the presence of LV dyssynergy were evaluated in 33 pts.

LVEF determined by the CdTe module correlated with first-pass radionuclide angiocardiography (r=0.78) and sodium iodide nuclear probe studies (r=0.80). Comparable correlations were obtained in 18 pts with nl LVEF (r=0.79), 15 pts with abnl LVEF (r=0.75), and 10 pts with dyssynergy (r=0.76). In these groups, there were no significant differences in LVEF by the 3 techniques. In 5 pts with increased chest diameter due to lung disease and/or obesity, the CdTe module underestimated LVEF in each pt (mean±SEM, 9±3%). In the remaining pts, LVEF by CdTe module and gamma camera were not different. In 11 pts, the absolute interstudy difference from 5 serial supine studies was 7±2%. LVEF obtained from supine and sitting studies correlated well (r=0.86), although LVEF was consistently lower in the sitting position (absolute difference, 5±2%; $p<0.01$).

Thus, the miniaturized CdTe module is suitable for continuous monitoring of LV performance in either the supine or sitting position. In its present design, the straight bore single hole collimator does not appear to be appropriate for pts with increased chest diameter due to diminished detector sensitivity with increased depth.

VALIDATION OF THE DETAILS OF THE RADIONUCLIDE LEFT VENTRICULAR TIME ACTIVITY CURVE. P.T. Makler, B.S. Denenberg, A.A. Bove, N.D. Charkes, L.S. Malmud, and J.F. Spann, FACC, University of Pennsylvania, Philadelphia, PA.

The first third ejection fraction has been reported to be useful in separating normal subjects from those with coronary disease when the data is acquired in a first pass manner but not when the data has been acquired using gated equilibrium techniques. One possibility is that the intermediate points obtained with the gated equilibrium technique may not reflect the true changes in ventricular volume during the cardiac cycle. We investigated this question by comparing the form of the left ventricular time activity curve (LVTAC) with computer assisted analysis of byplane contrast ventriculography (XR). Ventricular volumes were calculated with each technique at ten equal times during systole in each of sixteen patients. The data was expressed as the percent of the stroke volume remaining in the ventricle at each time. dV/dT was also calculated at each of the ten points. The results show that the RNTAC depicts the point by point changes in left ventricular volume with high fidelity. This was true for normal subjects as well as patients with coronary artery disease and myopathy. At no point on any curve was there more than a 4% difference between the RN value and the XR value. We conclude that because the volume curve by RNTAC is identical to the volume curve by XR, the RNTAC is accurately depicting the instantaneous changes in the left ventricular volume curve and thus, the failure to separate normals from CADs with the first third ejection fraction is because both groups have the same pattern and is not an artifact of the gating techniques.

FIRST THIRD EJECTION FRACTION: ARE RADIONUCLIDE MEASUREMENTS ACCURATE? A. Yamashina, N. Roistacher, M.I. Friedman, R.N. Pierson, Jr., St. Luke's-Roosevelt Columbia, N.Y.C.

Early systolic ejection phase indices by contrast angiography (CA) have been accepted as providing greater sensitivity for detection of abnormalities of left ventricular (LV) performance in coronary artery disease (CAD) than holosystolic indices. Recently a first pass radionuclide (RN-FP) count method for the measurement of first third ejection fraction (1/3EF), demonstrated good correlation with CA evaluations. However, the LV time activity curve (TAC) is only an approximation of the true LV volume cycle, being variably contaminated by crosstalk from other chambers and structures, and is most accurate at the peak of levophase transit.

In 15 patients with EF$>$0.50 (with and without CAD), 1/3EF in 4 consecutive beats showed the following problems:

1) Timing of end diastole (ED) and end systole (ES) cannot be derived from the TAC alone: the position of relative maxima often preceeded or followed the R wave (range -60 to 140 msec), and the largest inter-beat R-ES variation in each patient averaged 100 msec).
2) At FP LV ED count rates of ~200/40 msec, the standard deviation of a 30% 1/3 EF is ~ 8%, a coefficient of variation of ~26%. Smoothing of the TAC may reduce this by~$\sqrt{2}$.
3) In 15 patients at steady state, inter-beat coefficient of variation for first third EF was 0.38 + 0.19, vs 0.10 + .06 for total EF.
4) A 40 msec frame time is too long for evaluation of a curve whose slope is rapidly changing within 100-150 msec, even when statistical smoothing is employed.
5) Only 2 or 3 beats accurately represent holosystolic EF (Schelbert); certainly no more should be used for 1/3 EF.

Inter-beat variations, statistics at low count rates, and long framing times, contribute to the failure of the LV TAC to represent a high frequency rendition of the LV volume curve, and render this method invalid for 1/3EF.

SCINTIGRAPHIC MEASUREMENT OF LEFT VENTRICULAR VOLUMES USING THE COUNT DENSITY DISTRIBUTION. O. Nickel*, N. Schad*, E. J. Andrews, Jr., M.D., J.W. Fleming, and M. Mello. *Stadtiches Krankenhaus, Passau, West Germany and Medical Center Clinic/West Florida Hospital, Pensacola, Florida.

An experimental model was developed using ellipsoidic balloons of different volumes to derive an empirical formula for the relation of the "normalized" total count-rates on gamma camera images to volume. The Normalized Total Count rate (NTC) is defined by the total count-rate divided by the maximum count density. If an object is at a constant distance from the collimator, the NTC is a linear function of volume. This formula was then applied to calculate left ventricular end-diastolic volume in 71 consecutive patients from scintigraphic images obtained by radionuclide ventriculography. The distance from the left ventricle to the collimator was estimated by using the patient's height and weight. The volumes calculated by the nuclear method were compared with angiographic volumes obtained at cardiac catheterization and good correlation was found (r=0.95).

Scintigraphic measurement of left ventricular volume using an empirical formula based on count density distribution gives an accurate quantitative estimate of ventricular volume obtained in a non-invasive manner. Patient blood sample counting is not required and repeat studies can be performed with ease. The applications include evaluation of ventricular volume change in response to stress, drug intervention, and medical or surgical treatment. The method may also prove useful in following patients with valvular heart disease.

BIODISTRIBUTION OF TANTALUM-178 - A SHORT-LIVED RADIOPHARMACEUTICAL FOR BLOOD POOL IMAGING. R.A. Wilson, S.Y. Kopiwoda, J. Kochocki, R.J. Callahan, R.H. Moore, L. Camin, H.W. Strauss. Massachusetts General Hospital.

To determine if Tantalum-178 (Ta-178), a short-lived radiopharmaceutical (T 1/2p = 9.3 min) available from the Tungsten/Tantalum generator could be eluted and used directly for equilibrium blood pool imaging, biodistribution studies of the Ta-178 eluate were performed in mice and imaging and blood clearance studies were performed in dogs. Following intravenous injection of the radionuclide, the mice were sacrificed at intervals from 1 to 30 minutes after injection. The following organs were weighed and counted in a well scintillation counter and their activity compared to aliquot of the injected dose:

ORGAN	1 min	5 min	10 min	20 min	30 min
BLOOD	8.7±1.1	6.4±1.0	5.7±1.0	3.7±0.9	4.1±1.0
HEART	4.1±1.4	1.7±0.3	3.7±0.7	1.8±0.5	1.7±0.2
LUNG	5.5±0.7	4.8±0.5	3.2±0.4	2.5±0.3	2.8±0.4
LIVER	6.3±0.7	6.7±1.5	5.1±0.4	3.7±0.6	4.5±0.4
SPLEEN	3.7±0.5	6.0±0.5	2.9±0.4	2.2±0.2	3.6±0.6
KIDNEY	8.3±1.5	12.0±1.5	7.9±1.4	7.8±0.3	7.6±0.4
GUT	2.5±0.2	3.5±0.4	3.7±0.6	3.2±0.1	3.6±0.3
N	5	5	5	3	5

%dose/gm (mean ± SEM)

Two dogs and a rabbit were injected with Ta-178 and the biological half-life of the tantalum in the blood was found to be greater than 3 hours. The Ta-178 was associated with the plasma protein fraction of blood as determined by centrifugation and Sephadex gel filtration.

Two dogs had gated blood pool scans performed with Ta-178 after acute coronary artery ligation, followed by images recorded with technetium-99m labeled red blood cells in the same position. Blinded interpretation of the images suggested that image quality was similar with the two nuclides. These data suggest that Ta-178 can be used for equilibrium blood pool imaging and produces images of similar quality to technetium-99m.

IMPROVED IMAGE QUALITY IN CARDIAC BLOOD POOL SCINTIGRAPHY WITH SEMI-IN VITRO LABELED RED BLOOD CELLS. E. Busemann Sokole, A. Vyth, C.F.M. Raam, L.R. van der Wieken and J.B. van der Schoot. Wilhelmina Gasthuis, University of Amsterdam, Amsterdam, Netherlands.

Background (BG) activity in gated blood pool studies is still a key issue. Optimal labeling of red blood cells (RBC) is essential. We have replaced in vivo labeling of RBC with a simple semi-in vitro labeling method which takes about 30 min preparation time. Ten min after intravenous injection of Sn DTPA, 9ml of blood is withdrawn and centrifuged in the syringe. The plasma is removed and 550MBq of Tc-99m pertechnetate is added. After 10 min at room temperature the RBC are reinjected without washing.

The semi-in vitro RBC labeling in 10 patients (labeling percentage prior to injection, 95.9%±0.98%SEM) was compared to the in vivo RBC labeling in 9 other patients. In the first hour, labeling percentage, circulating RBC activity and urine activity were, respectively, (mean±SEM):

semi-in vitro	(96.1±0.35)%	(90.7±3.4)%	(4.6±0.7)%
in vivo	(90.0±0.93)%	(69.9±3.0)%	(4.6±0.8)%

The labeling remained almost constant.

In 40 patients, BG activity was assessed in the LAO view by the ratio of count densities in the center of the left ventricle (LV) and in the BG outside an automatically selected LV. This ratio was 3.5±0.3SEM (n=20) for the semi-in vitro and 2.2±0.1SEM (n=20) for the in vivo method.

Gated blood pool studies with semi-in vitro labeled RBC have been performed in 160 patients. Image quality was substantially improved facilitating wall motion assessment and automatic LV contour detection. Especially in stress gated blood pool studies, semi-in vitro RBC labeling is the method of choice, giving better statistics in a shorter time.

1:30-3:30 **ROOM E-1**

CARDIOVASCULAR III: MYOCARDIAL METABOLISM, ISCHEMIA, AND TOMOGRAPHIC IMAGING

Moderator: Heinrich R. Schelbert
Co-moderator: Kenneth A. Narahara

KINETICS OF C-11 PALMITATE IN ACUTELY ISCHEMIC MYOCARDIUM. H.R. Schon, H.R. Schelbert, G.D. Robinson, A. Najafi, J.R. Barrio, M.E. Phelps. UCLA School of Medicine, Los Angeles, CA

As demonstrated previously, the rate of β-oxidation in normal myocardium can be evaluated with C-11 palmitate (CPA). The purpose of this study was to examine the use of CPA for assessing the rate of β-oxidation in ischemic myocardium by determining the extraction fraction (E) and clearance (T) of CPA in acute ischemia produced by stenosing the left anterior descending cornary artery (LAD) in 15 experiments in 9 dogs. Myocardial blood flow (MBF) in ischemia was reduced to 54 ±25(SD) ml/min/100g from 124 + 25 ml/min/100 g at control ($p<0.001$) and myocardial oxygen consumption (MVO) from 12.7 ± 4.2 ml/min/100g to 7.9 ± 3.6 ml/min/100g ($p<0.01$). Consumption of free fatty acids (FFA) and glucose fell ($p<0.01$), while consumption of lactic acid decreased or frank production occurred. CPA was injected into the LAD and E and T were calculated from the peak and slope of the myocardial C-11 time activity curve recorded for 60 min. The curve consisted of a vascular, an early rapid and a late slow phase. E was independent of MBF and MVO, averaged 0.65 ± 0.07 and did not differ from control. T of the early rapid phase increased as MVO fell ($r=0.86$) and was proportional to the rate of residual C-11 CO_2 production ($r=0.88$) and to C-11 lipid washout ($r=0.46$, $p<0.05$). The ratio of peak C-11 CO_2 production to peak C-11 lipid washout decreased from 3.10 ± 1.77 at control to 1.72 ± 1.38 in ischemia ($p<0.01$). The ratio of the size of the early rapid to the size of late phase fell as MVO decreased ($r=0.78$) but was for the same MVO significantly lower than at control (0.75 ± 0.37 vs 2.80 ± 0.82 SD, $p<0.001$). We conclude that in acute ischemia a) E of CPA is unchanged from control; b) T of the early rapid phase is determined by β-oxidation but also C-11 lipid washout;and c) probably because of increased glycolysis, disproportionately more CPA is esterified rather than oxidized as compared to control.

RELATIONSHIP BETWEEN MYOCARDIAL BLOOD FLOW AND UPTAKE AND UTILIZATION OF FREE FATTY ACIDS (FFA). H.R. Schelbert, E. Henze, S.C. Huang, M.E. Phelps. UCLA School of Medicine, Los Angeles, CA 90024.

Several studies have compared myocardial imaging with Tl-201 and radiolabeled FFA analogs. Because uptake and β-oxidation of FFA are linked to myocardial blood flow (MBF) and to O_2 supply, myocardial images with FFA analogs may not provide information superior to that obtained with Tl-201. We therefore studied 7 dogs with pacing induced myocardial ischemia by positron computed tomography (PCT). MBF was evaluated with N-13 ammonia and microspheres and FFA metabolism with IV C-11 palmitate (CPA) and serial PCT imaging for 30 mins. Myocardial N-13 and C-11 activity and its clearance rate (defined as λ) were determined from multiple regions of interest assigned to the left ventricular myocardium on the PCT images. λ was derived from the early rapid phase of the myocardial C-11 time activity curve. Myocardial CPA activity was maximum between 3.0 to 6.0 min. and proportional to N-13 activity (r - values 0.70 to 0.98). In the ischemic segment, N-13 and CPA activity were depressed by 49.6±17.6SD% and by 49.0+17.4% compared to control myocardium. λ was reduced in ischemic segments by 57.6+41.2% and was inversely related to N-13 activity (r values from 0.70 to 0.94). However, the magnitude of λ in normal and ischemic segments varied considerably between individual dogs and was a function of FFA consumption (FFA consumption (meq/min/100gm) = $-0.1407 - 3.93\lambda$. We conclude Tl-201 myocardial perfusion images can provide information on the relative distribution of myocardial FFA uptake and utilization. However, quantitative estimates of FFA uptake and β-oxidation can only be obtained by imaging with tracers of FFA metabolism.

MYOCARDIAL ENERGY METABOLISM EVALUATED BY SINGLE PASS UPTAKE AND POSITRON EMISSION COMPUTED TOMOGRAPHY OF N-13 AND C-11 LABELED AMINO ACIDS. E. Henze, J. Egbert, J. Barrio, F. Baumgartner, M. Phelps, D. Kuhl, H. Schelbert. UCLA School of Medicine, Los Angeles, CA.

To determine the use of labeled amino acids (AA) for imaging regional myocardial ischemia by positron emission tomography (PCT) and their relationship to energy metabolism, myocardial uptake of N-13 and C-11 AA, oxaloacetate (OXA) and citrate (CIT) was studied at control, during ischemia and after transaminase inhibition in 14 dogs and 2 monkeys. In dogs, myocardial time activity curves after intracoronary injection revealed 3 phases with a short halftime (T) for the vascular phase (4-8 sec), a rapid second phase (20-60 sec) and a slower third phase (14-170 min). For all compounds tested, the residual fractions were 0.1-0.2 in normal myocardium and slightly but consistently higher by 0.02-0.07 for N-13 labeled to ALA, GLU, GLN and ASP during ischemia. T of C-11 labeled to OXA, CIT and ASP was similar and, compared to N-13 ALA, GLU and ASP was significantly ($p<0.001$) higher for the second (66.1±30.1 vs 25.5±12.5 sec) but lower for the third phase (20.9±7.4 vs 104.1±35.1 min). This was paralleled by C-11 CO_2 production. Following transaminase inhibition by aminooxyacetate, clearance of N-13 ALA, GLU and ASP was depressed but not for C-11 OXA and CIT. On the PCT images N-13 activity labeled to ALA and GLU was not decreased in ischemic segments despite a significant flow reduction. The whole body distribution of N-13 and C-11 AA in dogs showed low myocardial but high liver activity while in monkeys the myocardial activity was high. We conclude, that N-13 and C-11 AA are avidly extracted by myocardium. While in primates tracer concentration remains high, it rapidly declines in dogs because of transamination and metabolic breakdown. Because of increased uptake during ischemia and the relationship to the Krebs cycle labeled AA may be of value for imaging myocardial energy metabolism.

DETERMINATION OF MYOCARDIAL GLUCOSE METABOLIC RATE (MRGlc) BY POSITRON COMPUTED TOMOGRAPHY (PCT) AND FLUORO-18 DEOXYGLUCOSE (FDG). O. Ratib, M.E. Phelps, S.C. Huang, E. Henze, C. Selin, H.R. Schelbert. UCLA School of Medicine, Los Angeles CA.

The determination of the MRGlc by PCT imaging, using FDG and a three compartment model has previously been validated in the brain. However, data obtained from myocardial PCT images require correction for an object size related underestimation of indicator tissue concentrations and for a cross contamination of activity between blood pool (BP) and myocardium. We performed kinetic studies in 6 open chest dogs, with serial gated PCT imaging and by rapid sampling of arterial and coronary sinus blood. Myocardial blood flow was measured by the microsphere technique, and myocardial glucose, lactate and free fatty acid (FFA) consumption determined using the Fick principle. The myocardial wall thickness was measured by in vivo echocardiography and post mortem. The amount of contamination between myocardium and BP was estimated from PCT images obtained prior to FDG injection with O-15 CO labeled red blood cells. FDG tissue concentrations were determined from cumulative arterio-venous differences and from the corrected PCT images. The rate constants k_1 to k_4 of our model and the lumped constant (LC) were estimated by a least square fitting of the tissue curves. The rate constant "K" for transport and phosphorylation of FDG is equal to $k_1 \cdot k_3/(k_2+k_3)$. The mean LC was 0.88±.28. MRGlc derived with our model correlated to that by the Fick method by r=0.81. However, unlike the brain, the normal myocardial MRGlc showed high variations (mean 9.7±7.8 mg/min/100gm) due to the capability of the myocardium to utilize the alternative substrates of FFA and lactic acid. We conclude that accurate measurement of local MRGlc is possible provided gated acquisition is employed and appropriate corrections for wall thickness and for cross contamination between BP and myocardium are made.

THALLIUM STUDIES USING SINGLE PHOTON EMISSION COMPUTED TOMOGRAPHY (SPECT). R.E. Coleman, F.R. Cobb, R.J. Jaszczak. Duke University Medical Center, Durham, NC.

Animal studies have demonstrated that the early distribution of thallium-201 has a very good correlation with coronary blood flow determined by the microsphere technique. Thus, a method of accurately determining thallium-201 distribution should reflect relative coronary blood flow. SPECT has the ability to remove activity in front of and behind the area of interest and thus should offer advantages in determing thallium-201 distribution. The purpose of this study was to determine the effects of 180 degree (RAO to LPO) versus 360 degree data collection on rms noise and ventricle contrast since the area of interest (heart) is anterior in the left chest.

Phantom studies used a 10cm diameter cylinder with a 1cm ring (heart) which contained activity in ratios of 6:3:0:1 representing normal myocardium: ischemic myocardium: infarcted myocardium: background. Increased image contrast was observed for the 180 degree data collection as compared to the 360 degree data collection.

We have compared the effects of the 180 versus 360 degree data collection on 8 patient studies. Using our filtered backprojection algorithm, there are artifacts of reconstruction with the 180 degree sampling since the total object is not reconstructed, but there is no appreciable difference in the ventricular image. The rms noise over the same region of interest is larger for the 180 than the 360 degree collections.

Our SPECT system is a dual LFOV system, permitting simultaneous 180 and 360 degree collection. Reconstruction of either set of data is then possible.

TRANSAXIAL COMPUTED TOMOGRAPHY WITH ^{201}TL IN PATIENTS WITh PRIOR MYOCARDIAL INFARCTION. J.L. Ritchie, D.O. Olson, D.L. Williams, G. Harp, J.H. Caldwell, and G.W. Hamilton. Veterans Administration Medical Center, Seattle, Wa.

Eighteen patients with prior MI diagnosed on clinical grounds (ECG Q wave, history and/or enzymes) had planar imaging with ^{201}Tl at rest. Transaxial emission computed tomography employing a rotating gamma camera over 180° (64 collection angles) was also performed with no attenuation correction. Transaxial (standard body CT format) planes were reconstructed in 6mm increments from 128x128 projection images by filtered back projection. This volumetric data set was then rotated in 3 dimensions to realign the display axes to coincide with the major cardiac axes. Thus, serial slices from: 1) base to apex; 2) slices perpendicular to the septum along the long axis; and 3) slices parallel to the septum along the long axis were calculated and displayed for each patient (cardiac axial series). All images in this preliminary report were interpreted qualitatively.

Overall, 11 of 18 patients had perfusion defects in the planar images. In the transaxial or body CT format, defects were identified in 11/18 patients. In the realigned cardiac axial series, perfusion defects were identified in all 18 patients. Often, infero-apical defects were not contiguous with any normal myocardium in the body CT format and were thus not identified. Additionally, the geometric extent or number of slices in which the defect was seen was easily determined in the cardiac axial perspectives (Figure 2).

We conclude that transaxial tomography with realignment along the cardiac axes will improve defect detection for ^{201}Tl imaging.

ROTATING GAMMA CAMERA ECT OF TL-201 IN THE HUMAN HEART. M.C. Besozzi, H.R. Rizi, W.L. Rogers, N. Clinthorne, B. Pitt, J.H. Thrall, J.W. Keyes, Jr. The University of Michigan Medical Center, Ann Arbor, MI.

This study was undertaken to develop a clinical imaging technique for rotating gamma camera Tl-201 myocardial tomography and to establish standards for data analysis. Eleven volunteers and 42 patients with known coronary artery disease (CAD) received 2.0 mCi Tl-201 at peak treadmill exercise with imaging at 10 min. and 2 hr. using a G.E. 400T and high sensitivity collimator. Established acquisition parameters include: 32 equally spaced images over a 180° arc from RAO to LPO, 64 x 64 matrix, 30 sec/image for total counts of 2500K/study. Ten transaxial, 8 oblique (right angles to long axis of heart) and 8 rotated sagittal (parallel to long axis of heart) planes were reconstructed for each case. The oblique planes were quantitatively analyzed using circumferential profiles. Normal visual and quantitative distribution patterns were defined in the 11 volunteers. This tomographic technique with multiplane reformatting provides better anatomic definition than previous techniques by presenting full transmural views of all portions of the myocardium. In particular, the location of the apex and valve planes were unambiguously depicted in all cases. Post exercise and redistribution circumferential profiles were closely parallel with a maximum divergence during redistribution of 20% in the normals. Conclusion: with suitable acquisition parameters, tomography with a rotating gamma camera is clinically feasible. The technique, including multiplane reformatting, provides good definition of myocardial structure and the oblique planes appear well suited to currently available schemes for quantitation.

TL-201 TRANSAXIAL ECT: IN VIVO QUANTIFICATION OF MYOCARDIAL ISCHEMIA IN DOGS. H.R. Rizi, S. Pasyk, V.B. Fiedler, K.W. Mori, B. Lucchesi, B. Pitt, J.W. Keyes, Jr. University of Michigan Medical Center, Ann Arbor, MI.

There is need for a method to accurately quantify myocardial ischemia. Planar imaging gives good results for anterior lesions but poor results for inferior lesions. We have studied the quantitative accuracy of Tl-201 transaxial ECT for inferior wall myocardial ischemia. Distal left circumflex coronary artery was ligated in 10 dogs following a left thoracotomy. Three uninfarcted dogs were also studied. Ungated, in vivo Tl-201 imaging was performed in all dogs using a rotating camera tomograph and 2-3 mCi Tl-201. After imaging the dogs were killed and the hearts sectioned and differentially stained to define the ischemia area. Transaxial tomograms were reconstructed and the data reorganized to yield tomograms oriented perpendicular to the long axis of the left ventricle. Good quality tomograms were obtained in all dogs. The ischemic zone and the total left ventricle were measured by planimetry on both the tomographic and histologic sections. The percentage of the left ventricle that was ischemic was calculated. The results are summarized in the following table.

	Range %	Mean %	SD %
Tomo	0-45	25.15	17.7
Histo	0-53	25.69	17.9

The correlation found between tomographic and histologic measurements of extent of myocardial ischemia was: r = 0.90 (n = 13, y = 2.29+0.89 X). We conclude: 1) Good quality in vivo Tl-201 transaxial ECT is feasible; 2) Tomograms that are perpendicular to the long axis of the left ventricle are best for measurement of inferior wall ischemia; 3) Accurate quantification of inferior myocardial ischemia is feasible over a wide range of ischemic zone size.

1:30-3:30 **ROOM D-1**

RADIOPHARMACEUTICALS I: GENERAL

Moderator: Powell Richards
Co-moderator: Vincent J. Sodd

A NEW RADIOIODIDE EXCHANGE TECHNIQUE: THE MW2 METHOD. T.J. Mangner, J.L. Wu, D.M. Wieland and W.H. Beierwaltes. University of Michigan Medical Center, Ann Arbor, MI.

No general technique is available for the exchange labeling of aromatic iodides possessing neither strong electron-donating nor electron-withdrawing substituents. The melt method is applicable only to chemically activated compounds, is dependent on the vagaries of substrate melting point, and is generally inadequate for the production of compounds with high specific activities. We report here a general exchange method which entails a solid phase reaction of iodoaromatics with radioiodine.

Typically, 0.2-2.0 mg of substrate, 5-20 mCi of NaI-125, and 2-4 mg of ammonium sulfate are dissolved in water or alcohol, the solvent removed by heating, and the mixture heated at 120-160°C (below the melting point of the substrate) for 1-4 h. Isolated radiochemical yields of 40-98% have been obtained with 15 different iodoaromatics including various aralkyl amines, guanidines and amino acids. Specific activities of up to 150 mCi/mg have been achieved.

The function of the ammonium sulfate is to cause a gradual increase in the acidity of the exchange medium via in situ decomposition with resulting loss of ammonia. Sulfuric acid can be successfully substituted for ammonium sulfate to promote the exchange.

The mechanism of the exchange is likely an electrophilic process involving a higher oxidation state of the radioiodide: 1) The reaction proceeds in acidic media, 2) The exchange fails in the presence of reducing acids (e.g. oxalic), 3) A significant loss of volatile (molecular) radioiodine is observed when the reaction is carried out under a steady nitrogen flow.

Additional studies probing the mechanism and scope of this exchange reaction are in progress.

RADIOIODINATED FRAGMENT E1: A POTENTIAL THROMBUS-LOCALIZING RADIOPHARMACEUTICAL. L.C.Knight, S.A. Olexa, A.Z.Budzynski and L.S.Malmud. Thrombosis Research Center and Department of Nuclear Medicine, Temple University, Philadelphia, PA.

Fragment E1, derived from the plasmin digestion of crosslinked fibrin,is a dimeric molecule containing a pair of binding sites which are complementary to paired binding sites on linear polymers of fibrin. Fragment E1 does not bind to fibrinogen or to single fibrin monomer molecules, but only to aligned fibrin monomers in a fibrin strand. This specificity for the major constituent of venous thrombi makes Fragment E1 an ideal candidate for development as an agent for thrombus detection in vivo.

Fragment E1 was labeled with I-131 or I-123 by the Iodogen technique. The labeled material had the same electrophoretic mobility on polyacrylamide gels as the unlabeled Fragment E1, and it was incorporated into forming and preformed plasma clots in vitro (72% and 14% uptake, respectively). Labeled Fragment E1 was injected into pigs with pre-existing thrombi. Usually, I-125-fibrinogen was injected simultaneously as a control. The thrombi, induced in the jugular veins by a local electric current, were 1 to 120 hours old at the time of injection. Thrombi and blood samples were removed 24 hours post injection.

Radioiodinated Fragment E1 localized substantially in thrombi of all ages tested. Thrombus:Blood (T:B) ratios (cpm/g thrombus ÷ cpm/g blood) as high as 108 were obtained and the mean T:B ratio was 47 ± 34 in thrombi 2 to 5 days old. As expected, I-125-fibrinogen did not localize well in aged thrombi (the mean T:B ratio was 2 ± 1 in thrombi ≥ 20 hours old). These results suggest that radiolabeled Fragment E1 is an excellent tracer for detection of both fresh and aged thrombi in vivo.

BRAIN IMAGING WITH I-123 LABELED DIAMINES: A KIT PREPARATION SUITABLE FOR ROUTINE CLINICAL USE. K.M. Tramposch, H.F. Kung and M. Blau. State University of New York at Buffalo and V.A. Medical Center, Buffalo, N.Y.

As part of a continuing program to develop practical single-photon brain imaging agents, a novel series of radioiodine labeled diamines was synthesized and evaluated.

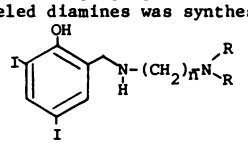

These compounds were synthesized by treating 4,6 -diiodosalicylaldehyde with the appropriate amine followed by reduction of the intermediate schiff base with sodium borohydride. The compounds were labeled with either I-125 or I-123 in greater than 95% radiochemical yield by a rapid (15 min, 100°) aqueous exchange reaction which is amenable to kit preparation. The partition coefficients (n-octanol: buffer pH 7.4 and pH 7.0), serum protein binding and biodistribution in rats were studied. The brain uptake in rats at 2 minutes after iv injection ranged up to 2.8% dose/organ.

Two I-123 labeled diamines were studied in monkeys. Compound 1 (n=3, R=Me) showed very fast brain uptake (complete at 2 min) and no clearance of brain activity over the 30 minute imaging procedure. Compound 2 (n=2, R=Me) showed higher initial brain uptake and 75% of the initial activity remained at 1 hour.

These I-123 labeled diamines would be useful as brain imaging agents for routine clinical use in conjunction with single-photon tomographic devices.

SYNTHESIS OF RADIOTRACERS FOR IN VIVO MAPPING AND QUANTIFICATION OF DOPAMINE RECEPTORS. E.G. Corley, H.D. Burns, J.J. Frost, T. Duelfer, M.J. Kuhar, and H.N. Wagner, Jr. Johns Hopkins Medical Institutions, Baltimore, MD.

Autoradiographic studies in animals have demonstrated that tritiated neuroleptic drugs such as spiperone localize selectively in tissues which have high concentrations of dopamine receptors. Drugs of this type, if labeled with positron or gamma emitting radionuclides, may be useful for the non-invasive, in vivo study of these receptors in man. An essential step in this project was to develop rapid, high yield syntheses of F-18 and C-11 labeled drugs such as spiperone and benperidol as well as I-123 labeled analogs of these neuroleptic drugs. F-18 labeled benperidol and an I-123 labeled analog of benperidol have been prepared at high specific activity via the Wallach reaction. These compounds were prepared rapidly by methanesulfonic acid decomposition of the appropriate triazene in the presence of no-carrier-added radionuclides (CsF-18 or NaI-123). Both the F-18 and I-123 labeled compounds were prepared in bromobenzene. However, higher yields of the I-123 labeled compound were obtained when tetrahydrofuran was used as the solvent. Reverse phase HPLC purification was required for both compounds to remove by-products formed in the reaction which compete with the radiotracer for receptor binding. Preliminary biodistribution studies in mice suggest that F-18 labeled benperidol preferentially accumulates in the caudate nucleus, a region of the brain which is rich in dopamine receptors. (We thank Drs. M. Ter-Pogossian and M. Welch of Washington University, St. Louis, Missouri, for kindly supplying the F-18.)

NEW BRAIN IMAGING AGENTS: Se-75 (*Se) AND Te-123*m* (*Te)-LABELED BARBITURATES. R. A. Grigsby**, F. F. Knapp, Jr., A. P. Callahan, L. A. Ferren and K. J. Irgolic**, Nuclear Medicine Technology Group, Oak Ridge National Laboratory (ORNL), and **Chemistry Department, Texas A&M University, College Station, TX.

Barbiturates are lipophilic drugs that freely cross the intact blood-brain barrier. In order to assess the potential use of barbiturates radiolabeled with gamma-emitting radionuclides, several *Se and *Te labeled barbiturates were prepared by coupling selenols or tellurols with 5-alkyl-5-(ω-bromoalkyl) diethylmalonates. The barbiturates, prepared by ring closure with urea-t-BuOK in DMSO, were purified on SiO_2 columns. The TLC, UV, IR, low and high resolution MS and NMR properties were consistent with the proposed structures. The *Se and *Te-labeled barbiturates were prepared similarly, and after column purification were administered to female Fischer 344 rats. Pronounced brain uptake was observed after 5 min indicating that the structurally modified barbiturates freely pass through the intact blood-brain barrier. These results suggest that radiolabeled barbiturates may be a potentially useful class of new agents to monitor regional cerebral blood flow.

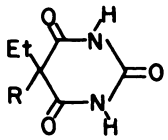

R	Range, 3 rats, % dose/gm
ϕ-*Se-Butyl	0.71-0.95
Butyl-*Se-Propyl	0.78-0.85
ϕ-*Te-Butyl	0.88-1.00
Butyl-*Te-Propyl	0.44-0.49

ORNL is operated by Union Carbide Corporation under contract W-7405-eng-26 with the U.S. Department of Energy.

LIPOPHILIC CHELATES OF TECHNETIUM-99m:TROPOLONE. L.A. Spitznagle, C.A. Marino and S. Kasina, Departments of Medicinal Chemistry/Pharmacognosy and Radiology, University of Maryland at Baltimore, Baltimore, MD

The design of radiopharmaceuticals labeled with technetium-99m has been limited by the small number of ligands which will form neutral chelates with technetium-99m. A literature search revealed that the compound, 2-hydroxy-2,4,6-cycloheptatrienone (tropolone) formed lipophilic chelates. The lipophilicity togther with its chelating properties led us to study the binding of tropolone with technetium-99m. The general procedure for the preparation of the chelate involved the reduction of Tc-99m-pertechnetate with stannous chloride in the presence of tropolone and extraction of the neutral chelate into chloroform. Radiochemical yields of the chelate were 90-95%. The radiochemical purity of the neutral chelate as determined by HPLC was greater than 95%. Incubation of the labeled chelate with rat blood resulted in binding to the RBC (55%) and to plasma proteins (22%), while incubation of the chelate with washed RBC's resulted in 73% binding. Likewise, incubation of the labeled chelate with solutions of human serum albumin or rat plasma proteins resulted in protein binding of 60% and 65%, respectively. Whole body distribution studies of the labeled chelate were carried out in rats. The results of these studies and their implications on the design of future radiopharmaceuticals will be discussed.

This investigation was supported by Grant #HL 18744, National Heart, Lung and Blood Institute, and Grant #CA 28561, National Cancer Insitite, DHEW.

SPECIFIC RECEPTOR LABELING *IN VIVO* WITH C-11 SPIROPERIDOL. C.D. Arnett, A.M. Findley, A.P. Wolf, J.S. Fowler, and R.R. MacGregor, Brookhaven National Laboratory, Upton, NY.

An important consideration in the use of positron-emitting radiopharmaceuticals for *in vivo* labeling of neurotransmitter receptors is the proportion of receptor-bound to free and non-receptor bound activity in the live animal. To evaluate this relationship we have studied the time course of specific binding of C-11 spiroperidol, a dopamine receptor antagonist, in mouse brain. Mice were pretreated with (-)- or (+)-butaclamol to assess total and non-specifically bound activity, respectively, and then killed at various times up to 60 min after intravenous injection of C-11 spiroperidol. A crude particulate-bound activity (PBA) fraction of cerebral cortex or cerebellum was isolated by rapid filtration and washing of the tissue homogenate. There was no difference in cerebellum PBA between (-)- and (+)-butaclamol pretreated animals. However, in the (-)-butaclamol controls the ratio of PBA in the cortex to that in the cerebellum increased to about four fold at 30 min. Since dopamine receptors are present in the mouse cerebral cortex but not in the cerebellum, we interpret these results to indicate that specific receptor labeling can be achieved with C-11 spiroperidol with an *in vivo* time course which is reasonable for positron emission transaxial tomographic studies.

We thank Ayerst Laboratories for making butaclamol available to us.

ON THE SYNTHESIS OF FLUORINE-18 LABELED SPIROPERIDOL: MECHANISTIC STUDIES. H. Ku and J.R. Barrio. UCLA School of Medicine, Los Angeles, CA.

There is considerable interest in the mapping and evaluation of neuroreceptors by the use of positron emission tomography. In this regard the synthesis of F-18 labeled spiroperidol and related neuroleptics have recently received increasing attention. As part of our efforts on the synthesis of fluoro compounds of medicinal interest, p-(3,3-dialkyl-1-triazeno) analogs of spiroperidol, acetophenone and other models have been prepared and thoroughly characterized. Their sensitivity to substitution with F-18 fluoride and several other nucleophiles have also been tested under a large variety of conditions (solvents, acids, temperature). For example refluxing p-(3,3-dialkyl-1-triazeno)acetophenone in THF containing methanesulfonic acid and F-18 cesium fluoride for 30 minutes gave acetophenone as the major product and all attempts to detect fluoro aromatic compounds in the reaction mixture failed. An intermolecular hydrogen abstraction mechanism is postulated for this reaction. However, use of aprotic solvents (e.g. CCl_4) favored nucleophilic substitution and allowed a smooth transformation to F-18 p-fluoroacetophenone. Acetophenone was not observed. This result indicates that CCl_4 effectively inhibited the free radical chain reactions, and prevented the formation of unwanted protodediazotization products. The effect of para-substituents on the aromatic dialkyl triazenes toward nucleophilic substitution with F-18 fluoride vs radical hydrogen substitution as well as the application of this reaction to the synthesis of F-18-spiroperidol will be discussed.

1:30-3:30 **ROOM G-1**

COMPUTER AND DATE PROCESSING I: GENERAL

Moderator: Nathaniel Alpert
Co-moderator: C. Leon Partain

THE USE OF THE TEMPORAL HADAMARD TRANSFORM FOR EFFICIENT DATA COMPRESSION DURING IMAGE ACQUISITION AND PROCESSING. F. Deconinck, A. Bossuyt, R. Lepoudre, M. Jonckheer. A.Z. - V.U.B., Laarbeeklaan 101, 1090 Brussels, BELGIUM.

This paper discusses an image acquisition and processing technique that provides efficient and relevant data compression for dynamic isotope studies. Data compression techniques to which functional imaging techniques belong optimize the information density in the data set according to particular criteria which are choosen to favor information which is most relevant in a particular application (e.g. Fourier amplitude of change vs. activity in equilibrium gated nuclear angiography (EGNA)). The Fourier transform which uses sine and cosine basis functions is hard to implement on a real time basis. We propose the use of the temporal Hadamard transform in which the basis functions are square waves. The convolution of the temporal data with the basis functions can be performed during the acquisition as only additions and substractions are required. When 64 k-byte memory is available, different acquisition options for EGNA are 1 x (256 x 256), 4 x (128 x 128), 16 x (64 x 64)... images per heart cycle. In those applications where the temporal information carried by the first harmonic is satis - factory, only 4 images are required to calculate the first harmonic amplitude and phase on a pixel to pixel basis. In

this case high spatial resolution images can be acquired. In EGNA this is essential when tomography by means of a 7-pinhole collimator is performed. In standard imaging it is of great use when edge detection is required. An integrated data acquisition and processing technique that provides efficient and relevant data compression such as the temporal Hadamard transform, can allow smaller digital imaging systems to handle sophisticated functional imaging procedures.

OBLIQUE ANGLE TOMOGRAPHY-A RESTRUCTURING ALGORITHM FOR TRANSAXIAL TOMOGRAPHIC DATA. J.H. Borrello, N.H. Clinthorne, W.L. Rogers, J.H. Thrall, and J.W. Keyes, Jr. University of Michigan Medical Center, Ann Arbor, MI

A set of contiguous transaxial tomograms obtained with a rotating camera tomograph represents the full three-dimensional distribution of activity within a volume of the body. Tomographic sections in any orientation can be produced from such data by resorting the data appropriately. Such restructured tomograms can be particularly useful for studying the heart because the images can be tailored to the individual patient's anatomy. A simple and efficient algorithm was developed for producing tomograms of the heart oriented at either right angles or parallel to the long axis of the left ventricle. The relative rotation of the ventricular axis to the left (horizontal angle) and downward (vertical angle) are determined with an interactive display program. A correction for the horizontal angle is introduced during reconstruction of the transverse sections and the vertical angle is compensated for during the restructuring step using an interpolation algorithm. For a typical Tl-201 study, the program will produce 29 rotated sagittal and 34 oblique angle tomograms in 5 minutes. The program has produced good quality studies in over 70 consecutive patients. The reoriented tomograms have specific advantages for imaging the heart and are free of some of the limitations seen in tomograms obtained by limited angle tomography.

SOFTWARE RELIABILITY: EDGE DETECTION ALGORITHMS. P.T. Cahill, R.J.R. Knowles, and O. Tsen. The New York Hospital-Cornell Medical Center, Polytechnic Institute of New York, and The Long Island College Hospital, New York,NY

A comprehensive approach to the evaluation of eleven edge detection algorithms was developed: (a) the nature of nuclear medicine images and borders were determined; (b) evaluative criteria relevant to nuclear medicine applications were evolved, and (c) simulated and experimental phantoms that correspond to the essential features of clinical cardiac and renal images were constructed. Criteria used for evaluation of edge detection algorithms were accuracy of area delineation, ROC analysis, and shape preservation. Studies were performed using simulated phantoms, experimentally measured phantoms and three types of clinical images over a range of information densities (ID). In these studies, adaptive and nonadaptive second step thresholding (10 values) was performed.

Results of these studies revealed that the accuracy of area delineation was the most critical parameter and that ROC and shape analysis were considerably less sensitive. For low ID images, only the totally adaptive nearest neighbor algorithm met area, ROC and shape criteria over a wide range of threshold values. The use of adaptive thresholding proved essential in avoiding excessive high false positive rates for medium and high ID images. With adaptive filtering the Kirsch and Sobel algorithms provide satisfactory results at ID's considerably higher than encountered in clinical images.

Our results represent the initial phase of a systematic validation of software performance under the image conditions unique to nuclear medicine.

QUANTITATIVE DIGITAL AUTORADIOGRAPHY BY VIDEODENSITOMETRY. Y. Yonekura, M. Meyer, A. B. Brill, P. Som, H. Lee, J. A. G. Russell, and G. W. Bennett. Medical Department, Brookhaven National Laboratory, Upton, NY.

Macroautoradiography (M-ARG) has played and will play an important role in the development of knowledge ranging from establishing the anatomical localization of radiolabelled drugs to increased understanding of biochemical mechanisms underlying different pathophysiological processes. New tissue sectioning equipment permits the preparation of whole body-ARGs. Simple, relatively low cost equipment is now available, which when added to a conventional minicomputer system makes it possible to do quantitative ARG, based on the measured optical density in each region.

Digital images of the ARG are obtained using a video camera equipped with a zoom lens, and stored in a disk storage system. Digitized sampling provides 256x256, 512x512, or 1024x1024 arrays. Therefore, a 1 cm^2 image can be digitized and analyzed for 80, 40, or 20 μ^2 elements in the sample with 256 grey levels. Several standard samples with serial dilution of the radioactivity are also digitized to make a standard curve. The number of each pixel in the digital image is converted to the value of the radioactivity according to the standard curve. Attenuating films between the ARG film and the sample permit dual isotope analysis using digital image subtraction. Triple isotope analysis can be accomplished using short half-life high energy positron emitters along with C-14 and H-3 labelled compounds. These digital images are displayed as color-coded images, which assist in recognition of anatomical correlations and facilitate selection of regions of interest, or as 3-dimensional plots of the light intensities.

A MONTE CARLO STUDY OF THE FLUORESCENT EXCITATION OF I-127. F.B. Atkins, R.N. Beck and D.B. Charleston. Walter Reed Army Medical Center, Washington, D.C. and the Franklin McLean Memorial Research Institute, Univ of Chicago, Il.

Quantitative elemental analysis by the use of stimulated fluorescent x-rays has a number of medical applications; in particular, imaging the relative and absolute concentration of stable iodine in the thyroid. However, little work has been done on the analysis and optimization of fluorescence techniques in the area of imaging.

To investigate the fundamental components which affect spatial resolution and quantitation, we have developed Monte Carlo computer codes to simulate this process. This permits an analysis of aspects of the excitation process which are not readily accessible experimentally, e.g., the spatial distribution of the sites of x-ray stimulation within the medium. Using these methods, we have investigated the effects of excitation energy, organ depth, and scatter. The fluorescent yield demonstrates that lower energy photons (40-45keV) are more efficient (about a factor of 2 at 2cm depth) than the γ-rays from Am-241.

A significant component of the fluorescent yield is due to photons scattered from the excitation beam, but which can still produce x-rays. The ratio of scatter to primary increases with increasing source energy and iodine depth, being about 83% at 60keV compared to 59% at 45keV at a 2cm depth. The function defined as the relative number of such fluorescent sites within annular regions about the beam axis has FWHM values of about 3-5cm with very broad tails. In optimizing the excitation energy, we can consider the detection of the K_α x-rays superimposed on a continuous spectrum. Using this criterion, the SNR is maximum around 45keV at depths <2cm, and is relatively constant from 45-70keV at 4cm depth.

EFFECT OF VALVULAR REGURGITATION AND REGION OF INTEREST SELECTION ON FIRST-PASS CARDIAC OUTPUT DETERMINATIONS. E.C. Glass, H.A.Cohen, H.H.Hines. Saint John's Hospital & Health Center, Santa Monica, CA and University of California, Davis

Indicator dilution theory suggests that time-activity curves derived from any portion of the central circulation through which the entire cardiac output passes should yield identical cardiac output (CO) values in the absence of shunts. This assumption was tested in 30 patients (pts) using first-pass left anterior oblique radionuclide angiography. All pts also underwent gated blood pool imaging and contrast ventriculography: 15 showed aortic or mitral regurgitation (REG) and 15 did not. First-pass Stewart-Hamilton CO were calculated from three regions of interest (ROI): right heart, left heart, and whole heart. Systematic differences resulted among CO determined from different ROI ($p<.001$), seemingly due to differences in apparent washout rates in ROI (Table: CO as mean ± SD in liters/minute).

ROI	ALL pts (n=30)	REG (n=15)	No REG (n-15)
Right heart	6.1 ± 1.7	6.3 ± 2.0	5.9 ± 1.4
Left heart	5.3 ± 1.6	5.1 ± 1.8	5.6 ± 1.3
Whole heart	5.1 ± 1.4	5.0 ± 1.6	5.2 ± 1.2

Differences between right and left heart CO values were greater in pts with REG (mean difference 21 ± 10%) than in pts without REG (mean difference 7 ± 4%), p<.001. Furthermore, differences between right and left first-pass CO more accurately predicted the presence or absence of REG than did differences in gated right and left ventricular stroke counts (93% vs. 77% accuracy, respectively, p<.05).

Therefore, (1) valvular REG and ROI selection significantly affect first-pass CO measurements, and (2) comparisons of first-pass CO from right and left heart ROI have proven useful in clinically assessing mitral or aortic regurgitation.

SHORT ACQUISITION TIME RADIONUCLIDE ANGIOGRAPHY FOR CALCULATION OF LEFT VENTRICULAR EJECTION FRACTION: COMPARISON WITH STANDARD ACQUISITION TIMES. G.B. Trobaugh, D.L. Williams, S.D. Hartnett, G.D. Harp, R.C. Tutt, K. Namey, Harborview Medical Center, Seattle, WA.

Although most equilibrium radionuclide angiographic studies performed at rest are acquired for about 5 minutes, shorter acquisitions would be valuable during changing events, or could also permit higher resolution collimation, lower radionuclide dosage, or both. We compared the left ventricular (LV) ejection fraction (EF) in 24 patients (pts) calculated from an acquisition of 225K/.04 sec frame (our standard study) to serial acquisitions of 2 min, 1 min, 30 sec, 15 sec, 7 sec and a second 225 K study. The patient's own red blood cells were labelled with 25 mCi of Tc-99m. Studies were acquired in the 45° LAO position by a gamma camera with all-purpose collimation into a minicomputer as a 64x64 array. The studies were processed as follows: (1) noise smoothing and subsequent resolution recovery (RR) by a stationary cylindrical filter, (2) isolation of the left ventricle by an interpolative background technique with threshhold edge detection of the LV and (3) automatic background selection beneath the LV. The regions of interest calculated from the RR images were applied to the corresponding background corrected raw images.

Correlation of LVEF derived from the first 225 K image vs. each of the following:

	Second 225 K	2 Min	1 Min	30 Sec	15 Sec	7 Sec
r =	.981	.978	.959	.963	.898	.804
Sy.x =	.037	.042	.052	.048	.080	.117

We conclude that appropriate image processing of acquisitions of 30 sec or more prior to calculation of LVEF can be clinically satisfactory. In special circumstances, even shorter acquisitions may be appropriate.

GATED BLOOD POOL IMAGING IN PATIENTS WITH ATRIAL FIBRILLATION. D.D. Watson, E.M. Leidholdt, B.A. Carabello, M.E. Read, C.D. Teates, and G.A. Beller, University of Virginia Medical Center, Charlottesville, VA.

Atrial fibrillation is a common problem which interferes with conventional R-wave gated blood pool imaging. This study investigated the variations in systolic time intervals in patients with atrial fibrillation (AF). The interval from R-wave peak to end-systole (R-S) was measured from aortic pressure tracings obtained during catheterization with chart speeds of 100 mm/sec. Thirteen patients were studied and 307 cardiac cycles analyzed. The average R-R interval for all patients was 774 ± 155 msec. The average R-S interval was 354 ± 15 msec. There was no correlation between current R-R and R-S but R-S intervals were slightly dependent on the previous R-R interval with average regression slope = 0.074 indicating 7.4 msec shift in R-S per 100 msec shift in previous R-R. The average scatter in R-S (SD = 15 msec) was much less than R-R (SD = 155 msec). The maximum error in average left ventricular ejection fraction caused specifically by gate synchronization errors at end-systole was calculated to be 0.75% based on 20 frames per cardiac cycle and using constant preset frame intervals. We conclude: 1) The interval of electromechanical systole is relatively stable in patients with AF. 2) The systolic ejection phase of the cardiac cycle and the average ejection fraction (but not the diastolic phase) can be adequately determined by conventional gating. 3) In patients with AF, gate intervals should be constant and not dependent on the R-R interval.

1:30-3:30 **ROOM A-1**

SYMPOSIUM: MARTIN REIVICH AND SELECT NEUROLOGY PAPERS

Moderator: Abass Alavi
Co-moderator: Martin Reivich

INVITED SPEAKER

Martin Reivich, Cerebral Vascular Research Institute, University of Pennsylvania Medical School, Philadelphia, PA. THE FDG METHOD: PHYSIOLOGIC AND CLINICAL STUDIES.

LOCAL CEREBRAL GLUCOSE METABOLISM IN HUNTINGTON'S DISEASE DETERMINED BY EMISSION COMPUTED TOMOGRAPHY OF ^{18}F-FLUORO-DEOXYGLUCOSE. D.E. Kuhl, C.H. Markham, M.E. Phelps, J. Winter, J. Metter. UCLA School of Medicine, Los Angeles, California 90024

Previously we demonstrated that local cerebral metabolism determined by the ^{18}F-fluorodeoxyglucose (FDG) scan was a more sensitive indicator of local cerebral dysfunction than was the associated structural alteration determined by CT in both stroke and epilepsy. To learn if this were true also in Huntington's Disease (HD), we studied 13 HD patients ranging in age from 28-71 years who had disease durations from one year-15 years. We performed ECAT positron tomography using FDG and measured local cerebral glucose utilization ($LCMR_{glc}$) for major grey and white matter structures. Using CT scans, we determined the extent of caudate, central and cortical atrophy. These results were then compared to those from age-matched controls.

Severity of choreoathetosis and dementia correlated with duration of illness, but not with global or regional glucose utilization. The most severely demented patients had marked cortical and central atrophy, but some individuals with the worst atrophy had the least dementia. Not all patients had caudate atrophy; when present, striatal atrophy was greater in those with longer disease durations. But all patients had profound striatal hypometabolism, and three patients with early disease had little or no evidence of striatal atrophy. Finding demonstrable hypometabolism in striatum of normal or near normal bulk suggests that an alteration in metabolism precedes cell loss. We will test subjects at risk for HD to learn if demonstrable striatal hypometabolism precedes symptoms.

BLOOD BRAIN BARRIER PERMEABILITY AND INTRAVASCULAR FLOW-VOLUME MEASUREMENTS USING RUBIDIUM-82 AND DYNAMIC POSITRON EMISSION TOMOGRAPHY. T.F. Budinger, C.-K. Yen, Y. Yano, R.P. Friedland, and H.A. O'Brien, Jr.* Donner Laboratory, University of California, Berkeley, CA, and Los Alamos Scientific Laboratories*, Los Alamos, NM.

Rubidium does not normally pass the blood brain barrier and in the form of Rb-86 chloride has been used to measure changes in blood brain barrier permeability in in vitro studies. Rubidium-82 ($T_{\frac{1}{2}}$=75 sec) produced from a portable generator was used with the Donner 280-crystal positron tomograph to study brain blood volume, regional permeability changes associated with blood brain barrier disruption, and blood flow in normal subjects, patients with brain tumors, and patients with arterio-venous malformations. These studies followed dog and monkey experiments using purposeful blood brain barrier disruption with intracarotid infusion of urea. Both i.v. bolus and constant infusion techniques were used with a maximum dose of 60 mCi which gives a whole body absorbed dose of 0.07 rad and a dose to the kidney of 4.3 rads. Constant infusion was used to show blood volume changes associated with stimulation of the motor cortex. With an injected dose of 20 mCi or less, blood brain barrier disruption near tumors can be detected with a signal-to-noise greater than that noted on contrast enhanced x-ray CT studies. With a simple bolus infusion

and dynamic PET imaging, arterial and venous phases of the cerebral circulation are easily discerned.

The past emphasis on the use of Rb-82 has been directed toward heart and kidney studies. It is shown in these studies that this readily available positron emitter can also be used for the efficient detection of tumors and evaluation of blood brain barrier permeability.

MAPPING LOCAL CEREBRAL BLOOD FLOW BY MEANS OF EMISSION COMPUTED TOMOGRAPHY OF N-ISOPROPYL-p (^{123}I)-IODOAMPHETAMINE (IMP). D.E. Kuhl, J.L. Wu*, T.H. Lin*, C. Selin, and M. Phelps. UCLA School of Medicine, Los Angeles, California 90024 and *Medi-Physics, Inc., Emeryville, California 94608.

Winchell et al have proposed that the initial cerebral distribution of IMP may be useful for imaging relative regional brain perfusion. Since the physical properties of ^{123}I are favorable for single-photon emission computed tomography (ECT), we explored using IMP for determination of local cerebral blood flow (LCBF).

Increases and decreases of LCBF were induced in dog brains. Labeled microspheres were injected into the left atrium simultaneous with intravenous injection of IMP during constant rate sampling from an artery. LCBF, (ml/100g/min), was calculated as the arterial sampling flow times the ratio of brain sample to arterial blood sample activity. At 5 min after injection, there was good agreement between LCBF values based on IMP and those based on microspheres, but this relationship deteriorated at high flow values; microsphere determined flow increases of 100% and 500% were associated with IMP determined flow increases of only 74% and 280%, respectively.

The same method for determining LCBF was applied to human subjects, but local brain IMP activity was determined by Mark IV, a single-photon detecting tomograph, rather than by sample counting. Images resembled those of $^{13}NH_3$ and ^{18}FDG obtained by positron ECT. There was a 40% increase in brain activity between 5 min and one hour after injection, and during this time good distinction was maintained between gray and white matter. Gray matter LCBF values were in a normal range when one considered the contrast loss associated with spatial resolution. These studies suggest that IMP should be further investigated as an LCBF indicator compatible with single-photon ECT, a combination that could serve as an alternative to positron ECT.

0-15 WATER CLEARANCE METHOD FOR MEASUREMENT OF LOCAL CEREBRAL BLOOD FLOW (LCBF) WITH POSITRON COMPUTED TOMOGRAPHY (PCT). SC Huang, ME Phelps, RE Carson, EJ Hoffman, D Plummer, N MacDonald, DE Kuhl. UCLA School of Medicine, Los Angeles, CA.

Since the development of PCT, which provides quantitative radioactivities in vivo, a number of methods have been used to measure LCBF. However, they are limited either by metabolic trapping or by nonlinear responses. We have developed a method which employs the mean clearance time of O-15 water to measure LCBF with PCT.

The method requires the subject to inhale O-15 CO_2 (30 mCi) in a single breath, and PCT scanner to collect data continuously for 8 minutes. Each projection measurement of PCT scan is thus measured repeatedly in time. The distribution volume (V) and the mean transit time (T) of tracer through a local tissue region can be obtained respectively from the area and the 1st moment of the time activity curve of each projection measurement by PCT reconstruction. After V and T are obtained, LCBF is calculated by central volume principle (LCBF = V/T). PCT studies using physical decay of O-15 in phantoms to simulate biological clearance of tracer showed T in local regions was obtained correctly (177±20 sec) by the method. In human studies, recirculation of tracer was removed by exponential extrapolation. O-15 water input function was obtaind form blood samples and the delay time of the input function was subtracted from mean transit time image before applying the central volume principle. Preliminary results showed good quality images of LCBF with gray to white matter ratio of V,T and LCBF to be 1.2, 0.6 and 2 respectively. Quantitative LCBF in gray matter was about 60 ml/min/100 gm.

The method is convenient to use and allows rapid measurements of LCBF. Its characteristics such as noise and error propagation are currently under investigation.

QUANTITATIVE MEASUREMENTS OF TOMOGRAPHIC REGIONAL CEREBRAL BLOOD FLOW USING XE-133 CLEARANCE METHOD AND EMISSION TOMOGRAPH (HEADTOME). I.Kanno, K.Uemura, Y.Miura, S.Miura, S.Takahashi and Y.Kawata., Division of Radiology, Research Institute of Brain and Blood Vessels, Akita, JAPAN.

Tomographic regional cerebral blood flows (rCBF) were measured using an emission tomograph (HEADTOME) [1] and the Xe-133 clearance technique. Resolutions of HEADTOME in single photon dynamic scan were 15 and 12 mm FWHM at the center and at 10 cm radius, respectively. Sensitivity for Xe-133 was 13 kcps/(μCi/ml) with slice thickness of 30 mm. Scattered fractions were 49 % and 25 % at the center and at the periphery, respectively. In rCBF studies Xe-133 was administered noninvasively. Continuous scan was performed for 15 min and sequential pictures of every 20 sec were reconstructed. The rCBF at each pixel was determined by "time integrating" method [2], in which, a couple of early pictures were summed, then local clearance rate (ki) was determined by referring the pixel value to table of integrals calculated for various k's using the endtidal Xe-133 curve, local solubility coefficient (λi) by fractionating the pixel value of total picture of 15 min, and finally from these two parameters; rCBFi = λi·ki.

Several studies have been carried out in patients with the cerebral infarcts. The rCBFs of infarcted regions were measured quantitatively to 25-35 ml/100g/min. The method, however, involves several problems to be solved; how to elminate the scattered fractions, to delineate the brain on the picture in order to accurately determine λi, and to rapidly and effectively input Xenon into the brain, and errors involved in the time integrating method. These were empirically examined and discussed in detail.

[1] Kanno,I, et al: J Comp Ass Tomo 5 (in press), 1981.
[2] Kanno,I, Lassen,NA: J Comp Ass Tomo 3: 71-76, 1979.

WEDNESDAY, JUNE 17, 1981

10:30-12:00 **ROOM A-1**

CARDIOVASCULAR IV: CORONARY ARTERY DISEASE

Moderator: William L. Ashburn
Co-moderator: Harvey S. Hecht

EFFECTS OF HIGH DOSE ORAL PROPRANOLOL ON EXERCISE LEFT VENTRICULAR PERFORMANCE IN CORONARY ARTERY DISEASE. H. J. Berger, A. Lachman, R.W. Giles, M. Sands, R. Zito, A.V.N. Goodyer, B.L. Zaret. Yale Univ., New Haven, Ct.

The left ventricular (LV) functional consequences of high dose oral propranolol (PROP) were evaluated during upright bicycle exercise (EX) in 14 patients (pt) with coronary artery disease (CAD). LV ejection fraction (EF), end-diastolic volume (EDV), cardiac output (CO), and regional function were determined by first-pass radionuclide angiocardiography. Studies first were obtained on PROP (660±101mg/day {mean ± SEM}; serum level, 320±58ng/ml) at rest and during symptom-limiting EX. After ≥96 hrs off PROP, EX studies were repeated at the same rate-pressure product (RPP), the same external workload (WL), and the new symptom-limiting maximum (MAX).

	EX-ON PROP	EX-OFF PROP		(*p<.01 vs PROP)
	MAX	SAME RPP	SAME WL	NEW MAX
EF (%)	70±3	70±4	59±3*	57±4*
CO (l/min)	18.2±1.8	18.0±1.8	20.7±2.1	21.3±2.5
RPP ($\times 10^{-2}$)	141±30	152±30	258±60*	273±71*

On PROP, 10/14 pts had a normal (nl) LV response to EX, and LVEF increased with EX by +11±2%. Off PROP, all pts had abnl LVEF responses, and 7/14 also developed regional dysfunction. However, EX CO was maintained due to LV dilatation. At the same EX WL, EDV increased from resting values by 55±10ml on PROP and by 39±8ml off PROP (pNS). At rest, PROP decreased heart rate from 78±6 to 54±2 beats/min (p<0.001). LVEF decreased from 71±3 to 59±3% (p<0.01), while EDV increased from 192±18 to 214±13ml (p<0.05).

Thus, for diagnosis of CAD, EX LV function studies should not be performed on high dose PROP. At the same level of myocardial oxygen consumption, there is no difference in EX LVEF on and off PROP. However, at the same external WL, PROP prevents EX-induced LV dysfunction.

REPRODUCIBILITY OF EXERCISE RADIONUCLIDE ANGIOGRAPHY IN CORONARY ARTERY DISEASE. H.S. Hecht, M.A. Josephson, J.M. Hopkins, and B.N. Singh. Wadsworth VA Medical Center and University of California, Los Angeles, CA.

Before using exercise induced changes in radionuclide ejection fraction (EF) and regional wall motion abnormalities (RWMA) to evaluate interventions, reproducibility of exercise radionuclide angiography (RA) must be established. Thus, 18 stable coronary artery disease (CAD) pts underwent maximum multistage, supine equilibrium exercise RA on 2 occasions on placebo (P1 and P2), separated by 2 weeks. The results are:

	Baseline EF		MEx-EF		MEx-Baseline EF	
	P1	P2	P1	P2	P1	P2
mean	.56	.58	.51	.54	-.05	-.04
SD	.14	.12	.18	.18	.12	.11
r	.90*		.92*		.69*	
SD(d)	.06		.07		.09	

MEx-maximum exercise r-correlation coefficient SD(d)-SD of difference *p<0.001

Using the conventional criteria of a decrease or <0.05 increase in EF and/or new RWMA, in 16 of the 18 pts P1 and P2 agreed on the diagnosis of CAD; 12 had similar EF response and 15 agreed in RWMA.

Conclusions: 1) A significant correlation exists in both baseline and exercise EF and exercise-baseline EF. 2) Despite this correlation, the differences (SD(d)) emphasize the need for inclusion of reproducibility studies in all evaluations of interventions by exercise RA. 3) The variations in EF response based on directional changes and in RWMA result in a lack of uniformity regarding the diagnosis of CAD.

COMPARISON OF THALLIUM-201 MYOCARDIAL IMAGING AND REGIONAL WALL MOTION STUDIES AFTER CORONARY VASODILATATION WITH DIPYRIDAMOLE

H. Sochor, O. Pachinger, E. Ogris, M. Klicpera, P. Probst, F. Kaindl.
University of Vienna, Cardiol. Dept.-Austria

This study was undertaken to study the reliability of Tl-201 imaging after coronary vasodilatation and the suitability of this technique for wall motion studies. Perfusion defects (PD) after coronary vasodilatation with Dipyridamole (DIP) can be caused by regional perfusion deficits or by stealphenomena. DIP-Tl-201 imaging was performed in 287 pts. 142 had coronary artery disease (CAD) verified by contrast angiography. Sensitivity of a Tl-201-DIP scan in pts without prior myocardial infarction was 79 %. Overall accuracy of predicting vessel involvement by segmental PD was 88 %. To evaluate the appearance of a Tl-201-PD and a regional wall motion (RWM) abnormality, 40 pts were studied with 2 DIP-tests utilizing Tl-201 stress and redistribution scans and MUGA-blood-pool scintigraphy.80 % (32/40) had PD according coronary anatomy, 58 % (23/40) had PD without any RWM abnormality. 9 pts (22 %) with PD had angina pectoris with ECG changes. In 7 of them PD correlated with a RWM abnormality.
The sensitivity for detecting CAD in pts without infarction using Tl-201-DIP stress scintigraphy was 79 %.
Only 22 % of the CAD pts has RWM abnormalities after coronary vasodilatation.
Dipyridamole is not suitable for gated blood-pool exercise studies.
Regional differences in Tl-201 scans after DIP can be caused as well by ischemic reactions as by steal- and maldistribution phenomena.

SIGNIFICANCE OF EXERCISE INDUCED ST ELEVATION IN PATIENTS WITH LEFT VENTRICULAR ANEURYSM. S. Winter, A. Kiers, M. Sullivan, A.S. Most, H. Gewirtz.
Rhode Island Hospital (Brown U),Providence, RI

The significance of exercise induced ST segment elevation (STE) in patients (PTS) with left ventricular aneurysm (LVAN) is uncertain. Thallium (Tl) stress tests were performed in 16 PTS with LVAN to study the role of myocardial ischemia in this phenomenon. Imaging in anterior and LAO projections was begun 5 min after Tl injection with delayed scans made 2 hrs later. A computer was used to determine time related changes in Tl activity in abnormal and normal scan zones, to quantitate the size of initial Tl defects and to size the LVAN (% akinesia/dyskinesia of total LV circumference on anterior gated blood pool scan). Sum of STE (Σ ST-mm) in precordial leads V1-6 was determined at rest and immediately post exercise. Marked STE (ST $\geq$ 10.0mm) occurred at peak stress in 7 PTS (Group - I mean $\pm$ 1SD = 13.1 $\pm$ 1.9), while only modest (Σ ST=5.3$\pm$1.4;N=6) or no additional (N=3) STE occurred at peak stress in 9 PTS (Group II). LVAN size in Group I PTS (51$\pm$8) was greater (P. <01) than in Group II (27$\pm$8) and ejection fraction lower (.24$\pm$.09 vs .38$\pm$.09, P <.01). Likewise, initial anterolateral wall defect score was higher (P <.01) in Group I (278$\pm$117) than in Group II (124$\pm$72). In Group I the initial defect:normal zone Tl ratio (0.30+.08-anterior view) increased to 0.49$\pm$0.20 in the late scan (P=.01). Although the initial defect:normal Tl ratio did not change significantly in Group II (Initial - 0.49+.13 to Late - 0.57+.17), 5/9 PTS exhibited increases (20 to 45%) comparable to that of PTS in Group I. Thus, exercise induced marked STE is indicative of extensive anterior wall damage and large LVAN. Reversible ischemia may also contribute but by itself is not sufficient to account for exercise induced marked STE in these PTS.

REGIONAL MYOCARDIAL PERFUSION AFTER CORONARY ARTERY BYPASS SURGERY: ASSESSMENT BY QUANTITATIVE EXERCISE THALLIUM-201 SCINTIGRAPHY. G.J. Taylor, J.A. Austin, D.D. Watson, I.K. Crosby, H.A. Wellons, P.T. Stebbins, G.A. Beller, University of Virginia, Charlottesville, Virginia.

To better understand angina relief by coronary artery bypass surgery (CAB), 34 patients (pts) had exercise (Ex) thallium-201 (Tl) scintigraphy and angiography before and 7.7 ± 1.4 wks (± SD) after CAB. Graft patency was 89% (86/97), and 31 pts had resolution of angina. Changes in regional Tl activity were computer quantitated from serial Tl images obtained 10, 60 and 180 min. post-Ex. Segment (seg) perfusion was defined as normal (Nl), showing a persistent defect (PD) or a redistribution (RD) defect. A total of 97 scan segs receiving grafts were analyzed. Pre-CAB, 36 segs were Nl; post-CAB, 33 remained Nl and 3 became PDs associated with intraoperative damage. Pre-CAB there were 45 RD defects; post-CAB, 40 (89%) became Nl, 3 remained as RD defects and 2 became PDs. There were 16 pre-CAB PDs thought to represent scar, post-CAB 9 remained as PDs and surprisingly 7 became Nl. Of pre-CAB PDs, 5 had $\geq$ 50% reduction in regional Tl counts and none improved post-CAB; 7 of the 11 PDs with 25-49% reduction in Tl counts normalized after surgery.

Thus, improved perfusion can be demonstrated by quantitative Tl scintigraphy in most myocardial segments showing abnormal perfusion pre-CAB. Furthermore, quantitative imaging pre-CAB appears useful in predicting potential reversibility of perfusion abnormalities. Some persistent defects may revert to normal Tl uptake post-CAB.

LEFT VENTRICULAR DYSFUNCTION DURING ANESTHESIA INDUCTION FOR CORONARY ARTERY SURGERY ASSESSED WITH THE COMPUTERIZED NUCLEAR PROBE. R.W. Giles, H.J. Berger, P. Barash, S. Tarabadkar, P. Marx, B.L. Zaret, Yale Univ., New Haven, Ct.

Laryngoscopy and intubation produce reflex changes in heart rate (HR) and systolic blood pressure (SBP) during anesthesia induction. Therefore, left ventricular (LV) performance was studied during induction prior to elective coronary artery surgery (CABG) using the labeled equilibrium blood pool and the computerized nuclear probe. LV ejection fraction (EF) was obtained during induction immediately before endotracheal intubation (PREINTUB), immediately post-intubation (INTUB), and at 1-minute (min) intervals thereafter (Recovery=10 min). HR, SBP, pulmonary capillary wedge pressure (PCWP), and cardiac index (CI, l/min/m^2) were recorded simultaneously. In 25 patients (pts), anesthesia was induced by standard techniques using diazapam 0.3mg/kg i.v., inhalation of nitrous oxide/oxygen (3:2), and enflurane 0-2% q.s. During INTUB, LVEF decreased in all pts, averaging $\pm$SEM, 16$\pm$1% (range, 4-26% EF units). LVEF did not recover to PREINTUB levels in 7 pts by 10 min.

	LVEF	HR(bpm)	SBP(mmHg)	PCWP(mmHg)	CI
PREINTUB	50$\pm$2	57$\pm$3	116$\pm$3	16$\pm$1	2.7$\pm$0.2
INTUB	32$\pm$3*	72$\pm$3*	152$\pm$4*	23$\pm$2*	2.8$\pm$0.2
RECOVERY	47$\pm$3	59$\pm$3	114$\pm$4	16$\pm$4	2.8$\pm$0.2

*p<0.001, compared to PREINTUB

In a group of 7 additional pts, induction with a synthetic high potency narcotic, fentanyl 75µg/kg i.v., blunted

the hemodynamic and LVEF changes occurring during intubation.

Thus, there is profound depression of LV performance during intubation, associated with reflex hypertension and tachycardia, which may be modified by appropriate therapy. These data highlight the need for monitoring LV performance during anesthesia induction for CABG.

10:30-12:00 **ROOM B-1**

CARDIOVASCULAR V: VENTRICULAR FUNCTION AND VOLUME

Moderator: Ernest V. Garcia
Co-moderator: Kenneth P. Lyons

A CRITICAL EVALUATION OF THE ACCURACY OF EJECTION FRACTION FROM FIRST PASS RADIONUCLIDE ANGIOGRAMS: COMPARISON TO BIPLANE CONTRAST ANGIOGRAPHY. D.S. Dymond, R.P. Grenier and D.H. Schmidt, University of Wisconsin-Mt. Sinai Medical Center, Milwaukee, WI.

Conventional corrections for background(BG) in LV ejection fraction(EF) calculations from first pass radionuclide angiograms(FPRA) assume that the major contribution to BG is from right heart and left lung. This study examined the residual BG present, mainly scatter, when activity in right heart and left lung was eliminated. During cardiac catheterization, 17 patients had FPRA performed immediately prior to contrast ventriculography. Imaging was carried out in the anterior projection using a multicrystal detector, the bolus of Tc99m being injected into the distal right pulmonary artery. Biplane contrast EF ranged from 4% to 69%. EF from FPRA was calculated (a) from LV time-activity curve assuming BG only in lung and right heart and (b) from time-activity curve corrected for BG by subtracting a curve generated from a circular region of interest around the LV, including the aorta. Method (a) correlated closely with contrast EF (r=0.97) but significantly underestimated EF compared to contrast EF (34.7% vs.48.6%, $p<0.001$). Method (b) also correlated closely with contrast EF (r=0.98) with no significant difference in absolute values (45.8% vs.48.6%). Direct measurement of BG in method (b) showed it to be $30.5 \pm 6.5\%$ of observed end diastolic counts over the range of EF. These data indicate 1) there is a major scatter contribution to BG in addition to right heart and left lung; 2) BG components due to scatter are readily estimated with the circular region of interest technique; and 3) with appropriate evaluation of BG and with contrast and radionuclide studies performed together, equality, not only proportionality between FRPA EF and biplane contrast EF may be achieved.

INFLUENCE OF THE COLLIMATOR ON THE MEASUREMENT OF EJECTION FRACTON IN SIMULATED GATED CARDIAC IMAGES. J.A. Rothendler, K.A. Brown, R.A. Wilson, G.M. Pohost, H.W. Strauss . Massachusetts General Hospital, Boston, MA.

Selection of the optimal collimator for recording equilibrium cardiac blood pool images during supine bicycle exercise is frequently based on the need to record a maximum number of events in a short imaging time. To define which collimator is best suited for this purpose, we utilized a "beating" balloon cardiac phantom model to study the effect of collimator on ejection fracton (EF) determinations. The model was designed to simulate a gated cardiac image in the left anterior oblique position in regard to left ventricular (LV) size, counts and LV to background ratio. Gated images of the phantom were obtained at known EF's of 30 to 70% in 5% increments for each of three collimators: "high resolution" (HR), "general purpose" (GP), and "high sensitivity" (HS). Images were obtained to simulate two levels of activity; one analogous to an average two minute collection, the other analogous to a 35% reduction in activity. EF's were determined semi-automatically using a combination of threshold and second derivative criteria for LV edge detection. There were no significant differences in regression coefficients between the two levels of activity. For the combined data from the two levels, the following results were obtained:
(m = measured, t = true)

COLLIMATOR	REGRESSION EQUATION	R	VARIANCE
HR	EF(m)=.753EF(t)+13.83	.969	6.87
GP	EF(m)=.877EF(t)+ 5.11	.931	22.08
HS	EF(m)=.698EF(t)+ 9.69	.900	21.45

There were significant differences in the regression equations for GP vs. HS ($p<.01$) and HR vs. HS ($p<.0001$). The variance for HR regression line was significantly lower ($p<.05$) than that for GP and HS.

We conclude that the choice of collimator may have a significant effect on the accuracy of ejection fraction determinations. The basis for this effect is probably multifactorial, although a difference in edge characteristics produced by the collimators may play an important role.

THE PHASE IMAGE: AN ACCURATE MEANS OF DETECTING AND LOCALIZING ABNORMAL FOCI OF VENTRICULAR ACTIVATION. MA Frais, EH Botvinick, JW O'Connell, DW Shosa, MM Scheinman, RS Hattner University of California, San Francisco, CA

Since the phase image provides a means of detecting the sequence of ventricular contraction, which is linked to the sequence of electrical activation, we applied it to the identification of the earliest site of ventricular contraction in 12 patients (pts) with abnormal foci of ventricular activation. Four pts with W-P-W syndrome and pre-excitation at rest and 8 pts with ventricular pacemakers were studied. Phase analysis of the equilibrium blood pool scintigram was performed by fitting the fundamental Fourier harmonic to the multiple-gated left ventricular (LV) counts data in the anterior and "best septal" LAO projections. The site of earliest ventricular contraction in each patient was determined from phase data displayed as composite static and dynamic images and phase histogram of each visually determined ventricular region. In those pts with W-P-W, foci of earliest contraction were seen in the anterior wall of the LV in 1 pt and in the septum in 2 pts, and corresponded exactly to the sites of pre-excitation determined on electrophysiologic mapping. Similarly among 8 pts with pacemakers the site of earliest activation was localized to the RV in 7 pts and to the LV in 1 pt. Within each ventricle the site corresponded to the radiographic location of the pacemaker electrode.

The phase image provides an accurate, non-invasive visual means of detecting and localizing abnormal foci of ventricular activation.

CORRELATION OF PHASE IMAGE PATTERNS WITH VARIOUS CARDIAC ACTIVATION PATTERNS INDUCED BY PACING. E. Byrom, S. Swiryn, D. Pavel, C. Meyer-Pavel, B. Handler, K. Rosen. University of Illinois Medical Center, Chicago

The phase image is a potentially useful tool for non-invasive evaluation of electrical disurbances of the heart. Detailed validation is essential before routine clinical use can be suggested. We have studied various effects of pacing in 4 patients (pt), simultaneous with ECG monitoring and, in the case of ventricular pacing, with X-ray visualization of the pacer location. Only changes obtained without significant increases in heart rate were compared, to avoid any possible effect of heart rate itself. Three groups (G) of changes were evaluated: G1) Atrial pacing (AP) with and without left bundle branch block (LBBB) (2pt), G2) AP versus right ventricular pacing (VP) (3 pt), G3) VP from two different sites (1 pt). For each ventricle (LV,RV) the mean and standard deviation (SD) of the phase distribution were calculated, together with the location and phase of the areas of lowest (early) and highest (late) phase, and the phase differences between the ventricles (LV minus RV) Δ mean, Δ early and Δ late. Results: G1) LBBB was characterized by increases in all Δ parameters, increased LV SD values and displacement of the LV early area, as compared to AP without LBBB. G2) VP was characterized by increases in Δ mean and Δ early, and in LV and RV SD values, and by displacement of LV and RV early areas. G3) When the pacer was moved from the upper septum to the lower septum, a clear change in pattern was seen, RV early area corresponding to the pacer site. Conclusion: With each case serving as its own control phase images show clearly the effect of different activation patterns, both as phase differences between ventricles, and as changed phase distribution within ventricles.

QUANTIFICATION OF LEFT VENTRICULAR (LV) VOLUME IN GATED EQUILIBRIUM RADIOVENTRICULOGRAPHY. M.H. Bourguignon, J.G. Schindeldecker, G.A. Carey, K.H. Douglass, R.D. Burow, E.E. Camargo, L.C. Becker, H.N. Wagner, Jr. The Johns Hopkins Medical Institutions, Baltimore, MD.

A simple method for measuring LV volume using a semi-automated analysis of 40° LAO gated blood images has been developed. The essence of this method is the use of the dimensions and radioactivity within a segment of aorta to convert observed LV count ratios to volume. Four assumptions were made: 1) the aortic arch is nearly parallel to the collimator face when a patient is in the proper LAO position; 2) a segment at the top of the aortic arch, approximately 1 cm wide, is a right cylinder; 3) the edges of the aorta can be delineated as the lines where the second derivative of a cross sectional profile equals zero; 4) LV and aortic arch counts undergo the same attenuation because they are nearly the same distance from the chest wall in the proper LAO position. By measuring the counts and volumes of two regions of known shape, one in the middle, the other at the edge of the aortic arch, and calculating their differences, a background-independent volume count ratio ($\Delta V/\Delta C$) can be obtained. The LV end diastolic volume (LVEDV) is calculated with the equation: LVEDV = ($\Delta V/\Delta C$) · LVEDC, where LVEDC represents LV end diastolic counts. Twenty-six patients were evaluated by equilibrium radio- and contrast ventriculography, the latter analyzed by planimetry. The radionuclide method yielded an end diastolic volume that correlated well with contrast ventriculography ($r=0.96$, $Y=0.91 x + 21$ ml). In addition to its simplicity and objectivity, a major advantage of this method is that it does not require a blood sample.

MODELS FOR ATTENUATION CORRECTED VENTRICULAR VOLUMES. E. Fine, J.P. Wexler, S. Heller, S. Scharf and M.D. Blaufox, Albert Einstein College of Medicine, Bronx, NY.

There is imprecision in volume data determined from radionuclide ventriculograms. This determination requires correction for attenuation which is geometry dependent. We have derived equations for attenuation correction to determine the contribution of attenuation to the observed imprecision: I) $V=N/a$ (uncorrected); II) $V=(N/a)e^{\mu z}$ (point source surrounded by uniform attenuating medium); III) $V=(2N e^{\mu d}\mu^2 M^2/3a)[(1-1/\mu M)+e^{-2\mu M}(1+1/\mu M)]^{-1}$ (ellipsoid of revolution with diverging attenuator); IV) $V=(4N e^{\mu d}\mu^2 M^2/3a)[(\mu M-1/2\mu M)+e^{-2\mu M}(1+1/2\mu M)]^{-1}$ (ellipsoid of revolution with rectangular attenuator); where N=measured balloon activity, a=specific activity and u=attenuation coefficient, M=major axis of ellipsoid of revolution, d=thickness of attenuator; z=d+M. Equations were tested with 99m-Tc in balloon phantoms of known water volumes ranging from 31 to 330cc. Linear regression (V=MX+B) between calibrated volumes (X) and calculated volumes (V') using the equations revealed:

		I		II		III		IV	
Range of X	n	M	B	M	B	M	B	M	B
30-330cc	21	0.20	0.8	1.34	-18.3	1.30	-16.0	1.12	-9.2
30-100cc	10	0.21	-0.3	1.19	-7.9	1.17	-7.3	1.05	-5.3
100-330cc	11	0.19	3.6	1.40	-33.1	1.34	-27.2	1.13	-12.4

Models II,III,and IV more accurately predicted left ventricular volume than did the uncorrected model I($p<0.05$). Analysis of variance did not demonstrate a statistically significant difference among II,III, and IV. Model IV appeared to be more accurate than II and III. These data support the contention that attenuation correction is necessary for determination of left ventricular volume. However, the imprecision in data collected by present instrumentation does not yet justify use of specific models for correction.

10:30-12:00 **ROOM D-1**

RADIOPHARMACEUTICALS II: RADIOHALOGENATED COMPOUNDS

Moderator: Kenneth Krohn
Co-moderator: W. C. Eckelman

RAPID INCORPORATION OF RADIOBROMINE VIA THE REACTIONS OF BROMINE OR SODIUM BROMIDE WITH ORGANOBORANES. G.W. Kabalka, K.A.R. Sastry, University of Tennessee, Knoxville, TN.

The halogens have more potential as cyclotron-produced nuclides of choice for radiopharmaceuticals than any other family in the periodic table. Until recently, most research efforts in the halogen area were directed towards the insertion of the radioiodines. Recently there has been a significant interest in radiobromine because of the increased stability of the resultant organic bromides as compared to organic iodides.

The standard syntheses of organic bromides parallel those of the corresponding iodides and are frought with the same difficulties: inefficient utilization of the radiohalide, lack of regiospecificity, etc. We recently reported a new synthesis of organic iodides via the reaction of organoboranes with iodine monochloride which was applicable to a wide variety of functionally substituted molecules (1).

We wish to report that radiobromine labeled materials can be readily prepared via the reaction of either bromine or bromide ion under extremely mild conditions.

$$R_3B \xrightarrow{Br_2} RBr$$

$$R_3B \xrightarrow{Br^-} RBr$$

We have synthesized a variety of bromine labeled organic molecules and will discuss the advantages and disadvantages of each method.

(1) KABALKA GW, GOOCH EE: J Org Chem 45:3578, 1980

RADIOBROMINATIONS UTILIZING N-CHLOROSUCCINIMIDE AND NO-CARRIER-ADDED SODIUM BROMIDE-77. D. S. Wilbur and H. A. O'Brien, Jr. Los Alamos National Laboratory, Los Alamos, NM

In-situ generation of no-carrier-added (nca) radiohalogenating agents provides an efficient method of preparing the high specific activity radiolabelled compounds that are required for receptor binding radiopharmaceutical studies. It has been observed that bromide ions are rapidly converted in-situ by N-chlorosuccinimide (NCS) to an electrophilic brominating agent. The brominating species, generated in solvents such as MeOH, EtOH, THF, dioxane, and acetonitrile, readily brominates activated aromatic compounds (e.g. phenol, aniline) and alkenes (e.g. cyclohexene, styrene) at room temperature. The exact nature of the electrophilic species is unknown. Reaction with aromatic compounds in ethanol yields the corresponding bromo isomers, whereas addition to alkenes such as cyclohexene in ethanol yields one major product in which Br-OET has formally added across the double bond. Unlike N-chlorotetrafluorosuccinimide employed by Stöcklin et al, NCS does not require anhydrous reaction conditions.

The utility of NCS in nca radiobrominations was demonstrated by A-ring radiobrominations of phenolic steroids. For example, estradiol(E2) and 17α-ethynylestradiol(EE2) were rapidly brominated (<30 minutes) with nca sodium bromide-77 in ethanol with very high overall radiochemical yields. Separation of the reaction components by HPLC gave the pure 2-bromo-Br-77 and 4-bromo-Br-77 isomers. The 4-bromo-Br-77 isomers of both E2 and EE2 were estimated to have specific activities of 600-1200 Ci/mmole. Such specific activity is within the range believed to be necessary for target tissue localization of radiolabelled steriods.

TISSUE DISTRIBUTION, CLEARANCE RATES AND RADIATION DOSIMETRY OF 16α[Br-77]-BROMOESTRADIOL-17β. K.D. McElvany, J.A. Katzenellenbogen,* S.G. Senderoff,* B.A. Siegel, M.J. Welch. Washington University School of Medicine, St. Louis, MO; *University of Illinois, Urbana, IL; and LANL Medical Radioisotope Group, Los Alamos, NM.

16α[Br-77]-Bromoestradiol-17β (BE) of high specific activity has been synthesized and shown to have selective, receptor-mediated uptake in uteri and mammary tumors in rats. Mature rats bearing DMBA-induced mammary tumors have been injected with 100-200 μCi BE and imaged with a scintillation camera fitted with a pinhole collimator, allowing visualization of the tumors. These studies suggest that BE may be a useful agent for imaging estrogen receptor positive human breast tumors.

Tissue distribution of BE was determined in mature female rats and these data were used to estimate the

absorbed radiation dose resulting from administration of BE to humans. The critical organs are the upper and lower large intestine, which receive 0.34 and 0.43 rads/mCi, respectively. A factor which must be considered in determining the dosimetry of BE in humans is the slower clearance of estrogens in humans as compared to rats due to increased enterohepatic circulation.

Clearance of BE in a monkey was studied to investigate the rate and route(s) of excretion of the compound. The clearance half-time was 36 hrs, with roughly equal amounts of activity present in the urine and feces. This rate of clearance has been confirmed by studies in several patients, and scintillation images also suggest similar routes of excretion in humans.

IN VIVO COMPARISON OF 16α[Br-77]-BROMOESTRADIOL-17β AND 16α[I-125]-IODOESTRADIOL-17β. K.D. McElvany, K.E. Carlson,* M.J. Welch, S.G. Senderoff,* J.A. Katzenellenbogen.* Washington University School of Medicine, St. Louis, MO; *University of Illinois, Urbana, IL; and LANL Medical Radioisotope Group, Los Alamos, NM.

16α[Br-77]-Bromoestradiol-17β has been synthesized with specific activities of ~400-1000 Ci/mmole, as determined by Scatchard analysis. 16α[I-125]-Iodoestradiol-17β was obtained commercially, and its specific activity was verified to be ≥1000 Ci/mmole.

Tissue distribution of the Br-77- and I-125-estradiols was studied in immature and mature female rats; animals were injected intravenously with 5 μCi 16α[Br-77]-bromoestradiol and 2-3 μCi 16α[I-125]-iodoestradiol. Both labeled estradiols showed selective receptor-mediated uptake by target tissues, confirmed by depression upon co-administration of 18 μg unlabeled estradiol. Uterus-to-blood ratios at 1 hr were 14.3±6.6 for the bromoestradiol and 14.8±7.7 for the iodoestradiol; the ratios at 3 hrs were 24.0±8.4 and 25.5±12.3, and those at 6 hrs were 15.2±3.8 and 13.1±5.1.

The uptake ratios vary significantly between animals; however, comparisons of the ratio for the bromoestradiol to that for the iodoestradiol in a given animal are very consistent. The ratios of the uterus-to-blood ratio for bromoestradiol to that of iodoestradiol are 1.02±0.10 at 1 hr, 1.06±0.19 at 3 hrs and 1.23±0.22 at 6 hrs. These results stress that discrepancies may arise when comparing tissue uptake ratios in different animals, and indicate that the radioiodinated estradiol may be a useful standard when measuring selective uptake of radiolabeled estrogen derivatives.

NEW HALOGENATED ESTROGENS WITH HIGH BINDING AFFINITY AND SELECTIVITY FOR THE ESTROGEN RECEPTOR: POTENTIAL BREAST TUMOR IMAGING AGENTS. J.A. Katzenellenbogen, S.G. Senderoff, S.W. Landvatter, K.D. McElvany,* M.J. Welch* University of Illinois, Urbana, IL; *Washington University School of Medicine, St. Louis, MO; and LANL Medical Radioisotope Group, Los Alamos, NM

The bromosteroids 1 and 2 were prepared by halogenation of the corresponding estrone enol diacetates, followed by hydride reduction, and the pentestrols 3-5 and hexestrols 6-8 were prepared by displacement reactions on the corresponding alcohols (obtained by total synthesis). The receptor binding affinity (RBA) and the binding selectivity index (BSI), that considers both receptor and non-receptor binding, were determined for each compound by in vitro assay. 1-6 have the highest BSI values and should show the greatest receptor mediated uptake by target tissues in vivo. Studies in immature rats with Br-77 labeled 1 and 2 have shown uterus to non-target tissue ratios (± SEM) of 19.3 ± 2.4 and 18.9 ± 2.6 (n=6), respectively; these compounds have been used to image mammary tumors in rats. Routes to compounds 3-6 suitable for radiolabeling have been developed.

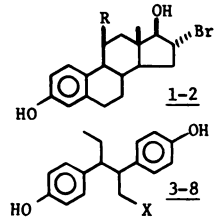

Cpd. No.	R	RBA	BSI
1	H	139	91
2	OMe	20	42
	X		
3	F	135	163
4	Br	200	110
5	I	172	67
6	CH_2F	127	89
7	CH_2Br	65	21
8	CH_2I	60	12

ANALOGUES OF 3-QUINUCLIDINOL BENZILATE FOR MYOCARDIAL IMAGING. W.J. Rzeszotarski, R.E. Gibson, W.C. Eckelman, D.A. Simms, E.M. Jagoda, and R.C. Reba. George Washington University Medical Center, Washington, D.C.

Recently, we reported that the potent muscarinic antagonist: 3-quinuclidinol benzilate (QNB) localizes in the myocardial tissue by a receptor mechanism. To further our understanding of the molecular requirements leading to a high affinity, muscarinic-cholinergic receptor binding radiotracer we synthesized seven analogs of QNB. The synthetic route was based on the formation of a Grignard intermediate (I) and its reaction with the ethyl ester of benzoylformic acid (II). Transesterification of the resulting α-aryl (or alkyl)-α-hydroxy-benzeneacetic acid ethyl ester (III) with 3-quinuclidinol in the presence of sodium 3-quinuclidinilate gives the analogues (IV).

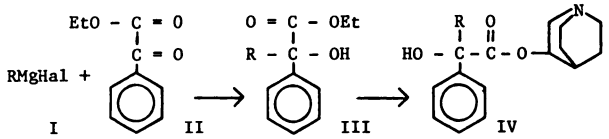

R = (A) C_6H_5-, (B) C_6H_5,N-CH_3, (C) $CH_3(CH_2)_3$-, (D) C_5H_9-, (E) C_6H_{11}-, (F) 4-FC_6H_4-, (G) 3-FC_6H_4-, (H) 4-BrC_6H_4-, (I) 3-BrC_6H_4-

Each relative binding index (RBI) was determined in a displacement study using ^{3}H-QNB and rat ventricular muscle preparation. Statistically, analogues IV A,C,D and G have the same affinity constant. All compounds had an affinity constant equal to or greater than N-CH_3 QNB (B). Since N-CH_3 QNB gives heart to blood ratios of greater than 20 in dogs and rats, these analogues are good candidates for radiolabeling.

THE MECHANISM OF m-IBG LOCALIZATION: DRUG INTERVENTION STUDIES. D.M. Wieland, L.E. Brown, D.D. Marsh, T.J. Mangner, W.H. Beierwaltes. University of Michigan Hospital, Ann Arbor, Michigan.

Radioiodinated meta-iodobenzylguanidine (m-IBG) a neuron-blocking derivative, shows promise as a radiopharmaceutical for the heart (H) and adrenal medulla (AM). Drugs known to lower the accumulation of norepinephrine (NE) in adrenergic nerves have been evaluated for their effect on the in vivo distribution of m-IBG.

Dogs were maintained on drug regimens, administered 100 μCi of I-125-m-IBG or H-3-NE and sacrificed at various times. Treatment with 6-hydroxydopamine (OHDA), a destroyer of adrenergic nerve fibers, caused a decrease (-50%) of m-IBG in the H. The spleen (-77%) and pancreas (-65%) showed a greater decrease. The AM, known to resist the action of 6-OHDA, showed an increase (+40%). The increase may be due to higher blood levels of m-IBG or homeostatic response of the AM to functional impairment of the nerves. H-3-NE was also decreased in the H (-82%) and increased in the AM (+47%).

Desmethylimipramine, a specific inhibitor of uptake 1, had no effect on the left ventricular concentration of m-IBG but lowered H-3-NE (-30%). AM accumulation of m-IBG (-89%) and NE (-97%) were strikingly lowered.

Pre- or post-treatment with reserpine, a vesicular storage blocker, caused depletion (-85%) of the AM content of m-IBG. Reserpine treatment precluded otherwise clear I-131-m-IBG images of the dog AM. The AM showed no stereochemical preference for (+) or (-) I-125-m-iodo-α-methylbenzylguanidine.

10:30-12:00 **ROOM G-1**

COMPUTERS AND DATA ANALYSIS II: TOMOGRAPHY

Moderator: Ronald R. Price
Co-moderator: Peter D. Esser

ESTIMATION OF THE LOCAL STATISTICAL PRECISION OF EMISSION COMPUTED TOMOGRAPHY (ECT) N.M. Alpert, D.A. Chesler, J.A. Correia, J. Chang, R.H. Ackerman, G.L. Brownell and J.M. Taveras. Department of Radiology, Massachusetts General Hospital, Boston, MA.

In order to properly utilize the concentration of radioactivity obtained with ECT, it is essential to have a reliable estimate of the precision of the measurement. This is true whether one wishes to compare regional measurements in the same tissue for significant differences or to compare results obtained in subjects studied at different institutions. Until now, the only information on the precision of ECT measurements was from computer simulation of simple phantoms which could not be related directly to in vivo studies and which did not take into account the effects of photon absorption or random coincidence events. We have developed a relatively simple algorithm for the direct computation of the local variance of the activity concentrations in an ECT image, $\sigma^2(r)$, which is based on the filtered back projection reconstruction method. In the case of reconstruction with an analytic photon absorption correction using positron emitters

$$\sigma^2(r) = \int\int d\theta\, dr\, p_\theta(r)\, h^2(r-r')\, e^{2\mu D(r')}$$

where p_θ represents the projection data measured at angle θ, h is the reconstructive filter, D is the distance traversed in tissue by the photon pair and μ is the linear attenuation coefficient. The effect of random coincidence events is included according to the relation $\sigma^2 = \sigma^2_T + \sigma^2_R$, where R and P refer to random and prompt coincidences respectively. The validity of this approach was demonstrated by comparing the computed value to the results obtained from measurements on phantoms. We have applied the direct computation of local variance to data obtained in cerebral metabolism studies with the MGH positron camera. At a resolution of 2cm FWHM and 10^6 events per slice, the relative statistical error (σ/concentration) is about 2% in gray matter over the cerebral convexity and about 3% in deep gray matter structures. White matter structures typically have larger relative errors-about 6%.

We conclude, on the basis of these studies, that quantitative ECT measurements in the brain can be very precise, that the precision for any study can be readily determined and that by reporting routinely the precision of the measurements data can be more usefully compared.

A CONCENTRIC POLAR PLOTTING TECHNIQUE FOR ANALYSIS OF EMISSION CARDIAC TOMOGRAPHY. T. Johnson, D. Kirch, B. Hasegawa, J. Sklar, P. Steele, VA Medical Center, Denver, CO

Quantitative display of information derived from scintigraphic imaging is a particular challenge now that emission tomography of the heart has become practical. Two-dimensional techniques such as stereoscopic or isometric display of organs as transparent or solid objects fail to provide a simple, concise means to convey regional quantitative information from tomographic radionuclide studies of the heart. We have developed a single-frame display format termed the "bull's-eye plot" which maps quantitative information into a set of circumferential polar plots. Data from the apical slice is plotted in the centermost ring and proceeds concentrically to the basal data in the outermost ring. This technique is most readily used to consolidate up to six tomographic thallium-201 circumferential profile curves into a single plot which readily associates the points on the curve with their anatomic locations and relates the data between the various slices in space and time. The quantitative measures to which it can be applied include percentage redistribution, regional washout rates, absolute uptake, and epi-to-endocardial uptake ratios. Bull's-eye plots are equally well suited to the temporal problem of tomographic segmental wall-motion analysis. For this purpose, functional descriptors such as wall-motion, wall-thickening, or radius of curvature can be sequentially projected in a dynamic fashion which is not possible by conventional plotting methods. We have found bull's-eye plots to be an excellent modality for consolidating information regarding temporal and spatially varying phenomenon into a single unified presentation. This technique is potentially useful on any video digital graphic display device.

FIELD FLOOD UNIFORMITY CONSIDERATIONS FOR ROTATING GAMMA CAMERA ECT. W.L. Rogers, N.H. Clinthorne, K.F. Koral, and J.W. Keyes, Jr. University of Michigan Medical Center, Ann Arbor, MI.

The sensitivity of ECT image quality to deviations in Anger camera field uniformity has been described by others. Using computer simulation of disk source data we have verified that a gaussian defect with FWHM=2.4cm and amplitude of 2% will produce image structure with 16% amplitude when the defect is located at the center of rotation. This means that central camera uniformity must be maintained within 1/2% if false image structure is to be held to less than 4%. This accuracy imposes strict requirements on the techniques used for uniformity correction.

In examining the conventional approaches to uniformity correction we have found the following severe problems: 1) Commercial Tc flood sources bulge at the center and exhibit non-uniformities of 10% or more. 2) Flood response of our prototype camera was a function of angular position because of inadequate magnetic shielding. This also caused a 6mm image shift during camera rotation. 3) Statistical accuracy of the built-in camera uniformity correction was limited to 1.7% by the 10M count calibration image. 4) Insufficient computational accuracy in a standard flood correction program introduced structure in reconstructed images with an amplitude of 9%.

On the basis of these findings we conclude that ECT demands highly stable cameras and the development of greatly improved flood correction methods.

A COMPARISON OF IN VIVO MYOCARDIAL PERFUSION DEFECTS BY SINGLE PHOTON, TRANSAXIAL EMISSION COMPUTED TOMOGRAPHY TO PLANAR IMAGES OF IN VITRO MYOCARDIAL SLICES. J.H. Caldwell, D.L. Williams, J.L. Ritchie, G.D. Harp, D.L. Olson, G.W. Hamilton, A. Coleman, K. Amato. VA Medical Center, Seattle, WA.

This is a report of a study in progress to define the in vivo (VIV) tomographic capabilities of a single photon, transaxial emission computed tomography (ECT) system (GE 400T) for myocardial perfusion imaging. A snare was placed on the circumflex coronary artery in 2 dogs, the artery occluded, and 2 million Tc-99m MAA particles (30 mCi) were injected into the left atrium, and the snare released. Ten sec/image non-gated projection images (128) were acquired over 360°. The animal was sacrificed and the acquisition repeated. The heart was excised and 1.8 cm thick slices made from apex to base. These slices were positioned to approximate the VIV orientation and planar images acquired on a gamma camera with a single pinhole collimator. Using a filtered backprojection algorithm without attenuation correction, 1.8 cm thick slices were reconstructed in standard CT format and then reoriented into slices perpendicular to the long axis of the left ventricle. Qualitatively the shape of the VIV images was similar to the in vitro (VIT) slices and the shape and extent of the perfusion defects corresponded to those seen in the VIT slices. However, cardiac motion produced some blurring of the defect. Quantitatively, count ratios of nonperfused to perfused myocardium were compared between the nonbeating VIV slices and the VIT slices. For the 6 VIT slices in which a defect was visible, the ratio was .10 $\pm$ .08 (mean $\pm$ SD) compared to a ratio of .41 $\pm$ .07 for the VIV slices. We conclude that ECT produces tomographic images of myocardial perfusion defects that are representative of the actual perfusion abnormality. Cardiac motion, however, results in some loss of definition, and without attenuation correction there is an over estimation of count ratios in the regions of interest.

RETRIEVAL OF QUANTITATIVE INFORMATION FROM POSITRON EMISSION COMPUTED TOMOGRAPHIC IMAGES FOR CARDIAC STUDIES WITH C-11 PALMITATE. E. Henze, S.C. Huang, D. Plummer, E. Hoffman, M.E. Phelps, O. Ratib, A. Najafi, J. Barrio, H.R. Schelbert. UCLA School of Medicine, Los Angeles, CA.

While positron emission tomography (PCT) overcomes the limitations of photon attenuation encountered with single photon imaging and therefore should provide images that represent quantitatively tracer tissue concentrations, this is seriously limited in the heart because of object size related losses in count recovery and cross-contamination of activity between myocardium and blood pools. To correct for these limitations, we developed a mathematical model that determines the count recovery factor as well as the fractional spillover from myocardium to blood and from blood to myocardium considering myocardial wall thickness, chamber diameter and intrinsic resolution of the PCT. This model was tested with serial gated PCT imaging in 5 open chest dogs and intravenous C-11 palmitate. Arterial blood samples for well counting were withdrawn at the midpoint of each image. The fractional spillover from blood to myocardium was determined by blood pool labeling with C-11 CO inhalation. The diameter and wall thickness of the imaged cardiac cross section were measured by ultrasound. When the PCT data were not corrected, blood C-11 concentration measurements were accurate only on the initial image, with high C-11 blood activity but were consistently too high on the late images. After employing the mathematical model for correction, the in vivo and in vitro measured blood activi-

ties correlated well in all 5 dogs (r=0.98, y=0.97 x +0.35, SEE=1.6). Further, the myocardial C-11 time activity curves were similar to those observed after intracoronary injection of C-11 palmitate in normal and ischemic tissue. We conclude that noninvasive serial in vivo evaluation of myocardial fatty acid metabolism by PCT is feasible because myocardial and blood C-11 concentrations can accurately be derived from PCT images.

THREE-DIMENSIONAL DISPLAY OF SINGLE PHOTON ECT IMAGES. K. Minato, Y. Ishii, T. Mukai, Y. Yonekura, K. Yamamoto, N. Tamaki, N. Maeda, H. Ito, T. Maekawa, M. Kuwahara and K. Torizuka. Dept. of Radiology and Nuclear Medicine, Kyoto University Medical School and Automation Research Laboratory, Kyoto University, Kyoto, Japan.

Recently a variety type of tomographic expression of radionuclide emission images can be obtained. This type of expression necessitates 3 dimensional display to complete clinical diagnosis.

Present report describes an attempt to display 3-D shaded images, easily perceptible to physician's eye, those of which derived from a series of tomographic images obtained by using a rotating gamma camera or a 7 pinholes collimator.

The creating procedure of the 3-D shaded images are as follows. The contours of the tomographic images were determined primarily. Then the 3-D geometric model of the organ of interest was summed up to be constructed in a computer. This 3-D model was projected on a screen (128 X 128 pixels) and the images were shaded to emerge up surfaces of the organ vividly.

The system can be implemented in a standard gamma camera data processing system (PDP-11/60), which necessitates about 1 minute computing time, and thus, help a physician to recognize the spatial relationship among several tomographic images. Further, cinematic display of a beating myocardial image, constructed from a series of gated Tl-201 myocardial tomography, seemed to be the most contributory to understand entire picture of wall motion abnormality.

10:30-12:00 **ROOM E-1**

SYMPOSIUM: TRENDS IN MEDICAL EDUCATION

Moderator: Robert M. Donati

WHERE DOES NUCLEAR MEDICINE FIT IN THE FUTURE OF MEDICAL EDUCATION. E. James Potchen, Michigan State University, East Lansing, MI.

TRENDS IN UNDERGRADUATE MEDICAL EDUCATION. Frederick J. Bonte, University of Texas S.W. Medical School, Dallas, TX.

REDESIGNING THE PREMEDICAL EDUCATION REQUIREMENT. Richard C. Reba, George Washington University Hospital, Washington, DC.

1:30-3:30 **ROOM B-1**

CARDIOVASCULAR VI: CLINICAL VENTRICULAR FUNCTION STUDIES

Moderator: F. David Rollo
Co-moderator: Alan D. Waxman

VENTRICULAR FUNCTION IN PATIENTS TREATED BY MEDIASTINAL IRRADIATION FOR HODGKIN'S DISEASE. D.H. Feiglin, B. Bar-Shlomo, M. Druck, J. Morch. G. Jablonsky, D. Hilton, B. Gilbert, D. Perrault, J. Herman, K. Moore, P.R. McLaughlin. Toronto General Hospital, Toronto, Ont. Canada.

To assess left and right ventricular function in asymptomatic patients after mediastinal irradiation for Hodgkin's disease we studied 12 patients who received a mean dose of 3545 ± 626 Rads (2000-4650) to the heart 10-26 years (mean 14.5 years) prior to testing. Their mean age was 42 years (25-55 yrs). These patients were compared to 19 normal controls with a mean age of 28 years (22-34). All subjects had radionuclide gated angiography at rest and during each level of maximal graded supine bicycle exercise. There were no significant differences between radiation patients and controls in maximal workload, heart rate and systolic pressure. The left and right ventricular ejection fractions are shown (Mean + SD):

	LVEF		RVEF	
	Rest	Ex	Rest	Ex
Radiation Patients	66±9	67±12	42±5	41±8
Controls	70±7	79±5*	46±6	57±4
Controls Vs Pat.	NS	P<.001	NS	P<.0001

*Rest Vs Ex P<.0001

In summary, patients who had mediastinal radiotherapy demonstrated an abnormal right and left ventricular response to exercise. These data suggest unrecognized underlying ventricular disease in these patients and indicate the need for careful long term cardiac followup of post irradiation patients.

USE OF GATED BLOOD POOL SCINTIGRAPHY TO OPTIMIZE PACING RATE IN PATIENTS WITH PERMANENT PACEMAKERS. K.A. Narahara, M.L. Blettel. UT Southwestern and VAMC, Dallas, TX.

Rate adjustable ventricular pacemakers (RAVP) are widely prescribed for patients (pts). To assess the effect of pacing rate on left ventricular function, gated blood pool scintigraphy (GBPS) was performed in 17 pts. Ejection fraction (EF), end diastolic volume index (EDVI), end systolic volume index (ESVI), stroke volume index (SVI), cardiac index (CI) and double product (DP) were determined at six pacing rates. Pts were grouped according to heart size (HS) on standard chest x-ray. Values are means ± SEM.

RATE	50	60	70	80	90	100	
	(pts with normal heart size) N=10						
EDVI	81±6	75±4	69±4	64±4	60±4	59±4	(cc/M²)
ESVI	35±3	35±2	34±2	33±2	32±2	33±2	(cc/M²)
SVI	46±3	40±2	35±2	31±2	28±2	25±2	(cc/M²)
CI	2.3±.2	2.4±.1	2.5±.2	2.5±.1	2.5±.2	2.5±.2	(L/M²)
EF	59±1	57±1	54±1	52±1	49±1	45±1	
DP	67±3	82±3	95±3	108±3	122±4	135±5	
	(pts with increased heart size) N=7						
EDVI	149±23	141±22	135±23	129±23	121±21	112±19	(cc/M²)
ESVI	94±25	90±23	88±24	86±24	84±22	79±20	(cc/M²)
SVI	55±5	51±4	47±4	43±3	38±2	33±2	
CI	2.8±.2	3.1±.2	3.3±.3	3.4±.2	3.4±.2	3.2±.2	
EF	43±7	42±7	41±7	40±7	38±7	35±6	
DP	60±4	73±4	86±5	101±6	111±6	126±6	

We conclude: 1)Pacing rate does not affect estimated CI in pts with normal HS although higher pacing rates depress the EF. 2)Pts with increased HS may benefit from pacing rates>70, but pacing at>90 results in a significant decrease in EF and CI despite an increased DP. 3) GBPS may be uniquely suited for optimizing pacing rates in pts with RAVP - particularly those with an increased HS.

RESTING AND STRESS LEFT VENTRICULAR FUNCTION IN PATIENTS WITH HYPERTROPHIC CARDIOMYOPATHY. D.E. Manyari, W. Paulsen, D.R. Boughner, P. Purves, W.J. Kostuk, University Hospital, London, Ontario.

The response of the left ventricle (LV) to exercise in patients with hypertrophic cardiomyopathy (HCM) is not well defined. Accordingly, ECG-gated blood pool cardiac scintigraphy was used to assess the LV function both at rest (R) and during symptom limited supine ergometer exericse (Ex). Studies were obtained in 16 patients (pts) (mean age 43 years) who were off all medications for at least 72 hours prior to cardiac catheterization and prior to the radionuclide studies, which were performed within 3 weeks of each other. They were subdivided into 3 groups based on

hemodynamic data: group I, no demonstrable obstruction, 4 pts; group II, latent obstruction, 4pts; group III, obstruction present at rest, 8 pts. The LV ejection fraction (EF) response to Ex was also assessed in 20 normal subjects (N), mean age 40 yrs. The results were (mean±SEM):

	N	I	II	III
Rest - EF(%)	62±4	58±4	71±4*	68±4*
Ex - EF(%)	74±3	72±5	67±1	62±4*

*=$p < 0.05$ vs normal values.

Pts in group I had normal EF both at R and during Ex. Those in Group II and III had an elevated EF at R and showed either no change or a diminished EF on Ex. Both, Ex duration and maximal heart rate-pressure product achieved during Ex were higher in pts of Group I than in pts of groups II and III, despite similar double product at R. Therefore, there are significant differences in the resting and exercise LV function between these three hemodynamic subgroups of HCM. These results may have important therapeutic implications.

THE USE OF A SCINTILLATION PROBE TO INVESTIGATE ISCHEMIC HEART DISEASE.

GJ Davies, S Chierchia, F Crea, M Morgan, A Maseri.
Royal Postgraduate Medical School, London, U.K.

Observation of the sequence of events preceding chest pain is important in the investigation of ischemic heart disease (IHD). We have monitored the ECG, arterial pressure (AP) and a left ventricular (LV) volume index in 10 patients (pts) with suspected IHD at rest in the basal state, with hyperventilation and after intravenous ergometrine. LV volume monitoring was achieved by counting the ^{99m}Tc-labelled blood pool (in vivo labelling) using a scintillation probe.

Eight pts with angiographic evidence of IHD showed an increase in end-diastolic volume (EDV) and end-systolic volume (ESV) after ergometrine, associated with typical "ischemic" chest pain in all pts but with unequivocal ECG changes in only 3. Four of these pts developed a similar increase in EDV and ESV after 5 min hyperventilation; these changes preceded the development of S-T segment elevation on the ECG which was accompanied by a marked fall in stroke volume (SV) and further rise in EDV, indicating a severe reduction in ejection fraction (EF). Amyl nitrite caused a rapid fall in EDV and ESV with an increase in SV and EF, associated with a transient, marked fall in AP and regression of ECG changes. Two pts with no evidence of IHD showed no change after ergometrine and a reduction in EDV and ESV during hyperventilation, but no other changes. The above method of monitoring LV function is therefore useful for the evaluation of patients with suspected IHD.

EVALUATION OF LEFT VENTRICULAR FUNCTION AT PROGRAMMABLE PACEMAKERS(RA,RV PACING) BY MULTI-GATED RADIONUCLIDE CARDIOANGIOGRAPHY. T.Nishimura, Y.Kosakai, T.Uehara, K.Hayashida, Y.Kitoh, T.Fujita, T.Kozuka, H.Manabe.
National Cardiovascular Center,Suita,Osaka,JAPAN.

Multi-gated radionuclide cardioangiography combined with dye dilution method were applied to evaluate left ventricular function in cardiac pacing at various heart rates(50-120/min.). The parameters calculated from multi-gated and dye method were cardiac output(CO),end-diastolic volume(EDV), end-systolic volume(ESV), ejection fraction(EF), and dV/dT. The storoke volumes(SV) from counts method were good agreements with those by dye method(r=0.96).

9 patients with complete atrioventricular block implanted by ventricular pacemaker and 5 patients with sick sinus syndrome by atrial pacemaker were studied at intervals of 10 beats from 50 to 120/min. At ventricular pacing, according to the increase of heart rate(HR), rate-output curve showed the flat and peaked type. EDV,ESV,SV were decreased gradually and EF was unvariable. On the other hand, at atrial pacing,according to the increase of HR, rate-output curve showed the flat type. EDV,ESV,SV were only slightly decreased in comparison with those of ventricular pacing.

Left ventricular function by increase of HR at cardiac pacing were mainly determined from the decrease of EDV caused by the shortening of filling time of left ventricle, other parameters were changed by the Starling's law of cardiac function amd contractility of myocardium. The differences of hemodynamic changes between atrial and ventricular pacing were thought to be caused by atrial kick phenomenon.

RIGHT VENTRICULAR EJECTION FRACTION FROM FIRST PASS RADIONUCLIDE ANGIOGRAMS: COMPARISON WITH CONTRAST RIGHT VENTRICULOGRAPHY. D.S. Dymond, R.P. Grenier and D.H. Schmidt.University of Wisconsin-Mt.Sinai Medical Center,Milwaukee,WI.

This study was undertaken to investigate whether right ventricular ejection fraction(RVEF) could be assessed accurately from first pass radionuclide angiography(FPRA). 18 patients had right anterior oblique(RAO) contrast right ventriculograms performed supine at cardiac catheterization, and in all patients RAO FPRA was carried out supine within 24 hours of contrast studies using a multicrystal gamma camera. Contrast RVEF was measured from traced silhouettes using a single plane area-length formula. For FPRA, an RV region of interest(ROI) was obtained with an iterative technique which minimized count contributions from pulmonary artery(PA) and right atrium(RA). Only beats preceded by a complete diastolic phase were used. A background ROI was selected as a ring, 2 cm wide, immediately adjacent to the RV ROI but excluding the PA and RA. Background counts per pixel at end diastole(ED) were uniformly subtracted from the RV pixels. RVEF was calculated from the ratio of stroke volume counts to corrected ED counts. RVEF from FPRA correlated with contrast RVEF (r=0.74, SEE 6.5%) for a range of RVEF from 21% to 61%. Background counts were found to be directly proportional to observed counts at ED (mean 0.27 ± 0.06 of ED counts) so that

$$\text{EF corrected} = (1.37 \pm 0.11)\ \text{EF uncorrected}$$

RVEF from FPRA also showed high inter-observer reproducibility (r=0.93, SEE 2.9%). In conclusion, 1) RVEF from FPRA correlates acceptably with contrast RVEF, despite the limitations of contrast RV angiograms; 2) the values are highly reproducible; and 3) the proportionality between background and ED counts may eliminate the need for background ROI in the RAO view.

EFFECT OF VALVE REPLACEMENT ON LEFT VENTRICULAR FUNCTION AT REST AND DURING EXERCISE IN AORTIC VALVULAR INSUFFICIENCY. D.E. Manyari, P. Purves, W. J. Kostuk, University Hospital, London, Ontario.

Symptomatic patients (pts) with aortic valve insufficiency (AI) and subnormal resting left ventricular (LV) ejection fraction (EF), have been shown to improve both, their resting and exercise EF after aortic valve replacement. However only the resting, but not the exercise, EF returned to normal values indicating residual LV dysfunction. The effect aortic valve replacement on LV function in pts with AI and normal resting EF has not been reported. Therefore, we studied 8 pts with significant AI and normal resting EF, before and after aortic valve replacement using ECG-gated blood pool cardiac scintigraphy at rest and during supine bicycle exercise. Decisions for surgical treatment in this group of pts were made by the attending physicians and the surgeons, based upon symptoms allegedly from cardiac origin. The results were compared to those obtained in 20 normal subjects (N). In pts with AI the pre-operative (op) EF at rest was 61±2% (mean ±SEM) which was not statistically different from that in N (64±3). During exercise the EF decreased to 54±4 ($p < 0.01$) in pts with AI, which was markedly lower ($p < 0.001$) than the exercise EF in N subjects (72±3). After aortic valve replacement the resting EF was unchanged (62±4), but EF during exercise improved to 69±5 ($p < 0.01$) from pre-op values. The exercise post-op EF was indistinguishable from that in N subjects (72±3). Thus, the results of this study suggest that EF during exercise may be normalized by aortic valve replacement in pts with AI when surgery is performed before resting LV function has deteriorated.

COMPARISON OF THE VARIABILITY OF CONTRAST AND RADIONUCLIDE ANGIOGRAPHIC ESTIMATES OF HEART VOLUME. I.P. Clements, M.L. Brown, and H.C. Smith. Mayo Clinic and Mayo Foundation, Rochester, MN.

In 23 patients the inter-observer variability of left ventricular volumes assessed by radionuclide and contrast

angiographic techniques were compared. Contrast angiographic volumes were obtained from orthogonal biplane images. The count rate from gated blood-pool images using 99m-Tc labeled erythrocytes (background corrected) in the left ventricle, normalized for number of cardiac cycles processed, time per frame, isotope decay, and count rate in a 10 ml blood sample taken at equilibration (counted by the same Anger camera), exhibited a good correlation with the contrast angiographically determined end-diastolic ($r = 0.85$; S.E.E. = 28 ml) and end-systolic volume ($r = 0.94$; S.E.E. = 18 ml). Regression equations relating contrast angiographic volume (V) and normalized count rate (C) of $V = 68.7C - 3.8$ (end-diastole) and $V = 69.2C + 0.32$ (end-systole) were used to determine left ventricular volume by the radionuclide technique. Both radionuclide and contrast angiographic volumes were reassessed some months apart by different observers, and the change between the two estimates was similar and not significantly different ($P > 0.05$) with each technique (Table).

Δ Volume	Contrast	Radionuclide
End-diastole	9 ± 7 (0-23)*	16 ± 16 (1-65)
End-systole	8 ± 6 (0-23)	9 ± 9 (0-29)

* mean ± SD (range) ml

It is concluded that left ventricular volume obtained noninvasively by the radionuclide technique is accurate and subject to similar inter-observer error as the contrast technique.

Thirty-one patients (pts) resuscitated from out-of-hospital ventricular fibrillation (VF) who did not have acute myocardial necrosis (isoenzymatic criteria) had thallium (Tl) myocardial imaging within 9 hours after VF. Studies were repeated 1 week later in 22 pts. All studies were read independently by two observers.

On admission, 22 pts (71%) had Tl abnormalities (ABN), 6 of whom (27%) had in-hospital cardiac death; none of the 9 pts with a normal Tl scan had an in-hospital cardiac death ($p<0.005$). Of the 9 deaths, 6 were cardiac (congestive heart failure or arrhythmia) and 3 were neurological. All 6 of the cardiac death pts had an ABN Tl scan, as did one of the neurological death pts who had known coronary artery disease (CAD). In the 9 pts with normal Tl scans, only one had documented CAD (single vessel), two had suspected CAD, and 6 did not have CAD (4 cardiomyopathy, 2 accidents).

Of the 22 pts with repeated images, 8 scans improved which were initially ABN and 10 remained unchanged (7 normal, 3 ABN). In this group whose defects became smaller or were unchanged, there was subsequent in-hospital cardiac death in 1 (6%) versus 2/4 whose defects became larger ($p=.15$).

The improvement in myocardial blood flow patterns on serial studies in 8/15 (53%) patients presenting with abnormal images suggests that ischemia is associated with VF in about half of these pts. A primary electrical event may be the etiology in the remainder. In those pts without neurological death, a normal T1 myocardial scan on admission was associated with survival.

1:30-3:30 **ROOM E-1**

CARDIOVASCULAR VII: CLINICAL APPLICATIONS OF Tl-201

Moderator: Daniel S. Berman
Co-moderator: Gene B. Trobaugh

SERIAL THALLIUM IMAGING IN PATIENTS WITH UNSTABLE AND STABLE ANGINA: RELATIONSHIP OF MYOCARDIAL PERFUSION AT REST TO PRESENTING CLINICAL SYNDROME. K.A. Brown, H. Phillips, R.D. Okada, C.A. Boucher, H.W. Strauss, H.K. Gold, G.M. Pohost. Massachusetts General Hospital, Boston, MA.

Unstable and stable angina pectoris comprise a heterogeneous collection of clinical syndromes whose underlying pathophysiology is incompletely understood. To determine whether the different anginal syndromes are associated with differences in regional coronary blood flow at rest, serial myocardial thallium imaging at rest was performed in 19 patients with unstable angina presenting with rapidly worsening or new onset exertional symptoms (Group IA), 9 patients with unstable angina presenting with rest angina alone without exertional symptoms (Group IB), and 34 patients with chronic stable angina (Group II). Thallium imaging was recorded in the anterior and 45 degree left anterior oblique positions at 5-10 minutes and 2-3 hours after injection. No patient had had angina or ST depression within 2 hours of imaging or injection.

Transient defects were found on rest thallium studies in 100% (19/19) of patients in Group IA, compared with only 33% (3/9) of patients in Group IB ($p<.0001$), and 12% (4/34) of patients in Group II ($p<.0001$). Persistent defects were found in 80% (15/19) of Group IA, 89% (8/9) of Group IB, and 82% (28/34) of Group II (p=NS for all comparisons).

There was no significant difference among the three groups in distribution or severity of angiographic coronary artery disease or angiographic collateralization.

These findings suggest that: (1) In unstable angina patients with exertional symptoms, evidence of ischemia at rest is common, suggesting the presence of coronary artery lesions that are hemodynamically significant at rest. (2) In unstable angina patients with rest symptoms alone, evidence of ischemia at rest is uncommon in the absence of angina, suggesting a dynamic component of coronary artery disease. (3) In chronic stable angina patients, evidence of ischemia at rest is uncommon, consistent with their lack of rest symptoms. (4) Differences in rest regional coronary blood flow among the three groups of patients are not reflected in angiographic coronary anatomy or collateralization.

ACUTE THALLIUM MYOCARDIAL IMAGING FOLLOWING RESUSCITATION FROM OUT-OF-HOSPITAL VENTRICULAR FIBRILLATION. G.B. Trobaugh, J.L. Ritchie, B.W. Gross, J.A. Werner, H.L. Greene, G.W. Hamilton, L.A. Cobb. Harborview Medical Center, Seattle, WA.

DETECTION OF MULTIVESSEL CORONARY DISEASE AFTER TRANSMURAL INFARCTION USING STRESS ECG AND TL-201 IMAGING. M.E.Siegel, H. Ahmadpour, P. Colletti, and L.J. Haywood. LAC/USC Medical Center, Los Angeles, CA

Most patients surviving an acute myocardial infarction (MI) have diffuse coronary artery disease. Identification of these patients is important to their prognosis and management. This study assesses exercise ecg and Tl-201 imaging in detecting multivessel coronary disease (MVCD) in patients with prior MI.

Fifty patients with acute transmural MI's were studied. Six weeks post CCU discharge, patients had combined stress ecg/Tl-201 imaging. Tl-201 administered during stress was followed by immediate and 4-6 hour delayed imaging in three projections. Segmental analysis of images was performed for location and sizing of defects. One week later, coronary arteriography was performed.

37/50 patients had multivessel disease, > 50% stenosis, angiographically. Ecg detected 40%; reversible thallium defect detected 48%. Specificities were 92% and 84%. Combined Tl-201 and ecg detected 75% with a specificity of 76% and a positive predictive value (PPV) of 93%. 21/26 patients had previous inferior-posterior MI and MVCD. Sensitivity by ecg, Tl-201 and combined were 42%, 61% and 85%. Combined PPV was 94% with 80% specificity. 14/22 patients had prior anterior MI's and MVCD. Ecg and Tl-201 detected 42% and 35%. Combined results detected 64% with a specificity of 75% and PPV of 81%.

Combined exercise ecg and Tl-201 imaging can reliably detect the presence of significant multivessel disease after transmural MI. In our patients, Tl-201 imaging appears more sensitive in identifying significant coronary disease in patients with previous inferior MI compared to those with prior anterior MI.

CHANGES IN MYOCARDIAL PERFUSION AND LEFT VENTRICULAR FUNCTION AFTER PHYSICAL CONDITIONING. J. TUBAU, K. WITZTUM, D. JENSEN, E. ATWOOD, V. FROELICHER AND W. ASHBURN, UNIVERSITY OF CALIFORNIA, SAN DIEGO, CA.

Seventeen coronary patients (pts), were studied before and after 6 months of physical conditioning (C), using exercise Thallium (Tl) and radionuclide ejection fraction (EF). Myocardial perfusion (MP) changes were assessed by three observers comparing circumferential profiles (CP), from multiple views at peak exercise pre and post C. CP displayed the activity in percentage of the maximum, for 120 three degree sectors. Differences in CP, were considered significant when extended for at least an 18° sector. Each image was grossly divided into 6 equal regions related to coronary distribution. The maximum interobserver variability was 6% and the maximum differences pre/post C in 52 normal regions was also 6%; therefore, CP changes of

12% extending for at least 18°, were considered a significant alteration in MP. Of 159 regions available, total agreement occurred in 144 (90.5%). Although maximum double product was similar pre and post C, 11 regions (5 pts), improved and 2 (1 pt) worsened. The EF response to exercise (EFR) before C, was normal (NL) increasing by 11% in 4, flat (F) in 7 and severely abnormal (↓>4%), in 6 pts. Mean EF values, did not change after C whether at rest, .55 vs .53, or at peak exercise, .55 vs .55 (NS); but pts exercised to a higher workload, 791±214 vs 955±210 Kp (p<.001). Six pts improved their EFR, 9 did not change and 2 worsened Of 5 pts improving their Th,1 improved the EFR, 2 were already NL and of 2 who did not change, 1 increased the resting EF by 23%. One pt worsened with both techniques.

CONCLUSION: Changes in perfusion and left ventricular performance occur after C but are not always concordant. Further randomized controlled studies are needed.

MECHANISM OF IMPROVED DETECTION OF INDIVIDUAL CORONARY ARTERY STENOSES BY ADDITION OF QUANTITATIVE ASSESSMENT OF MYOCARDIAL WASHOUT TO ANALYSIS OF THALLIUM-201 SCINTIGRAMS
A. Abdulla, J. Maddahi, E. Garcia, J. Gutman, A. Waxman, A. Rozanski, D. Berman. Cedars-Sinai Med. Ctr., L.A., CA.

Mechanisms for myocardial Tl-201 (Tl) washout (W/O) abnormalities (abn) in the absence of perfusion defects (PD) reported with quantitative Tl analysis (QA) are not well understood. Thus, we studied 153 pts {94 with coronary artery (CA) disease, and 59 normals (nls)} undergoing QA of 3 view 10 min Tl scintigrams (Sc) obtained 6 mins and 4 hrs after stress. In 232 vessels with CAD, the sensitivity for detection of individual CA stenoses (S) (≥50%) was 64% by PD and increased to 78% (specificity 88%) by additional W/O analysis (p<.001). Isolated W/O abn was present in 32 myocardial segments (SEG), all supplied by diseased vessels, and all without prior myocardial infarction. Sc in 9/32 SEG also showed isolated W/O abn in the contralateral (CL) SEG, and CAs to these SEG revealed identical % S in 9/9 (balanced reduction of blood supply). QA in 13/32 showed PD+ W/O abn in the CL SEG, 12 of which were supplied by vessels with greater S than those supplying the SEG with W/O abn alone (imbalanced reduction of blood supply). The remaining 10/32 had no Q abn in the CL SEG. In these 10 SEG with W/O abn alone, the initial myocardial Tl profiles showed decreased counts compared to the CL SEG, but the degree of decrease was just within the range of nl (unappreciated PD) and all 10 were supplied by CAs with greater stenosis than those to the CL SEG. Thus, 1) mechanisms for absence of PD in ischemic myocardial segments with W/O abnormality are described and are mainly due to the relative nature of assessment of PD; and 2) being spatially nonrelative, additional analysis of % W/O significantly improves detection of ischemic myocardial segments.

QUANTITATIVE ANALYSIS OF Tl-201 MYOCARDIAL STRESS DISTRIBUTION AND WASHOUT IMPROVES THE IDENTIFICATION OF LEFT MAIN AND TRIPLE VESSEL CORONARY ARTERY DISEASE.
J. Maddahi, A. Abdulla, D. Berman, E. Garcia, A. Rozanski, A. Waxman, J. Forrester, H.J.C. Swan. Cedars-Sinai Med. Ctr., L.A., CA

To improve the suboptimal accuracy of visual (V) analysis of Tl-201 (Tl) scintigraphy (Sc) and exercise (Ex) ECG for detection of left main (LM), LM equivalent (E) and triple vessel (TV) coronary artery (CA) disease (D)(≥50% stenosis), we studied the ability of quantitative (Q) analysis of EX distribution (DIST) and 4 hr % washout (W/O) of Tl to identify these patients (pts) with high risk (HR) D. VTl, QTl, EX ECG, EX hypotension (↓BP), and CA angiography were compared in 108 consecutive pts with suspected CAD. HRD was present in 61 pts (14 had LMD, 1 LME, and 46 TVD) and 47 had either less extensive CAD (32) or normal (nl) CAs (15). Using sequential 3 view 10-min planar images, circumferential profiles of stress Tl DIST and % W/O were obtained and compared to previously determined lower limits of nl. EX ECG was considered positive for HRD if ≥2mm ST depression occurred in the 1st 6 mins of EX. With Sc, HRD was considered present if VTl or QTl were abnl in either combined anterior, septal, and posterolateral LV regions or in the regions of all 3 CAs. Sensitivity and specificity for detection of HRD pts were as follows:

	EX BP	EX-ECG	VTl	EX-ECG+VTL	QTl	EX-ECG+QTl
Sensitivity	20%	36%	16%	48%	64%*	79%*
Specificity	98%	96%	94%	89%	89%	85%

(*p<.01 vs others). For overall detection of CAD, all 61 HRD pts were detected as diseased by combined EX-ECG+QTl; however, individual pts were missed by all other test combinations. Thus, quantitative analysis of myocardial Tl stress distribution and washout significantly improves the noninvasive identification of pts with high-risk CAD.

VALUE OF THALLIUM-201 SCINTIGRAPHY WITH ONLY SUBMAXIMAL EXERCISE IN THE EARLY PREDICTION OF OUTCOME AFTER UNSTABLE ANGINA PECTORIS.
K.A. Narahara, M.C. Hillert, T.C. Smitherman, L.L. Burden. VAMC and UTHSC, Dallas, TX.

The clinical usefulness of Tl-201 scintigraphy (Tl) has been evaluated primarily with maximal exercise. We tested the predictive value of Tl with only sub-maximal exercise testing (SubMaxETT) in 25 patients (pts) whose unstable angina pectoris (UAP) had been stabilized on medical therapy. These pts underwent SubMaxETT-Tl 1-2 days before hospital discharge (dc). End points were: typical angina pectoris (AP), 1 mm ST segment depression (ST↓), ventricular ectopic activity (VEA), fatigue (F) or target heart rate (HR) of 120. No complications occurred.

The pts were then classified according to the worst anginal symptoms which occurred in the 12 wks after dc. Thirteen pts were in Functional Class (FC) I-II (Group A) and 12 were in FC III-IV (Group B).

	Group A	Group B	
SubMaxETT-Tl results:			
AP or ST↓	6/13	6/12	ns
F or HR	7/13	5/12	ns
VEA		1/12	
reversible Tl defect	2/13	10/12	p<.005

Conslusions: (1) SubMaxETT is sufficient to produce reversible Tl defects in a substantial fraction of pts tested after UAP (2) the presence of a reversible Tl defect with SubMaxETT is associated with a poor clinical outcome after UAP (3) the presence of a reversible Tl defect after SubMaxETT may define a group of pts who would benefit from early cardiac catheterization and possible coronary artery bypass surgery.

THE INDEPENDENT CLINICAL VALUE OF EXERCISE THALLIUM SCINTIGRAPHY.
M. Hlatky, E. Botvinick, B. Brundage. University of California, San Francisco, CA

To determine the effect of stress perfusion scintigraphy with Tl-201(SPS) on diagnostic accuracy and the use of coronary angiography (CA), 51 consecutive patients without prior myocardial infarction or other heart disease who had undergone SPS and subsequent CA were evaluated. After review of history, physical examination, and stress (S)ECG, patients were divided into 4 groups: 1-typical angina and a positive S-ECG; 2-typical angina and a negative S-ECG; 3-atypical angina and a positive S-ECG; 4-atypical angina and a negative S-ECG. For each patient, a single observer prepared a clinical summary in a uniform format, including a detailed history of the chest pain, risk factors, rest and S-ECG, and physiologic stress test data without interpretation. Each of 91 cardiologists were presented 8 patients, 2 different patients chosen at random from each of the 4 groups. The cardiologists first assessed the probability of coronary disease and the necessity for coronary angiography. They were then presented the results of SPS and revised their assessments if warranted.

With knowledge of SPS results, diagnostic accuracy improved significantly beyond the accuracy attained with history, physical exam, and S-ECG data (groups 1-3, p<0.0001; group 4, p<0.01). The amount of improvement was greatest in group 3, and lowest in group 4. Requests for CA were increased in groups 2 and 4 (p<0.01), unchanged in groups 1 and 3, decreased in patients without coronary disease, and increased in patients with coronary disease (p<0.001). Thus, SPS improved diagnostic accuracy in all clinical groups, while its impact on requests for coronary angiography depends on the specific clinical subgroup.

1:30-3:30 **ROOM D-1**

BONE AND JOINT

Moderator: N. David Charkes
Co-moderator: Vidya V. Sagar

Tl-201 SCINTIGRAPHY BY INTRAARTERIAL INJECTION IN BONE AND SOFT TISSUE LESIONS OF LOWER EXTREMITIES.
N. Tonami, K. Tomita, T. Michigishi, K. Koizumi, K. Kuwajima, K. Hisada, S. Hayashi, I. Shima and S. Nomura. Department of Nuclear Medicine and Orthopedic Surgery, Kanazawa University, Kanazawa, Japan.

Bone and soft tissue tumors can be sometimes visualized by intravenous injection of Tl-201-chloride. However, radioactivities in the lesions usually are not enough to evaluate. This came to the idea of the intraarterial injection of the agent from femoral artery (selective Tl-201 scintigraphy) to evaluate various bone and soft tissue lesions of lower extremities. This study was performed in 23 cases of 7 malignant tumors, 10 benign tumors and 6 inflammatory conditions. All of 7 malignant tumors showed intensive Tl-201 concentration corresponding to the lesion, whether there was any calcified tissue or not. Benign tumors with cellularity, such as osteoid, giant cell tumor and hemangioma showed positive, but not intensive concentration, while most tumors with cystic lesions, such as bone cyst, fibrous dysplasia did not show any apecific concentration. Most of inflammatory conditions such as osteomyelitis or fasciitis showed positive, but none of them showed intensitive concentration. The results obtained suggest that selective Tl-201 scintigraphy seem to have several advantages which are (1) it is useful to differentiate between malignant and benign lesions, (2) the degree of Tl-201 concentration reflects somewhat the local metabolic activity, cellularity and the vascular condition, (3) it gives a more accurate outline than that by Tc-99m MDP bone scintigram, (4) as it's an easy and fast technique, out-patient can have this examination.

COMPUTER-SIMULATED Tc-99m-MDP BONE SCAN CHANGES IN SOME SYSTEMIC DISORDERS. N.D.Charkes, P.T. Makler, Jr.,Temple University Hospital, Philadelphia, PA.

In earlier studies, we showed that computer modeling of skeletal tracer kinetics by compartmental analysis techniques can satisfactorily describe the time-varying distribution of tracer in normal bone, both in animals and in man. In this study we simulated changes in Tc-99m-MDP kinetics in some systemic disorders by perturbing appropriate intercompartmental rate constants, using a program written for a small digital computer. The bone-to-soft tissue ratio, a commonly used criterion of contrast, was calculated as a discrete time function for up to 6 hr postdose. The term "bone" is inclusive of exchangeable bone, bone extracellular fluid (ECF) and 10% of blood volume, summed and divided by estimated skeletal volume; "soft tissue" is the sum of 90% of the blood volume and non-bone ECF, divided by non-skeletal volume. In normals, contrast rises for 2 hr, then much more slowly for 4 more hr;the mean $\pm$ 20% was used to evaluate changes in disease states. Mild congestive heart failure (CHF) (cardiac output 0.5x nor with 25% edema) does not affect the scan, but marked CHF produces a low contrast scan up to 4 hr postdose. High cardiac output states do not affect contrast after 1½ hr. Edema greater than 25% produces a low contrast scan. As little as a 25% increase in skeletal avidity for MDP increases contrast and produces a "super-scan". Acute renal failure does not affect contrast but chronic renal failure can produce a low contrast study from 25% edema or a "super-scan" from a 30% increase in bone avidity for MDP. Conclusion: Computer simulation studies predict bone scan abnormalities in a variety of systemic disorders, suggesting an important role for modeling in scan interpretation.

BONE IMAGING IN PRE AND POSTOPERATIVE EVALUATION FOR HAND SURGERY. A.H. Maurer, D. A. Espinola, H. Rupani, L.E. Holder. Union Memorial Hospital and The Johns Hopkins Medical Institutions, Baltimore, MD.

We have performed three phase bone scans (TPBS) consisting of a radionuclide angiogram (RA), an immediate post-injection "blood pool" (BP) image, and 3-4 hour delayed images (DI) to assess various clinical problems encountered in a regional center for hand surgery. In order to evaluate the utility of TPBS we analyzed 132 consecutive TPBS. The normal pattern of a TPBS of the hand was established by examining patients sent for metastatic surveys or non-hand related pathology. The radial and ulnar arteries as well as flow through the palmar arch could be delineated by the RA. Blood flow to the digits was visualized in the RA and relative vascularity of the digits was assessed in the BP. Metabolic activity of the bones was evaluated in the DI.

Patients were referred for a TPBS for evaluation of pain of uncertain etiology (PUE), to preoperatively assess the vascularity of suspected lesions, and postoperatively to assess graft patency and viability. A final diagnosis was established for 63 patients with surgery and arteriography (n=44), by arteriography alone (n=1), and by clinical course (n=18). Specific vascular patterns were correctly recognized for aneurysms, hemangiomas, arteriovenous malformations, radial or ulnar artery occlusion, and digital artery spasm or thrombosis in 21/24 cases. Post traumatic or post surgical graft patency and viability was correctly diagnosed in 13/13 cases. A correct diagnosis was made in 18/20 cases of PUE. Overall accuracy of TPBS was 92%. We conclude that the TPBS is a valuable technique for diagnosing clinical problems that present in a hand surgery center.

EVALUATION OF THREE PHASE BONE IMAGING IN SUSPECTED OSTEOMYELITIS. A.H. Maurer, D.C. Chen, E.E. Camargo, H.N. Wagner Jr. and P.O. Alderson. The Johns Hopkins Medical Institutions, Baltimore, MD.

It is often difficult to separate nonosseous inflammatory disease from osteomyelitis scintigraphically. In this study we have attempted to evaluate the utility of performing a three phase bone study consisting of a radionuclide angiogram, an immediate post injection "blood pool" image and 2-3 hour delayed images for patients (pts) with suspected osteomyelitis. We analyzed 223 consecutive three phase bone studies performed on pts with suspected osteomyelitis. A final diagnosis was established for 98 pts using biopsy material (n=10), joint fluid cultures (n=6) or clinical course and x-rays (n=82).

The value of performing a three phase bone study was evaluated by first interpreting only the delayed images, next the combination of delayed images and "blood pool",and finally the three phase bone images. In 20 of 64 (31%) pts with abnormal studies the "blood pool" image and/or radionuclide angiogram resulted in an improved scintigraphic diagnosis. In 11 of 64 (17%) pts the "blood pool" alone led to the correct diagnosis and was most helpful in identifying noninfectious skeletal disease. In 9 of 64 (14%) pts the radionuclide angiogram was essential for an accurate diagnosis, particularly in cases of soft tissue infection. There was no change in the sensitivity for detecting osteomyelitis (92%) but the specificity improved from 75% using the delayed images alone to 92% using three phase bone imaging. Diagnostic accuracy improved from 69% using delayed images alone to 90% using three phase bone imaging. Both the radionuclide angiogram and "blood pool" images augmented the accuracy of bone imaging in pts with suspected osteomyelitis.

SCINTIGRAPHY VS. RADIOGRAPHY IN THE DIAGNOSIS OF STRESS FRACTURES OF THE HEEL. R.L. Laughlin, F.H. Gerber, and R.B. Greaney. Balboa Naval Hospital, NRMC, San Diego, CA

The diagnosis of stress fracture has rested on the presence of classic x-ray changes. As part of a larger project we have evaluated bone scan and x-ray findings in the heels of 95 Marine Recruits of which 43 had 2 or 3 exams at 2-4 wk. intervals. These 43 had 73 focal scan abnormalities of the calcaneus on initial exam, 60 with normal x-rays. The table shows results of follow-up radiographs as compared to initial findings. In each case initial and follow-up scans were focally abnormal.

Initial X-ray	Follow-up X-ray		
	Normal	Subtle	Classic
Normal	9	17	26
Subtle	0	4	8
Classic	0	0	9

Previous investigations have suggested that the diagnosis of stress fracture can be made by scintigraphic findings, however, sequential radiographic and scintigraphic comparison was incomplete. We found that many patients with persistently abnormal scintigrams progressed through a spectrum of radiographic changes ranging from normal, to previously unrecognized subtle changes, and finally to the classic findings of stress fracture. In our group of patients, 70% (51/73) showed such progression on follow-up studies while the scintigrams remained focally abnormal. Based on this experience we feel that radiography is a relatively insensitive indicator of the presence of acute stress fracture and that a focally abnormal bone scintigram accompanied by a normal radiograph in a patient with a clinical history for stress fracture establishes the presence of the disease.

ROTATING SLANT HOLE TOMOGRAPHY OF THE HIP. D.G. Pavel, C. Meyer-Pavel, D. Mess, J.Zwirowski, B. Patel, E. Byrom R. Barmada. University of Illinois Medical Center, Chicago

Due to the hip structure, the superimposition of normal and abnormal areas is common. This fact generates difficulties in the evaluation of planar images. The rotating slant hole tomography (RSHT) appears particularly suited for the hip because of its wide field of view close to the collimator face, simplicity and low cost. We have evaluated the feasibility of routine hip RSHT on 31 patients. A portable camera was used as close as possible to the hip area. Each acquisition had 6 rotations of the collimator, 60° apart. Each of the 6 views required 2 minutes for an average value of 130K/each. The reconstruction was started routinely at 3cm from the collimator and in obese patients at 5cm. A total of 12 planes was generated of 1cm thickness each. Results: In all but two of the patients the quality of the images was very good. The 2 suboptimal cases were probably due to motion and excessive bladder activity. The normal ilieofemoral joint showed a clear delineation of the semicircular contour of the acetabulum in at least 1 or 2 planes and the femoral head area appeared homogeneous or with a smooth transition towards decreased concentration in the upper and lateral aspect, particularly in elderly patients. The abnormal joints enabled a very precise separation of areas of decreased, absent or increased uptake. In particular, the areas of necrosis surrounded by reactive bone were unequivocally elicited as such. While most of the abnormalities detected were seen on the planar images as well, the details , the contrast and the depth information were clearly superior on RSHI. The clinical significance and usefulness of this additional information is under evaluation.

TC-99m MDP SKELETAL SCINTIGRAPHY FOR EARLY DETECTION OF STRESS FRACTURES IN SOLDIERS: L.D. Samuels and I.Shaskolsky Depts. of Medical Biophysics and Nuclear Medicine and Radiology, Hadassah University Hospital, Jerusalem, Israel.

Stress fractures in healthy young adults have often been overlooked because of the early absence of roentgenographic findings, yet early diagnosis of stress fractures is imperative to prevent serious complications due to continued stress. Because of this, we have studied the role of MDP bone scanning for the early diagnosis of stress fractures in soldiers who complained of pain, usually after strenuous marching. Skeletal scintigraphy was performed three to four hours after IV injection of 15-20 mCi Tc-99m MDP. Initial scans were performed within hours to days of onset of pain and followed by later scans after 3-12 weeks when possible. Scan findings were correlated with roentgenographic findings and with clinical course. In an initial series of thirty soldiers, scans in nineteen soldiers showed clear evidence of one or more lesions, characteristic of stress fractures, although the majority of these men did not have positive roentgenographic findings, in agreement with other investigators. In a few patients there was later evidence of callus on followup Xrays, but this was unusual if treatment has begun promptly. We conclude that skeletal scintigraphy is a very sensitive method for early diagnosis of stress fractures, that skeletal scans should be mandatory when patients complain of severe leg pain after heavy exercise and that when scans are positive for stress fracture appropriate therapy must be given whether or not Xrays are positive, since roentgenography alone is not a reliable method of diagnosis, nor is it required to confirm the scintigraphic diagnosis.

SCINTIMAGING OF SKELETAL INFECTIOUS PROCESSES WITH A NEW LEUKOCYTE LABELLING TECHNIQUE UTILIZING IN-111 ACETYL-ACETONE. H.N. Wellman, P. Giorgi, H. Sinn, and K. Scheer. IUMC, Indianapolis, IN and DKFZ, Heidelberg, FRG.

Leukocytes can be labelled readily by acetyl-acetone and In-111(In-111 AAL) with high efficiency (80%) and viability (90%) as evidenced by vital stain and mobility tests, not requiring absolute alcohol or oxine use. In vivo normal distribution of viable In-111 AAL consistently demonstrates predominate uptake in liver with lesser amounts in spleen and bone marrow and absent uptake in lung. A high purity leukocyte preparation for labelling is paramount and is accomplished with initial dextran separation and differential density gradient centrifugation separations with metrizamide to especially eliminate reticulocytes. Because of the reported uptake of Ga-67 citrate in reactive bone formation, such as in osteomyelitis (OM), differentiation of skeletal infectious processes may be difficult. Thus In-111 AAL have been utilized in a population of 97 patients suspect of skeletal infectious processes with positive conventional Tc-99m MDP bone scans.

Of the patients, 79 have had pathological confirmation. Imaging of the involved skeletal sites and liver-spleen region was performed with a large crystal multi-photopeak γ camera 24 hr. after 3mCi In-111 AAL IV. Six clinical groups of differing skeletal infectious processes were studied, with 21 true and 3 false positives and 21 false and 34 true negatives for a sensitivity of 50%, a specificity of 92%, and accuracy of 70%. The high specificity complements the high sensitivity of conventional bone imaging.

Best results were obtained in post-, trauma, surgery and prosthetic and joint infectious processes. An interesting finding of complementarity of In-111 AAL contiguous uptake to bone imaging abnormalities was consistently observed.

1:30-3:30 **ROOM G-1**

GI II: ESOPHAGEAL AND GASTRIC FUNCTION

Moderator: Manuel L. Brown
Co-moderator: Edward A. Eikman

RADIONUCLIDE TRANSIT (R.T.) - NON-INVASIVE TEST FOR ESOPHAGEAL MOTILITY DISORDER. C.O.H. Russell, E.R. Holmes, F. Allen, D.A. Hull, L.D. Hill. Mason Clinic, Seattle, WA.

Esophageal motor function is generally assessed by radiology and manometry. The former often fails to detect abnormality and the latter is invasive and has low patient acceptance. We have tested the hypothesis: radionuclide transit studies are a sensitive test of esophageal motor function.

A homogenous bolus of 250μCiTc sulfur colloid in 10 ml of water was swallowed while in the supine position under a low energy all-purpose collimator of a gamma camera linked to a microprocessor. Transit of 3 such boluses was recorded at 0.4 sec. intervals. The esophageal area was divided into 3 equal areas of interest which were then analyzed graphically using counts (representing volume) against time. A low compliance, high fidelity esophageal manometry system was used to record peristalsis of wet swallows (10 ml).

A) Control group (20 volunteers). The R.T. graphs showed 3 sequential peaks of activity (proximal, middle and distal) in all cases demonstrating smooth coordinated bolus transit in <15 seconds. B) Patients with obvious motility disorder by manometry and radiology (n=15). All cases demonstrated transit time (>15 sec) and the graphs described the functional problem in most cases. C) Dysphagia patients (n=24). Obstruction was excluded in all cases. The incidence of abnormality by R.T. was 19/24 (79%) and 12/19 (63%) by manometry. The correlation between test results was positive ($P<0.05$).

Radionuclide transit studies are a safe, non-invasive alternative for studying esophageal motor function and has a sensitivity at least equal to that of manometry.

MEASUREMENT OF ESOPHAGEAL MOTOR FUNCTION. JW Ryan, B Brunsden, G O'Sullivan, P Kirchner, T DeMeester, and M Cooper. The University of Chicago Hospitals, Chicago, IL.

Recent studies using digital processing techniques show that there are critical and limiting factors which must be considered when using scintigraphic approaches to esophageal motor function. These are (1) attenuation, (2) temporal resolution, (3) physical form of bolus, and (4) patient position. Each factor has been assessed using an LFOV camera, parallel-hole collimator, a positioning frame, and a microprocessor for digital processing from list mode. Three 150 μCi Tc-99m radiolabelled boluses consisting of water (15cc), pudding (10cc) and gelatin capsule with water were swallowed. Studies were performed in both supine and upright positions using all three materials with frame rates of 0.15 sec and 3 ROIs over esophagus and stomach.

Results of attenuation and temporal resolution studies in normal volunteers and patients with achalasia show esophageal clearance is not exponential but is an intermittent linear or step function. Supine studies revealed abnormalities not evident when upright. Clearance of pudding in both positions was markedly different from water and the capsule studies revealed a rebound phenomenon not previously described. In achalasia using a water bolus a "shuttling" phenomenon also not previously described was clearly evident using ROI analysis. In one patient with aspiration induced recurrent pulmonary infiltrates, delayed clearance with "shuttling" was the only evidence of esophageal dysmotility. These studies reveal that a posterior view is essential (attenuation), fast frame rates are necessary to accomodate bolus transits as short as 0.15 sec and various patient positions using different bolus materials are required to quantitate normal and abnormal esophageal motor functions.

EFFECT OF VOLUME ON GASTRIC EMPTYING: A NEW THEORY, AND A STUDY BY RADIONUCLIDE TECHNIQUES. Richard P. Spencer, Dept. Nuclear Medicine, University of Connecticut Health Center, Farmington, CT.

Gastric emptying does not follow "steady state" kinetics, but initial events can be approximated by an effective $T_{\frac{1}{2}}$. The effects of different meal volumes on emptying $T_{\frac{1}{2}}$ have been little studied. We devised a conceptual model and checked it against literature data as well as on volunteers (informed consent). As the size of the meal increases, retention should increase. Thus $T_{\frac{1}{2}} \sim$ a function of amount ingested. The stomach is a muscular organ; it contracts against a surface of ingested materials (related to the amount A, raised to a power p). With a proportionality constant, this can be written in logarithmic form as: $\log T_{\frac{1}{2}} = \log k + p.\log A$. A similar expression can be derived from the Nelson-Kohatsu gastric pressure/volume law if duodenal pressure is small. A log plot of $T_{\frac{1}{2}}$ should be a linear function of log (amount ingested). Depth-corrected gastric emptying data of Christian et al (J. Nucl. Med. 21:883, 1980) were plotted for meal sizes of 300, 900, and 1,692 grams. Results. 1. The three points for the solid meal form a line on the log-log plot. 2. The points from the liquid meal also form a line. 3. These 2 lines are parallel (they are displaced by a multiplying constant). This suggests that once solids are liquified, they can not be distinguished from the liquid phase. 4. The value of the exponent is about 0.75. Our data on low and high volume meals in normals tend to confirm these findings. By use of 2 distinct volumes, it may be possible to more accurately assess gastric emptying with radionuclide techniques.

Tc-99m-OVALBUMIN LABELED EGGS:COMPARISON WITH OTHER SOLID FOOD MARKERS IN VITRO. L.C.Knight and L.S. Malmud. Temple University Hospital, Philadelphia, PA.

A radiolabeled solid food marker for gastric emptying studies should be physiologic and the label should not dissociate from the solid phase. Labeling the liver of a live chicken by systemic injection of Tc-99m-sulfur colloid (in vivo Tc-SC-CL) provides a good label, but handling live chickens is inconvenient and some patients refuse a liver meal. We have labeled ovalbumin, the major constituent of egg white, in a effort to develop a labeled egg meal.

Commercial ovalbumin (OA), labeled with Tc-99m by an electrolytic technique, was added to a beaten whole raw egg and cooked. This label was compared for stability with eggs labeled by adding common technetium radiopharmaceuticals (Tc-SC,Tc-MAA,Tc-HSA) to beaten eggs before cooking them. In vivo Tc-SC-CL was also evaluated. Labeled foods were agitated in warm 0.1N HCl or gastric juice. Aliquots of each suspension were removed to test for dissociation of label by filtration through thin glass wool or by centrifugation at 640xg.

In 0.1N HCl, all labels were highly stable. In gastric juice,the in vivo Tc-SC-CL was the most stable (1% dissociation/3hr). Tc-OA-egg and Tc-SC-egg were of approximately equal stability (5-14% dissociation/3 hr). Tc-MAA-egg appeared of similar stability, but this may be misleading as Tc-MAA also sticks to glass wool and is centrifuged down without egg present. Tc-HSA-egg was the least stable (26-35% dissociated/3 hr).

We conclude that while in vivo Tc-SC-CL is the firmest label for solid food in gastric juice, Tc-OA-egg and Tc-SC-egg are sufficiently stable to be regarded as more clinically optimal agents.

THE INCREASED SENSITIVITY OF SOLID SCINTIGRAPHIC GASTRIC EMPTYING. H.A. Goldstein, A. Alavi, W.J. Snape. Hospital of the University of Pennsylvania, Philadelphia, PA.

This investigation reviews 11 patients with vomiting and/or epigastric pain who had scintigraphic gastric emptying with both solid and liquid meals. These were patients with gastroparesis (diabetic and idiopathic), gastric outlet obstruction, scleroderma, or irritable bowel syndrome.

All patients fasted before the study. The liquid meal consisted of 150 cc orange juice, 150 cc normal saline, and 100-250 uCi Tc-99m sulfur colloid. The solid meal consisted of 100-250 uCi Tc-99m sulfur colloid in 100 cc of cooked egg albumin. After the test meal the patient was imaged for 60 minutes in the supine position. The percent gastric emptying (decay corrected) was plotted using a computer.

In all patients, the gastric emptying was less with the solid meal (mean: 26.6 ± 25.9%) than with the liquid meal (mean: 62.1 ± 23.3%). Both the solid ($p < .001$) and liquid ($p < 0.05$) emptying was significantly reduced from normal gastric emptying, (67 ± 19%) and (79.5 ± 10.6%) respectively for these meals. Of six patients with normal liquid gastric emptying, four had reduced solid gastric emptyings, while two had normal values, albeit less than the liquid gastric emptying. The severity of decreased solid emptying was unrelated to the value of the liquid emptying.

The technique of scintigraphic gastric emptying with a solid meal provides a more sensitive indicator of decreased gastric motility than with a liquid meal.

LOSS OF LIQUID-SOLID DISCRIMINATION IN GASTRIC EMPTYING OF AGED SUBJECTS: F.L. Datz, P.E. Christian, and J.G. Moore. University of Utah Medical Center, Salt Lake City, UT.

The purpose of this study was to evaluate the effect of aging on gastric emptying rates in man. Eight healthy young men (mean age 32.3 years, range 25-43) and ten aged men (mean age 76.4 years, range 71-88) were studied. All denied a history of gastrointestinal disease or diabetes, and none were taking any medications. Subjects were given a standardized 900 gm meal (total caloric value = 621 Kcal; 81% carbohydrate, 14% protein, 6% fat; liquid-solid ratio = 1). Chicken liver labeled with Tc-99m SC (600 μCi) and In-111 DTPA (100 μCi) were used as the solid and liquid-phase markers, respectively. Images were obtained at 30 minute intervals on a gamma camera interfaced to a computer. The data was corrected for radioactive decay, attenuation, and the effect of depth within the body.

Liquid-phase emptying was significantly more rapid than solid-phase in the young group (liquid $T_{\frac{1}{2}} = 82 \pm 13$ min.; solid $T_{\frac{1}{2}} = 145 \pm 28$ min.; $p < .02$). Liquid-phase emptying described a curvilinear pattern whereas solids displayed a linear pattern. However, in the aged group no statistically significant difference was observed in liquid versus solid-phase emptying rates (liquid $T_{\frac{1}{2}} = 100 \pm 9$ min.; solid $T_{\frac{1}{2}} = 117 \pm 24$ min.; $p > .05$). Both liquid and solid-phase emptying described in a linear pattern.

We conclude a defect exists in liquid-solid discrimination in the gastric emptying pattern of aged subjects

manifesting itself primarily as a delay in liquid-phase emptying.

QUANTITATIVE GASTRO-CHOLECYSTOSCINTIGRAPHY-EFFECTS OF VARIED MEALS. E.Rock, L.S.Malmud, Z.Rattner, R.S.Fisher. Temple University Hospital and Medical School, Philadelphia, PA.

Previous studies have demonstrated that meals of various physical and chemical composition affect both gastric and gallbladder (GB) emptying. The purpose of this study was to quantitate the response of the stomach and GB in man to monocomponent meals of fat, carbohydrate (CHO), amino acids (AA), saline and multicomponent mixed solid or mixed liquid meals. This technique involves simultaneous GB and gastric scintigraphy using a Tc-99m HIDA derivative and In-111 DTPA meal, respectively.

During the first 90 minutes, both gastric and GB emptying were slower in response to the mixed solid meal in comparison to the mixed liquid meal. Beyond that time, the maximal GB response was similar for both the solid and liquid meals. GB and gastric emptying rates in response to isovolumic, isocaloric, monocomponent fat meals did not differ significantly from the mixed liquid meals. By contrast, the maximal GB response to a 5% or 50% CHO meal and to the AA meal were 34.6±9.1 (P<.01), 43.0±8.4 (P<.01), and 38.6±.2% (P<.01) respectively in comparison to the mixed meal. The gastric emptying rate was more rapid for the 5% CHO, than for the 50% CHO meal. No significant GB emptying was observed following a normal saline meal ingested orally. However, a 2.5% saline meal resulted in a maximal response of 33.1±8.9% (P<.01).

In conclusion, these studies suggest that GB emptying is a complex phenomenon, and a function of gastric emptying, as well as, of the physical and chemical composition, osmolality, and caloric content of the ingested meal. Scintigraphic techniques permit the quantitation of these phenomena non-invasively in man.

QUANTITATIVE CHOLECYSTOSCINTIGRAPHY - CHOLINERGIC EFFECTS. R.S.Fisher, E.Rock, Z.Rattner and L.S.Malmud. Temple University Hospital and Medical School, Philadelphia, PA.

Gallbladder function may be quantitatively approximated scintigraphically using the Tc-99m HIDA agents and a gamma camera on line to a computer. The purpose of this study was to determine the effect of cholinergic stimulation of the gallbladder, using bethanechol or sham feeding; and to compare cholinergic stimulation to cholinergic blockade by atropine or vagotomy. A total of 48 subjects was studied using 5mCi Tc-99m-Pipida administered intravenously. Of these 35 were normal asymptomatic volunteers and 13 were patients who had previously undergone vagotomy for peptic ulcer disease.

Following oral administration of a 315ml standard liquid meal containing 36gm carbohydrate, 10gm protein and 20gm fat, the maximal gallbladder response was 77.9±3% compared to almost no gallbladder emptying over two hours without a meal stimulus.

Cholinergic blockade by atropine following the standard meal reduced maximal gallbladder emptying to 56.6±9% (P<.01), while vagotomy reduced gallbladder emptying to 60.2±7% (P<.01). In the absence of the meal, bethanechol induced gallbladder emptying of 25.1±6.4%, while sham feeding induced 61.4±6.6% emptying (P<.05).

In conclusion, cholescintigraphy has been employed to demonstrate the effects of cholinergic and anticholinergic stimulation on gallbladder function. Cholinergic blockade by atropine or surgical vagotomy decreases gallbladder emptying, while cholinergic stimulation increases gallbladder emptying both by sham feeding and to a lesser degree by urecholine administration.

1:30-3:30 **ROOM A-1**

SYMPOSIUM AND WORKSHOP ON EMISSION TOMOGRAPHY

Moderator: Thomas F. Budinger
Co-moderator: Michael E. Phelps

"PHYSICS, ENGINEERING, COMPUTER SCIENCE ASPECTS AND DETECTOR TOPICS"

PHYSICAL ATTRIBUTES OF EMISSION TOMOGRAPHY FOR MEDICAL SCIENCE. T. F. Budinger, University of California, Berkeley, CA.

DETECTOR CONSIDERATIONS IN SINGLE PHOTON TOMOGRAPHY. W. J. MacIntyre, Cleveland Clinic Foundation, Cleveland, OH.

DETECTORS, SAMPLING, SHIELDING, AND CIRCIUTS OF PETT. S. E. Derenzo, University of California, Berkeley, CA.

EMISSION TOMOGRAPHY WORKSHOP

"DATA ACQUISITION AND PROCESSING ARCHITECTURE FOR MULTIPLANE ECAT"

Moderators: Thomas F. Budinger and Michael E. Phelps, University of California, Los Angeles, CA.

Participants:
C. Williams, ORTEC, Inc.
L. Carroll, Cyclotron Corporation
C. Thompson, Montreal Neurological Institute
D. Ficke, Washington University
J. Blaine, Washington University
N. Mullani, University of Texas
J. Keyes, University of Michigan
A. Jaszczak, Duke University

THURSDAY, JUNE 18, 1981

8:30-10:00 **ROOM B-1**

CARDIOVASCULAR VIII: SPECIAL STUDIES

Moderator: Richard N. Pierson, Jr.
Co-moderator: J. Peter Lavender

MYOCARDIAL IMAGING IN HUMANS WITH I-123-PALMITIC ACID. R. Kline, H. Rizi, T. Mangner, M. Besozzi, J. Thrall, D. Swanson, J. Copp, L. Brown, W. Beierwaltes. University of Michigan Medical Center, Ann Arbor, MI.

I-123-ω-palmitic acid [IPA] (16-iodohexadecanoic acid) is potentially useful as a clinical imaging agent because it can be readily synthesized in an analytically pure form from the commercially available alcohol juniperic acid. By comparison, the purification of 16-iodo-9-hexadecenoic acid (which has been characterized as a myocardial imaging agent in humans) is complicated by commercial unavailability of a pure precursor and by the presence of cis- and trans-isomers.

In order to establish the imaging characteristics of IPA, 10 normal volunteers were studied. After the intravenous injection of 3.0 mCi IPA, 30 sequential 1-minute images were obtained for each subject in the 40° LAO projection. Following interpolated background subtraction, time-activity curves were generated from a region of interest over the left ventricle.

Myocardial images were comparable in quality to thallium images. Mean peak target:background ratio was 2.3:1 (range 2.0-3.0, ± 0.3 SD). Mean peak accumulation of IPA activity in the left ventricle was at 6.7 min (range 4.0-9.0, ±2.0 SD). Mean myocardial halftime from peak was 22.1 min (range 17-25, ±2.8 SD). Linear regression analysis of the period from 9 to 32 minutes post injection revealed linearity with $-.93 \leq r \leq -.98$.

Myocardial time activity curves generated from background subtracted IPA images reflect myocardial metabolism. IPA imaging should prove useful in the characterization of myocardial disease states with deranged fatty acid metabolism.

INDIUM-111 PLATELET SCINTIGRAPHY FOR THE DIAGNOSIS OF LEFT VENTRICULAR THROMBI; OPTIMUM VIEW AND IMAGING TIME AFTER INTRAVENOUS INJECTION OF PLATELET SUSPENSION IN A SURGICALLY VERIFIED SERIES. M.D.Ezekowitz, E.W.Allen, R.W.Burow, S.W.Herren, Department of Medicine, University of Oklahoma Health Sciences Center, Oklahoma City, OK.

Imaging patients for cardiac thrombi in multiple views on consecutive days following injection of the platelet suspension consumes a considerable amount of camera and technician time. Therefore, the purpose of this study was to determine the optimum view and time (from injection of the platelet suspension) for scintigraphic study of cardiac thrombi. The patient population consisted of 22 patients with LV aneurysms located in the apical or anterior LV. All patients required aneurysmectomy and had the platelet suspension injected 6 days prior to aneurysmectomy. Thus, both surgical confirmation and proof by direct tissue analysis of the scintigraphic diagnosis was possible in every case. Each patient was imaged daily or on alternate days in the LAO, RAO, anterior or L.lateral views. For analysis, images were randomized with respect to view, patient identity and time. All images were interpreted by 3 blinded observers. Sensitivity and specificity was determined for each observer for each view and time. The optimum sensitivity and specificity for observers 1 and 3 was found in the LAO view on day 4 following injection of the platelet suspension and was 82 and 70% for sensitivity and 100% for specificity. Observer 2 recorded a maximum sensitivity on day 2 (76%;LAO view) and specificity day 3 (84%;LAO view). Thus, we conclude that: 1) the optimum view for imaging was the LAO view with the optimum imaging time being between day 2 and 4 following injection of the platelet suspension; 2) the diagnostic accuracy is not enhanced by obtaining multiple views on other days.

NONINVASIVE RADIOISOTOPIC TECHNIQUE OF QUANTIFICATION OF PLATELET DEPOSITION IN EXTRACARDIAC CONDUITS IN HUMANS. K.C. Agarwal, M.K. Dewanjee, R.H. Feldt, H.W. Wahner, J.S. Robertson, M.L. Brown, V. Fuster, J.H. Chesebro, M.P. Kaye, F.J. Puga, G.K. Danielson. Mayo Clinic and Mayo Foundation, Rochester, MN.

In right-sided extracardiac conduits inserted for surgical correction of certain congenital heart defects, obstruction is a significant late complication requiring conduit replacement. Our histopathologic study indicates a significant role of platelets in the pathogenesis of conduit obstruction. This study was designed to evaluate the feasibility of imaging procedure with 111-Indium-labeled platelets to localize and later quantify platelet accumulation in the conduits. Four patients with pulmonary atresia and 1 with truncus arteriosus underwent conduit placement, 2 with and 3 without porcine valve. Autologous platelets collected from 43 ml of blood were labeled with 111-Indium-oxine in ACD-saline medium (labeling efficiency 50-60%). 400-500 uCi of autologous 111-Indium-labeled platelets were administered intravenously immediately after surgery in 4, and five days after surgery in 1 patient. Imaging was performed at 6 hours and daily for 1-4 days using a portable Picker gamma camera interfaced with a computer and fitted with medium-energy parallel hole collimator. Platelet deposition was noted at the site of the conduit in all 5 patients. Maximum accumulation (0.1-0.3% of injected dose) of platelets was seen within the first 24 hours. Activity over blood pool and lungs declined and over liver and spleen increased in a predictable manner over the imaging period. This technique has potential use as a noninvasive quantitative tool to study the effect of platelet inhibitor drugs in preventing platelet deposition and possibly conduit obstruction.

THE AVALANCHE RADIATION PROBE: MONITORING OF REGIONAL MYOCARDIAL BLOOD FLOW AUTOREGULATION IN SMALL VOLUMES IN VIVO. R. P. Karlsberg, V. L. Gelezunas, H. N. Konchigeri, K. P. Lyons. VA Hospital, Long Beach, Univ. of Ca., Irvine .

A miniature, solid state, avalanche radiation probe (ARP), has been developed for measurement of regional myocardial blood flow. Since the device is sensitive only to low penetrating radiation which travels short distances in tissue (0.01 to 1 cm) enhanced spatial resolution has been achieved. Flow measurements with ARP correlate to radioactive microsphere measurements in 0.3 gm biopsies. We tested the linearity of the ARP over a wide range of myocardial blood flows and the detector efficiency as a function of distance in 5 open chest dogs. Blood flow alterations were produced by adenosine (0.1 to 1 mg/Kg), a metabolic vasodilator, and by reactive hyperemia after temporary coronary occlusion (15 sec to 2 min). Regional flow measured with ARP from the washout of intracoronary injected Xenon-133 was compared to coronary flow measured with electromagnetic meters (EM). Regional flow ranged from 40 to 120 ml/min/100 gm before adenosine or hyperemia. The average increase in flow after adenosine (200±30%) was similar to the increase in flow during hyperemia (220± 20%) when measured regionally with ARP or proximally with EM (230±40% vs 210±20% SEM). ARP flow correlated to EM flow (r=0.87±.05). The calculated detection volume was approximately one-half cubic centimeter. We conclude that adenosine can reproduce the highly regional changes in flow seen with reactive hyperemia. This new device allows repetitive monitoring of myocardial flow in vivo in small volume during autoregulatory phenomenon and is linear over a wide range.

THE DISTRIBUTION OF CARDIAC OUTPUT IN MAN RECORDED BY INTRAVENTRICULAR INJECTION OF MICROSPHERES. J.P.Lavender, A.Maseri, G.J.Davies, B.Oliveira, D.Sugrue and M.Myers, Hammersmith Hospital and Royal Postgraduate Medical School, London, England.

There are few records of the distribution of cardiac output in man in contrast to data on blood flow to individual organs. Little is known about re-distribution of cardiac output in states of poor left ventricular function. The purpose of this study is to record such distributions using intraventricular injections of labelled microspheres. Approximately 4 x 10^6 microspheres of mean diameter 15 microns were labelled with technetium 99m and injected into the left ventricle in 7 patients undergoing angiography for investigation of myocardial pathology. Cardiac output was determined by Fick principle. Static planar views and tomographic reconstruction of the myocardial distribution of radioactivity were used for diagnostic purposes. Whole body emission and transmission scans were used to calculate the distribution of radioactivity throughout the body. Transmission scans using cobalt 67 were used for correcting attenuation on the emission images. Comparison of calculated to actual retained activity showed relative error of ± 5.6%. Myocardial images of high quality showed focal defects in 4 and normal myocardium in 3. Mean blood flow to the myocardium was 4.8%, cardiac output 232 ml per minute, (range 156 - 406). Cerebral flow was 14.8%, 578 ml per minute; to the spleen 6.0%, 293 ml per minute, and to the left kidney 9.9%, 477 ml per minute. This method, therefore, allows images of myocardial perfusion as well as measurements of blood flow distribution throughout the body.

ENDOTHELIAL PERMEABILITY AND C-14- AND I-131-CHOLESTEROL UPTAKE OF AORTOCORONARY FEMORAL VEIN BYPASS GRAFT IN DOGS. M.K. Dewanjee, N. Shapira, M. Tago, V. Fuster, and M.P. Kaye. Mayo Clinic and Mayo Foundation, Rochester, MN.

Eighteen dogs underwent aortocoronary femoral vein bypass graft surgery. All dogs were injected with 300 µCi of I-131-iodocholesterol and 100 µCi of C-14-cholesterol and sacrificed 24 hours postoperatively: group I dogs, 1 day; group II dogs, 3 days; group III dogs, 7 days; and group IV dogs, 1 year after surgery respectively. Radioactivity in blood, grafted femoral vein (GFV), control femoral vein (CFV), femoral artery, aorta and vena cava were determined with Beckman gamma and beta counters. The GFV/CFV and GFV/blood ratios of these two cholesterol tracers in three groups are tabulated:

	I:1-day (n=5)	II:3-days (n=5)	III:7-days (n=5)	IV:1-yr (n=3)
$\frac{GFV}{CFV}$	6.2±2.7	5.2±1.7	3.9±1.1	1.38±0.1
$\frac{GFV}{Blood}$	1.0±0.2	0.9±0.2	0.5±0.1	0.22±0.01

Results indicate a sixfold increase in permeability and uptake of cholesterol in grafted vein with respect to

control vein in the 1-day period postsurgery. The cholesterol uptake in GFV ($p<.01$) decreases to half of this value seven days after surgery. Scanning electron microscopy demonstrates patchy endothelial cell loss from GFV and slow re-endothelialization which decreases cholesterol uptake. Vein graft permeability and cholesterol uptake thus provide a sensitive marker of graft re-endothelialization and permit evaluation of platelet-inhibiting drugs on graft repair after aortocoronary bypass surgery.

8:30-10:00 **ROOM A-1**

GI III: GI BLEEDING AND SINGLE PHOTON EMISSION

Moderator: Philip O. Alderson
Co-moderator: Kenneth A. McKusick

CLINICAL EFFICACY OF SINGLE PHOTON EMISSION COMPUTED TOMOGRAPHY OF LIVER. K.Yamamoto, T.Mukai, Y.Dodo, N.Tamaki, Y.Ishii, R.Morita and K.Torizuka. Kyoto University Hospital, Kyoto, Japan.

Clinical efficacy of single photon emission computed tomography(SPECT) was comparatively evaluated with conventional liver scintigraphy(CLS) for detecting small space occupying lesions(SOLs).

SPECT images were obtained with a rotating gamma camera, GE 400T, linked to DEC PDP 11/60 computer system.

On administration of 4mCi Tc-99m colloid, it took about 10 min. to collect sufficient counts to reconstruct SPECT images. 85 cases suspected of liver tumor were examined.

Among 51 cases of confirmatory SOLs proved by angiography, surgical operation and so on, CLS showed 73% of sensitivity and 85% of specificity, while the use of SPECT improved to 86% and 94% respectively, so that the accuracy rate was increased from 78% to 89%.

Resolving capacity of these modalities were investigated in 59 SOLs smaller than 6cm in diameter, summarized as followed;

	-2 cm	2-4 cm	4-6 cm	total
CLS	0/16	11/28	14/15	25/59
SPECT	2/16	19/28	15/15	36/59

(No.of SOLs detected/ No.of SOLs confirmed)

The smallest SOL resolved by SPECT was 1.7cm in diameter with excellent contrast.

In conclusion, greater sensitivity and specificity for detecting small SOLs in the liver was achieved by SPECT using rotating gamma camera, which was a feasible device for routine clinical use.

SINGLE PHOTON EMISSION TOMOGRAPHY IN DIAGNOSIS OF LIVER METASTASIS. C. Raynaud, A. Syrota, F. Soussaline, A. Todd-Pokropek, C. Kellershohn. Service Hospitalier Frédéric Joliot. Département de Biologie, C.E.A., Orsay, France.

Single photon emission tomography, also called gamma-tomography(GT), with a rotating gamma camera GE 400 T connected to a SIMIS 3, provides 3 D images and an image contrast 2 to 3 times higher than in conventional scintiscans.These advantages should be useful in detecting liver metastasis where other competitive methods are not ideal.However it has been found that the interpretation of liver GT sections requires an excellent knowledge of the liver anatomy to prevent a high incidence of false positive results. To facilitate the reading of the GT images, anatomical diagrams of normal transverse, sagittal and frontal sections have been established and are presented. They indicate the localization of the liver surface landmarks and limits of segments and areas.

The correct interpretation of GT images of metastasis has been found to be more difficult than anticipated. To establish guidelines, ten patients having liver metastasis surgically confirmed and localized, had a GT. In 7 patients the metastases were easily recognized. In 2 cases they were missed in first reading but were found when the images were interpreted with greater care. In 1 case the metastasis was detected only afterwards when surgical information was added. After an appropriate training an observer should have detected lesion in at least 9 out of the 10 cases. The site of the metastasis was exactly localized during surgery in 6 patients. In all these cases the localization found on GT sections with the help of the anatomical diagrams was satisfactory. These results are encouraging and justify an extensive double blind study to evaluate GT in the detection of liver metastasis.

EVALUATION OF PORTAL CIRCULATION BY Tl-201-CHLORIDE PER-RECTAL SCINTIGRAPHY. N. Tonami, K. Nakajima, T. Michigishi, H. Matsuda, K. Koizumi, T. Aburano, K. Hisada, K. Kobayashi and N. Hattori. Kanazawa University, School of Medicine, Kanazawa, Japan.

A new method of per-rectal scintigraphy using Tl-201-chloride was performed in 25 patients (normal 5, cirrhosis 13, chronic hepatitis 5, acute hepatitis 2) to evaluate portal circulation. Two mCi of Tl-201-chloride was given rectally after emptying the rectum with the enema. Scintigrams were taken sequentially at 5 minutes interval up to 25 minutes using gamma camera and time activity curves of the regions of interest over liver, heart, spleen and lung were obtained. The 20 minutes' heart/liver activity ratios were chosen to evaluate the degrees of porta-systemic collateral circulation. In normal subjects, the liver was visualized in 0-5 minutes' image after administration, while other organs were obscure even in 20-25 minutes' image. On the contrary, in patients with significant porta-systemic shunts the liver was not clearly visualized, while Tl-201 appeared in the systemic circulation and accumulated in other organs. The 20 minutes' heart/liver activity ratios (mean $\pm$ S.D.) were 0.13 ± 0.06 in normal, 0.91 ± 0.26 in cirrhosis, 0.17 ± 0.02 in chronic hepatitis, 0.22 ± 0.02 in acute hepatitis, respectively. All of the patients with esophageal varix showed 20 minutes' heart/liver ratios of more than 0.60. Our data suggest that this noninvasive method seem to be essential to discriminate between normal or chronic hepatitis and cirrhosis and might be useful to evaluate the degrees of porta-systemic collateral circulation.

SCINTIGRAPHIC LOCALIZATION OF THE LOWER GI BLEEDING SITES: COMPARISON WITH ARTERIOGRAPHY AND SIGMOIDOSCOPY. A. Alavi, University of Pennsylvania School of Medicine, Philadelphia, Pennsylvania.

Successful management of patients with acute lower GI bleeding generally depends on accurate localization of the site of hemorrhage. There are shortcomings to both arteriography and endoscopy in the evaluation of these patients. 47 patients with acute onset of lower GI bleeding were studied by scintigraphy following intravenous administration of 10 mCi of 99m-Tc sulfur colloid (Tc-SC). The findings on the scans were compared to those noted on arteriography (in 45 patients) and sigmoidoscopy (in 5). In 20 patients with negative scintigrams for bleeding the arteriograms appeared negative as well. On follow-up these patients evidenced cessation of hemorrhage. In 25 patients with scintigraphic evidence of hemorrhage, arteriograms were positive for bleeding only in 11. In 2 patients the arteriography was unsuccessful because of technical difficulties. Based on clinical follow-up, none of the 25 patients with evidence of hemorrhage on the scan, proved to have false positive results. In 5 patients with a bleeding site in the rectum, the scintigrams correctly identified the site of hemorrhage in all 5, while the sigmoidoscopy suggested a bleeding site above the rectosigmoid junction. Arteriography performed on 3 patients in this group confirmed the scan findings. The management of patients with either negative arteriogram or endoscopy and positive scans was significantly influenced by the findings on the scintigrams. The data presented above suggest that Tc-SC scans should be the study of choice in the evaluation of patients with rectal bleeding. Angiography and sigmoidoscopy can be performed following the scan to either confirm the findings or to stop the hemorrhage.

EARLY DETECTION OF EXPERIMENTAL MESENTERIC ISCHEMIA WITH INTRAPERITONEAL XENON. F. Gharagozloo, G. B. Bulkley and P.O. Alderson. Johns Hopkins Medical Institutions, Baltimore, MD and Columbia University, New York, NY.

Scintigraphic detection of intestinal ischemia has been limited by poor entry of activity into the ischemic area and high background in adjacent abdominal (ABD) organs. These problems can be obviated by the intraperitoneal (IP) administration of Xe-133 in saline. Xe-133 is absorbed passively across the peritoneum and selectively retained in tissues with poor perfusion. To demonstrate this, rats (n=24) and dogs (n=18) were divided into four equal groups: control, sham operation, simple mechanical obstruction and strangulation obstruction (STO) of an ileal segment. Following IP injection of 0.6-1.0 mCi of Xe-133, ABD activity was sequentially monitored at 30 min intervals by a camera-computer system. Each species showed 2-3x greater retention of Xe-133 activity at 60 min in STO than the other groups ($P < 0.001$). Images (n=52) were read independently by 6 observers. Sensitivity to strangulation was 100% in rats and 92% in dogs. Specificity was 100% in rats and 97% in dogs. In a second experiment, controls (n=6) were compared with rats who underwent superior mesenteric (SM) or portal vein ligation (n=6 each) or SM artery occlusion (n=6). Six dogs also underwent SM artery occlusion. All vascular obstruction groups showed marked Xe-133 retention at 60 min, while controls showed background activity. Histologic exams revealed that this discrimination was achieved prior to the development of tissue necrosis. ABD imaging and quantification of activity clearance following IP administration of Xe-133 in saline is an excellent method for early detection of mesenteric ischemia.

DETECTION OF GI BLEEDING BY AN IMPROVED RED BLOOD CELL (RBC) LABELING TECHNIQUE. E.A. van Royen, J.B. van der Schoot, A.Vyth. Dept. Nuclear Medicine, Univ.Hospital Wilhelmina Gasthuis, Amsterdam, the Netherlands.

Scintigraphic detection of gastrointestinal bleeding may be helpful in patients intermittently bleeding from a site not detectable by endoscopy. Tc-99m labeled RBC are an ideal blood pool labeling agent which permits prolonged follow-up in case of intermittent bleeding. In vivo labeling of RBC has a major drawback of relatively high background activity and visualization of the stomach by unbound Tc-99m pertechnetate.

We developed a simple semi-in vitro technique for Tc-99m RBC labeling. After intravenous injection of Sn-DTPA, 10 ml of blood is taken, the syringe is centrifused the plasma removed by means of a 3-way cock and 15 mCi pertechnetate added. After 10 min incubation the labeled RBC are reinjected without further washing. The procedure takes about 20 - 30 min. No visualization of the stomach occurs. Background activity is about 25% lower than that found for the in vivo technique. Until now 14 patients with recurrent GI bleeding from unknown sites (negative endoscopy, negative angiography) have been studied. In 9 patients it was possible to demonstrate the most probable origin of the bleeding by repeated scintigraphy during 24 hr after injection. The method proved to be useful in subacute and chronic GI bleeding from unknown origin, especially when located in the lower GI tract, for the determination of the most probable site and for the determination of the most suitable time for angiography in case of intermittant bleeding.

The detection limit of the method was calculated to be about 1 ml of blood per cm^2 for a 10 min acquisition time

8:30-10:00 **ROOM E-1**

RADIOPHARMACEUTICALS III: BIFUNCTIONAL CHELATES AND MECHANISMS

Moderator: Mathew L. Thakur
Co-moderator: Richard M. Lambrecht

BIFUNCTIONAL CHELATES FOR TUMOR IMAGING. C.H. Paik, W.C. Eckelman, K.S. Lei, K.E. Friend and R.C. Reba. George Washington University Medical Center, Washington, D.C.

p-Aminobenzylethylenediaminetetraacetic acid, synthesized according to the method by Meares, et al. (Anal Biochem 100: 152, 1979), was diazotized and then azo coupled to methyl-p-hydroxybenzimidate to give methyl-(4-hydroxy-3-azobenzylethylenediaminetetraacetic acid)-benzimidate. This compound was conjugated to the lysine residues of an antibody in an attempt to prepare a tumor imaging agent. In these studies, anti human serum albumin was used as a model system. The antibody (2.0×10^{-6}M) was reacted with the imidate at molar ratios of 1:100, 1:500, and 1:1000 for 20 hrs in 0.1M borate at pH 8.3 at 23.5°C. The reaction solution was purified by affinity chromatography through a 0.9 x 30 cm combination column containing Sephadex G-50 (24 cm long) and Sepharose 4-B conjugated to HSA (4 cm long). The amount of active or deactivated antibody was detected by a UV monitor. The results showed that conjugation of the chelating agent to lysine residues of the antibody via the amidination reaction at the above reagent ratios did not diminish the antibody-binding activity. Via a mixed anhydride reaction at the same molar ratios, the conjugation of diethylenetriaminepentaacetic acid to the lysine residues of the antibody also did not decrease the antibody-binding activity. In previous studies, we showed that the In-111 labeled diethylenetriaminetetraacetic acid conjugate of human serum albumin (HSA) prepared via the amidination reaction cleared from plasma much faster than I-125 labeled HSA when 1:10 or 1:100 molar ratios of HSA to chelating agent were reacted. This suggests that a specific tumor imaging agent with a high target to blood ratio may be prepared by conjugating a chelating agent to lysine residues of a tumor specific antibody.

SELECTIVE CELL LABELING: A POTENTIAL RADIOACTIVE AGENT FOR LABELING HUMAN NEUTROPHILS. S.S. Zoghbi, M.L. Thakur, A. Gottschalk. Yale University School of Medicine, New Haven, CT and W.A. Marisco, E.L. Becker. University of Connecticut Health Center, Farmington, CT.

A radioactive agent that may selectively label a given type of cells in whole blood would be a great improvement in cell labeling technique. A new radioactive agent that would facilitate such a labeling of human neutrophil is being investigated. The technique uses a synthetic chemotactic attractant N-formyl-methionyl-leucyl-phenylalanine (FMLP) for neutrophils each of which is shown to have 2000 receptor sites. Tritiated FMLP was covalently bound to human transferrin (TF) using 1-ethyl-3-(3-dimethylaminopropyl) carbodiimide HCl as a coupling agent. Knowing the protein concentration and tracing the tritium label we were able to perform quality control on preparations that indicated the FMLP to TF ratios of 1:1 to 8:1. The use of TF allowed an efficient incorporation of In-111 at pH 7 in 30 mins. incubation at 37°C in the presence or absence of added bicarbonate ions. The unbound In-111 was eliminated on a mini gel column.

Preliminary studies for defining optimum labeling conditions showed that 20 minutes incubation in plasma at 22°C was required and that the labeling efficiency was dependent of the FMLP:TF molar ratios. When an aliquote of In-111-TF-FMLP containing 322 million FMLP molecules with FMLP:TF ratio of 8:1 was added to 220 million cells, 60% of the added In-111 became cell associated and could not be removed from cells upon repeated washings with plasma.

The results indicate that In-111-TF-FMLP is a promising agent worthy of further investigations.

DEFEROXAMINE, AN EXCELLENT BIFUNCTIONAL CHELATING AGENT FOR LABELING PROTEINS WITH GALLIUM : 67-Ga-HSA. A. Yokoyama Y. Omomo, K. Horiuchi, H. Saji, K. Yamamoto, Y. Ishii, H. Tanaka, and K. Torizuka. Faculty of Pharmaceutical Sciences and School of Medicine, Kyoto University, Kyoto.

Deferoxamine (DF) is a well known chelator of trivalent metal ions, such as Fe(III), Ga(III) and In(III) with 1:1 molar ratio. The presence of free amino group in its molecule was regarded as an available functional group for coupling reaction with protein. So, these features appeared as promising for the development of bifunctional chelating agents.

The coupling reaction of DF with HSA was carried out in the presence of glutaraldehyde. The DF-HSA conjugate was

stable for more than three months. The labeling reaction of DF-HSA conjugate with 67-$GaCl_3$ was performed at pH 7.4. A very stable complex with a labeling efficiency near 100 % was obtained. The entire procedure required only 10-15 min after the addition of 67-$GaCl_3$.

Comparative in vivo studies of this 67-Ga-DF-HSA complex with the commercially available RIHSA (CEA) in rats showed a superior physiological behavior with blood clearance half life of 234 min as opposed to 121 min obtained with RIHSA. The great in vivo stability could be observed for more than three hours.

Development of this new bifunctional chelating agent of DF is an outstanding achievement since 68-Ga, a positron emitter is already available from a generator. Also its use as RIHSA substitute or as prospective enzyme, hormone and antibody containing radiopharmaceuticals hold considerable promise.

THE INFLUENCE OF ATP AND OTHER MEDIATING IONS ON THE IN VITRO TRANSFER OF Ga-67 FROM TRANSFERRIN TO FERRITIN. R.E. Weiner, G. Schreiber, and P.B. Hoffer. Yale University School of Medicine, New Haven, CT.

Iron binding molecules such as Transferrin (TF) and Lactoferrin have been shown to play a role in Ga-67 localization. Ferritin (FE), the iron storage protein, would appear to be another potential Ga-67 sequestering agent present in cells. Indeed, Larson et al., have demonstrated in vivo, Ga-67 binding to FE. We have examined in vitro, the effect of a variety of ions on the ability of FE to remove and bind TF bound Ga-67.

Equilibrium dialysis and sephadex gel chromatography were used to determine the fraction of Ga-67 bound to the respective proteins. A 2 chamber dialysis system was used to determine the amount and rate of transfer of Ga-67 between FE and TF. FE bound 70% of the added Ga-67 citrate after 80 hr incubation at pH 7.4. When the TF-Ga-67 complex (30 μM) was challenged by FE (3 μM), with no mediator present, a small transfer of Ga-67 from TF to FE occurred (∿6% at 90 hr). However, when either citrate, ATP, lactate or EDTA ions were added to the incubation mixture there was enhancement of the rate and amount of transfer. ATP and citrate were the most effective mediators. In presence of 1 mM ATP, TF bound activity was reduced from 72% to 17% and FE bound increased to 61% after 98 hours. Ga-67 did not dissociate from TF-Ga-67 complex when challenged by albumin over a similar time period, in the presence of 1 mM ATP.

These results suggest that FE, present in cells can remove and retain Ga-67 entering the cell in the form of the Ga-67-TF complex. In addition, small ions present in the cytoplasm would possibly facilitate this transfer.

TL-201 UPTAKE IN ISOLATED ADULT RAT CELLS. B.Rauch,F.Helus,A.Wieland,E.Braunwell, W.Hasselbach,and W.Kübler. Abt.Innere Med.III d.Universität, Nuklearmed. Inst. DKFZ u. Max-Planck Inst. f. med. Forschung Heidelberg.

To study kinetics of cellular Tl-201 uptake, myocardial cells of adult rats were isolated by perfusion with collagenase and hyaluronidase. Intact cells showed rhythmic contractions when stimulated by alternating current. Using the flow dialysis method according to Colowick et. al., the following results were obtained: 1) When extracellular Tl(Tl-201) concentration was 10 nmol/ml, 18±2 nmol/ml cell volume were extracted by myocardial cells within 90 seconds. 2) Myocardial cells, destroyed by calcium overload, were not able to extract a detectable amount of Thallium. 3) Tl(Tl-201) is bound by valinomycin, known as an ionophore, specific for potassium ions. Moreover, Tl(Tl-201)extraction was enhanced in the presence of valinomycin by at least 25%. 4) In the presence of Tetraaethylammonium, known as a blocker of the inward rectifying potassium channel in twitch muscle, Tl(Tl-201) sequestration was reduced by 40%. These results indicate a considerable part of Thallium being passively accumulated by myocardial cells by way of membrane channels specific for potassium. Unspecific binding to cell membrane probably does not participate in Thallium extraction by myocardial tissue.

TRANSFERRIN RECEPTORS AND GALLIUM-67 UPTAKE. D.C. Chen, B. Newman, R.M. Turkall and M-F. Tsan, The Johns Hopkins Medical Institutions, Baltimore, Maryland.

It has been shown that transferrin (TF) stimulates the in vitro uptake of gallium-67 (Ga-67) by a variety of neoplastic cells and that this Ga-67 uptake may be mediated by TF receptors. However, the relationship between TF receptors and Ga-67 uptake remains uncertain.

We have studied TF receptors and in vitro uptake of Ga-67 by human cells, including 3 normal lines (WI-38 fibroblasts, foreskin fibroblasts, and MRC-5 embryonic lung fibroblasts), 2 transformed lines (AV-3 amnion cells and Chang liver cells) and 2 neoplastic lines (HEp-2 larynx cancer and HeLa cervical cancer). The cellular TF receptors were determined by an indirect immunofluorescence technique based on their ability to bind purified human TF. Ga-67 uptake was determined after a 24 hour incubation of cells with Ga-67 in the presence and absence of TF (0.1-2.5 mg/ml).

The fraction of cells with TF receptors was low in normal cell lines (3-40%), intermediate with transformed cell lines (37-50%) and high in neoplastic cell lines (60-61%). Transferrin stimulated Ga-67 uptake by all cell lines, e.g. 50-350% stimulation at 1 mg TF/ml. However, there was poor correlation between the number of TF receptor positive cells and Ga-67 uptake either in the presence (R=0.27) or absence (R=0.26) of human transferrin.

Our results confirm previous observations that human TF stimulates Ga-67 uptake by human cells in vitro. However, Ga-67 uptake correlates poorly with TF receptor bearing cells.

8:30-10:00 **ROOM G-1**

INSTRUMENTATION I

Moderator: John Correia
Co-moderator: Stephen R. Thomas

SPECIFICATION TESTING OF A SINGLE-PHOTON EMISSION TOMOGRAPH (DCAT) FOR MEASURING BRAIN BLOOD FLOW PERFUSION IN MULTIPLE TRANSVERSE SECTIONS E.M. Stokely, F.J. Bonte, E.E. Griffin, S. Horner, R.W. Parkey, Dallas, TX

Measurements were made of the sensitivity, resolution, energy discrimination, and slice and channel separation characteristics of a new single-photon emission tomograph for studying regional brain blood flow (RBBF). The sensitivity using a 17cm diameter cylindrical phantom and a threshold setting of 60 keV was 19,145 cps/μCi/cc/slice (57,434 total) for Xe-133 in water. The resolution of the current collimator is 0.8 cm FWHM at 8.4 cm from the center of the rotation axis, and 1.6 cm FWHM at the center. The resolution in the slice dimenson is 2.1 cm FWHM at 8.4 cm from the center of the rotation axis, and 1.9 cm FWHM at the center (Figs. 1 and 2). Slice crosstalk could be adjusted to 5-8% for a point source in a nonscattering medium. Slice crosstalk was 9.4±1.1% for a point source in a cylindrical water bath. Adjacent crystal crosstalk was less than 2.0% using a Xe-133 point source. The energy discrimination resolution is 38% at 81 keV for Xe-133, and the threshold is normally set at 60 keV. We believe that DCAT possesses the required characteristics for reliable, reproducible measurement and display of RBBF.

AN IMPROVED TWELVE-PINHOLE SYSTEM FOR EMISSION CARDIAC TOMOGRAPHY. D. Kirch*, B. Hasegawa*, D. Stern+, J. Sklar*, P. Steele*,*VA Medical Center and +Research Systems, Inc., Denver, CO.

The availability of a high-resolution, large-field camera (Picker Model 4/61C) has made it possible to extend the seven pinhole concept to twelve pinholes configured with four central views (of 13° obliquity) surrounded by eight outer views (of 32° obliquity with respect to the mean line-of-sight). This design provides a 12/7ths increase in sensitivity and more complete angular sampling over the eight-inch reconstruction volume, reducing imaging time and lessening the crucial need to position the heart for symmetric viewing coincident with the long axis. A compound pinhole design is used to produce a more uniform sensitivity over the projected area of each view on the detector. The increase in the number of available views requires that the computer reconstruction programs achieve greater processing speeds and a multiplicative estimation process has been used to improve convergence of the tomographic data with a single iteration. Attenuation correction and edge enhancement are accomplished iteratively and study-to-study quantitative relationships are preserved by applying an integral count constraint. The analysis programs have been modified to present a unified set of circumferential profile curves as a single display which better delineates regional perfusion defects and improves correlation with specific arterial lesions. The performance improvements of increased sensitivity and improved depth resolution provide clinical and investigative advantages in terms of rapid dynamic sequence imaging of thallium-201 tracer kinetics and the ability to perform stress gated blood pool tomography.

A STUDY DEMONSTRATING THAT THE HEART IS THE ONLY SUITABLE ORGAN FOR COLLIMATOR TOMOGRAPHY. W. Chang, S. L. Lin, and R.E. Henkin. Loyola Univ. Med. Center, Maywood, IL.

Since the introduction of the 7-pinhole collimator(7PH) and its application to cardiac imaging, a number of investigators have examined the applications of this technique to other organs. The initial results have not been encouraging. Cold areas which are artifactual in nature were often created at the center of the imaging field.

The quadrant slant hole collimator (QSH) has combined the advantages of slant hole collimation and the multiple view simultaneous acquisition of the 7PH system. It is currently employed in a clinical trial for cardiac imaging.

This collimator system was investigated for applications to other organs by employing phantoms simulating the liver, brain and the myocardium. The QSH system suffers from the same problems as the 7PH system. The origin of the problem is related to the limited and discrete angle of data sampling. Anger previously has well demonstrated that ring tomography (of which both 7PH and QSH are variants) could potentially produce artifact in images of a liver phantom. We have concluded that the main reason why the 7PH and QSH systems are acceptable for myocardial imaging is because of the favorable geometry. In addition, it is now known that limited angle tomography does not favor the low spatial frequency information. Myocardial images do not have as much low spatial frequency information as do images of other organs.

The system allows only for the reconstruction of a hollow object, which has its own axes of rotational symmetry aligned with the axis of symmetry in data sampling. Therefore, the heart appears to be the only organ which has the proper size and geometric configuration for collimator tomography.

NONCARDIAC APPLICATIONS OF THE SLANT HOLE COLLIMATOR. H.D. Royal, J.A. Parker, G.M. Kolodny. Division of Nuclear Medicine, Beth Israel Hospital, Boston, MA.

The usefulness of the slant hole collimator in cardiovascular nuclear medicine to better separate atrial and ventricular activity is well recognized.

The slant hole collimator permits the acquisition of oblique views with the collimator flat against the surface of the patient. This permits acquisition of oblique views which would be physically impossible to obtain with a parallel hole collimator. In the last two years, we have investigated the slant hole collimator's usefulness in noncardiac studies and have found it to be useful in the following situations.

1. Examination of the posterior fossa during a brain scan is improved with posterior views obtained with the slant hole collimator with the holes directed cephalad.
2. Differentiation between pubic bone activity and bladder activity can be aided by a pair of anterior slant hole views of the pelvis, one obtained with the holes directed cephalad and one obtained with the holes directed caudad. A superficial structure such as the pubic bone will translate less than a deeper structure such as the bladder when these two views are compared.
3. LAO views of the gall bladder during a hepatobiliary study have been found to give better separation of the gall bladder and the hepatic and common bile duct.
4. Renal morphology can be more completely delineated using the slant hole collimator to obtain the contralateral posterior oblique image of each kidney.
5. Obliques of the vertebral column have been helpful in clarifying abnormalities in these regions.
6. Cephalad and caudad views of the spleen have been helpful in assessing splenic trauma.

A PHYSICAL COMPARISON OF A ROTATING GAMMA CAMERA AND SEVEN PIN-HOLE EMISSION TOMOGRAPHY SYSTEM. E.I. Holodny, W.P. Kowalsky, R.L. Van Heertum and A. Lando. St. Vincent's Hospital and Medical Center of New York, N.Y.

A comparison was made between two modalities (seven pinhole and transaxial) of single photon emission computed tomography using a large field of view (37 PM tubes) gamma camera. Physical parameters evaluated included: line spread function in X, Y, and Z coordinates, minimum detectable lesion using a variable defect size myocardial phantom, slice thickness reconstruction and distortion of reconstructions as a function of depth. The full width half maximum (FWHM) measurements of a line source were used as an indicator of spatial resolution. The FWHM (X,Y plane) measurements for the seven pinhole technique ranged from 1.2 cm at 5 cm from the face of the collimator to 2.9 cm at 15 cm, while the FWHM (Z plane) values were 2 cm and 12 cm at 5 cm and 14 cm distances respectively. On the other hand, the FWHM (X,Y plane) determination for the transaxial reconstruction technique was 1.9 cm at the 15 cm distance. Our results to date suggest that the rotating gamma camera system offers important physical advantages over the seven pinhole approach.

COMPARISON OF 201-TL PLANAR IMAGES OF MYOCARDIAL PERFUSION WITH SINGLE PHOTON TRANSAXIAL TOMOGRAPHIC IMAGES. S.A.Cook, R.T.Go, C. Napoli, W.J. MacIntyre, G. Rincon, D. Underwood. Cleveland Clinic Foundation, Cleveland, OH.

Several studies of conventional 201-Tl images for myocardial perfusion have been reported comparing the conventional planar images with longitudinal tomographic images obtained with the seven pinhole or slant hole collimators. Since longitudinal tomography does not exhibit good z-axis resolution, the present study has utilized a transverse tomographic system, the GE-400T rotating camera, to obtain transverse, saggital and coronary sections of the myocardium.

Patients were injected at stress following a dose of 2.0mCi 201-Tl and imaged by a Nuclear Ohio 100 camera within 5 minutes, recording conventional planar images in the anterior, 45° and 60° left anterior oblique views. Immediately following the planar studies, the patient was placed under the GE-400T and scanned transversely with 64 views at 30 sec. per view. Reconstruction was made of 0.5 cm. slices at approximately 50 sec. per slice on the Informatek SIMIS 4. Regional defects from both studies were identified independently and compared in each case to results of cardiac catheterization.

Previous correlation of 80 patients in this institution has shown a sensitivity of 72% for conventional 201-Tl imaging when compared to cardiac catheterization. Preliminary results of the present study of 25 patients have shown an improvement on this figure with the tomographic method. Of perhaps greater importance is the more discrete localization of ischemic areas and the possible delineation by use of multiple slices, of the actual volume of the segments involved.

8:30-10:00 **ROOM D-1**

FIRST JOINT SNM ALASBIMN ROUNDTABLE

Moderators: Eduardo F. Touya and Jose O. Morales
Co-moderators: Barbara J. McNeil and Leon S. Malmud

(1) Osvaldo J. Degrossi. EFFECTS OF RADIATION OF THE THYROID FOR NONTHYROIDAL DISEASE.

(2) Alfredo C. Santisteban. HOW TO EXTRACT ADDITIONAL INFORMATION FROM THYROID IN VITRO STUDIES.

(3) Nestor Arreaza. RADIONUCLIDE VENTRICULOGRAPHY IN PATIENTS WITH CHAGAS' MYOCARDIOPATHY.

(4) Kenneth A. McKusick. RADIONUCLIDE STUDIES IN PATIENTS WITH NONCORONARY ARTERY MYOCARDIOPATHY.

10:30-12:00 **ROOM B-1**

ONCOLOGY I

Moderator: David A. Turner
Co-moderator: William D. Kaplan

A PROSPECTIVE STUDY OF COMPUTED TOMOGRAPHY (CT), ULTRASOUND (US) AND NUCLEAR IMAGING (NI) OF THE LIVER IN PATIENTS WITH BREAST OR COLON CARCINOMA. P.O. Alderson, D.F. Adams, B.J. McNeil, R. Sanders, S.S. Siegelman, H. Finberg, S.J. Hessel, H.L. Abrams. Johns Hopkins, Baltimore, MD and Harvard Medical School, Boston, MA.

A prospective independent evaluation of CT, US and NI of the liver was performed in 189 patients (pts) who had either colon (n=129) or breast (n=60) carcinoma. Fourth generation CT scanners were used. US studies were obtained using gray-scale or phased array scanners. Multiple-view nuclear scans were obtained using 37 tube gamma cameras. The exams were obtained in random order. All 3 exams were obtained in 122 of the 189 pts (65%); 45 of these (37%) had liver metastases. Tissue diagnoses were available in 41 of the 122; the others were diagnosed by clinical means. Studies were classified into one of 5 categories (definitely abnormal, probably abn, etc.) so receiver operating characteristic (ROC) curves could be constructed. A 2x2 matrix analysis was also done. In pts with all 3 exams the matrix analysis showed that CT had a slightly higher sensitivity (0.93) than NI (0.86) or US (0.82). Specificities were 0.88, 0.83 and 0.85, respectively. These differences were not statistically significant. However, ROC curves showed that CT had the highest true positive rate (TPR) at every false positive rate (FPR). At a FPR of 0.1 the TPRs were 0.92-CT, 0.80-NI and 0.70-US. Differences were greatest for pts with breast cancer; at an FPR of 0.1 the TPRs were 1.00-CT, 0.83-NI and 0.60-US. CT provides the most accurate means for detecting liver metastases from breast or colon carcinoma. NI is nearly as good and represents a reasonable alternative exam.

EMISSION AND TRANSMISSION TOMOGRAPHY IN THE DETECTION OF SPACE OCCUPYING DISEASE OF THE LIVER O. Khan, P.J. Ell, I. Cullum, P.H. Jarritt. Institute of Nuclear Medicine, The Middlesex Hospital Medical School, London, UK.

Radionuclide Planar and Section Scintigraphy (RNPL and RNSS) and Computerized X-ray Transmission Tomography (CTT) were compared in the detection of space occupying disease in the liver. A total of 242 patients were studied. 134 females (age range 18-25) and 108 males (age range 10-80) were investigated. There were 72 Ca breast, 28 Hodgkin's, 22 non-Hodgkin's lymphoma, 29 Ca bronchus, 15 primary liver tumour, 22 GI tract tumour, 13 malignant melanoma, 4 Ca ovary, 8 Ca prostate and 29 miscellaneous tumour patients. RNPL and RNSS were compared in these 242 patients. There were 71% concordant results (171 patients) and 15% discordant results (36 patients). Doubtful RNPL were obtained in 6%, doubtful RNSS in 5% and doubtful RNPL + RNSS in 3% of all cases.

In 107 patients, RNPL, RNSS and CTT were compared. Criteria in the final evaluation of these patients included histology, obvious lesion progression and one year follow-up. There were 76 concordant (71%) and 31 discordant (29%) studies. RNSS was correct in 23 out of these 31 cases, RNPL and CTT in 7 out of these 31 cases. Final analysis of this data offers accuracy ranges for RNPL of 79-82%, for CTT 79-82% and RNSS of 88-98%.

TUMOR IMAGING WITH I-131 MONOCLONAL ANTIBODY AND ANTIBODY FRAGMENT IN MICE. G. Levine, B. Ballou, J. Reiland, D. Solter, L. Gumerman and T. Hakala. University of Pittsburgh Schools of Medicine and Pharmacy, Pittsburgh, Pa.

The recent development of tumor specific monoclonal antibodies derived from hybridomas offers a potent tool for tumor detection. We report three related studies in which a tumor specific antibody or $F(ab')_2\mu$ fragments labeled with I-131 was injected into MH-15 teratocarcinoma bearing BALB/c mice and into human choriocarcinoma bearing nude mice. For kinetic studies, 15 uCi were administered in 0.2 ml., I.V.; for imaging studies, 100-150 uCi were used. In the first study using I-131 whole antibody (IgM) specific to mouse and human teratocarcinoma, we found tumor to blood ratios of about 15:1 at 5 days post administration with an accumulation of 15% of the administered dose per gram in the tumor. In the second study I-131 $F(ab')_2\mu$ fragments were injected into MH-15 teratocarcinoma bearing BALB/c mice. As with whole IgM, the fragments appeared to be eliminated from nontumorous tissue via two compartment first order perfusion kinetics. Whole body elimination was greater with the $F(ab')_2\mu$ fragments at 48 hours than with whole antibody. Images at 48 hours post administration also were appreciably better with $F(ab')_2\mu$. In the third study a human choriocarcinoma (BeWo) was detected in nude mice using I-131 labeled $F(ab')_2\mu$ fragments.

RADIOIMMUNODETECTION OF HUMAN MELANOMA USING RADIOLABELED MONOCLONAL ANTIBODIES. S.M. Larson, P.W. Wright, J.P. Brown, I. Hellström, and K.E. Hellström. Veterans Administration Medical Center and Hutchinson Cancer Research Center, Seattle, Wa.

Monoclonal antibodies (mouse hybridoma) have been produced against 2 cell surface antigens of human melanomas: cell surface protein, p97 (Proc Natl Acad Sci 77:2183,1980) and Ming-Yeh antigen (Proc Natl Acad Sci 76:2927, 1979). We have performed 6 biodistribution studies of these radiolabeled antibodies in 3 patients with advanced melanoma, in order to determine their potential usefulness as agents for diagnostic imaging and/or therapy of malignant melanoma. Three different antibody preparations have been used alone or in combination in each of these studies: a monoclonal IgG_1 "normal control"; an anti-p97 IgG_{2A}; and an anti-Ming-Yeh IgG_1. Sterile and pyrogen free antibody preparation was injected intravenously, approximately 1 mCi per patient (200 µg protein), and blood samples were drawn at intervals after injection. Images were performed, beginning at 3 hours with final pictures at 48-72 hours. In comparison to the normal control immunoglobulin (plasma $t_{\frac{1}{2}}$=24 hours) there was very rapid clearance of immune specific antibody ($t_{\frac{1}{2}}$=30 minutes). For anti-p97, radiolabeled immune complexes were documented in serum. Imaging studies showed that the bulk of radiolabel localized in the liver, although immune specific uptake was noted in some, but by no means all documented tumor deposits.

The imaging procedure was well tolerated, no febrile

reaction or abnormalities of renal function, liver chemistry, or blood and platelet counts were noted. Preliminary clinical studies in humans are promising enough to justify further studies using radiolabeled antibodies and immune fragments.

THE UTILITY OF Ga-67 SCINTIGRAPHY FOR DETECTION OF CLINICALLY UNSUSPECTED METASTATIC MALIGNANT MELANOMA. R.D. Neumann, D.R. Vlock, P.B. Hoffer, J.E. Myers, A. Gottschalk, and J.M. Kirkwood. Yale University School of Medicine, New Haven, CT.

Previous retrospective studies of the value of gallium scanning in the staging and follow-up of patients with malignant melanoma have given conflicting results. We therefore embarked on a prospective study of its value. The protocol patients were studied with a tomographic instrument (Siemens Pho/Con) using 10 mCi Ga-67 citrate with initial imaging at 48 hrs. Each patient had a complete physical and neurologic exam, head CT scan, chest x-ray or full lung tomographs within 2 mos. of each gallium study. When metastatic disease was suspected additional radiologic exams, body CT scans, ultrasound, and biopsy were done. Sixty-seven patients with a total of 114 gallium studies are included in this report. Evaluation was done of 5 regions in each patient study: lymph nodes/soft tissues, lung, abdomen, skeleton and brain, for a total of 570 sites. The gallium scan findings and clinical (including laboratory, biopsy, etc.) results were concordant in 532 sites. Of the 38 discordant sites, the gallium scan correctly detected subsequently proven disease in 17 sites and was falsely positive in 2 sites. Gallium failed to identify 15 sites of disease. Clinical findings were falsely positive (gallium true neg) in 4 sites. Gallium scans missed 4 instances of brain metastases and 7 instances of pulmonary metastases. Scans were particularly useful in detecting unsuspected lymph node-soft tissue lesions (7) and abdominal-visceral lesions (6). Gallium imaging in patients with melanoma appears to be particularly useful in detecting unsuspected sites of metastases.

GALLIUM-67 AND LIVER SCANNING IN CANCER OF THE ESOPHAGUS. M Osborne, JW Ryan, S Sepahdari, P Kirchner. The University of Chicago Hospitals, Chicago, IL.

Ga-67 scans were obtained prior to therapy in 75 patients with biopsy proven cancer of the esophagus. 67/75 had colloid liver scans. 56/75 underwent surgical exploration. The primary tumor was resected in 44. Ga-67 concentration in the primary tumor was detected in 37/75 (49%) and more in squamous (30/49 = 61%) than in adenocarcinoma (6/25 = 24%). None of the 8 adenocarcinomas arising in Barrett's esophagus were Ga-67 positive. One carcinosarcoma was Ga-67 positive. Tumor detectability with Ga-67 did not correlate with the location of the primary nor with tumor penetration of the esophageal wall except for extramural squamous extension. For resected tumors, Ga-67 scans were positive in 0/4 primaries < 2 cm, 15/35 tumors 2-7.9 cm, and 4/5 lesions ≥8 cm.

Tumor spread precluding operation was detected by Ga-67 in 11/12 patients including 8/8 with distant metastases. Of 8 tumors unresectable due to extensive local disease in the chest, 7 were squamous with dense tracer accumulation. Of 4 unresectable due to distant metastases, 3 were adenocarcinomas with Ga-67 negative primaries. Colloid and Ga-67 scans detected 3/5 with metastatic liver disease while 2 hepatic malignancies were not evident on either study.

Ga-67 scanning yielded the most useful information in squamous tumors. It proved as accurate as colloid liver scanning in the detection of hepatic metastases and is promising as a screening test for distant metastases. However, its role in defining regional disease precluding resection is still uncertain.

10:30-12:00 **ROOM D-1**

PEDIATRICS

Moderator: David L. Gilday
Co-moderator: H. Theodore Harcke, Jr.

PHASE ANALYSIS IN PEDIATRIC NUCLEAR CARDIOLOGY. M. deSouza, D.L. Gilday, S. Houle. The Hospital for Sick Children, Toronto, Ont. and D.G. Hall. Medical Data Systems, Ann Arbor, MI.

The use of temporal Fourier phase analysis in the study of patterns of ventricular contraction, and selection of cardiac regions of interest in equilibrium gated studies is becoming common in adult cardiology. The same applications are pertinent to the study of cardiac function in children where complex congenital abnormalities provide challenges for diagnosis and evaluation. The technique displays both an amplitude and a phase parametric image, and requires little operator intervention, except to view the dynamic display.

We have applied this technique to 30 pediatric cardiac patients and found it yielded extra information in 16 cases. In those children with complex congenital abnormalities, phase analysis of gated studies has provided additional information to traditional regional wall motion assessment. Phase analysis is especially useful in postoperative studies of children when there has been a disruption of conduction pathways. In addition, this technique can provide better selection of ventricular regions of interest for ejection fraction calculation important in cases where congenital abnormalities makes this difficult. Where atrial activity overlapping the ventricle results in errors in ejection fraction calculation phase analysis has been particularly useful.

The technique can be applied to data acquired in frame or list mode. Reconstructed list mode gated first pass studies can be analyzed using the technique, as well as low and high density equilibrium studies acquired at rest or stress.

GASTROESOPHAGEAL SCINTISCANNING IN CHILDREN. A. PIEPSZ, and B. GEORGES. St Peter's Hospital, Brussels, Belgium.

Tc-99m colloid "milk scan" is accepted as a sensitive technique for the detection of gastro-esophageal reflux in children. The present study is devoted to some factors which could influence the sensitivity of the method, namely the duration of monitoring and the position of the patient under the camera. For this purpose, a quantification index of reflux was used, taking into account the number and the height of the reflux peaks, as well as their duration. In a first study on 60 patients with G.E. reflux, supine position was found superior to prone or left lateral position : the detection of the reflux phenomenon, the number of reflux episodes and the total amount of refluxing material were all higher in the supine position. Compared to this last position, a 30° right lateral position did not improve the results. It was also obvious from this first study that in prone and in left lateral positions, reflux was more likely to occur during the 20 first minutes after the meal, rather than between 40-60 minutes. In supine position however, no such effect was observed. In a second series of 25 patients with G.E. reflux, a 1 Hr continuous monitoring in supine position increased by 25% the detection of reflux, in comparison with a 30 min. test. In 7 patients, reflux occured only during the 1st half hour. In 6 patients, reflux was noted only during the 2nd half hour.

GFR MEASUREMENT IN CHILDREN BY MEANS OF A CdTe PORTABLE DETECTOR.
A.Piepsz,H.R.Ham,M.Hall,J.L.Froideville,M.Ectors, St Peter's Hospital. Free University of Brussels Belgium.

The overall estimation of GFR is still a difficult problem in the pediatric population. The chemical methods were found either impracticable (inulin clearance) or unreliable (creatinine clearance). The plasma disappearance curve of a radiotracer like Cr-51 EDTA or Tc-99m DTPA requires at least 3 blood samples between 2 - 4 hrs after injection. With the portable CdTe detector it is possible to determine a plasma curve by means of serial external measurements calibrated by only one blood sample. The small size of the detector allows accurate repositionning for the external countings and the possibility of measuring GFR in several patients during the same time interval.

In 25 adult patients, comparison with the classical Cr-EDTA (3 blood samples) has shown identical results. In children, good concordance was generally found with the creatinine clearance, although discordances related to gross overestimation of creatinine clearances were observed.

The method is particularly well suited to the pediatric population and allows a continuous monitoring of GFR, for instance in the postoperative period of renal transplantation or during the course of a prolonged aminoglucosides treatment.

Factors affecting the accuracy of the method were analyzed : site and number of external measurements, best time schedule for blood sampling, magnitude of error on GFR due to errors on the slope.

EXPERIENCE WITH DYNAMIC IMAGING UTILIZING DIDA IN THE DIFFERENTIATION OF NEONATAL HEPATITIS, BILIARY ATRESIA, AND PATENT BILIARY SYSTEM IN INFANTS. J.C. Leonard, D.C. Hitch, C.V. Manion. Oklahoma Children's Memorial Hospital , Oklahoma City, Oklahoma

Twenty-seven infants under one year of age were imaged for one hour following the injection of 0.6mCi/kg of Tc-99m-Diethyl-IDA (DIDA). Computer processing with equal sized regions of interest over the liver, heart and bladder produced a series of related curves which document the bio-distribution of DIDA. At least three distinct sets of curves can be defined based on the relationship of these curves. Neonatal hepatitis was characterized by an absence of hepatic accumulation of thus essentially parallel hepatic and cardiac (IV disappearance) curves. Biliary atresia (BA) is characterized by good hepatic uptake but with minimal decrease in activity over time and thus the terminal portion of the hepatic curve is parallel with the cardiac curve. In the patent biliary system good hepatic accumulation with subsequent convergence toward the cardiac curve was noted.

Inadequate studies were obtained in four patients due to excessive movement during the study. The technique was accurate in 20 of the remaining 23 cases, 87%, with 2 false positive and 1 false negative study for BA, giving a sensitivity of 86% and specificity of 88%.

A mathematical model has been defined to describe the observed curves and work is currently directed to determine the equilibration constants. Application of the technique reduces the need for repeat studies after pharmacologic intervention as well as the need for delayed imaging as advocated by the proponents of I-131 Rose Bengal.

RADIONUCLIDE ANGIOGRAPHY AND VENTRICULOGRAPHY AFTER OPEN HEART SURGERY. G.G. Janos, M.J. Gelfand, G. Benzing, S. Kaplan. E.L. Saenger Radioisotope Laboratory and Division of Pediatric Cardiology, Children's Hospital and University of Cincinnati Medical Center, Cincinnati, OH.

First-pass (FP) and gated radionuclide ventriculography (RNV) was performed in 38 patients (pt) 2-24 hours after repair of intracardiac defects using cardiopulmonary bypass (CPBy) and cold cardioplegia. Thirteen had ventricular septal defect (VSD), 7 tetralogy of Fallot (TOF), 4 atrial septal defect (ASD), 4 aortic stenosis, 4 AV communis, 3 transposition of the great vessels (TGV) and 3 other defects.

FP excluded residual left to right shunt (L-R) in 10 VSD, 3 ASD and 3 TOF. Significant L-R was detected in 3 VSD, 2 required reoperation and one died. FP right ventricular (RV) ejection fraction (EF) was calculated in 19 pt; in the 6 successful TOF repairs, post-operative (PO) RV EF was ≥0.61. Pulmonic valvular insufficiency precluded L-R estimation in 4 TOF. FP also identified decreased left lung perfusion in a PO TOF at the site of a previous left Blalock-Taussig shunt. Superior vena cava obstruction was noted by FP in one PO TGV.

Left ventricular (LV) EF and wall motion was evaluated by gated RNV in 36 pt. Seven had depressed PO LV EF (<0.50). LV wall motion abnormalities were noted in 6 pt, all had apical hypokinesis probably related to LV venting at CPBy. Gated RNV showed a large hemopericardium in one other pt requiring surgical drainage. In 2 pt with transient PO respiratory insufficiency, LV EF was normal on repeated studies.

RNV is a non-invasive, safe technique for evaluation of cardiac function and detection of significant complications in the immediate PO period.

Tc-99m HEAT DENATURED RBC FOR SPLENIC SCINTIGRAPHY IN CHILDREN. C.P. Ehrlich, N. Papanicolaou, S. Treves, Children's Hospital Medical Center, Harvard Medical School, Boston, MA. P. Richards, Brookhaven National Laboratory, Upton, NY.

The purpose of this investigation was to develop a Tc-99m heat-denatured red blood cell (RBC) technique suitable for pediatric patients (pts.) and evaluate its clinical utility.

Seven pts. aged 4 days to 16 years in whom Tc-99m sulfur colloid (SC) scintigraphy failed to confidently identify the spleen were studied with a modification of the Brookhaven National Laboratory (BNL) RBC kit. Only 1 ml of blood was needed compared to 6 ml with the adult kit. Labeling efficiency averaged 95%. Denaturation was achieved by heat at 49.5° for 15 min. Labeling efficiency remained high (≅90%) following denaturation.

The indications were: asplenia in the heterotaxia syndrome (3), accessory spleens in pts. with recurrent idiopathic thrombocytopenic purpura (ITP) following splenectomy (2), splenic trauma (1), intrathoracic mass (1).

In two of the three pts. diagnosed as asplenic with SC the spleen was detected with RBC's. An accessory spleen was found with SC in one of the two pts. with ITP. This was confirmed by the RBC study which made the visualization of the small spleen much easier. A questionable splenic hematoma by SC was unequivocally demonstrated by the RBC study. An intrathoracic mass found to be either liver or spleen by SC was identified as spleen by the RBC study.

The pts. suspected of being asplenic and proven to have spleen(s) were spared long-term prophylactic antibiotics. Thus splenic scanning can be of usefulness in selected pts. Use of the modified BNL kit limits blood loss and makes the test applicable in infants and small children.

10:30-12:00 **ROOM G-1**

RENAL

Moderator: Joe C. Leonard
Co-moderator: Manuel L. Brown

Tc-99m-DTPA AND I-131-HIPPURAN FINDINGS IN CYCLOSPORIN A NEPHROTOXICITY IN LIVER TRANSPLANT RECIPIENTS. G.B.G. Klintmalm, W.C. Klingensmith III, S. Iwatsuki, G.P.J. Schroter, and T.E. Starzl. University of Colorado Health Sciences Center, Denver, CO.

Cyclosporin A (CyA) is a new immunosuppressive agent which is likely to be widely used in renal transplant recipients despite its known nephrotoxicity. To study the effects of CyA nephrotoxicity on Tc-99m-DTPA and I-131-hippuran imaging without the confounding effects of acute tubular necrosis (ATN) and rejection, we performed serial postop Tc-99m-DTPA and I-131-hippuran in nine liver transplant recipients treated with CyA. In the Tc-99m-DTPA study perfusion, clearance, and parenchymal transit were visually graded 1 to 5 (1= normal); in the I-131-hippuran study only clearance and transit were

graded. In addition the effect of CyA on renal function was determined by measuring serum creatinine levels during the second postop week in the CyA group and retrospectively in a control group of 29 liver transplant recipients not treated with CyA. The creatinine level in the control group was 0.87±0.24 mg/dl (mean±S.D.) and in the CyA group 3.31±2.47 mg/dl (mean±S.D.) ($p<0.01$). Eight of 9 CyA patients showed imaging abnormalities in 13 of 15 studies (3 patients had multiple studies); 5 of 8 patients with abnormalities showed an ATN-like pattern (relatively preserved perfusion) in at least 1 studies. In conclusion, the immunosuppressive drug CyA causes nephrotoxicity which may mimic either ATN or rejection in Tc-99m-DTPA and I-131-hippuran studies. This finding suggests that the differentiation of ischemic ATN and rejection from CyA nephrotoxicity will be diffficult in renal transplant recipients treated with CyA.

A NEW FORMULA FOR CALCULATION OF ERPF. W.N.Tauxe, E.V. Dubovsky, T.Kidd, R.Lewis, L.R. Smith, M.V.Yester. University of Alabama in Birmingham, Birmingham, Alabama.

In 1971, we developed a method for estimation of effective renal plasma flow (ERPF) in 116 patients, based on the concentration remaining in the plasma 44 min after injection. The original data base consisted mostly of patients with various nephrological diseases and contained relatively few normal subjects. Regression equations relating the plasma concentrations to other estimates of ERPF (C_{PAH}, C_{OIH}), described a parabola which occasionally underestimated ERPF in upper limits of the normal range. The purpose of this paper is to present new regression formulae for estimation of ERPF in subjects with high normal renal function. Additional adults were chosen for study, including 63 normal kidney donors (with high ERPF) and 10 anephric patients to secure the lower end of the regression curve. Each subject was injected with 50 μCi chromatographically pure ^{131}I-orthoiodohippurate (OIH). Plasma was sampled at 10, 15, 20, 25, 30, 40, 44, 50, 60 mins. Rate constants and intercepts were derived from bi-exponential plots and ERPF was calculated using Sapirstein's two compartment models. ERPF was then plotted against percent dose reciprocals at 44 min (in liters), the time of the errof nadir. Two types of regression equations resulted, one a quadratic: $ERPF=-54.0+7.47X-0.020X^2\pm32$ ml/min; and one exponential, $ERPF = 1126.2\left[1-e^{-(0.0080x-7.80)}\right]\pm32$ ml/min. The latter theoretically is more related to the exponential physiological processes than the former, and ultimately does not deflect negatively, but the former may be slightly easier to use in practice. Both formulae predict ERPF better than the 1971 formula.

CLINICAL COMPARISON OF Tc-99m-N,N'-BIS(MERCAPTOACETAMIDO)ETHYLENEDIAMINE (Tc-DADS) AND I-131-HIPPURAN (I-H) FOR EVALUATION OF RENAL TUBULAR FUNCTION. W.C. Klingensmith III, J.P. Gerhold, A.R. Fritzberg, C. Singer, V.M. Spitzer, C.C. Kuni. University of Colorado Health Sciences Center, Denver, CO.

Animal studies indicate that Tc-DADS is excreted by the renal tubular cells at a faster rate than renal glomerular excretion of Tc-99m-DTPA and is thus a potential Tc-labeled replacement for I-H (J Nucl Med 20:641, 1979). We conducted a direct comparison between Tc-DADS and I-H in ten renal transplant patients with a creatinine range of 0.9 to 16.3 mg/dl. Each patient was studied with Tc-DADS and I-H sequentially in one sitting. For each agent digital images were recorded for 30 min. At 30 min the patient voided and additional images were recorded for 5 min. These data were analyzed in order to quantitate in relative terms: 1) renal extraction efficiency, 2) parenchymal transit time, and 3) excretion. The kidney to background ratio at 2.5 min was used as an index of extraction efficiency. The Tc-DADS extraction efficiency was 76 ± 0.04% (mean ± SEM) of I-H ($p<0.05$). The time of appearance of activity in the collecting system was used as an index of parenchymal transit time. Tc-DADS appearance time was 39 ± 12% (mean ± SEM) longer than I-H ($p<0.05$). The percent of injected dose (%ID) excreted into the bladder by 30 min was determined from bladder counts at 30 min before and after voiding and % ID in the voided specimen. Tc-DADS excretion was 27 ± 8% (mean ± SEM) of I-H ($p<0.05$). In conclusion, the biologic properties of Tc-DADS are inferior to those of I-H; analogues of Tc-DADS should be explored in an attempt to find a Tc-labeled replacement for I-H.

10:30-12:00 **ROOM E-1**

INSTRUMENTATION II

Moderator: Gordon L. Brownell
Co-moderator: Nizar A. Mullani

THE NEUROECAT: A NEW HIGH-RESOLUTION MULTIPLANE POSITRON COMPUTED TOMOGRAPH FOR IMAGING THE BRAIN. M. Phelps, E. Hoffman, S.C. Huang, D. Plummer, D. Kuhl. UCLA School of Medicine, Los Angeles, CA. M. Crabtree, M. Burke, R. Keyser, R. Highfill, C. Williams. ORTEC, Oak Ridge, Tenn.

The NeuroECAT consists of 3 octagonal rings of 88 BGO detectors (17x 27x 29mm) providing 5 simultaneous images. Unique geometry and shielding design provides uniform image and axial resolution and minimizes scatter and random coincidences (hardware substrated on-line). System has electronically controlled selection of low (11.0±0.4mm) and high (7.7±0.5mm) in plane resolution. Axial resolution is 13.4mm and 15.5mm with interplane septa in and out. Efficiency with a 20cm diam phantom is 39,000, 78,000 and 270,000 CPS/ Ci/ml for straight across, interplane and total system with interplane septa retracted. With septa in place, straight across and system efficiency are 23,500 and 70,500. Scatter is 12 and 28% with septa in and out and a 20cm diam x 20cm long phantom. Septa are inserted or retracted under electronic control. Gantry tilt (±25°) allows flexible image plane selection. Reconstruction with an array processor is 9.4 sec per plane. Coincidence time resolution is 20nsec. Tomographic images of full brain are rapidly viewed in a cinegraphic format (variable speed) in transaxial, coronal or saggital planes for convenient and rapid tracking of structures and extraction of local physiologic variables from image data and tracer kinetic models resident in system software.

Patient studies with FDG show the highest quality brain studies performed to date. Images show clear delineation of the convolutions of the cortical ribbon, separation of cerebellar cortex, cerebellar white matter, vermis and dentate, internal grey nuclei, internal and external capsule and other sustructures of the brain.

NOVEL TWO-POSITION SAMPLING SCHEME FOR DYNAMIC POSITRON EMISSION TOMOGRAPHY. R.H. Huesman, S.E. Derenzo, G.T. Gullberg, and T.F. Budinger. Donner Laboratory, University of California, Berkeley, CA.

Stationary circular positron emission tomographs with closely packed detectors combine the capability to do dynamic studies with excellent sensitivity, but their spatial resolution (FWHM) is limited to approximately the distance between detector centers and varies with source position. Several schemes have been developed to improve the linear sampling so that the geometrical detector pair resolution of ½ the detector size can be realized. These schemes involve taking data at typically 8-16 positions of the detector array, severely limiting the potential for dynamic quantitative imaging.

We demonstrate a novel sampling scheme that requires only two mechanical positions to provide a uniform linear sampling distance of ¼ the detector spacing. The detector array consists of two semi-circles that are hinged like a clamshell. With the clamshell closed, the array is a circle with an even number of detectors. With the clamshell open to provide a one-detector gap at the point opposite the hinge, the array closely approximates a circle with an odd number of detectors (one missing). Although each of these configurations has a sampling distance of ½ the detector spacing, their combination provides a sampling distance of ¼ the detector spacing. (The "missing detector" data can be estimated by interpolation without artifact.) Reconstructions of computer-generated data show that the combined data from even and odd rings provide a significant improvement in resolution over data from a stationary array. In addi-

tion, this technique has virtually eliminated artifacts associated with spatial variability of the resolution.

TIME-OF-FLIGHT SAMPLING OF ARTERIAL CONCENTRATIONS OF POSITRON-EMITTERS. RJ Nickles, RD Hichwa and GD Hutchins, University of Wisconsin, Madison, WI.

The sequential sampling of radiotracer concentrations in arterial blood is needed for the input function to many dynamic nuclear medical procedures. An example is the time-course of 2FDG plasma levels required to convert a β^+-tomograph into a quantitative map of rCMGlu. For β^+-emitters, time-of-flight (TOF) techniques have long held the promise of true isolation in depth. A prototype camera employing a pair of plastic scintillators (5x5 cm Pilot U on RCA 31024 phototubes; 30% dynamic range with snap-off diode CFTD) can resolve distances to less than 5cm (FWHM=300psec) with CsF roughly twice that figure.While this is inadequate for detailed imaging, it is suitable as a "sharp-focus probe" into the contents of the cardiac chambers. The left atrium and ventricle form a pool of arterial blood with an axial dimension of 10 cm in the LAO projection. Conventional focussing collimation is ineffectual, being unable to exclude off-plane activity in a stationary counting measurement. To investigate non-invasive TOF arterial sampling, the above scintillator pair was mounted on the gantry of a retired dual 5" scanner, with the interdetector axis laser-aligned LAO to the supine subject. This axis also passes through the focus of the original, collimated NaI detector. In this way, the great chambers can be conventionally localized with Tc-99m HSA before acquiring the time-to-pulse-height (TAC)spectrum with its arterial β^+-activity information. Point-source fiducial markers calibrate the TAC spectrum in distance and the depth dependence of the sensitivity. Initial tests with phantoms and C-11 CO are encouraging. However, F-18 2FDG raises more challenging problems, clearing rapidly from the blood into the myocardium itself.

LIMITED TIME-OF-FLIGHT TOMOGRAPHY - WILL IT HELP? F.B. Atkins. Walter Reed Army Medical Center, Nuclear Medicine Service, Washington, D.C. 20012

In an ideal situation, the difference in the time of arrival of the two annihilation photons following a positron decay permits a precise localization of the decay site along the ray joining the detector elements. However the temporal resolution of real coincidence detection systems is generally too poor for accurate localization. A time uncertainty (FWHM) of 0.5 nsec results in a corresponding standard deviation in the spatial coordinates of approximately 6.4 cm. While this is still coarse compared to the overall spatial resolution of positron cameras, this can have a significant effect on the statistical character of the reconstructed image.

The time-of-flight information results in a generalization of the profile data at each angle in a 2-dimensional function:

$$P_\theta(t,s) = \int f_\theta(t,\tau)\cdot q(s-\tau)d\tau$$

where the object distribution along the ray at (t,θ) is convolved with the spatial response function of the time-coincidence technique, $q(s-\tau)$. Computer simulations have been performed to assess the effects of limited time-of-flight localization on the noise magnitude and character in the reconstructed images of phantom data. Results indicate that significant improvements can be achieved with temporal resolutions of about .5 nsec, and modest improvements at 1.0 nsec.

QUALITY CONTROL: MEASUREMENTS OF CONTRAST AS A FUNCTION OF NOISE IN CONVENTIONAL AND TOMOGRAPHIC IMAGES. A. Todd-Pokropek, S. Huggett, M. Short and F. Soussaline. U.C.H., London U.K. and Dept. de Biologie C.E.A. Orsay, France.

A transmission phantom measuring small differences in contrast in conventional images, called the 'strip wedge phantom' has been designed. It comprises thin Cu wedges such that the inherent contrast varies along one axis, and spatial frequency along the other. This phantom has been tested under a wide variety of conditions i.e. total counts, count rate, scatter, energy window, and for various displays. Results are expressed as curves with Minimal Detectable Contrast (MDC) plotted against other parameters, e.g. the noise level.

Quality control of tomographic systems is notoriously difficult, and it is suggested that MDC is a good parameter to study. An emission phantom, based on the 'strip wedge phantom' made of Perspex strips is proposed to compare perceived contrast for both conventional and tomographic images, relying on the partial volume effect to generate tomographic contrast.

While there is a significant increase ($\sim$3) in detected contrast in tomography, there is a corresponding increase in noise level. However, the MDC in tomography is significantly affected by the size of the object and the noise power spectrum (with amplified high frequencies). Tomographic MDCs have been found to be significantly better than predicted from a knowledge of the overall signal to noise ratio alone.

LESION DETECTABILITY OF ROTATING CAMERA-BASED SINGLE PHOTON EMISSION COMPUTED TOMOGRAPHY(SPECT). R.J. Jaszczak, F.R. Whitehead, C.B. Lim, R.E. Coleman, Duke University Medical Center, Durham, NC.

The fundamental strength of SPECT in lesion detection lies in its capability of enhancing object contrast free from superposed background activity. The purpose of this study was to experimentally evaluate an analytical model of our dual scintillation camera SPECT system. The model was derived using a linear systems analysis and describes the reconstructed image contrast, %rms noise, and the minimum counts required for statistically reliable detection of centrally located spherical sources placed within larger background sources.

The %rms noise in attenuation corrected SPECT images of a Tc-99m source uniformly distributed in a water-filled 22cm diameter cylindrical phantom was measured using various reconstruction filters and agreed well with theoretically derived values. To further verify the model a 20cm diameter cylindrical water-filled phantom containing a centrally located 2cm lesion was imaged. A 0.8cm annular Tc-99m source having the same concentration as the lesion surrounded the water-filled cylinder. The minimum number of total events required for reliably detecting the 2cm diameter lesion within the "hot-ring" phantom in the reconstructed image was between 14,000 to 26,000 counts depending on the reconstruction filter used. The model predicted 18,000 counts were required. The conventional static images did not reliably detect the central lesion even with up to 1,000,000 counts. The measured lesion image contrasts (defined as the difference between the lesion count density and the background count density, divided by the background count density) for the conventional and SPECT images were 0.1 and 22.0, respectively.

10:30-12:00 **ROOM A-1**

SYMPOSIUM: HEINRICH R. SCHELBERT AND SELECT CARDIAC PAPERS

Moderator: Heinrich R. Schelbert
Co-moderator: H. William Strauss

INVITED SPEAKER

Heinrich R. Schelbert, UCLA Center for the Health Sciences, Los Angeles, CA. RECENT ADVANCES IN BASIC CARDIOLOGICAL NUCLEAR MEDICINE RESEARCH.

IDENTIFICATION OF ISCHEMIC MYOCARDIUM USING 18-FLUORO-DEOXYGLUCOSE, N-13-AMMONIA AND POSITRON COMPUTED TOMOGRAPHY. R.C. Marshall, H.R. Schelbert, J.H. Tillisch, M.E. Phelps and E. Henze. UCLA School of Medicine, Los Angeles, CA.

Since previous work has shown that the myocardial metabolic rate for glucose (MMRGlc) accelerates during ischem-

ia if residual perfusion is adequate to wash-out metabolic end products, the ratio of myocardial 18 fluoro-deoxyglucose (FDG) to N-13-ammonia (NH) activities detected by positron computed tomography should be higher in reversibly ischemic myocardium than non-ischemic or dead tissue. To test this hypothesis, 4 patients (pts) with clinical evidence of resting ischemia (RI) were compared to 5 pts with previous infarcts but with no evidence of ischemia at rest (NI). In NI pts, regional FDH and NH activities correlated well (r=0.82, n=149). After normalizing regional FDG and HN activites to their respective average values for the entire heart, the average variability of the FDG/NH ratio was (±S.D.) 11.9±4.4%. For NH activities less than average, the average FDG/NH ratio was 1.05±0.21. For NH activities greater than average, the value was 0.97±0.09. In RI patients, the average variability of the FDG/NH ratios was significantly higher (32.5±15.1, p<0.05). In addition, regional beds of myocardial ischemia, identified as having FDG/NH ratios greater than 2 S.D.'s above the average value at corresponding NH activities in NI pts, were observed in all 4 RI pts in areas that correlated with clinical criteria for ischemia.

We conclude that these data support the hypothesis that FDG/NH ratios and PCT can be used to identify reversibly ischemic myocardium.

SERIAL RADIONUCLIDE EVALUATION OF DOXORUBICIN CARDIOTOXICITY IN CANCER PATIENTS WITH ABNORMAL BASELINE RESTING LEFT VENTRICULAR EJECTION FRACTION. H.J. Berger, W. Choi, J. Alexander, P. Schwartz, F. Wackers, B. Zaret. Yale Univ., and Danbury Hospital, New Haven, Ct.

Previous studies from this laboratory have established guidelines for safe administration of doxorubicin to cancer patients (pts) with normal (nl) left ventricular (LV) performance. Over 36 months (mos), 48/329 pts (15%) referred for first-pass radionuclide evaluation of LV function had abnl (<55%) baseline resting LV ejection fraction (EF) prior to receiving doxorubicin. Thirty-seven/48 pts had no evidence of antecedent heart disease. Eighteen/48 pts had received prior thoracic radiation therapy. Serial LVEF measurements were obtained over 2-15 mos of therapy in 29 pts. Of 18 pts not studied serially, 9 were denied doxorubicin because of abnl LVEF.

Initial LVEF averaged (±SD) 48±5% (range, 30-54%) in the 29 pts followed serially. After receiving 313±144 mg/M^2 (120-600 mg/M^2) of doxorubicin, final LVEF was unchanged (47±9%, pNS). In the 12 pts who received ≥350mg/M^2, final LVEF was less than initial values (48±8 vs 43±4%, p<0.05). LVEF declined by ≥10% in only 4 pts (12-18% EF units). One of these pts developed congestive heart failure (CHF) at 480mg/M^2. No other pt developed CHF during therapy or follow-up of 5-20 months. Eleven/48 pts are still receiving doxorubicin in spite of abnl LVEF; the remaining 14 pts are either in remission or have died due to progression of disease.

Thus, abnl LV function is present in a substantial number of cancer pts without clinically evident antecedent heart disease. Doxorubicin can be administered safely in the presence of abnl baseline LV function using serial radionuclide studies as a means of monitoring therapy.

CNILICAL EVALUATION OF THALLIUM-201 MYOCARDIAL EMISSION TOMOGRAPHY USING A ROTATING GAMMA CAMERA: COMPARISON WITH PLANAR IMAGING AND SEVEN-PINHOLE TOMOGRAPHY. N.Tamaki, T. Mukai, Y.Ishii, K.Yamamoto, Y.Yonekura, T.Fujita,K.Torizuka, H.Kambara, and C.Kawai. Kyoto University Hospital,Kyoto, JAPAN.

Clinical efficacy of single-photon emission tomography (SPECT) of thallium-201 myocardial imaging using a rotating gamma camera (Maxi 400-T;GE) was comparatively evaluated with planar imaging (PLAN) and seven-pinhole tomography(7P). Data collection of SPECT was carried out from the left anterior oblique projection, so that the frontal and sagittal tomograms could show cardiac cross and longitudinal sections, respectively. Imaging time was 22 min for SPECT, 10 min for 7P, and 20 min for PLAN upon I.V. administration of 2 mCi of Tl-201. Myocardial imaging using these methods was performed in patients with an evidence of myocardial infarction and in normal subjects.

Scintigraphic results:

	PLAN	7P	SPECT
sensitivity	17/23 (74 %)	21/23 (91 %)	22/23 (96 %)
specificity	16/17 (94 %)	12/17 (71 %)	15/17 (88 %)
accuracy	33/40 (83 %)	33/40 (83 %)	37/40 (93 %)

Our study showed that the use of 7P tomography as compared with PLAN improved the sensitivity but decreased the specificity, with no significant increase in the overall accuracy. But the use of SPECT provided very high sensitivity and specificity, and consequently high accuracy could be estimated. In 7P method, choice of tomographic section was limited, whereas in the SPECT the most appropriate section, either transaxial, frontal, or sagittal can be selected, allowing a most clear observation of the defect. In conclusion, SPECT provided most accurate informations and seemed to be the best choice among those described methods.

1:30-3:30 **ROOM B-1**

CARDIOVASCULAR IX: THALLIUM MYOCARDIAL IMAGING

Moderator: Denny D. Watson
Co-moderator: Robert S. Gibson

THALLIUM-201 KINETICS IN ISCHEMIC MYOCARDIUM. D.D. Watson, H.H. Holzgrefe, A.M. Grunwald, R.S. Gibson, C.D. Teates, and G.A. Beller, University of Virginia Medical Center, Charlottesville, VA.

Delayed thallium-201 (Tl) redistribution (RD) is observed with myocardial ischemia and may reflect either altered extraction of Tl or altered cellular washout. These experiments measured the myocardial extraction and intrinsic myocardial efflux of Tl at normal and reduced myocardial blood flow. The average myocardial extraction fraction at normal blood flow in 10 anesthesized dogs was 82 ± 6% at normal coronary arterial perfusion pressures (CAPP) and increased insignificantly to 85 ± 7% at CAPP of 10-35 mmHg. Thé intrinsic Tl washout rate in the absence of systemic recirculation was measured in 12 additional dogs by external counting following intracoronary injection of Tl and also by measurement of arterial-venous saturations. At normal CAPP the intrinsic myocardial washout $T\frac{1}{2}$ was 54 ± 7 min and rose markedly to $T\frac{1}{2}$ of 300 min at CAPP of 25-30 mmHg. A second component of intrinsic washout with $T\frac{1}{2}$ = 2.5 min and representing 7% of the total initially extracted Tl was also observed and presumed to represent interstitial washout. We conclude that myocardial redistribution of Tl in states of reduced myocardial perfusion cannot be the result of increased myocardial extraction efficiency but is the result of slower intrinsic cellular washout rate at reduced blood flow. The blood flow dependence of intrinsic myocardial Tl washout offers the potential to classify the relative severity of perfusion defects observed by myocardial Tl scintigraphy.

ANALYSIS OF LATE THALLIUM CLEARANCE FROM MYOCARDIUM IN SUBJECTS WITH CORONARY DISEASE AND NORMALS. J. Sklar, D. Kirch, T. Johnson and P. Steele, Division of Cardiology, VA Medical Center, Denver, CO

We have extended the quantitative seven-pinhole methodology to serially follow the dynamics of thallium redistribution after exercise and have observed a pattern of slow late thallium clearance that appears to be characteristic of myocardium supplied by obstructed coronary arteries. Quantitative thallium scintigrams (7-pinhole tomography, circumferential count profiles) and blood samples for thallium concentration (counts/ml) were taken immediately, 2 hours and 4 hours after maximal treadmill exercise on 27 subjects: 20 with coronary artery disease (CAD) and 7 normals. The rate of thallium clearance from the blood (TCB) was compared to the rate of thallium clearance from each segmental region of myocardium (TCM--derived by ratioing corresponding segments of the absolute circumferential count profiles) between the 2 and 4 hour images. In

6 of the 7 normals, TCM exceeded TCB in all regions of all images. Seventeen of the 20 CAD patients had at least one region where TCM was less than TCB. Of the 13 pts with multiple vessel CAD (MVCAD), 11 had multiple regions with TCM<TCB. Of the total of 39 obstructed coronary arteries, this analysis detected 30. Of the 40 regions which were abnormal by this analysis, (i.e., TCM<TCB), 30 corresponded to obstructed coronaries. In contrast, while standard normalized quantitative analysis also was abnormal in 17 of the 20 CAD pts, it diagnosed MVCAD in only 5 of the 13 pts that had it. These results show that slow late thallium clearance from myocardium is characteristic of regions of myocardium supplied by diseased coronaries, and that observation of this phenomenon may improve diagnostic sensitivity for the presence of MVCAD.

QUANTITATIVE 201-THALLIUM SCINTIGRAPHY AT REST IN A MODEL OF SUSTAINED REGIONAL FLOW REDUCTION. R.M. Steingart, T. Yipinstoi, J.P. Wexler, R. Bontemps, J. Scheuer, Montefiore Hospital, Albert Einstein College of Medicine, Bronx, NY.

Quantitation of 201-Tl scintigrams is dependent on the determination of regional activity both in the ventricle and the backgrounds. To evaluate various methods of quantitation, 5 minute sequential scintigrams were obtained for 125±27 minutes in 7 open chest dogs with fixed, stable, regional flow reductions. Scanning was begun 10 minutes after the intravenous injection of 201-Tl at rest with data acquisition in 64x64 matrixes.

Time activity curves (TACs) from regions within the ventricle were generated with and without background subtraction. Uncorrected ventricular TACs and those corrected using interpolated background demonstrated no significant change in myocardial activity in regions of normal or reduced flow. In contrast, when ventricular TACs were corrected for lung background, reduced flow regions demonstrated a significant increase of activity with time (135± 94 to 236±107 counts/pixel/5 minutes, $p< 0.01$) from initial to final scans respectively. In normal flow regions, TACs demonstrated no significant change (391±194 to 412±102, p=N.S.) from initial to final scans. However, even with this background correction there was considerable overlap in TAC patterns between regions with reduced flow and those with normal flow.

These findings demonstrate that quantitative analysis of 201-Tl scintigrams is highly sensitive to the type of background correction. Further, TAC's are too variable among animals to allow separation of normal from reduced flow regions at rest. The significance of quantitative patterns of 201-Tl redistribution at rest requires redefinition.

REDISTRIBUTION OF THALLIUM-201 AT REST: CORRELATION WITH DEGREE OF CORONARY STENOSIS IN PATIENTS WITH ANGINA. G.A. Beller, R.S. Gibson, J.A. Gascho, A.M. Grunwald, B.C. Berger, D.D. Watson, University of Virginia, Charlottesville, Virginia.

Defects observed on initial thallium-201 (Tl) rest images may not represent myocardial scar. Some show delayed redistribution (Rd) suggesting rest hypoperfusion. To determine the frequency of rest Rd and relate it to severity of coronary stenoses (STEN), 73 patients (pts) with postinfarction, unstable or severe stable angina underwent serial imaging at rest prior to coronary angiography (CA). Anterior and 45° LAO images were divided into 3 vascular segments corresponding to the 3 major arteries for quantitative image analysis. Of 219 vessels analyzed by CA in the 73 pts, 24% were normal or had <70% STEN, 20% had 70-90% STEN and 57% had >90% STEN. Below, Tl Rd and persistent defects (Pd) are correlated with severity of STEN:

Tl Uptake	<70%	70-90%	>90%
Normal	39/52(75%)*	12/43(28%)	22/124(18%)
Rd	8/52(15%)**	17/43(40%)	60/124(48%)
Pd	5/52(10%)	14/43(32%)	42/124(34%)

*p<0.0001 versus >70% STEN; **p<0.002;***p<0.001

Of 43 STEN between 70-90%, 31 (72%) were associated with initial defects, 59% (17/31) of which showed Rd. Of 124 STEN >90%, 102 (82%) correlated with initial defects, of which 59% (60/102) showed Rd. Thus, in pts with severe coronary artery disease, there is a high prevalence of initial resting Tl defects in myocardial segments perfused by ≥70% STEN. More than 50% of these show delayed Rd suggesting viable but hypoperfused myocardium.

THE EFFECT OF INDERAL, EXERCISE LEVEL, AND SUBCRITICAL DISEASE ON THE SPECIFICITY OF EXERCISE THALLIUM-201 IMAGING. M.D. Osbakken, R.D. Okada, C.A. Boucher, H.W. Strauss, G.M. Pohost. Massachusetts General Hospital, Boston, MA.

Recent experience with Tl-201 exercise (ex) imaging suggests that positive results may be more common in patients without critical coronary artery disease than initially reported. In a series of 100 patients with <50% stenosis in all coronary vessels, ex Tl imaging was positive in 32 patients(specificity=68%). The coronary angiogram showed subcritical disease defined as 25-49% stenosis (SC) in 27 and no SC defined as <25% stenosis in 73. Images were reviewed by 3 independent observers and segmental Tl scores averaged. The incidence of positive scan for the NoSC and SC groups follow. The effect of propranolol(PROP)and level of exercise as determined by percent of peak predicted heart rate(PPHR) were examined (*p<.05).

	Total (N=100)	No SC(N=73)	SC(N=27)
Overall	32/100=32%	19/73=26%--*--13/27=48%	
PROP	19/42 =45%	13/29=45%	6/13=56%
No PROP	13/58 =22%	6/44=14%	7/14=50%
>85% PPHR	15/41 =37%	6/28=21%	9/13=69%
<85% PPHR	17/59 =29%	13/45=29%	4/14=29%

The relatively high incidence of positive scans in this population is due in part to SC disease, especially when HR indicates that ex level is approaching maximum. In the NoSC group, patients receiving PROP have significantly more false positives. In conclusion, in this large group of patients, a low incidence of false positives, 6 of 44 (specificity=86%), is obtained in patients off PROP with normal coronary arteries. These data suggest that PROP should be discontinued before the Tl-201 ex test, and further that angiographic interpretation frequently underestimates the severity of disease.

DIPYRIDAMOLE INTERVENTION REGIONAL BLOOD FLOW AND HEMODYNAMIC STUDY IN MAN. T.K. Chaudhuri, S. Sorenson, and B.M. Groves. University of Texas Health Science Center and Veterans Administration Hospital, San Antonio, TX

Dipyridamole induced coronary vasodilatation may be useful in the study of Thallium-201 myocardial imaging for the detection of coronary artery disease. We measured regional myocardial blood flow (RMF;ml/100g/min) and hemodynamics before and after intravenous dipyridamole (0.56 mg/kg for 4 min) in 11 patients employing a gamma camera/computer system for the detection of disappearance curves of intracoronary xenon-133 injections. Mean ± SEM heart rate (HR), systolic blood pressure (SBP), double product (DP), cardiac output (CO), normal artery RMF (RMF/NL; N=15), and RMF for arteries with greater than 50% stenosis (RMF/CAD;N=10) were:

	HR	SBP	DP	CO	RMF/NL	RMF/CAD
CONTROL	75±3	144±7	106±5	6.5±.4	67±3 *	52±7
D	87±6	131±6	112±7	6.8±.6	116±3 Δ	78±10
P	.01	.03	NS	NS	.001	.001

In 20 patients, RMF before and after nitroglycerin (NTG) was unchanged (RMF/NL 57vs49; RMF/CAD 59vs55). This data suggests that 1) RMF differences occur after intravenous D, but not NTG, which separate NL from CAD vessels 2) maximal coronary vasodilatation may not occur in man after intravenous D 3) RMF/CO ratios after D are favorable to improve thallium uptake.

*NS Δp< .01

DIFFERENCES IN THALLIUM REDISTRIBUTION AFTER EXERCISE AND DIPYRIDAMOLE INFUSION. J. Sklar, D. Kirch, J. Routh, F. Gold and P. Steele, VA Medical Center, Denver, CO

Dipyridamole (DPY) alters myocardial blood flow distribution in patients with coronary artery disease (CAD) such

that focal defects may be seen in their thallium images as frequently after DPY infusion as after exercise. The dynamics of thallium redistribution after DPY infusion have not been studied. We performed thallium tomography (7-pinhole collimator, quantitative circumferential count profiles) on 20 patients with CAD after maximal treadmill exercise (EX) and, one week later, after infusion of 0.60 mg/kg of intravenous DPY at rest. Images were acquired immediately and 4 hrs post stress (EX or DPY) and again after 24 hrs. A pt's images were considered abnormal if any region's count density fell below normal or if it demonstrated positive redistribution (RED)--a 15% or greater relative increase in count density on normalized count profile--at 4 hours. Of the 10 pts with multiple vessel CAD (MVCAD), 9 were abnormal after both EX and DPY. RED was seen in 6 pts after EX and 5 after DPY (p=NS). Of the 10 pts with single vessel CAD, 8 were abnormal after both EX and DPY. RED, however, was seen in 6 pts after EX but none after DPY ($p<.01$). By 24 hrs, images were similar after EX and DPY.

These results show that early patterns of RED are different after EX and DPY. Unlike EX, RED after DPY is seen only in pts with MVCAD. Since DPY causes "coronary steal"--a true reduction in regional myocardial blood flow leading to ischemia--in animals with MVCAD but not single vessel CAD, this suggests that early RED is a marker for myocardial ischemia, not just a response to transient myocardial blood flow maldistribution.

HEMODYNAMIC SIGNIFICANCE OF 201 THALLIUM PULMONARY UPTAKE DURING STRESS MYOCARDIAL SCAN.
J.P. Smeets, P. Rigo, P. Collignon, V. Legrand, M. Oury, H. Kulbertus, University of Liege, Department of Medicine, Liege, Belgium.

Pulmonary uptake of 201 Tl during stress myocardial scintigraphy has been reported as indicative of left ventricular ischemia or dysfunction during exercise. To determine the practical value of this sign we have studied 58 patients, 3 months after MI, and performed stress Thallium scans and stress hemodynamic measurements within 24 hours of each other. The LV EF was also determined. Patients achieved similar heart rates and work loads during both tests.
An abnormal pulmonary uptake was observed in 25 patients (group A) while 33 patients (group B) had no such sign. Groups A and B had similar cardiac index and incidence of residual ischemia with exercise (by clinical, electrocardiographic or scintigraphic criteria). Group A was characterized by an increased frequency of anterior MI (76% v. 48%, $p < .05$), of LV aneurysms (42% v. 12%, $p < .01$), and of LAD scintigraphic defects (76% v. 48%, $p < .05$), by larger rest TL defects (6.1 ± 2.4 v. 4.7 ± 2.5, segments involved $p < .05$) as well as by a lower resting EF ($34\% \pm 13.5$ v. $48\% \pm 13\%$, $p < .05$). Pulmonary wedge pressure during exercise was higher in group A (23.3 ± 10.6 mm Hg v. 17.7 ± 9.8 mm Hg, $p < .05$). 67% of patients with a wedge pressure $\geq$ 23 mm Hg belonged to group A.

We conclude that TL pulmonary uptake mainly reflects LV dysfunction during exercise, but only constitutes an accessory evidence as it lacks sensitivity and specificity.

1:30-3:30 **ROOM D-1**

PULMONARY

Moderator: Merle K. Loken
Co-moderator: Philip O. Alderson

NEW METHOD FOR THE DETECTION OF PULMONARY EMBOLI: METHYL IODIDE-131 AND METHYL IODIDE-123 INHALATION "HOT SPOT" IMAGING. Z.D. Grossman, J.G. McAfee, G. Subramanian, C. Ritter, F.D. Thomas, B. Lyons, G. Gagne, A. Zens, F. Farrar, T. Feld, P. Fernandes, and A. Johnson. The Upstate Medical Center, Syracuse, NY.

At room temperature methyl iodide is a lipid-soluble gas. After a single inhalation of CH_3I-131 or CH_3I-123, radioactivity appears in the pulmonary capillary and venous blood, whereas little activity appears in expired gas. Where pulmonary blood flow exists, the radioactivity is immediately washed out of the lungs into the systemic circulation. Where pulmonary blood flow is compromised, however, a transient "hot spot" is seen. The pulmonary wash out of radioactivity after inhalation is analogous to that of inhaled O-15-labeled CO or CO_2, and a "hot spot" is diagnostic of good ventilation and poor perfusion.

We have imaged anesthetized dogs with lobar, segemental, or subsegemental pulmonary arterial occlusions produced by Swan-Ganz balloon catheter. Each animal was radiographed, evaluated with Tc-99m-MAA and Xe-133, and imaged with .1-.6 mCi CH_3I-131 or .5-2 mCi CH_3I-123. Five of six lesions studied with CH_3I-131 and three of four lesions studied with CH_3I-123 were identified. Each missed lesion was associated with airway obstruction. The "hot spots" associated with positive studies washed out in several minutes, unless balloons were extremely tight or cardiac output was low, both of which markedly prolonged wash out.

Since CH_3I-131 is stable, inexpensive, and simple to produce, and since the energy of I-131 permits initial study with Tc-99m-MAA and Xe-133, this technique may prove to be a useful supplement for embolus detection, as a less invasive alternative to pulmonary angiography. The potential of CH_3I-123 remains to be defined.

INCIDENCE OF ABNORMAL PULMONARY PERFUSION SCANS IN NORMAL INDIVIDUALS. J.M. Wallace, K.M. Moser, M.T. Hartman and W. L. Ashburn. University of California, San Diego, CA.

A vital factor relating to the utility of the pulmonary perfusion (Q) scan in the evaluation of patients suspected of pulmonary embolism is the prevalence of abnormal Q scans in individuals free of cardiopulmonary disease. Because this prevalence is not well-defined, we performed Q scans in 80 normal subjects. METHODS: 46 male and 34 female nonsmoking volunteers, age 18-29, having no history of active cardiopulmonary disease are studied. Each subject underwent a history, physical examination, ECG, spirometry and PA chest roentgenogram. The subjects then received 1.5 mCi of ^{99m}Tc-MAA followed by imaging in 6 views. Subjects demonstrating a Q defect underwent a ventilation (V) scan. Known abnormal Q scans were randomly interspersed with the study Q scans. All scans were then interpreted independently by 2 experienced readers (KM and WA) and read as: 1) normal or 2) abnormal if lobar, segmental or subsegmental defects were seen on at least 2 views. RESULTS: There was 100% agreement between the two reader's interpretations and between duplicate interpretations by the same reader. Seventy-nine of the 80 study scans were read as normal. No subject demonstrated a lobar or segmental defect. One of the 80 subjects demonstrated a small left upper lobe segmental defect. She had a mild pectus excavatum, but the PA chest film was normal. The V scan showed no defect. CONCLUSION: Based on statistical analysis of these results, the expected incidence of a normal nonsmoking individuals in this age group having a lobar or segmental Q scan defect is 0-3.7% and 0-4.1% for a subsegmental defect (95% confidence limits). Thus it is highly improbable that Q scan defects, particularly lobar or segmental, ar due to normal variations; and in this age group should be considered as evidence of vascular or parenchymal ("airways") lung disease.

A COMPARISON OF Xe-133 VENTILATION AND Tc-99m AEROSOL INHALATION IMAGING AS AIDS TO PERFUSION SCANNING IN THE SCINTIGRAPHIC DETECTION OF PULMONARY EMBOLISM. P.O. Alderson, E.V. Kotlyarov, M.K. Loken and F.H. DeLand. Johns Hopkins, Baltimore, MD; GWU, Washington, DC; University of Minnesota, Minneapolis, MN.

Tc-99m DTPA aerosol (A) imaging has been suggested as an alternate to Xe-133 ventilation (V) imaging as an aid to perfusion (P) scanning in the detection of pulmonary embolism (PE). To determine their relative utility, a comparison was performed in 67 patients (pts) at 3 institutions. Each pt had a V study consisting of a posterior single breath inhalation, 3-5 min washin and 5 sequential 60 sec washout images, including posterior oblique views. A standard 6-view P scan was then performed. Next the pts inhaled the Tc-99m aerosol until the lung count rate at 140 keV was triple that seen with the P agent alone. A 6-view study was then performed. The 67 VP and AP studies were interpreted

independently at each institution as high or low probability (prob) for PE or indeterminate (IND). Ten of the 67 pts had pulmonary angiography within 72 hrs of the radionuclide study. There was agreement between the VP and AP diagnoses in 60 of the 67 cases (90%). In pts with angiography the positive predictive value (PV) of VP imaging was 0.67 (4/6) and that of AP was 0.83 (5/6). The negative PV of both was 100% (2/2) and each had 2 IND cases. There was disagreement in 2 pts with angiography. One pt with PE had an IND VP scan and a high prob AP scan. A pt without PE had a high prob VP scan and an IND AP scan. The results suggest that AP imaging with DTPA aerosol is a reasonable alternative to V imaging as an aid to the detection of PE by P lung scanning.

COMPUTER ASSISTED INTERPRETATION OF VENTILATION-PERFUSION IMAGING IN PULMONARY EMBOLISM. D.F.Wong, E.E. Camargo, P.O. Alderson, D. Biello, R.D. Katz, O. Malpica, K.H. Douglass, H.N. Wagner, Jr. The Johns Hopkins Medical Institutions, Baltimore, MD. and The Mallinckrodt Institute of Radiology, St. Louis, MO.

A computer-assisted diagnostic algorithm has been developed to assist physicians in the diagnosis of pulmonary embolism (PE) based solely on combined ventilation-perfusion (VP) scanning and chest radiography. The current data base consists of 239 patients who had Xe-133 single breath, equilibrium and delayed washout ventilation studies immediately followed by Tc-99m microsphere perfusion scans, chest x-ray within 12 hrs and pulmonary angiograms within 72 hrs of the scans. The program is based on a sequential response of the physician to serial questions posed by the computer with regard to the number and size of perfusion defects together with the relationship of ventilation and perfusion, and the presence, absence and size of an abnormal radiographic opacity for each defect. Using the characteristics of the scans in the data base the computer estimates the probability of PE. The program also generates curves relating post vs. pre test probability for various VP patterns. In 72 interpretations of 25 new studies by 3 experienced physicians, the mean computer-assisted probability (%) of PE was 10% ($p<0.01$) closer to the angiographic diagnosis than the physicians' unassisted diagnosis. Of the studies chosen by the computer to be in the probability ranges 0-20%, 20-40% and 80-100% the frequencies of PE by angiography were respectively 11%, 26%, and 82%. Because of the complexity of interpreting V-P scans, the computerized data aids the physician in the interpretation of the studies and in the future can provide a means of combining a priori clinical data with the results of nuclear studies.

RELATIVE ACCURACY OF TWO DIAGNOSTIC SCHEMES FOR DETECTION OF PULMONARY EMBOLISM BY VENTILATION-PERFUSION SCANNING. W.D. Carter, T.M. Brady, J.W. Keyes, Jr., J.H. Thrall, D.R. Biello, B.A. Siegel, P.O. Alderson. University of Michigan, Ann Arbor, MI, Washington University, St. Louis, MO, Columbia University, New York, NY.

The relative accuracy of two diagnostic schemes for detecting pulmonary embolism with ventilation (V)-perfusion (P) scintigraphy was evaluated. One scheme was recently proposed by Biello while the other was based on literature published prior to 1978 and was used at the University of Michigan. Seven observers at 3 institutions reviewed the Xe-133 and Tc-99m scans and chest radiographs of 70 patients who underwent angiography to diagnose pulmonary embolism. Group A (3 observers) used the newer criteria while Group B (4 observers) used the older approach to categorize scans as high or low probability or indeterminate for pulmonary embolism. Interobserver variability was also evaluated. All 70 patients had abnormal V-P studies, 75% had abnormal chest X-rays and 60% showed Xe-133 retention. Emboli were angiographically visualized in 25 patients. Both groups had similar sensitivity and specificity for scans not classified as indeterminate. Group A, using the newer diagnostic scheme, correctly diagnosed more patients by accurately categorizing scans that were called indeterminate by Group B. Group A also had a significantly better average proportion of agreement between observers (0.75) than group B (0.60, P=.002). Wide interobserver variability in V-P scan interpretation was noted however. We conclude the newer criteria are more accurate, less subjective and reduce the number of indeterminate scans. The indeterminate category plays an important role by allowing a "buffer zone" for equivocal cases and identifying to our clinical colleagues a subset of patients requiring further evaluation.

MECHANISMS OF AEROSOL DEPOSITION DOWNSTREAM OF AIRWAY OBSTRUCTION. H. Itoh*, D.L. Swift, G.C. Smaldone, P.O. Alderson, H.N. Wagner Jr. Kyoto University*, Kyoto, Japan, and Johns Hopkins Medical Institutions, Baltimore, MD.

The problem in giving therapeutic aerosols to the patient with COPD is less penetration of the aerosols in the lung because of their premature deposition in the obstructive airways. This has been noticed for years since the advent of radioaerosol imaging of the lung; however, no extensive study has been done regarding the mechanism of such deposition. The purpose of the study was to evaluate physical parameters regulating the aerosol deposition at the obstructed site, and to provide theoretical basis for proper delivery of the aerosols to the patient with airway obstruction.

Monodisperse sebacate aerosols tagged with uranine were given to a half inch i.d. plastic tube with a circular constriction. The amount of uranine deposited downstream of the orifice was determined fluoroscopically. The individual parameters such as particle size, flow rate, density of carrier gas and degree of stenosis were put together to form two dimensionless numbers. They were Stokes number (Stk) and Reynolds number (Re), indicating inertial force of the aerosol and intensity of local turbulence, respectively. The study showed that the downstream deposition is controlled by both numbers, in other words, the deposition is determined by Stk at constant Re and vice versa, independent of the individual parameters.

In conclusion, the model study suggested that increased aerosol deposition in COPD is caused by enhanced inertia of the aerosol and local turbulence. Slow inhalation of small sized aerosols is recommended, because it helps to minimize these factors simultaneously.

DETERMINATION BETWEEN HEMODYNAMIC AND NONHEMODYNAMIC PULMONARY EDEMA BY INHALED SOLUBLE RADIOAEROSOL. J.M. Uszler, G. Mason and R.M. Effros, Harbor-UCLA Medical Center, Torrance, CA.

Pulmonary edema may be produced by elevations of capillary pressures or injury to the alveolar-capillary membranes. Diagnosis of such injury is generally based upon indirect evidence: presence of edema in the absence of elevated pulmonary artery wedge pressures. We recently developed a procedure for directly detecting increased alveolar-capillary permeability in a study of patients (pts) with various forms of chronic interstitial lung disease (ARRD 121:105-117, 1980). Pts inhale an aerosol containing Tc-99m-DTPA (diethylenetriamine-pentaacetate) for 2 minutes and during the immediately following 7 minutes the regional (3-4/lung) clearance (expressed as % decrease per minute) of radioactivity from the lungs is measured with a scintillation camera and minicomputer system.

In the present study, DTPA regional clearance rates were determined in 5 pts with congestive heart failure and 5 pts with non-hemodynamic pulmonary edema (3 of septicemia, 1 near-drowning and 1 uncertain cause). Roentgenographic evidence for interstitial/alveolar edema was present in all pts. Seven normals were studied to determine normal DTPA clearance rate (1.56 ± 1.10%/min, $\bar{x} \pm 2$ SD). In pts with congestive heart failure only 2 of 29 regions had accelerated clearance. In contrast, clearance rates were accelerated in 21 of 30 regions in the pts with non-hemodynamic pulmonary edema ($p<.001$). It is suggested that acute injury to the alveolar-capillary membranes increases the permeability of this barrier to small hydrophilic solutes, a phenomenon which can be quantitated by this simple, non-invasive procedure.

Supported by NIH Grants HL 18606 and HL07388

QUANTITATIVE MEASUREMENTS OF REGIONAL LUNG DENSITY AND BLOOD VOLUME USING POSITRON EMISSION AND TRANSMISSION TOMOGRAPHY. P. Wollmer, C.G. Rhodes, F. Fazio and T. Jones. MRC Cyclotron Unit, Hammersmith Hospital, London, UK.

Using positron emission tomography (ECAT) in the transmission and emission mode, we have developed a technique

for the quantitative measurement of regional lung density, blood volume and extravascular lung density and obtained values for normal subjects. A measurement of lung density is given by a transmission scan, using a ring source containing Ge-68/Ga-68 which emits monoenergetic γ-rays (511 keV). The pixel counts in the transmission scan are proportional to physical density in the range 0.02-1 g/cc. Regional blood volume in the lung is measured following a bolus inhalation of C-11O and scanning in the emission mode. Both the blood volume (emission) scan and the lung density (transmission) scan can be normalized to the counts/pixel in blood. This allows the blood component to be subtracted from the lung density scan to give a measurement of extravascular lung density.

In normal subjects, studied in the supine posture at the level of the sternal insertion of the 4th rib, we found an anterior-posterior gradient in lung density from 0.20 to 0.38 g/cc. This difference is almost entirely due to the difference in blood volume. The blood content rose from 0.075 ml/cc anteriorly to 0.21 ml/cc posteriorly. The distribution of extravascular lung density is thus almost flat, values being 0.11 g/cc in the anterior and 0.16 g/cc in the posterior part of the lung.

We think that this simple and non-invasive technique will provide new information about the functional anatomy of the lung, especially in pulmonary edema and infiltrative lung diseases. This is supported by preliminary data in patients.

1:30-3:30 **ROOM A-1**

SYMPOSIUM: S. JAMES ADELSTEIN AND SELECT DOSIMETRY/RADIOBIOLOGY PAPERS

Moderator: Robert H. Rohrer
Co-moderator: Jack Coffey

INVITED SPEAKER

S. James Adelstein, Harvard Medical School, Boston, MA. THE MICROSCOPIC DISTRIBUTION OF ENERGY IN RELATION TO DOSIMETRY AND RADIONUCLIDE THERAPY.

THE USE OF CHELATING AGENTS FOR REDUCTION OF RADIATION DOSE. Z.H. Oster, P. Som, D.F. Sacker, N. Cicale, A.B. Brill and H.L. Atkins. Brookhaven National Laboratory and SUNY at Stony Brook, NY.

The possibility of reducing radiation exposure after completion of a radionuclide study by chelating agents was studied in rats.

Groups of 6 Sprague-Dawley rats were given Tc-99m pertechnetate (Tc) or Ga-67 citrate (Ga-67) I.V. followed at 1-24 hrs by one of the following: desferioxamine (DFO), BAL, Bleomycin (Bleo), DMSA, DTPA and DTPA+Sn. Whole body retention was determined with a gamma camera interphased to a minicomputer and activity in selected organs was assessed by direct counting of samples in a well type counter. Matched groups of animals receiving the radiopharmaceutical only, served as controls.

DFO given 5 hrs after Ga caused a 25% reduction in the whole body radiation dose as compared to controls whereas, when given 24 hrs after Ga, an 11.9% reduction is observed. BAL lowers Ga blood activity by 41.28% ($p<0.001$) and also decreases activity in muscle, liver, GI tract and bone. DMSA did not affect Ga distribution. Tc was only slightly affected by BAL and not at all by the following: Bleo, DMSA, DTPA and DFO. BAL induced a slight reduction in the whole body retention as well as in Tc concentration in blood, thyroid, kidney and stomach. DTPA+Sn decreased Tc activity in thyroid, stomach, and intestines whereas blood activity was higher (3.86%g vs. 0.65%g). After separation and washing, 70% of the blood activity was in the RBC, an effect similar to that of PYP+Sn.

These results support the view that chelating agents are of value for reducing the radiation dose after radionuclide studies.

Research carried out under the auspices of the U.S. Dept. of Energy under Contract No. DE-AC02-76CH00016.

COMPARATIVE BIOKINETICS IN MICE OF THE CARBOXYL CARBON ATOM OF SOME AMINO ACIDS. K.A. Lathrop, P.V. Harper, and P.F. Faulhaber. The University of Chicago, Chicago, IL.

Carbon-11 incorporated into biomolecules at essentially carrier-free levels, allows biochemical processes to be studied without perturbation of the system with abnormal amounts of the tracer, and offers a means to follow quantitatively the entire biokinetic process in humans, to compare similar biomolecules, and to note deviations in disease. A study of carboxyl labeled straight and branched chain amino acids of corresponding chain lengths has been initiated with racemic compounds synthesized in our laboratory. This report describes results in mice, at intervals to 45 min after i.v. injection, for straight chain lengths three through six, i.e., 2-aminopropanoic (alanine), 2-aminobutanoic, 2-aminopentanoic (norvaline), and 2-aminohexanoic (norleucine); and for branched chains 2-amino-3-indolylpropanoic (tryptophan), 2-amino-3-methylbutanoic (valine), 2-amino-3-methylpentanoic (isovaline), and 2-amino-4-methylpentanoic (leucine). Urinary excretion, little or none for all straight chain acids and leucine, is 15% to 30% at 45 min for tryptophan, valine, and isoleucine. C-11 carbon dioxide excretion is 15% to 30% at 45 min for all straight chain acids, isoleucine, and leucine, but is essentially zero for tryptophan and valine. In all cases, blood content at 5 min is less than 10% of the injected C-11. Concentration of C-11 in the pancreas is 5 to 6 times that of the liver at all times observed, except that alanine is about 3:1, possibly associated with its rapid conversion to carbon dioxide. Pancreas/blood ratios after 30 min tend to be higher for branched chain than for straight chain acids. The four branched chain acids can be used to visualize the human pancreas, but the straight chain acids do not localize satisfactorily in the human.

NEW PROTOCOL FOR DETERMINATION OF DOSE IN RADS TO ISOLATED NECK LESIONS FOR I-131 THYROID-CANCER-THERAPY PATIENTS. K.F. Koral, R.S. Adler, R.C. Kline, J.E. Carey, W.H. Beierwaltes. University of Michigan Medical Center, Ann Arbor, MI.

A new technique describes the determination of the dose in rads to metastatic lesions of the neck following the administration of radioiodine for treatment of thyroid cancer. The goal is to relate dose level to therapeutic results.

A high-energy pinhole collimator is mounted on an Anger camera which can rotate about an axis that passes through the region of the neck. Anterior images are obtained daily if possible after the therapy injection with images at 1,2, 3 and 7 days being essential. Anterior and lateral images are taken at 2 days, both with and without a marker on the the skin surface, all without moving the patient. A single flood image is recorded so that a correction can be made for pinhole-collimator falloff. From the 2-day data, the magnification and distance below the skin surface are calculated for each lesion. Then a computer edge-detection program delineates tumor extent. An upper bound to the volume of an ellipsoid which is used to represent the lesion is then calculated. The uptake in counts is determined from the daily anterior images after an appropriate background subtraction. This uptake is converted to microcuries by use of an in-air calibration curve which takes into account the dependence of pinhole efficiency upon distance. The apparent uptake is then corrected for attenuation by using the calculated value for depth below the skin and an assumed attenuation constant. Finally, the dose rate is calculated and integrated to infinity by fitting a single exponential to the later data. Radiation doses to 5 lesions in 2 patients ranged from 2,500 to 31,000 rads per 175 millicuries.

UPTAKE AND RADIOTOXICITY OF Br-77-BROMODEOXYURIDINE IN MAMMALIAN CELLS. A.I. Kassis, S.J. Adelstein, Harvard Medical School, Boston, MA, C. Haydock, K.S.R. Sastry, University of Massachusetts, Amherst, MA, and K.D.

McElvany, M.J. Welch, The Edward Mallinkrodt Institute of Radiology, St. Louis, MO.

The uptake and radiotoxicity of Br-77-5-deoxyuridine have been studied in V79 Chinese hamster cells and compared to those of NaBr-77. Br-77-UdR was synthesized by the reaction of 2-UdR with gaseous oxidized bromine-77 species and separated by HPLC. The incorporation of Br-77-UdR into the DNA of dividing cells is dependent on extracellular radioactivity concentration and is linear. Incubation of cells with NaBr-77 did not result in measurable intracellular uptake. Survival of V79 cells was assessed by the colony-forming assay. Both NaBr-77 and cold BrUdR were non-toxic (50μCi/ml and 0.6μM respectively). The survival curve for Br-77-UdR had no detectable shoulder and a D37 (a relative index of toxicity) of 0.13 pCi/cell. In comparison, the D37 values for I-125-5-deoxyuridine and H-3-thymidine are 0.10 and 1.64 pCi/cell, respectively. Our results illustrate the extreme radiotoxicity of this Auger emitter when incorporated into the DNA of dividing mammalian cells and reiterate the effectiveness of this mode of decay in cell killing. Indeed, theoretical estimates indicate that deposition of 100 eV in a 1 nm sphere around the decay site in DNA is sufficient to produce high LET type cytocidal effects. The high toxicity, short half life (2.38 days) and lack of thyroid uptake of bromine suggests a possible role for this compound in the radiotherapy of tumors.

We wish to acknowledge the technical assistance of W.E. Guptill.

UPTAKE AND RADIOTOXICITY OF F-18-2-FLUORO-2-DEOXYGLUCOSE IN MAMMALIAN CELLS. A.I. Kassis, S.J. Adelstein. Harvard Medical School, Boston, MA, and J.S. Fowler, A.P. Wolf, Brookhaven National Laboratory, Upton, NY.

The introduction of positron emitting radionuclides as intracellular tracers has raised a number of questions regarding the dose of radiation delivered to sensitive cellular targets. To this end, we have measured the uptake and radiotoxicity of F-18-2-fluoro-2-deoxyglucose in Chinese hamster V79 lung fibroblasts. The rate of uptake of this radionuclide was found to be linear with increasing radioactive concentrations in the external medium, the slope of the curve rising with increased incubation periods. Survival of cells, as determined by the colony-forming assay, was also found to depend on the radioactive concentration and the exposure time. Thus, the radioactive content of whole cells which resulted in 37% survival fractions was 0.82, 0.56, and 0.45 pCi/cell for incubation periods of 110, 220, and 440 minutes respectively. A linear relationship was observed when these values were plotted as a function of the radioactive concentration in the external medium, respectively 66, 40, and 28 μCi/ml. Traditional dosimetry, based on MIRD calculations, underestimates the radiation dose to the radiosensitive targets of the cell by neglecting the high intracellular concentrations. These results suggest that an alternate dosimetric approach needs to be developed to explain the radiotoxicity observed. An attempt to correlate the latter in vitro toxicity with the in vivo MIRD based calculations will be made.

We wish to acknowledge the assistance of K. Karlstrom, A. Farrell, R. MacGregor and the cyclotron team at BNL in the preparation of the compound.

1:30-3:30 **ROOM G-1**

RADIOASSAYS IN CARDIAC DISEASE AND OTHER RADIOASSAYS

Moderator: Bernard J. Shapiro
Co-moderator: George J. Kollmann

RIA FOR DETECTION AND QUANTITATION OF CK-MB. L.R.Witherspoon, S.E.Shuler, C.F.Genre, J.F.Mackenzie, M.M.Garcia, Ochsner Clinic, New Orleans, LA.

Detection of CK-MB in the blood is the most important laboratory finding following acute myocardial infarction (AMI). Recently, RIAs employing hibridized CK-MB (Mallinckrodt (M)) or CK-B (Nuclear Medical Systems (NMS))have become available. Method M uses anti-CK-BB, CK-BB-125I, synthetic CK-MB standard and a PEG-second antibody separation. Total incubation time is 60 min. Zero standard binding was 10-20% of total activity (TA), nonspecific binding (NBS) 3-5% and did not differ between patient sera and standards. Sensitivity (B/B_o= 90%) was 10 ng/ml. Precision (CV) for serum pools (14,48,132 ng/ml) was 15,7 and 9% (between assay, 20 assays). Recovery of CK-MB added to patient sera (10,20,40 and 100 ng/ml) was 89-100%. Parallelism was demonstrated between the standard curve and dilutions of patient sera with high concentrations of CK-MB but not CK-BB or atypical CK. Concentrations measured in 46 ambulatory, noncardiac patients were 6.0±8.2(sd) ng/ml; in 57 patients hospitalized for suspected AMI but who had not had it, 13±12(sd). Method NMS uses anti-CK-B, CK-B-125I, CK-B standard and a second antibody separation. Total incubation time is 120 min. Zero standard binding was 26-28% of TA, NSB 3-5% and did not differ between patient sera and standards. Sensitivity was 5 ng/ml. Precision (CV) for serum pools (6 and 24 ng/ml) was 16 and 6%(between assay, 9 assays). Recovery of CK-B (4,8,16,32 ng/ml) was 89-103%. Parallelism between the standard curve and dilutions of patient sera containing CK-MB, CK-BB and atypical CK was demonstrated. Concentrations measured in 46 ambulatory, noncardiac patients were 7±3(sd) ng/ml; in 57 patients hospitalized for suspected AMI but who had not had it, 9±5(sd) ng/ml. Both systems are potentially valid alternatives to electrophoresis for the quantitation of serum CK-MB.

IMPROVED DIAGNOSTIC SPECIFICITY OF SERUM MYOGLOBIN RADIOIMMUNOASSAY (RIA) FOR ACUTE MYOCARDIAL INFARCTION (AMI) USING AGE-, SEX-, AND RACE-ADJUSTED REFERENCE RANGES. H.R. Maxon, I.W. Chen, M. Gerson, M. Sperling, and E. Stein. Eugene L. Saenger Radioisotope Laboratory and Department of Pathology, University of Cincinnati, Cincinnati, OH.

Many investigators have demonstrated that myoglobinemia is an early quantitative index of AMI, but others find it to be less specific than serum creatine kinase isoenzyme MB (CPK-MB). We found serum myoglobin levels to be sex-, age-, and race-dependent (Clin. Chem. 26:1864, 1980) and were able to improve the specificity of serum myoglobin RIA for AMI by using different reference ranges according to age, sex, and race. The reference range (tolerance limits for the coverage of at least 99% of the population with 95% confidence) determined from 292 apparently healthy subjects was 18-63 ng/ml whereas if they were grouped according to age, sex, and race, the upper limits of reference ranges varied from 40 ng/ml (20-50 years, female, black) to 91 ng/ml (male, black, >20 years). Of 42 patients without AMI, 4 patients had elevated serum myoglobin levels (68, 90, 91, 267 ng/ml) using the single reference range (specificity 90.5%) whereas only one patient gave a falsely positive result using the age-, sex-, and race-adjusted reference ranges (97.6%). Of 20 patients with proven AMI, one (53 year old white male) had a normal myoglobin level of 64 ng/ml using the adjusted reference ranges (sensitivity 95.0%) whereas all of these 20 patients had elevated myoglobin levels using the single reference range (100%). The diagnostic specificity and sensitivity of serum myoglobin RIA compared favorably with serum CPK-MB when the age-, sex-, and race-adjusted reference ranges were used.

MYOGLOBIN AND CK-MB RADIOIMMUNOASSAYS IN ACUTE MYOCARDIAL INFARCTION. B. Shapiro, G. Kollmann, S. Gordesky, S. Winsten, and R. Parameswaran. Albert Einstein Medical Center, Philadelphia, PA.

The purpose of the study was to determine the usefulness of serum myoglobin and serum CK-MB radioimmunoassays in the diagnosis of acute myocardial infarction in patients placed in the Coronary Care Unit with this tentative diagnosis. The assays were carried out using kits manufactured by Nuclear Medical Systems, Inc. for both myoglobin and CK-MB. Fifty patients were studied, of whom 28 (56%) had a discharge diagnosis of acute myocardial infarction. Determinations were carried out at the time of admission and on the 3 subsequent days of hospitalization. Of the 28 infarcts, 19 had at least one positive myoglobin level (sensitivity 0.68) and 20 had at least one

positive CK-MB level (sensitivity 0.71). Of the 22 non-infarcts, there were 3 who had at least one positive myoglobin (specificity 0.86), and 3 who had at least one positive CK-MB (specificity 0.86). Of the 28 infarcts, 18 were transmural; 16 of these had a positive myoglobin level, (sensitivity 0.89), and 16 had a positive CK-MB level (sensitivity 0.89). Only one transmural infarct was missed by both assays. Of the 10 subendocardial infarcts, only 3 had a positive myoglobin level and only 4 had a positive CK-MB level. Five of the subendocardial infarcts were missed by both assays. The low sensitivity for subendocardial infarcts is unfortunate, since this is precisely where the cardiologist would appreciate help in making the diagnosis. The low sensitivity of myoglobin did not appear to be due to delay in the appearance of the patient at the hospital, since CK-MB, which declines from its peak value more slowly, was not better. More definitive assays are needed.

SERUM CREATINE KINASE B (CKB) LEVELS FOLLOWING EXERCISE INDUCED MYOCARDIAL ISCHEMIA. J.A. Franco, J.L. Brown, B. Kovaleski, K. Vanags, M. Morris, W. Bohlman and L. Prevost. O'Connor Hospital, San Jose Ca.

Purpose of the study was to find if there are significant elevations of serum CKB levels in association with exercise-induced myocardial ischemia.

31 patients referred for treadmill exercise testing were studied. Baseline and one hour post-exercise blood samples were obtained for the determination of serum CKB levels. The paired serum samples were stored frozen at 20°C until tested in duplicate. A commercially available radioimmunoassay system (NMS, Newport Beach, Ca.) was utilized. A 50% increase above baseline values was considered to be significant. Our cardiac panel criteria for significant ischemia were used.

20 patients had normal exercise test results, none of them had significant post-exercise elevation of serum CKB levels.

5 of 11 patients with abnormal exercise test results had no elevation of CKB or angiographic evidence of severe coronary artery disease.

6 patients had both abnormal treadmill results and significantly increased post-exercise CKB levels. 4 of them had angiographic evidence of severe coronary artery disease.

The results of this study suggest that significant elevations of serum CKB levels occur frequently in association with exercise induced myocardial ischemia.

RADIOIMMUNOASSAY OF PLASMA NETILMICIN FOR THERAPEUTIC DRUG MONITORING IN INTENSIVE CARE PATIENTS. D.Glaubitt, H.J. Drechsler, and T. Lichtenberg. Departments of Nuclear Medicine and Anesthesiology, Academic Teaching Hospital, D-4150 Krefeld, Federal Republic of Germany.

As aminoglycoside antibiotics have a narrow therapeutic index, treatment with them requires drug monitoring in order to avoid an excessive or insufficient dosage. After introduction of netilmicin we evaluated the clinical efficacy of monitoring its plasma level during therapy.

Twenty-five intensive care patients were examined in whom severe infections were treated with netilmicin. Daily or in intervals of several days, blood samples were drawn 15 to 30 minutes after intravenous administration of the drug. The concentration of plasma netilmicin was measured by radioimmunoassay.

This procedure provided the opportunity to rapidly adjust the dosage of netilmicin to the therapeutic range which was assumed to lie between 1,0 and 16,0 µg/ml plasma. In patients whose renal function deteriorated or improved fastly, the procedure was especially useful to keep the plasma level of netilmicin within the therapeutic range.

In conclusion, drug monitoring in patients treated with netilmicin considerably increased therapeutic safety.

DETERMINATION BY RADIOIMMUNOASSAY OF DNA LEVELS IN THE SERUM OF PATIENTS WITH GASTROINTESTINAL DISEASE. S.A. Leon, M. Chakrabarty, E. Cohn, and B. Shapiro. Albert Einstein Medical Center, Philadelphia, PA.

The purpose of the study was to compare the serum concentration of circulating free DNA in patients with malignant or benign GI disease, and to determine the diagnostic value of such measurements. Previously, we had found that some patients with cancer of various origins had abnormally high levels of DNA in their circulation. DNA concentration was measured by radioimmunoassay developed in this laboratory, utilizing I-125-IUdR-labelled DNA as the antigen, and antibody from the serum of a patient with SLE. Of the 386 patients studied consecutively, 199 (52%) had malignant disease with a mean ± SE of 412±63 ng DNA/ml serum, whereas 187 (48%) had benign disease and mean (±SE) DNA levels of 157±16 ng/ml. The difference is statistically significant at $p<0.001$. In comparison, DNA levels in 88 normal controls had a mean ± SE of 14±3 ng/ml, significantly lower than in benign GI disease at $p<0.001$. The DNA assay showed the greatest sensitivity in carcinoma of the pancreas: of 65 patients, 57 (88%) had DNA levels above 100 ng/ml, chosen as the upper normal limit. The specificity was less adequate since 8 out of 16 patients with acute or chronic pancreatitis, and all of 7 patients with pancreatic pseudocyst, showed levels above 100 ng/ml. We conclude that serum DNA concentration is markedly elevated in malignancy of the GI tract, and moderately elevated in benign GI disorders, as compared with normal controls. These findings may have diagnostic or prognostic value.

A SIMPLE RADIOMETRIC ASSAY FOR ACETYLCHOLINESTERASE ACTIVITY. T.R. Guilarte, H.D. Burns, R.F. Dannals, and H.N. Wagner Jr. The Johns Hopkins University School of Hygiene and Public Health, Baltimore, MD.

At present, acetylcholinesterase (AChE) activity and the effect of its inhibitors is measured by the hydrolysis of C-14 acetylcholine (ACh) with subsequent separation of the resultant C-14 acetic acid. This method, although sensitive and specific, is tedious and requires a great deal of manipulation. We have developed an alternative method that is simple, fast, sensitive, specific and has the potential for automation.

Our new radiometric technique is based on the hydrolysis of ACh by AChE to acetic acid and choline. The acetic acid reacts with C-14 bicarbonate to generate C-14 carbon dioxide which is measured in an ion chamber (Bactec). The C-14 carbon dioxide evolved is proportional to the amount of ACh hydrolyzed. In essence, the test consists of an unknown vial and a series of standard vials containing increasing amounts of AChE. Both sets of vials contain 60 mM ACh solution as substrate and 1 µCi of C-14 bicarbonate. Appropriate blanks to correct for nonenzymatic hydrolysis of ACh are prepared.

The test can be used for measuring AChE activity in fluids and homogenized tissue as well as for assaying AChE inhibitors. Preliminary studies with known AChE inhibitors have shown that the new radiometric method can be used to rank such compounds according to their inhibitory potency.

The method is not only applicable for assaying AChE activity and the relative activities of its substrates and inhibitors, but it can be extended to other enzyme assays in which a proton is generated as a result of the enzymatic action. This proton can then react with the C-14 bicarbonate ion to produce C-14 carbon dioxide.

PREPARATION OF LATEX PARTICLES FOR SCINTILLATION PROXIMITY ASSAY (SPA). H. Hart and E. Greenwald. Dept. of Nuclear Medicine, Montefiore Hospital and Medical Center, Bronx, N.Y.

Scintillation Proximity Assay has been reported earlier as a very sensitive research method for the direct and indirect assay of antigens and antibodies. In order to adapt the

method for more convenient use in clinical applications, improved homogeneous, stable latex particulates have been prepared. Background counts arising from self-induced scintillations of the tritiated (LH) particles have been reduced approximately 5 fold by incorporation of a substituted benzotriazole in the particles. Scintillant particles (L*) have also been prepared which are now homogeneous within ~ 2%, are stable at room temperature for weeks and under refrigeration at 4°C for over a year. With these improved particles, it is quite easy to detect as little as 100 picograms of human albumin/ml routinely.

FRIDAY, JUNE 19, 1981

8:30-10:00 **ROOM A-1**

CARDIOVASCULAR X: VENTRICULAR FUNCTION TESTING

Moderator: Elias H. Botvinick
Co-moderator: Ismael G. Mena

RADIONUCLIDE AND HEMODYNAMIC EVALUATION OF ACUTE EFFECT OF ORAL ISORDIL ON EXERCISE PERFORMANCE IN CONGESTIVE HEART FAILURE. H.S. Hecht, S. Karahalios, J.A. Ormiston, S.J. Schnugg, J.M. Hopkins, and B.N. Singh. Wadsworth VA Medical Center and University of California, Los Angeles, CA.

To evaluate the acute effects of oral Isordil (I) on exercise (E) ejection fraction (EF) and hemodynamics in congestive heart failure, 11 patients underwent supine, graded E equilibrium radionuclide angiography and hemodynamic monitoring before and 90 min after I 40 mg po qid given over 24 hr. Duration of E (pre-I 6.5 min, post-I 8.3 min) and total work (pre-I 2448 kg-m/min, post-I 3227 kg-m/min) were greater post-I ($p<0.01$). At submaximal levels matched for identical workloads and at maximum E the mean results were:

	Submaximal E			Maximum E		
	Pre-I	Post-I	P	Pre-I	Post-I	P
EF	.22	.23	NS	.21	.23	NS
CI	3.5	4.0	NS	3.8	5.0	<0.02
SWI	31.3	36.3	NS	31.4	44.0	<0.01
SVR	17.2	13.8	<0.01	16.1	12.4	<0.01
SVI	29.5	35.0	<0.01	30.5	39.9	<0.01
HR	119.3	113.3	<0.01	127.5	126.5	NS
MAP	110.3	102.1	<0.001	112.7	111.1	NS
PCW	32.3	26.2	<0.001	38.5	32.6	NS

CI=cardiac index, SWI=stroke work index, SVR=systemic vascular resistance, SVI=stroke volume index, HR=heart rate, MAP=mean arterial pressure, PCW=pulmonary capillary wedge.

In conclusion, Isordil produces: 1) no change in EF; 2) lower PCW, MAP, HR, SVR and higher SVI at submaximal E; 3) higher CI, SWI, SVI and lower SVR at maximal E and 4) increased duration of E and amount of work.

IMPORTANCE OF RAPID SEQUENTIAL SAMPLING OF LEFT VENTRICULAR FUNCTION DURING THE COLD PRESSOR TEST BY BEAT-TO-BEAT ASSESSMENT WITH THE COMPUTERIZED NUCLEAR PROBE. R.W. Giles, P. Marx, H.J. Berger, B.L. Zaret. Yale Univ., New Haven, Ct.

The cold pressor (CP) stimulus is a sympathetic response associated with a reflex increase in blood pressure (BP). The temporal sequence of changes in left ventricular (LV) performance was studied in 18 patients (pts) with severe coronary artery disease (CAD) using the labeled equilibrium blood pool and the computerized nuclear probe. LV ejection fraction (EF) and relative LV volumes were obtained on a beat-to-beat basis for 8-10 beats at 0.5 minute (min) intervals during 3 mins of hand immersion in ice water (0°C) and for 3 mins post-CP. Heart rate (HR) and BP were recorded simultaneously. LVEF decreased significantly (>5%) in 16/18 pts. Maximal (max) decrease in LVEF averaged ±SEM 12±1% (range, 3-25% EF units; $p<0.001$ compared to baseline) and occurred at 1.4 mins of CP (range, 0.5-3.0 mins). This was associated with a 12±4% relative decrease in stroke volume and 16±3% relative increase in end-diastolic volume. In 7 pts, max changes in LVEF occurred at ≥2.0 min of CP. The max increase in systolic BP was 34±4 mmHg and occurred at 1.8 mins (range, 0.5-3.0 mins). In 10 pts, the max decrease in LVEF preceded the max increase in BP. HR did not change during CP. LVEF did not return to baseline values in 3 pts at 3 mins post-CP, despite recovery of BP.

Thus, during CP there are wide fluctuations in the times of max changes in LVEF and BP in CAD. These data emphasize the importance of rapid sequential sampling of LVEF during CP for a comprehensive understanding of this reflex and suggest that the magnitude of LV functional changes may be underestimated using conventional gamma camera imaging.

RADIONUCLIDE VENTRICULAR VOLUMES DURING SUPINE-BICYCLE AND ISOMETRIC HANDGRIP EXERCISE IN NORMAL MEN: EFFECT OF PROPRANOLOL. D.W. Baron, M.L. Brown, I.P. Clements, W.T. Bardsley, and C.E. Harrison. Mayo Clinic, Rochester, MN.

Measurement of exercise LV volumes (V) may be a more sensitive method of detecting ventricular dysfunction than ejection fraction. The purpose of this study was to determine the LV volume responses in normal men (n=17) during two different modes of exercise: 50% maximal handgrip and graded supine bicycle exercise, both before and after propranolol (P,2 mg/kg/day). End-diastolic (ED) and end-systolic (ES) counts were corrected for cycles processed, time-per-frame, venous counts, and radiodecay for each acquisition. Corrected counts (C) were used in a previously developed regression formula ($r=0.93$) to obtain LVV in ml. During control supine bicycle exercise, EDV increased from 132 ± 5 (SE) to 141 ± 7 ml, ESV decreased from 47 ± 2 to 32 ± 3 ml, stroke V increased from 85 ± 4 to 109 ± 5 ml, and ejection fraction (EF) increased from 64 ± 1 to 77 ± 2% (all $P < 0.01$). Following P, rest EDV increased to 145 ± 6 ml, stroke V increased to 97 ± 5 ml (both $P < 0.01$), and EF remained unchanged (66 ± 1%); during exercise EDV increased to 154 ± 7 ml, ESV decreased from 48 ± 1 to 37 ± 2 ml, stroke V increased to 117 ± 6 ml and EF increased to 75 ± 1% (all $P < 0.01$). Peak exercise EDV and ESV were both increased following P administration. During isometric exercise no significant change in EDV, ESV, stroke V, or EF occurred, either during control conditions or after P. Increased cardiac output (CO) in normals during dynamic exercise is due to both increased HR and stroke V, the latter being due to increased preload and an enhanced contractile state. During isometric exercise increased CO is due to increased HR only, stroke V remaining unaltered.

FUNCTIONAL IMAGING OF GATED BLOOD POOL INVESTIGATIONS FOR QUANTIFICATION OF REGIONAL WALL MOTION ABNORMALITIES. W.E. Adam, F. Bitter, W. Nechwatal and M. Stauch, University of Ulm, D-7900 ULM, FRG.

68 patients with suspected or proven coronary artery disease (CAD) underwent a gated blood pool (GBP) study in MLAO 30° and contrast ventriculography (CV) in RAO 30°. GBP yielded the following parametric scans

1 Amplitude of the first Fourier coefficient
2 Phase of the first Fourier coefficient
3 Maximum contraction velocity (Peak ejection rate)
4 Maximum relaxation velocity (Peak filling rate)
5 Difference between enddiastole and endsystole
6 Difference between end of fast filling and endsystole.

The reliability of parametric scanning could be proven by comparing pixel curves with the global LV-curve yielding a scan of correlation coefficients (CC). The CC show values greater than .9 in more than 78% of a normal LV and tend to zero in regional wall motion abnormalities (RWMA).

7 segments from GBP are compared with 9 segments from CV. The results are presented. E.g. the amplitude scan shows 80.4% detectability of RWMA's with no false positive results. The size of RWMA's correlated with $r = .803$. The phase scan showed no phase shift in normokinetic hearts, but significant phase shift in 60% of all patients with RWMA's, by far exceeding the dyskinesis rate revealed by CV (16%). The combination of amplitude and phase scans yielded a conformity of 90.8%, a sensitivity of 86.4% and a specificity of 100%.

LEFT VENTRICULAR VOLUME CHANGES DURING SUPINE EXERCISE IN PATIENTS WITH AND WITHOUT CORONARY ARTERY DISEASE. D.E. Manyari, L. Melendez, A. Driedger, T. Cradduck, P. Purves, W. J. Kostuk, University of Western Ontario, London, Ont.

There are conflicting reports regarding left ventricular (LV) volume changes associated to supine exercise (Ex) in patients (pts) with coronary artery disease (CAD) and in normal (N) subjects. Thus, LV end-diastolic volume (EDV) and end-systolic volume (ESV) changes during supine Ex, were evaluated in 118 pts using ECG-gated blood pool cardiac scintigraphy, by counting techniques. Cardiac catheterization within 7 days of the study disclosed N coronary arteries in 40 and CAD in 78. Of those with CAD, 42 pts have had at least one myocardial infarction (MI) 3 months or longer prior to the study, and 36 have had no previous MI. The Ex protocol was one of increasing workloads each 3 min, with acquisition made during the last 2 min, until symptoms or undue fatigue. Forty-eight pts with CAD developed angina or ECG ST segment depression on Ex, and 30 pts exercised to end-point fatigue. The LV volumes during Ex were compared to those at rest. In the N group, EDV increased an average of 4%±2% (±SEM) ($p>0.05$), ESV decreased 35%±4% ($p < 0.001$). In pts with CAD as a single group, EDV increased 18%±3% ($p < 0.05$), and ESV increased by 36%±5% ($p < 0.001$). The subgroup of pts with CAD and no previous MI increased both, EDV by 26%±5% ($p < 0.05$) and ESV by 54%±9% ($p < 0.01$); while pts with previous MI increased EDV by only 11%±3% ($p> 0.05$) and ESV by 20%±5% ($p < 0.05$). Similarly, in those with evidence of ischemia on Ex, EDV increased by 32%±4% ($p < 0.01$); while in those that exercised to fatigue EDV increased only by 8%±4% ($p>0.05$). Thus, pts with CAD comprise various subsets, each with different LV volume response to supine Ex.

SIMULTANEOUS DETERMINATION OF LEFT VENTRICULAR EJECTION FRACTION, REGIONAL WALL MOTION, FILLING PRESSURE AND END-DIASTOLIC VOLUME DURING EXERCISE. W. Nechwatal, W.E. Adam, F. Bitter, H. Sigel, M. Stauch. Dept. Radiology and Dept. Internal Medicine, University of Ulm, Ulm, FRG.

Assessment of functional importance of myocardial ischemia (ISCH) is mandatory in patients with coronary artery disease (CAD) under consideration for aorto-coronary bypass surgery. Left ventricular (LV) ejection fraction (EF) and regional wall motion (RWM) by gated blood pool studies were determined simultaneously with pulmonary artery wedge pressure (PWP) and cardiac output (Swan-Ganz thermodilution catheter) at rest and during exercise--induced ISCH in 15 patients with CAD. LV end-diastolic volume (EDV) was calculated from EF and stroke volume. For analysis of RWM, amplitudes and phases of the first Fourier coefficient of regional time-activity curves were displayed and color-coded ("parametric scanning").

EF decreased from 57.3% at rest to 50.7% during stress ($p<0.01$). Simultaneously, PWP increased from 9.9 mm Hg at rest to 32.7 mm Hg during ISCH ($p<0.001$). Only two patients had normal PWP values during ISCH, but demonstrated abnormal response of EF during exercise. Two patients with normal EF response during exercise showed an abnormal rise of PWP. The increment of EDV during ISCH was moderate (158 ml vs. 181 ml; $p<0.05$), and there was only a slight correlation between PWP and EDV ($r=0.58$). RWM deteriorated from rest to exercise in 12 of 15 patients, according to the amplitude scan. The phase scan revealed new areas of dyskinesis during ISCH in three patients.

The results indicate, that simultaneous determination of filling pressures and volumes as well as systolic parameters of LV function may be supplementary in the assessment of the functional importance of coronary lesions.

8:30-10:00 **ROOM D-1**

CARDIOVASCULAR XI: PERIPHERAL VASCULAR

Moderator: Michael E.Siegel
Co-moderator: Stephen Karesh

TL-201 PERIPHERAL PERFUSION SCANNING: CLINICAL EXPERIENCE. M.E. Siegel, C.A. Stewart, J. Seto, J.K. Siemsen. LAC/USC Medical Center, Los Angeles, CA

The purpose of this report is to describe our clinical experience with Tl-201 peripheral vascular perfusion scanning as a means of evaluating peripheral vascular disease.

To date, 90 patients have been studied. Patients being studied for prognostic information regarding ischemic ulcers (60) are studied at rest using a 1.5 mci dose of Tl-201. Quantification of ulcer perfusion is done by point counting over ulcer and surrounding area. Patients evaluated for significance of arterial lesions are studied by injecting during reactive hyperemia with immediate imaging and repeat imaging in 4-6 hours. If studied pre- and post-op or pre- and post-angioplasty to assess effect of intervention, reactive hyperemia is used. Patients studied pre- and post-sympathetic block are done at rest.

Our findings are as follows: Ischemic ulscers able to develop a hyperemia $\geq$1.5:1 compared to surrounding tissue have an 85% chance of healing, while 85% of those without this hyperemia required amputation. The test appears to be more sensitive and specific than clinical findings or Doppler ultrasound. Stress and delayed images can be helpful in optimizing surgical approach by localizing levels of fixed arterial resistance. Perfusion scanning can help assess the effect of sympathectomy prior to the definitive procedure, and thus, aid in optimizing therapy. The long term effect of transcutaneous angioplasty is being monitored with perfusion imaging.

Non-invasive peripheral perfusion studies are useful adjuncts to the prognostication and therapeutic design of the patient with peripheral vascular disease.

MUSCLE BLOOD FLOW IN INSULIN DEPENDENT PATIENTS WITH DIABETES MELLITUS USING SMALL SOLID STATE CdTe DETECTORS AND XENON-133. J.J. Steinbach, D. Pendergast, and M. Blau. Veterans Administration Medical Center and State University of New York at Buffalo, Buffalo, NY.

Limb muscle blood flow was determined by the intramuscular Xe-133 clearance technique using miniature CdTe semiconductor detectors. Twelve male patients with insulin dependent diabetes mellitus were studied in comparison with 7 normal controls. Muscle blood flow was determined at 4 muscle sites simultaneously (R&L vastus lateralis, R&L tibialis anterior). Measurements were made at rest, during 75W exercise and recovery using a bicycle ergometer. Concomitant serum lactic acid determinations were also obtained. There was no difference in resting blood flow between the diabetic group and controls. During exercise, consistent significant reduction of muscle blood flow was demonstrated in the vastus lateralis muscles (L $p<0.04$, R $p<0.004$). The reduction of flow in the anterior tibial muscles was less consistent. Although there was a tendency for the recovery blood flow to remain higher in the diabetic group, this was not consistently significant in all muscles studied. The diminished blood flow during exercise was reflected in markedly elevated and prolonged lactic acid levels.

The diminished blood flow to the vastus musculature is quite remarkable and surprising. It has not previously been reported. In view of these findings proximal muscle blood flow measurements with Xe-133 may provide a very useful diagnostic marker for small vessel disease in patients with diabetes mellitus.

RADIOISOTOPIC DYNAMIC STUDY OF THE ASSESSMENT OF PERIPHERAL ARTERIAL DISEASE. M. Oshima, Y. Koh, H. Kobayashi, M. Akisada and H. Ijima. Institute of Clinical Medicine, The University of Tsukuba, Ibaraki, Japan.

A new tracer technique was performed for evaluation of peripheral vascular disease by injection of an intravenous bolus of 20 mCi of 99m-Tc albumin. A cuff is applied to each ankle or forearm and the manometric pressure is raised 50 mmHg above the systolic pressure. Ischemia is maintained for two minutes by active muscular exercise. 99m-Tc albumin is rapidly injected into the antecubital vein after releasing the cuff pressure. The time activity curves (TAC) and sequential images in bilateral toes and each finger of the hands were obtained during reactive hyperemia

using a Baird System 77. For about two years we examined 16 normal subjects and 71 patients; Buerger's disease, 26; Arteriosclerosis obliterans, 22; Raynaud's phenomenon, 8; Diabetes mellitus, 5; and Miscellaneous, 10.

TAC in bilateral toes and each finger were compared to: (1) normal subjects (16 cases), (2) occlusive lesions which were proved by constant arteriography (45 cases), (3) pre- and post-operative patients (8 cases), (4) Raynaud's phenomenon with ice water (8 cases).

Results are as follows: (1) In normal subjects, TAC showed a marked peak at the first phase. (2) TAC showed the peak activity in occlusive lesions with collateral system, whereas showed the slight peak or the absent of peak with a gradual upward slope in occlusive lesions without collateral system. (3) TAC correlated with the results of vascular surgery. (4) TAC in Raynaud's phenomenon with ice water showed abnormal pattern. TAC in bilateral toes and each finger which have not been reported are reliable vehicle for evaluation of the peripheral vascular disease.

PRACTICABLE LYMPHOSCINTIGRAPHY AS AN ADJUNCT TO MICRO-LYMPHATICO-VENOUS ANASTOMOSES. G.A. Sacks, M.L. Born, J.A. Clanton, W.W. Hunter, J. Franklin, F.D. Rollo. Vanderbilt Medical Center, Nashville, Tennessee

The lymphedematous upper extremity such as that resulting from a radical mastectomy, is now potentially correctable using the microsurgical technique of lymphatico-venous-anastomoses. Success of the procedure depends upon the identification of suitable lymphatic channels and is related to the number of patent anastomoses performed. Scintigraphic techniques have been developed for the preoperative assessment of these patients. Our studies determine the presence and location of lymphatic channels, provide a semi-quantitative assessment of lymphatic flow rates, and illustrate the extent of collateralization. A reproducible method for preparing a micro-colloid suitable for lymphoscintigraphy was developed using an approved radiopharmaceutical preparation as the precursor. Filtration of Tc-99m sulfur colloid from commercially available kits using 0.2 micron Nucleopore and 0.22 micron Millipore filters was studied. Kits from four manufacturers were evaluated for the fractional activity retained on the filters and that passed in the filtrate. Filtrate yields from three of the four kits using the Nucleopore filter were 25%, 36%, and 60% respectively. Millipore filtration yields from two of the four kits were 14% and 35%. A dose of 500 uCi of the sub 0.22u sulfur colloid is administered intradermally in the dorsum of the hand. Normal upper extremity images demonstrate a single lymphatic channel with early evidence of axillary activity. In contrast, multiple tortuous collateral vessels with marked prolongation of the lymphatic transit time hallmark the edematous extremity. Post-operative improvement in lymphatic kinetics can be followed by this technique.

KRYPTON-81m : A MUCH BETTER RADIONUCLIDE FOR VENOGRAPHY. H.R. Ham, J. Vandevivere, M. Guillaume Th. Niethammer, R. Sergeysels and A.M. Ermans. St Peter's Hospital. Free University of Brussels and Centre de Recherche de Cyclotron, Liège, Belgium.

The clinical value of radionuclide venography is widely recognized and accepted. The radionuclides commonly used have, however, an inherent disadvantage due to the limitation of the dose. Krypton-81m is a noble gas. After I.V. injection, it is entirely exhaled during its transit in the lung, hence no limitation of the dose and no build-up in background level. A high count number can be accumulated using a high resolution collimator to ensure good quality images. The study can be repeated without delay in different projections, without or with tourniquet(s), until a satifactory result is obtained.

Routine delivery and clinical use of improved Kr-81m perfusion generator have been made available from a new and highly reliable remote controlled gas target system using the ^{nat}Kr (p,2n) Rb-81 reaction. Optimisation of Kr-81m elution efficiency and Rb-81m breakthrough provided a continuous production of Kr-81m in an injectable non ionic sterile solution at a high constant rate.

The comparison of venography using Kr-81m and Tc-99m MAA showed an absolute superiority of Kr-81m. A complete study (without and with tourniquet(s) applied at different parts of the limb) gave precise localisation and extension of deep vein thrombosis and also the physiological pathway of venous return. Comparison with contrast venography showed a very good correlation.

SHORT- AND LONG-TERM FOLLOWUP OF GELFOAM (GF) INJECTED FOR THERAPEUTIC EMBOLIZATION AFTER LABELING WITH VARIOUS RADIONUCLIDES. S. Karesh, D. Pavel, D. Spigos, I. Iossifides. University of Illinois Medical Center, Chicago, Illinois.

Embolization of the spleen and other organs has recently gained acceptance as a therapeutic procedure. Rapid non-invasive determination of the placement of GF particles labeled with Tc-99m following a $SnCl_2$ reduction has been previously reported. Due to the unavailability of radiopharmaceutical grade $SnCl_2$ solution, we have developed and optimized a procedure using commercial Sulfur Colloid (SC) kits. The labeling mechanism appears to involve mechanical trapping of the Tc-SC as it is formed in the GF matrix. In addition, using this same trapping mechanism, procedures have been developed for labeling GF with In-111 and Hg-203 by precipitating salts of these radiometal cations within the GF matrix. Use of these longer-lived isotopes enables long range follow-up of the fate of radiolabeled GF. Tagging efficiencies for all 3 isotopes were good (>60% incorporation of added isotope; essentially 100% tag efficiency after washing). In vitro stability studies of Tc-99m labeled GF indicated no loss of activity in the 1st 3 hours post labeling. Following transcatheter placement of tagged GF into the spleens of several dogs, imaging at 1-hour post injection with a scintillation camera consistently produced high quality images of the radioemboli. In addition, due to the good in vivo stability of labeled GF, good quality images were obtained for up to 1, 9, and 125 days post injection for Tc-99m, In-111, and Hg-203 labeled GF, respectively. In conclusion, a simple, rapid, reliable, inexpensive, and reproducible method is available for use in humans in determining the fate of intra-arterially injected GF.

8:30-10:00 **ROOM B-1**

ONCOLOGY II

Moderator: William H. Beierwaltes
Co-moderator: Leopoldo L. Camin

RELATIONSHIP OF "COMPLIANCE" IN THERAPEUTIC PROCEDURES TO SURVIVAL TIME AND CURE IN 103 PATIENTS WITH METASTASES OUTSIDE THE NECK FROM WELL DIFFERENTIATED THYROID CARCINOMA. W.H. Beierwaltes, J.E. Copp, A. Kubo. University of Michigan Medical Center, Ann Arbor, MI.

Since ∿ 75% of patients with metastases outside the neck from thyroid carcinomas die within 5 years of histopathologic diagnosis (HD), we carried out a follow-up of 103 such patients with papillary (PC) and follicular carcinoma (FC) observed between 1-1-47 to 6-30-80 to relate the "compliance" to our 10 principal steps in surgical and I-131 treatment to survival time (ST) from the first HD and apparent freedom from thyroid Ca ("without disease"). Follow-ups to June 1980 were obtained in all but 2 patients (followed-up from 1969-73, and from 1968-74). Forty-eight patients with PC were alive and 30 dead. Nine patients with FC were alive and 16 were dead. The cause of death was documented in each patient. Therapeutic steps determined to have a statistically significant increased survival time free of their disease were: 1) bilateral lobectomy within one year of nodule detection; 2) off T4 and T3 6 weeks before I-131 scan; 3) scan within 3 months of surgery; 4) treat with I-131 for significant residual uptake; 5) if recurrence of uptake, retreat with >150 mCi of I-131. The ST of patients with PC alive and "without" disease (16.7 yrs) was 3 times that of patients dead "with" disease (5.8 yrs). The ST of patients with FC alive and "without" disease (19.0 yrs) was 3 times that of patients dead "with" disease (6.7 yrs). The patients with PC who died "without" disease (14.8 hrs) survived 3 times > those dead with their

disease (5.8 yrs). Although the numbers are small, these data offer guidance in deciding the efficacy of therapeutic steps in treatment with I-131.

Co-55-BLEOMYCIN IN THE DETECTION OF LUNG CANCER AND BRAIN METASTASES. O.E. Nieweg, D.A. Piers, H. Beekhuis, A.M.J. Paans, J. Welleweerd, W. Vaalburg, M.G. Woldring. Department of Nuclear Medicine, University Hospital, Groningen, The Netherlands.

The value of Co-57-bleomycin in the detection and staging of lung cancer is well established. However the long half-life of Co-57 (270 days) is a major drawback for its widespread use. The purpose of this investigation was to study Co-55, which has a half-life of 18.2 hours, as a label for bleomycin.

Eleven patients with histologically proven lung cancer and two patients with a brain metastasis of lung cancer were studied. Co-55, a positron-emitting radionuclide, was produced in a cyclotron by bombarding natural iron with 35 MeV protons. A quantity of 1 mCi Co-55-bleomycin was injected intravenously. Positron imaging was performed using two colinear positioned uncollimated large field of view scintillation camera heads, operating in a coincidence mode.

In ten patients the tumor in the lung was shown on the Co-55-bleomycin tomograms. In one patient the tumor, a small size adeno carcinoma (2.5 cm), was not visualized. The weighed mean of the tumor-lung ratios was 1.9 $\pm$ 0.1. In both patients with a brain metastasis this was clearly demonstrated on the tomograms. The total body radiation burden to the patient was 0.5 rad/mCi.

It is concluded that, using a positron camera, Co-55-bleomycin is useful in the detection of lung cancer and its brain metastases. The hazard of environmental contamination is avoided while the excellent tumor seeking properties of the Co-bleomycin complex are retained.

EVALUATION OF RADIOPORPHYRINS AS TUMOR SEEKING AGENTS IN EXPERIMENTAL ANIMALS. R.A. Fawwaz, T.S.T. Wang and P.O. Alderson. College of Physicians & Surgeons, Columbia University, New York, NY.

Various radiolabeled metalloporphyrins localize in tumors, but their use as tumor scanning agents has been limited by low tumor-to-background ratios. This investigation was designed to determine if the target-to-nontarget ratio could be improved by modifying the chemical structure of the porphyrins. A total of 16 porphyrins with differing physico-chemical properties were evaluated. Because of ease of preparation, the porphyrins were chelated with Co-57 and 20 uCi doses were administered i.v. to Fischer rats (n=4-8 per test group) bearing TCT-4904 bladder transitional cell carcinomas implanted subcutaneously. Animals were sacrificed and the tissue distribution of the radioporphyrins was determined at 2 and 5 days after tracer administration and compared to the distribution of Co-57 chloride and Ga-67 citrate in animals bearing similar tumors. The biodistribution of the radioporphyrins was influenced by a variety of factors including water and lipid solubility, protein binding and the site of charge. Hepatic localization and renal excretion were usually present. Certain water soluble radioporphyrins such as tetra-N-methyl-4-pyridyl porphyrin achieved high tumor-to-blood ratios at 2 d (21:1) and 5 d (44:1). These were superior to the Ga-67 ratios at the same times (11:1 and 23:1, respectively)($P<0.01$). The % ID/gm in tumor exceeded gallium by nearly a factor of 2:1 at both 2 and 5 d. Scintigraphy following administration of these compounds revealed good tumor visualization. The study suggests that more extensive investigation of certain metalloporphyrins as tumor-seeking agents is warranted.

ON THE MECHANISM OF RADIOGALLIUM UPTAKE OF TUMOR CELLS IN VITRO:EFFECT OF TRANSFERRIN,LACTOFERRIN AND pH. S.R.Vallabhajosula,H.Lipszyc,S.J.Goldsmith,and T.Ohnuma. Mt. Sinai Medical Center, New York, NY.

Transferrin(Tf)has been shown to promote gallium uptake (GaU)by tumor cells in tissue culture.We compared the effect of Lactoferrin(Lf),another trivalent metal binding protein on GaU by the human Burkitt lymphoma cells in tissue culture. Since tumor tissue is known to be acidic,we also studied the effect of pH on GaU by the cells.

Cells were incubated for 1hr at 37°C,with either Gallium-67 citrate(Ga),Ga-Tf,Ga-Lf or a mixture of Ga-Tf and Ga-Lf in tissue culture media.The concentration of the protein in the media varied from 4-800ug/ml.Both proteins promoted GaU by the cells and the Lf enhancement of GaU is greater than Tf effect(3.3%vs0.7%).Optimal concentration for either Tf or Lf is 40-80ug/ml,but when both proteins were present simultaneously,the optimal concentration was reduced to 30 ug/ml each.With Tf,GaU increased with time while with Lf, GaU is greatest earlier and gradually decreases.

To study the effect of pH,the cells were incubated with either I-125-Tf-Ga,or I-125-Lf-Ga,in MOPS buffer at pH range 6.0-7.5. With Tf,GaU increases significantly at acidic pH(2.7% at 6pH vs 0.3% at 7.5pH),while with Lf the pH effect is minimal(5.4% at 6pH vs 3.4% at 7.5pH). However,the amount of I-125 Tf or Lf associated with the cells is similar in both cases.

Lf causes greater enhancement of GaU by tumor cells than does Tf but the mode of interaction seems to be similar.At acidic pH and only with Tf,GaU is increased,similar to Ga citrate.These results suggest that the mechanism of GaU by tumor cells may not be mediated entirely through specific Tf receptors,but may also be influenced by other conditions such as pH of the incubation medium.

EVALUATION OF RADIOLABELED 5-FLUOROURACILS FOR NUCLEAR SCINTIGRAPHY. G.A. Russ, M.A. Campione. Memorial Sloan-Kettering Cancer Center, New York, NY.

Cancer therapy involving 5-fluorouracil (5-FU) would be augmented by the ability to identify 5-FU sensitive malignancies and to predict local 5-FU concentrations prior to initiation of treatment. It has been demonstrated that 5-FU (F-18) uptake is significantly higher in 5-FU sensitive tumors than 5-FU resistant tumors. However, most of the administered 5-FU is catabolized and regional assessment of tumor concentrations is impeded by high circulating background activities resulting from F-18 labeled metabolites. We have predicted that the Carbon 2 of 5-FU is catabolized and cleared more rapidly than the rest of the molecule; thus a short-term distribution study was performed to determine if a C-11 label at this position would be superior to the F-18 label for assessment of 5-FU sensitive tumors.

Two groups of thirty mice were implanted with L-1210 lymphocytic leukemia and were treated on the seventh day with 1μCi each of 5-FU 2-(C-14) or 5-FU 6-(C-14). Groups of animals were sacrificed at designated times up to two hours and the tissues of interest were excised and the activity counted. The results showed that the relative concentration of C-14 acitivity in the tumors was not dependent on the position of the label, but that activities in blood and muscle were much lower (~10%) with the 2-(C-14) label and were similarly reduced in other tissue. These studies indicate that a more satisfactory assessment of 5-FU tumor concentrations would be obtained using 5-FU 2-(C-11) than using 5-FU (F-18).

RADIOCOLLOID UPTAKE IN AKR SPONTANEOUS LYMPHOMA. B.M. Gallagher, M.L. Delano and L.L. Camin. New England Nuclear Corp., N. Billerica, MA.

The clinical application of lymphoscintigraphy in defining regional lymph node metastases has been hampered by insufficient data on the correlation between lymph node uptake of a suitable radiocolloid and the histopathological changes in lymph node structure. This study has explored this relationship in the spontaneous AKR lymphoma model in mice. Three groups of animals were studied, CD-1 normal albino mice and AKR/J mice either before or after the clinical onset of the disease as determined by general appearance, lymph node enlargement and elevated leukocyte counts (WBC). Groups of animals were injected via the footpad with Tc-99m minimicroaggregated albumin (mμAA), and imaged at 2 hrs. The correlation between the absolute lymph node uptake and the degree of neoplastic infiltration was determined. The results showed that the uptake of mμAA by the popliteal, lumbar and peri-renal nodes was

equivalent between CD-1 and pre-involved AKR animals. As the disease progressed, increasing percentages of the lymph node mass were replaced by neoplastic lymphoblasts. This could be readily observed by lymphoscintigraphy as a decreased intensity of the lymph nodes in the images. The WBC count did not correlate with the severity of the disease. In the advanced stages of the disease the absorption of mμAA from the injection site was decreased significantly, possibly the result of altered lymph flow. Taken collectively, these results show excellent correlation between the presence of histologically confirmed neoplastic infiltration and lymphoscintigraphy with Tc-99m-mμAA in a spontaneous mouse lymphoma. The clinical extension of these studies to a variety of neoplastic conditions appears warranted.

8:30-10:00 **ROOM E-1**

RADIOPHARMACEUTICALS IV: Tc-99m RADIOPHARMACEUTICALS

Moderator: Gopal Subramanian
Co-moderator: James F. Lamb

THE DEVELOPMENT OF A NEW CHOLESCINTIGRAPHIC AGENT, Tc-SQ 26,962, USING A STRUCTURE-DISTRIBUTION RELATIONSHIP APPROACH. A.D. Nunn, M.D. Loberg, R.A. Conley and E. Schramm. Squibb Institute for Medical Research, New Brunswick, N.J.

The Tc-HIDAs have experienced somewhat random efforts to improve their characteristics as hepatobiliary agents, and there are now many equivalent agents. Our directed approach, first developing suitable model systems and then developing structure-distribution relationships (SDRs) with subsequent synthesis of optimum compounds, has yielded a superior agent. Rabbits were imaged with a gamma camera connected to a computer to obtain time-activity curves from which the in vivo kinetics of each agent were obtained. A pool of a dozen animals was used to eliminate inter-or intra-individual differences. Tissue samples were taken from rats to determine the hepatobiliary specificity, and isolated hepatocytes were used to predict the effects of exogenous and endogenous compounds on liver uptake. The models were validated using currently ranked compounds. The lipophilicity and protein binding of the different HIDA derivatives were determined using HPLC and affinity chromatography. Information from thirty derivatives was used to develop SDRs. It was determined that each ligand could be divided into two parts, one influencing protein binding and hence the compounds hepatobiliary specificity and the other affecting both the stability of the compound and its complexes and also intrahepatic kinetics. Using this information we have synthesized Tc-99m SQ 26,962, a complex with vastly superior characteristics as an hepatobiliary agent. It has faster in vivo kinetics, higher specificity and is more resistant to bilirubin. The radioactivity passes through the hepatobiliary system as a bolus with all the advantages this implies.

SYNTHESIS AND BIOLOGICAL DISTRIBUTION OF A NEW HEPATOBILIARY AGENT (Tc-99m-NIBC)* M. A. Antar and S. N. Banerjee. University of Connecticut Health Center, Farmington, CT and V. A. Medical Center, Newington, CT.

In the course of developing radiopharmaceuticals for renal function studies, we synthesized several ortho-iodohippuran analogs and prepared their Tc-99m complexes. One compound of these series (Tc-99m-NIBC) showed much faster hepatic uptake and very fast clearance from the hepatobiliary system in rabbits compared to Tc-99m-HIDA. We made the 99m-Tc complex at a high specific activity (5mCi/mg). After intravenous administration in rabbits γ-camera imaging at different intervals up to 60 minutes showed greater concentration in the hepatobiliary system and much faster clearance from the gallbladder into the intestine compared to those after Tc-99m-HIDA. Our compound has also much less activity in the kidneys compared to Tc-99m-HIDA. At 15 minutes after injection, 47% of injected dose was secreted in the small intestine and 23% in the hepatobiliary system. Mean total urine activity was 1% of injected dose. Mean activity in other tissues (% dose per gm) are as follows: blood (0.038), renal cortex (0.142), renal medulla (0.138), muscle (0.001), and stomach wall (0.005). The low stomach activity indicates minimum cleavage of "free" technetium from our compound indicating relative in vivo stability. It appears that this new agent, Tc-99m-NIBC has a promising potential for hepatobiliary function studies. *(University of Connecticut Invention Disclosure)

DEVELOPMENT OF A Tc-99m MYOCARDIAL IMAGING AGENT TO REPLACE Tl-201: PART II - Tc-DMPE. V.J. Sodd, K.L. Scholz, D.L. Fortman and H. Nishiyama, Nuclear Medicine Laboratory, BRH, FDA, Cincinnati, OH and E.A. Deutsch, K.A. Glavan and W.C. Bushong, Department of Chemistry, University of Cincinnati, Cincinnati, OH.

Thallium-201 is used routinely in nuclear medicine as a myocardial imaging agent. Because of its higher cost and inferior scintigraphic and dosimetric properties as compared to Tc-99m, efforts have continued at our laboratories to find a Tc-99m labelled agent to replace Tl-201. A long search for this Tc-99m agent resulted in a report at last year's meeting by Deutsch (Part I, JNM 21, p56 (1980)) of a Tc-99m labelled organometallic arsenic compound (Tc-DIARS) that showed promise as an agent that localized in healthy myocardial tissue. However, because this compound was insoluble in water, it presented difficulties with the injection. Present work describes a second type of compound (Tc-DMPE) that has initially demonstrated better myocardial uptake and complete water solubility. This complex with a +1 chemical charge consists of organophosphorous ligands and a central technetium atom. Preparations were tested for heart uptake by injection into normal anesthetized dogs and visualization on a gamma camera with a high-sensitivity collimator. The best scintiphotos achieved to date appear to be comparable to those obtained using Tl-201. Uptake of this agent occurs rapidly (<5 min) with retention times greater than 1 hr with concomitant uptake in the gall bladder similar to that of the earlier reported DIARS agent. It is concluded that a useful Tc-99m labelled agent to possibly replace Tl-201 for imaging healthy myocardial tissue has been found.

RENAL TRANSPORT MECHANISM STUDIES OF Tc-99m-N,N'-BIS-(MERCAPTOACETAMIDO)ETHYLENEDIAMINE, A. R. Fritzberg, W. P. Whitney, C. C. Kuni, and W. C. Klingensmith III. University of Colorado Health Sciences Center and VA Medical Center, Denver, CO.

Biodistribution studies of Tc-99m-bis(mercaptoacetamido)ethylenediamine (Tc-DADS) have shown that it is predominately excreted into the urine without renal retention and at a rate slightly slower than I-131-o-iodohippurate (OIH) but faster than Tc-99m-DTPA. More rapid renal excretion than Tc-99m-DTPA, an indicator of glomerular filtration, and the fact that the complex is 95% plasma protein bound suggests that it is actively secreted by the renal tubular cells. The effects of probenicid, an inhibitor of renal tubular secretion, and 2,4-dinitrophenol (DNP), an uncoupler of energy supply for active transport were studied on Tc-DADS in mice in order to determine if 1) renal tubular cell transport is occurring and 2) the relative efficiency of renal excretion of Tc-DADS and OIH in the presence of reduced tubular cell function. Tc-DADS radioactivity in the blood, liver, and intestines was markedly increased with both inhibitors. OIH changes were small but in the same direction. Tc-DADS renal excretion at 15 min was 67% in controls, 31% with DNP, and 20% with probenicid. OIH renal excretion at 15 min was 78% in controls, 73% with DNP, and 71% with probenicid. No significant changes were observed with Tc-99m-DTPA. Active renal tubular secretion of Tc-DADS is thus indicated by the results. The much greater reduction of renal excretion of Tc-DADS than OIH indicates a lower affinity for the renal anion transport system. This suggests that Tc-DADS may be more sensitive to mild decreased in renal function, but not as effective as OIH in cases of poor renal function.

CHEMICAL AND BIOLOGICAL STUDIES OF Tc-99m-N,N'-BIS-(MERCAPTOACETAMIDO)ETHYLENEDIAMINE: A POTENTIAL REPLACEMENT FOR I-131-HIPPURAN. A.R. Fritzberg, W.C.Klingensmith III, W.P. Whitney, and C.C. Kuni, University of Colorado Health Sciences Center and VA Medical Center, Denver, CO.

A Tc-99m labeled radiopharmaceutical with the biological properties of I-131-o-iodohippurate (OIH) would result in an agent with a several fold greater extraction efficiency than Tc-99m-DTPA and would allow doses such that renal perfusion could be simultaneously evaluated. As a result of the report (Davison, et al., J Nucl Med 20 641,1979) that Tc-99m-N,N'bis(mercaptoacetamido)ethylenediamine (Tc-DADS) was rapidly excreted by the kidneys we synthesized the chelating agent precusor and evaluated its behavior in mice, rats, and rabbits.

Analysis of the Tc-99m chelate by HPLC indicated a main peak (85-90%) and a shoulder peak (10-15%) when prepared with dithionite, stannous chloride, or formamidine sulfinic acid as reducing agents. Plasma protein binding of Tc-DADS was 95%. Biodistribution studies in mice indicated rapid blood disappearance with less than 1% left at 30 min. Kidney radioactivity was 12.6% at 5 min and decreased to less than 1% at 120 min. In rats the blood disappearance slopes of Tc-DADS and OIH were similar although initial blood values of Tc-DADS were similar to Tc-99m-DTPA. Renal excretion measurements in rabbits indicated 73.9±6.0% for Tc-DADS, 85.2±9.1% for OIH, and 42.9±12.8% for Tc-99m-DTPA at 35 min post injection. Biliary excretion of Tc-DADS in rats at 90 min was 7% under normal conditions and 18% in the absence of renal function. HPLC analysis of urine and bile indicated no chemical change in urine and over 80% unchanged in bile. The rapid renal excretion without retention of Tc-DADS warrants clinical evaluation.

ANALYSIS OF Tc-HIDAs AND FACTORS AFFECTING THEIR LABELING RATE, PURITY AND STABILITY. A.D. Nunn, E. Schramm. Squibb Institute for Medical Research, New Brunswick, N.J.

We have investigated the variation with time of the radiochemical composition of various ortho substituted Tc-HIDAs using HPLC and found that the size of the substituent influences the radiolabelling rate, the radiochemical purity and the radiochemical stability. In the series O-Dimethyl, O-Diethyl, O-Diisopropyl-HIDA the rate of complexing with Tc under identical conditions decreases with increasing size of the substituent. The labeling rate is affected by the pH of the solution, being higher at a lower pH. The concentration of the ligand but not the concentration of stannous ion also affects the labeling rate. The labeling curves are biphasic with a rapid, ligand dependent first phase followed by a slower, ligand independent second phase. This suggests that the reaction proceeds via an intermediate which is either converted directly to the final product or into another metastable form. The stability of HIDAs and Tc-HIDAs is also affected by the size of the substituents, furthermore, as the size of the ortho substituent is increased additional radiolabelled species are observed. Some of these species (which are neither free nor reduced hydrolyzed technetium) modify the in vivo characteristics of the Tc-HIDAs. These results demonstrate that the Tc-HIDA system is complex and that paper or thin layer systems are incapable of resolving all of the radiolabeled species. The complexity of the Tc-HIDA system increases with increasing size of the ortho substituents with the higher members of the series presenting unique problems.

8:30-10:00 **ROOM G-1**

INSTRUMENTATION III

Moderator: L. Stephen Graham
Co-moderator: Stephen E. Derenzo

Tl-201 IMAGING ARTIFACTS NOT DETECTED BY Co-57 or Tc-99m QUALITY CONTROL TESTING. S.J. Lukes, L.W. Grossman, and H. Nishiyama. Nuclear Medicine Laboratory, BRH, FDA and University of Cincinnati, Cincinnati, OH.

Early stages of hydration in a sodium iodide crystal may cause artifactual hot spots on Tl-201 heart images. This hot spot phenomena on Tl-201 clinical images was observed with a mobile gamma camera even though the daily quality control field floods revealed no visual apparent abnormalities. As a follow-up to the clinical observation of artifacts, a series of one million count flood images were taken using several nuclides -- I-125, Tl-201, Xe-133, Co-57, Tc-99m and I-131. Hot spots were clearly visible on only the Tl-201 and Xe-133 floods. With assymetric photopeak positioning using a Tc-99m source, hot spots, in addition to phototube nonuniformities, were noted. Subsequently, the camera head was disassembled and the crystal visually inspected. It was obvious the crystal seal had broken. Although the crystal was not discolored, closer inspection revealed several small shadow areas within. These shadow areas correlated closely with the hot spots observed in the Tl-201 and Xe-133 flood images. A retrospective examination of the Co-57 quality control records occasionally revealed very faint hot spots over a period of several months. However, the degree of nonuniformity appeared to be well below clinical significance and did not reproduce from day to day. Hydration of the crystal was confirmed by the camera manufacturer. Although the exact mechanism of the hot spot production is not understood, it is concluded that quality control procedures should utilize those nuclides imaged in clinical studies.

POSITRON IMAGING WITH THE ANGER TOMOGRAPHIC SCANNER. E.A. Silverstein, E.W. Fordham, A. Chung-Bin, and T. Wachtor. Rush University Medical Center, Chicago, IL.

Positron imaging capability was added to an Anger tomographic scanner by operating the instrument without collimators and placing the upper and lower detectors in coincidence. Data from each accepted positron annihilation imaging event, consisting of an x,γ pair from each detector, is digitized and stored on a disk by a minicomputer based data acquisition system. Other data, such as the position of the detectors with respect to the scan table, are also acquired, allowing the complete specification of each event.

With a fast coincidence resolving time (2τ) setting of 20 nsec the coincidence losses were 13%, showing adequate time resolution for this application. A sensitivity of 3,600 counts/min/μCi was measured for a Ga-68 source placed midway between the detectors which were 60 cm apart. Spatial resolution measurement gave 1.5 cm FWHM for the point spread function.

Satisfactory phamtom images have been obtained and applications of the instrument for animal and human studies are in progress. The combination of high sensitivity and longitudinal, whole body capability make this instrument attractive for use with positron emitters such as F-18 and Fe-52.

LESION PERCEPTIBILITY VERSUS COUNT DENSITY AND IMAGING TECHNIQUE. L.W. Grossman, R.J. Van Tuinen, S.J. Lukes. Nuclear Medicine Laboratory, FDA, University of Cincinnati Cincinnati, OH.

Perceptibility of low contrast lesions in scintillation camera imaging is generally assumed to be dominated by count density statistics and largely independent of the imaging medium. To test that assumption, a series of perception tests were conducted to characterize minimum detectable lesion contrast at selected threshold criteria for transparency film and computer acquired images. Each test consisted of a series of 100 images of a stepwedge phantom with 12 identically sized zones. Simulated cold lesions of constant size but random strengths were randomly induced into each zone of the phantom. Test images were read by experienced readers and then the scores analyzed.

All sets of test images showed roughly similar results. The minimum contrast required for 50 percent detection changed approximately as the square root of count density. The film images showed deviation from this dependence at high and low optical densities consistent with low film contrast or excessive optical density. Results for the

computer acquired images were at least as good, if not better than, the film based images over the entire range of count densities. Also, the variable gray scale of the computer avoided the losses seen at the extremes of the film dynamic range. Deviation of the digital images from square-root dependence on count density was observed at high count densities consistent with threshold effects of the eye.

FIRST AND SECOND ORDER STATISTICAL ANALYSIS OF CAMERA UNIFORMITY. P.T. Cahill and R.J.R. Knowles. The New York Hospital-Cornell Medical Center, Polytechnic Institute of New York, and The Long Island College Hospital, New York, NY.

Quantitative analysis of scintillation camera images is impossible without statistical parameterization of detector response. First order statistical variation is summarized by a new global error estimator (GEE). GEE is independent of information density and correlates with camera performance. GEE is readily measured by the standard global irradiation techniques and yet serves as the upper bound of local irradiation variance - the factor relevant to meaningful quantitative results in clinical practice. For 5 cameras, GEE varied from 3.9 to 10.2 % over a range from 37 to 4440 counts/pixel and was demonstrated to be uncorrelated with the Poisson statistical error.

Second order statistical analysis (texture) was implemented by the spatial gray level dependency method in terms of nine parameters (energy, entropy, correlation, homogeneity, inertia and 4 moments as a function of discrete mappings of the camera field).The significance of these parameters was elucidated by computer simulations in which each phototube was assigned different statistical weighting functions based on the systematic error in the field (GEE). Both first and second order experimental effects were successfully simulated.

A NEW EDGE ENHANCEMENT OPERATOR AND ITS APPLICATION TO THE ANALYSIS OF GATED CARDIAC SCINTIGRAMS. E.G. Hawman, D.A. Turner, W.D. Erwin, P.C. Lee, and M.W. Groch. Siemens Gammasonics, Inc., Nuclear Medical Division, Des Plaines, IL, and Rush-Presbyterian St. Luke's Medical Center, Chicago, IL.

Most boundary detection methods that have been applied to nuclear medicine scintigraphy are based on first- or second-difference operators. Resulting edge positions are found from the positions of maxima or zero-crossing in the first- or second-difference enhancement images. These edge position estimates contain an objectionable bias error which results from the relatively low resolution of gamma cameras for the organ structures of interest. To overcome this bias problem, a hybrid edge enhancement based on a linear combination of first- and second-difference operators was developed. This hybrid edge detector has been applied in a program for the automatic analysis of left ventricular ejection fraction. In addition to the new hybrid edge enhancement, this program incorporates recursive aspects to ensure temporal boundary continuity. The left and right ventricular regions are automatically located by a simple algorithm. Details of these associated algorithms and, in addition, clinical results illustrating program performance will be shown.

USER SOLVABLE AND DETECTABLE PROBLEMS: IMAGE APPEARANCE AND QUALITY CONTROL. G. W. Enos and W. J. Carroll. Picker Corporation, Northford, CT.

Performance of routine and special quality control procedures can provide the end user of scintillation camera equipment with the ability to monitor performance and identify problems needing service attention. With microprocessor controlled correction of various parameters in today's scintillation camera market, the need to recognize problems which may be "covered up" by these correction devices is essential.

In addition to identifying routine and specialized quality control procedures, this paper will deal with identification of common and rare problems which can be identified clinically. Scintigraphic results will be shown to demonstrate the problem and the mechanism by which these problems can be identified.

1:30-3:30 **ROOM A-1**

CARDIOVASCULAR XII: MYOCARDIAL INFARCTION

Moderator: Pierre Rizo
Co-moderator: Frans J. Wackers

IN VIVO ASSESSMENT OF INFARCT SIZE IN DOGS USING A TRANSAXIAL SINGLE PHOTON EMISSION COMPUTED TOMOGRAPHY SYSTEM. C.-M. Kirsch, J.R. Darsee, T.C. Hill, and B.L. Holman. Brigham & Women's Hospital, New England Deaconess Hospital, and Harvard Medical School, Boston, MA.

The accurate in vivo assessment of infarct size could have important implications for diagnosis and treatment of acute myocardial infarction.

Twelve dogs had experimental myocardial infarction induced by occluding coronary arteries supplying the anterior, lateral and posterior wall. Three days after the infarction a dose of approximately 19 mCi 99m-Tc pyrophosphate was administered and the heart of the dog was scanned from the base to the apex in increments of 1.25 cm using a multi-detector SPECT system. Hearts were then removed, sliced transversely in 1.25 cm sections and stained in triphenyltetrazolium chloride (TTC) to delineate and measure the infarcted area by means of planimetry. Consequently the weight of the infarcted tissue was calculated multiplying the plane by the thickness of the section. Infarcts ranged from 1.4 to 75.5 gr. The infarct weights using the SPECT system were calculated by determining the number of volume elements associated with each slice containing 99m-Tc pyrophosphate uptake in the heart.

Correlation analysis of the ECT versus TTC infarct size resulted in good correlation (r = 0.91, slope = 0.8, y intercept = 9.3) with a small standard error of the estimate (SEE = 6.7 gr). ECT detected and localized all infarcts, even as small as 1.4 gm.

This study indicates that SPECT provides a sensitive and accurate method for quantifying infarcted myocardium in vivo.

QUANTITATION OF EXPERIMENTAL CANINE MYOCARDIAL INFARCT SIZE WITH TECHNETIUM STANNOUS PYROPHOSPHATE: A COMPARISON OF MULTIPINHOLE AND ROTATING SLANT HOLE EMISSION TOMOGRAPHY. S.E. Lewis, E. Stokely, L. Buja, R.W. Parkey, J.T. Willerson. University of Texas Health Science Center, Dallas, Tx.

Multipinhole (MP) and rotating slanthole (RS) tomography estimates of myocardial infarct volume measured from 1 cm thich re-constructed slices were compared to multiview planar (2D) estimages of infarct area and to histologic measurements of infarct weight. Infarcts were produced in 21 anesthetized dogs by ligation of the proximal or mid-level branches of the LAD coronary artery. Planar, MP, and RS images were acquired concurrently 24-72 hrs postinfarction, 1-2.5 hrs following i.v. injection of 5-10mCi (2.5mg) technetium stannous pyrophosphate. Results:

DETECTION OF MYOCARDIAL INFARCTION

	21 Infarcts	14 Transmural	7 Nontransmural
	1-23.0 gm, mean = 10.1	7.1-23.0 gm, mean = 12.9	1-9.0 gm, mean = 4.5
2D	18/27 (85.7%)	14/14 (100%)	4/7 (57.1%)
MP	19/21 (90.5%)	14/14 (100%)	5/7 (71.4%)
RS	21/21 (100%)	14/14 (100%)	7/7 (100%)

CORRELATION WITH INFARCT WEIGHT (ALL INFARCTS)

2D	r=0.72	y=0.34X=1.99	SE=±1.87 cm^2
MP	r=0.6	y=0.84X+2.36	SE=±6.37 cm^3
RS	r=0.89	y=0.97X2.04	SE=±2.78 cm^3

The differences between MP and RS estimates of infarct size were significant ($p<0.05$). We conclude: 1) tomographic imaging may aid in detection of small infarcts and 2) RS appears to be superior to MP for infarct sizing.

VALUE OF RADIONUCLIDE VENTRICULOGRAPHY IN THE IMMEDIATE CHARACTERIZATION OF PATIENTS WITH ACUTE MYOCARDIAL INFARCTION. C. Sanford, J. Corbett, S.E. Lewis, G. Curry, A. Anderson, B. Moses, G. Dehmer, P. Nicod, J.T. Willerson. University of Texas Health Science Center, Dallas, Tx.

We tested the hypothesis that admission radionuclide ventriculography (RVG) provides a different functional characterization of patients (pts) with acute myocardial infarcts (MI) than physical examination and chest x-ray (CXR). RVGs were performed in 75 pts with MI within 8±3.1 (S.D.) hours after the onset of pain. By clinical criteria, 29 pts were Killip (K) Class I, 38 K II and 8 K III. Mean LV ejection fraction (EF) was significantly lower in K III (.29±.08) than K I (.51±.13) or II (.44±.17). Pts were subdivided into 4 groups based on their LVEFs: NORM ≥ .55, MILD .40-.54, MOD .25-.39 or SEV <.25. In spite of their clinical classification, 21% of K I pts had MOD or SEV and 12% of K III had only MILD depression of LVEF. K II pts varied widely from NORM to SEV with no statistical distinction possible among LVEF subgroups. Anterior MIs exhibited a significantly lower mean LVEF than inferior (.39±.16 vs .54±.09) due to significantly elevated ESVI (51±27 vs 37±21). No significant differences in LVEFs, LV volumes or regional LV wall motion abnormalities were noted between pts with transmural and subendocardial MIs. Chest x-rays were graded by cardiothoracic ratio and degrees of pulmonary venous congestion (PVC). While increasing PVC was associated with a trend toward higher K class and lower LVEFs, CXRs frequently failed to distinguish among pts with widely varying K classifications and LVEFs. Thus, hospital admission RVG adds significantly to the discriminant power of clinical and radiographic characterization of ventricular function in pts with acute MIs.

COMPARISON OF GLOBAL AND SEGMENTAL VENTRICULAR FUNCTION AT HOSPITAL ADMISSION IN PATIENTS WITH ACUTE TRANSMURAL AND NONTRANSMURAL INFARCTS. P. Nicod, J. Corbett, F. Sanford, G. Dehmer, R. Rude, J.T. Willerson, S.E. Lewis, University of Texas Health Science Center, Dallas, Tx.

Transmural myocardial infarctions (TM) purportedly have a different prognosis than subendocardial infarctions (SEMI). In order to evaluate the effects of TM and SEMI on global and segmental ventricular function we performed radionuclide ventriculography in 118 patients (pts) within 5 days (mean=1.7±1.2, S.D.) following MI. Seventy-two pts had no previous MI. Eighteen had SEMI [15 anterolateral (AL), 3 inferior (I)] and 54 had TM (26 AL, 28 I). Pts with AL SEMI had significantly greater LV ejection fractions (58.3±13.5 vs 37.6±12.6, p <0.05) and fewer dyskinetic segments (1/15 vs 16/26) compared to pts with AL TM but not significant difference in LV end diastolic volume or right ventricular ejection fraction. No significant differences were found in pts with I SEMI vs pts with I TM. Forty-six pts had a previous MI of whom 17 had SEMI (all AL) and 29 TM (18 AL, 11 I). There were no significant differences in measured parameters between SEMI and TM in these pts. However, the overall group of pts with previous MIs had larger LV volumes (end diastolic, p=0.019; end systolic volume, p<0.001) than those without MIs. Thus, 1) initial AL transmural myocardial infarction results in significantly greater LV dysfunction than AL subendocardial myocardial infarction or I transmural myocardial infarction and subendocardial myocardial infarction; 2) this difference is not demonstrable in patients with previous myocardial infarcts but, 3) patients with previous myocardial infarctions have larger LV volumes than patients with their first myocardial infarction.

RADIONUCLIDE VENTRICULOGRAPHY FOR EARLY IDENTIFICATION OF HIGH AND LOW RISK SUBSETS AMONG PATIENTS WITH NO OR MILD POST-INFARCTION HEART FAILURE. P.K. Shah, A.G. Ellrodt, M. Pichler, D. Berman, F. Shellock, H.J.C. Swan. Cedars-Sinai Medical Center, Los Angeles, California

Clinical assessment early after acute myocardial infarction (AMI) may be insensitive in identifying pts at high risk of short-term mortality. Thus, left (LV) and right (RV) ventricular ejection fractions (EF) were determined by Tc-99m-RBC multiple-gated equilibrium scintigraphy within 22 hrs of admission for AMI in 115 pts with no or mild clinical heart failure (CHF). On admission, 77 pts were in Killip Class I (K_1) and 38 were in Killip Class 2 (K_2). Based on EF, 16 pts were in Group (Gr)1 (LVEF ≤0.30; RVEF< 0.39), 20 in Gr 2 (LVEF≤0.30; RVEF≥0.39), 25 in Gr 3 (LVEF >0.30; RVEF <0.39) and 54 in Gr 4 (LVEF >0.30; RVEF ≥0.39). In-hospital mortality from pump failure or arrhythmias was 9/77 (12%) for K_1 and 12/38 (31%) for K_2 pts (p<0.02) with an overall mortality of 21/115 (18%). However, mortality was 11/16 (69%) for Gr 1, 6/20 (30%) for Gr 2, 1/25 (4%) for Gr 3 and 3/54 (5%) for Gr 4. The mortality in pts with LVEF ≤0.30 and RVEF ≤0.39 (Gr 1) was significantly (p< 0.001) higher than in the remaining groups. These data suggest that in pts with acute myocardial infarction and no or mild clinical CHF, early determination of LVEF and RVEF is superior to clinical assessment alone in identifying high and low risk pts.

PRONOSTIC SIGNIFICANCE OF THALLIUM-201 SCINTIGRAPHY IN MYOCARDIAL INFARCTION.
P. Rigo, C. Rigo-Betz, JP. Smeets, JC. Demoulin, G. Foidart, H. Kulbertus; University of Liege, Liège, Belgium.

Myocardial imaging has been used to detect and localize coronary lesions and to assess myocardial infarct (MI) size.

We have analyzed the pronostic significance of parameters derived from Thallium scans performed in 154 patients between day 3 and 6 of the MI. The scans were acquired in 3 views and each of these were analyzed in 5 segments coded as normal (0), midly (1) or severely abnormal (2). An MI size score of 0-30 was calculated. The location of coronary lesions was predicted from the segments involved. Evidence for multivessel disease and proximal LAD lesions (anterolateral defects) were sought. Patients ranged in age from 31 to 75 (mean 58.7). None was in shock or severe heart failure at time of the study. Eighteen months mortality increased from 11.1% (score 0-4), 20.3% (score 5-9) to 39.5% (score ≥ 10). Within each group, pts with recurrent MI had higher mortality despite similar scores. Thirty-five patients had evidence for proximal LAD disease. Among these mortality was highest in the 20 pts with a scan suggestive of associated RCA or LCx disease (78.4% at 18 months). It was 26.7% in the 15 pts with scans suggesting isolated proximal LAD disease. Pts with first MI and isolated distal LAD, RCA or LCx defects had a good prognosis (18 months mortality 10%).

We conclude that both thallium infarct size and location estimates have pronostic significance. Evidence for proximal LAD disease and multivessel involvement carries an ominous prognosis.

IDENTIFICATION OF MULTIVESSEL DISEASE IN MYOCARDIAL INFARCTION PATIENTS PRIOR TO HOSPITAL DISCHARGE. R.S. Gibson, D. D. Watson, B.A. Carabello, G.J. Taylor, N.D. Holt, and G.A. Beller. University of Virginia, Charlottesville, Virginia.

Since patients (pts) are at the highest risk for cardiac events soon after MI, early detection of multivessel disease (MVD) and residual myocardial ischemia may be important. The goals of this study were to identify pts with MVD and compare exercise (Ex) ST depression (ST+) with thallium-201 scintigraphy (Tl-201) for detecting ischemia outside the infarct region. Thus, 66 pts underwent Ex Tl-201 testing (target heart rate:120) prior to coronary angiography (CA) 2 weeks post-MI. Thirty-seven pts had MVD by CA and 29 had single vessel disease (SVD). Ten pts with MVD and 8 with SVD had nontransmural (NT) MI. Four criteria (I-VI) were compared to determine which one best identified pts with MVD: I) Ex limiting angina, II) ST+, III) ST+ and/or angina, and IV) Tl-201 defects in 2 or 3 vascular scan segments.

	I	II	III	IV
Sensitivity(%)	8/37(22)	13/37(35)	15/37(41)	26/37(70)
Pred. Accuracy(%)	8/8(100)	13/19(68)	15/21(71)	26/28(93)

Detection of MVD by criteria IV was greater than I, II or III (p<0.01). The predictive accuracy of criteria II, III was low (68%, 71%) compared to criteria IV (93%)(p<0.05). The prevalence of ST+ was higher in NTMI pts than transmural (T) MI pts (9/18[50%] versus 9/48[21%], p<0.05). These data demonstrate that: 1) multiple Tl-201 defects after low level Ex is more indicative of MVD than ST+; 2) more pts

with NTMI have ST↓ than TMI, whether they have SVD or MVD; and 3) Tl-201 appears more useful in distinguishing remote ischemia from residual ischemia in the infarct zone than ST↓.

SERIAL THALLIUM IMAGING AT REST ON ADMISSION TO THE CORONARY CARE UNIT: AN ANALYSIS OF TRANSIENT AND PERSISTENT DEFECTS AND INCREASED LUNG UPTAKE IN PATIENTS WITH SUSPECTED ACUTE MYOCARDIAL INFARCTION. C.A. Boucher, A.G. Mulley, R.D. Okada, G.E. Thibault, H.W. Strauss, A.M. Green, G.M. Pohost, Massachusetts General Hospital, Boston, MA

Patients with chest pain suspicious for acute myocardial infarction (AMI) are usually admitted to a coronary care unit (CCU) and AMI is either confirmed by enzyme changes, or, if absent, coronary insufficiency (CI) or no acute event (NE) is diagnosed. Prior studies suggest there is substantial mortality after discharge with or without AMI. Because rest Thallium imaging may show defects due to high grade stenosis, serial rest Thallium images were obtained in 55 consecutive patients within 12 hours of CCU admission for suspected AMI. Patients with prior MI, heart failure or valve disease were excluded. Scans were interpreted by 3 observers without knowledge of clinical data. Myocardial defects were graded as transient (TD) or persistent (PD). In addition, the presence of increased lung/heart (L/H) activity ($\geq$.65) was determined. Increased (↑) L/H has been previously shown to correlate with elevated left ventricular filling pressures. Scan findings follow: ($p<.05$*)

	TD	PD	↑ LH
AMI (n=14)	5 (36%)	10 (71%)	8 (57%)
CI (n=26)	16 (62%) *	14 (54%) *	12 (46%) *
NE (n=15)	8 (53%)	5 (33%)	3 (20%)

In conclusion, the majority of CI or NE patients have TD, indicating ischemia at rest. In contrast, patients with AMI have more frequent PD and ↑L/H, indicating left ventricular dysfunction at rest. The Tl-201 findings suggest that severe disease, which may be inapparent by conventional clinical approaches, is often present in patients discharged with either CI or NE.

1:30-3:30 **ROOM D-1**

HEMATOLOGY

Moderator: Edward R. Coleman
Co-moderator: Heinz W. Wahner

USE OF INDIUM-111 LABELED PLATELETS TO ASSESS PLATELET DEPOSITION ON ARTERIOSCLEROTIC PLAQUES IN A PRIMATE MODEL. M.J. Welch, C.J. Mathias, W.J. Powers, L.A. Sherman, B.A. Siegel, and T.B. Clarkson*. Washington University School of Medicine, St. Louis, MO; *Bowman-Gray Medical School, Winston-Salem, NC.

Groups of primates (Macaca arctoides) were fed either a control (n=4) or a high-cholesterol diet (n=4) for a period of at least five years. Serum cholesterol levels in the experimental group were in excess of 250 mg/dl while the control group had levels from 150 to 200 mg/dl. In-111-labeled platelets and Tc-99m-labeled red blood cells were injected into each animal, and consecutive images were taken and stored in a computer immediately thereafter and 24 hours later. The Tc-99m-labeled red blood cell image was used to subtract the blood pool background from the In-111-labeled platelet image to enhance visualization of platelet deposition. The subtracted images allowed the platelet deposition in the regions of the abdominal aorta, femoral, carotid, and renal arteries to be determined. All of the experimental monkeys had abnormal accumulation versus only one of the control animals. Four of the animal studies were repeated (2 experimental and 2 control), and comparable results were obtained. The animals were then given 3 mg/kg/day of aspirin for 5 days and the studies repeated. No abnormal accumulations of platelets were seen in the animals after treatment with low-dose aspirin. Studies are in progress to examine platelet deposition during the administration of high dose aspirin (30 mg/kg/day) and prostacyclin (PGI_2). Our results suggest that In-111-labeled platelets may be useful to study the pathogenesis of arteriosclerosis and pharmacological techniques for its amelioration.

THE INFLUENCE OF HEPARIN ON THE IN VIVO DISTRIBUTION OF IN-111 PLATELETS (In-111-P) IN AN EXPERIMENTAL CANINE MODEL. S. Zoghbi, D. Sostman, R. Neumann, M. Thakur, P. Carbo, P. Lord, A. Gottschalk, R. Greenspan. Yale University School of Medicine, New Haven, CT.

Recent literature is abundant with reports of In-111-P for detecting vascular thrombi including influence of heparin (H) anticoagulation. However, the effect of H on in vivo distribution of In-111-P is unknown. This was examined during our studies of the effect of H on the detection of pulmonary emboli (P.E.) in canine model. After anesthesia, blood was drawn for platelet labeling, thrombi were formed in a jugular vein and embolized by the force of venous return. The in vitro aggregation of In-111-P ranged from 46 to 100%. No aggregates were seen under phase microscopy. One group of animals (N = 3) with a bolus injection of (H) (200 I.V./kg body weight) and a second group (N = 7) with no heparin (NH) were studied. After the I.V. administration of In-111-P, serial blood samples were drawn for 4-5 hours, followed by sacrifice. Samples of blood, liver, spleen, lungs, and emboli were excised and concomitant radioactivity expressed as percent of administered dose. Circulating In-111-P was significantly ($P < 0.01$) different between the two groups at 5 mins. post-administration (H; 59.4±7.8%, NH; 28.9±9.2%) as well as at time of sacrifice (H; 53.5±3.9%, NH; 38.5±4.9%). The liver radioactivity of H-animals was (19.2±2.4%) significantly ($P < 0.01$) lower than that of NH-animals (36.5±8.0%). Spleen and lung radioactivity in both groups was similar ($P < 0.1$). The H treatment did not alter the PE/blood activity ratio (H; 21.3±18.1; N = 9, NH; 30.1±24.4; N = 7). Thus, H treatment improves In-111-P recovery by reducing liver uptake but does not influence the affinity of In-111-P for experimental P.E.

PLATELET DEPOSITION IN ARTERIAL GRAFTS IN MAN. J.R. Stratton, J.L. Ritchie, B. Thiele, D. Bandyk, L.A. Harker, G.W. Hamilton, L. Warrick, and K. McFadden. VA Medical Center and U. of Washington, Seattle, WA.

Platelets have a dominant role in the thrombotic and embolic complications of arterial prostheses. To measure platelet deposition in grafts, we serially imaged ^{111}In platelets 2-4 times over 96 hrs in 6 pts with acute (< 21 days) and in 11 pts with chronic (> 12 months) dacron aortofemoral or aortoiliac grafts. To assess reproducibility, 3 pts with chronic grafts had repeat studies. To assess the effect of sulfinpyrazone (200 mg qid), 6 pts with chronic grafts were restudied on drug. Studies were visually interpreted as positive if activity in the graft was greater than adjacent native artery. In 21 of the 26 studies, serial quantitative ^{111}In activity in the graft was assessed by a ratio of total graft counts from a region of interest divided by counts in 5 cc of blood.

Four of 6 acute grafts had platelet deposition. All 11 chronic grafts had deposition. In chronic grafts, total graft/whole blood activity increased from 24 hr to 72 or 96 hr by 53 to 231% (mean increase 85% at 72 hours; $p < .01$), indicating ongoing platelet deposition in the graft region of interest. Acute grafts had similar increases. Although total graft activity increased relative to blood, the pattern of deposition in the graft varied over time, suggesting a dynamic process of platelet build-up and release. The 3 repeat baseline studies also had marked changes in the pattern of deposition, although all remained positive. None of the 6 sulfinpyrazone studies had a visual or quantitative decrease in platelet deposition compared to baseline.

We conclude that platelet deposition in grafts 1) occurs commonly, even in chronic grafts, which implies a lack of graft endothelialization; 2) is a dynamic process which varies over time and between areas of the same graft; and 3) is not interrupted by sulfinpyrazone.

COMPARATIVE UPTAKE OF CLOTTING FACTORS IN EXPERIMENTAL TUMORS AND ABSCESS. P. Som, Z.H. Oster, K. Matsui, G. Guglielmi, B.R.R. Persson, D.F. Sacker, H.L. Atkins, and

A. B. Brill. Brookhaven National Laboratory, Upton, NY, SUNY at Stony Brook, NY and Lund University, Lund, Sweden

The possibility of using labeled clotting factors for tumor and abscess localization and differentiation was investigated in a adenocarcinoma tumor model in mice and in rats with turpentine-induced abscess. Tissue distribution of Tc-99m-Plasmin (Tc-99m-PL), I-125-Fibrinogen (I-125-FB), I-131-Albumin (I-131-ALB) and Ga-67-Citrate (Ga-67-CT) were determined at 2,4,5,6, and 24 hours.

The highest concentrations(%/g) in the tumors for the above compounds were found to be: Tc-99m-PL 1.05±0.32 (2 hr); I-125-FB 4.67±1.07 (5 hr); I-131-ALB 5.82±0.80 (4 hr); Ga-67-CT 4.80±0.83 (24 hr). The highest tumor/blood (T/B) and tumor/muscle (T/M) ratios were achieved with Ga-67-CT (24 hr), although at earlier time intervals the ratios of the four agents were comparable.

The highest concentrations (%/g) in the abscess were found to be: Tc-99m-PL 0.25±0.03 (4 hr), I-125-FB 1.39± 0.20 (4 hr), I-131-ALB 1.16±0.25 (5 hr), Ga-67-CT 1.49± 0.32 (24 hr). The abscess/blood (A/B) ratios for Tc-99m-PL, I-125-FB and I-131-ALB were never higher than 1.0 at any time intervals but Ga-67-CT reached 3.63 at 24 hours. The range of maximum abscess/muscle (A/M) ratios were between 6.39 (I-131-ALB at 24 hr) and 18.78 (I-125-FB at 4 hr).

The difference in tumor/muscle and abscess/muscle ratios warrants further investigation for possible differentiation between the two processes. I-125 fibrinogen clot localization studies in patients with neoplastic or inflammatory reactions may give false-positive results by direct uptake of the radiopharmaceutical in these lesions.

INDIUM-111 LABELLED LEUKOCYTE SCINTIGRAPHY IN DIAGNOSIS OF INFLAMMATORY DISEASE, M.H. Rövekamp, J.B. van der Schoot, and W.H. Brummelkamp. Academic Hospital Binnengasthuis and Wilhelmina Gasthuis, University of Amsterdam, The Netherlands.

This investigation was undertaken to evaluate the diagnostic usefulness of In-111 labelled leukocytes in inflammatory lesions: A. located intraabdominally and B. after implantation of vascular grafts.

Scintigrams were performed 24 hrs after injection of 300-500 μCi In-111 oxine labelled autologous leukocytes. In patients suspected of an upper abdominal process additional Tc-99m colloid scans were performed. To eliminate liver and spleen uptake subtraction of both images was done.

Material consisted of A. 142 scans performed in 116 patients suspected of an abdominal inflammation, and B. 52 scans in 47 patients after implantation of a vascular graft.

In group A., 87% accuracy, 97% sensitivity and 75% specifity were obtained. Follow-up of patients with false positive scans revealed less intensive leukocyte reactions initiated by non-inflammatory processes. With aid of other clinical data no conclusions leading to re-intervention were drawn from false positive results.

In group B., 83% accuracy, 100% sensitivity and 77% specifity were obtained. False positive scans were present in the early postoperative phase due to non-inflammatory processes such as hematomas.

It is concluded that In-111 leukocyte scintigraphy becomes a reliable diagnostic procedure to detect inflammatory processes.

DETECTION OF PROSTHETIC GRAFT INFECTIONS WITH RADIOLABELED LEUKOCYTES. J.G. Rose, A.I. Serota, S.E. Wilson, and W.H. Blahd. Veterans Administration Wadsworth Medical Center, Los Angeles, CA.

The utility of radionuclide labeled leukocytes for the detection of arterial prosthetic graft infection was studied in 12 dogs in which 3 cm Dacron(R) infrarenal aortic interposition graft had been established. Six dogs received 10-8 Staphylococcous aureus intravenously on the third post-operative day, and six dogs were used as controls. Indium-111 oxine labeled leukocyte studies were performed on all dogs 24 and 72 hrs post-op. Radioactivity concentrated at the graft site in all dogs in the first post-operative week. Subsequent serial examinations of the graft site in control dogs revealed no radioactivity. Radioactivity also declined in all but one infected animal. However, graft radioactivity reappeared and increased in the infected animals at 3 weeks (1), 6 weeks (3), and 8 weeks (1). All six infected animals had histologic and bacteriologic evidence of graft sepsis.

Three patients with suspected graft infections were also studied. Two patients had negative imaging studies and the third patient had a positive study. All studies were confirmed upon graft removal.

Radiolabeled leukocytes appear to be a sensitive and specific method for identifying clinically occult and potentially serious complications of prosthetic graft infection.

A PROSPECTIVE COMPARATIVE STUDY OF THE SENSITIVITY AND SPECIFICITY OF In-111-LEUCOCYTE AND GALLIUM-67 SCINTIGRAPHY. G.N. Sfakianakis, W.Al-Sheikh, A. Heal, G. Rodman Jr, R. Zeppa and A. Serafini. University of Miami, Miami FL

Preliminary experimental work in rabbits with subcutaneous abscesses indicated to us that the sensitivity of In-111-oxine labeled leucocyte (In-111-WBC) and Ga-67 methods of imaging differ, depending on the acute and active nature of the inflammatory process.

In order to study the clinical sensitivity and specificity of the two scintigraphic approaches a prospective study was undertaken in patients with clinical suspicion of focal infection. 24 patients had 25 paired studies in the following order: total body imaging 24 hrs after iv reinjection of In-111-oxine labeled autologous leucocytes (200-700 μCi, 100-700 million leucocytes), followed immediately by injection of 5 mCi of Ga-67 citrate and imaging at 24 and 48 hrs. The scintigrams were interpreted independently by different specialists with knowledge of the clinical condition. Both In-111-WBC and Ga-67 methods detected correctly 3 abdominal, 4 thoracic, 2 hepatic and 2 skeletal focal infections, and both missed an endocardiac lesion. Ga-67 was alone positive in 1 abdominal wall abscess and in 1 case of resolving septic pulmonary emboli. In-111-WBC was alone positive in 1 pyogenic liver abscess and in 3 patients with pulmonary and or pleural lesions. Ga-67 however, gave confusing abdominal images (in 9 patients intestinal or healing wound activity could not be differentiated from potential foci of infection) and it accumulated within neoplastic lesions(liver and lung) whereas In-111-WBC gave normal results. There was some indication that Ga-67 had a higher affinity for old or resolving lesions whereas In-111 WBC detected a few acute lesions not accreting Gallium.

COMPARISON OF In-111 LABELED PLATELETS, LYMPHOCYTES AND LEUKOCYTES FOR DETECTING EXPERIMENTAL CARDIAC ALLOGRAFT REJECTION. T.S.T. Wang, R.A. Fawwaz, S. Oluwole, M.A. Hardy and P.O. Alderson. College of Physicians & Surgeons, Columbia University, New York, NY.

This study evaluates the utility of infused In-111 labeled cells for detecting rejection in rat heart allografts. Heterotopic and syngeneic hearts were transplanted into the peritoneal cavity of Lewis rats. The mean survival time was 6.5 days in control recipients (n=10). Syngeneic leukocytes, lymphocytes or platelets were isolated, labeled with In-111 oxine and given i.v. to rats carrying allograft or syngeneic (control) hearts 0-6 d post-transplantation. Recipients were imaged 24 hrs after infusion of labeled cells. The animals were then sacrificed and both native and transplanted hearts were excised and cts/gm determined. Labeled leukocytes accumulated progressively in allografts. The transplant was visualized (positive scan) by day 4. The mean ratio of allograft to native heart isotope counts rose from 1.25 on day one to 10.07 ($P<0.0001$) on day 7. The transplant:blood ratio on day 7 was 10:1. In-111 platelets gave positive scans on days 5 through 7. Allograft to native heart count ratios rose sharply from 6.55 on day 5 to 16.98 ($P<0.005$) on day 7. The allograft: blood ratio on day 7 was 9:1. Labeled lymphocytes gave positive scans on days 6 and 7 but maximum allograft to native heart ratios were 5.3:1 and heart:blood ratios were 4:1. Syngeneic grafts showed no significant activity accumulation or positive scans with any labeled cells. The results suggest that labeled platelets or leukocytes may be effective agents for scintigraphic detection of allograft rejection.

1:30-3:30 **ROOM B-1**

RADIOPHARMACEUTICALS V: GENERAL

Moderator: Joanna S. Fowler
Co-moderator: H. Donald Burns

PRODUCTION OF SIMPLE CARBON-10 GASES FOR STEADY-STATE IMAGING. RJ Nickles, RD Hichwa and D Comar, University of Wisconsin, Madison, WI and CEA, Service F. Joliot, Hopital d' Orsay, France.

Carbon-10 (β^+,γ)-decays with a 717 keV gamma in $t_{\frac{1}{2}}$=19s. Production on the UW EN tandem employs $^{10}B(p,n)^{10}C$ on a molten target of 98%-enriched, mixed B/B_2O_3, shown below in a flow-through gas cell and tuned pipeline. Published cross sections predict a saturation yield of 4 mCi/μa at 10 MeV, a factor of ten greater than observed in the gas stream. The sensitive dependence of yield on power density in the beam strike suggests a holdup as $^{10}CO_2$ diffuses out of the fused target.

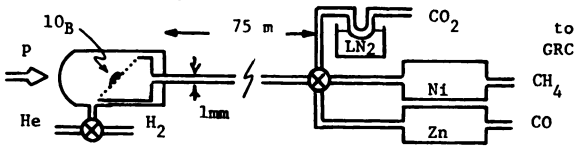

Target and beam parameters, as well as sweep gas and chemical maneuvers were varied to find peak ^{10}C-activities, with a 6:1 $^{10}C/^{11}C$ ratio observed by Ge(Li) spectroscopy and $t_{\frac{1}{2}}$-analysis. Cryotrapping of He-borne activity concentrates the predominate $^{10}CO_2$, verified by gas radiochromatography with parallel detection of 511 keV coincidence and 717 keV singles events. Conversion to $^{10}CH_4$ is quantitative as H_2-borne $^{10}CO_2$ sweeps over a Ni catalyst at 195º Similar conversion to ^{10}CO results as He-borne $^{10}CO_2$ passes through Zn-on-asbestos at 700ºC. The goal is a flow through synthesis of $^{10}C_2H_2$. Acetylene, an inert, diffusable tracer with ideal solubility, invites β^+-imaging of rCBF in the steady state.

EXTRACTION AND TURNOVER OF C-11 PALMITATE IN NORMAL MYOCARDIUM. H.R. Schön, H.R. Schelbert, G.D. Robinson, S.C. Huang, M.E. Phelps, J.R. Barrio. UCLA School of Medicine, Los Angeles, CA.

In order to define the potential of C-11 palmitate (CPA) for noninvasive assessment of myocardial fatty acid (FFA) metabolism with positron emission computed tomography (PCT), the influence of myocardial blood flow (MBF), oxygen (MVO), glucose and FFA consumption and C-11 CO_2 production on CPA extraction fraction (E) and halftimes (T) was investigated in 32 experiments in 19 dogs. MVO was altered by pacing, IV methoxamine or local application of xylazine to the sinus node; MBF was increased by IV dipyridamole. Following CPA injection into the left circumflex coronary artery, E and T were determined from the peak and slope of the myocardial C-11 time activity curve recorded with a scintillation probe for 45 min. E averaged 0.65 ± 0.10 SD in controls, increased with MVO ($r=0.39$, $p<0.05$) and, under physiologic conditions, was not influenced by MBF, arterial FFA and glucose concentrations or myocardial FFA and glucose consumption. Myocardial C-11 time activity curve consisted of a vascular phase, an early rapid and a late phase. T of the early rapid phase (T=3.39 min ± 0.70 SD in controls) was a function of MVO ($r=-0.84$) and C-11 CO_2 production ($r=0.97$), but independent of MBF. The size of the early rapid phase increased with MVO ($r=0.76$) while the size of the late phase decreased ($r=-0.65$). T of the late phase (T=166.55 min ± 46.53 SD in controls) was unaffected by MVO, MBF and C-11 CO_2 production. This phase probably represents intracellular storage of esterified CPA. We conclude that because of the strong dependency of the early rapid phase on β-oxidation noninvasive quantification of β-oxidation is possible with PCT from the size and slope of the early CPA phase.

LABELING AMINE LIGANDS WITH Tc-99m BY LIGAND EXCHANGE IN AQUEOUS SOLUTION. W.A. Volkert, D.E. Troutner and R.A. Holmes. University of Missouri and Harry S. Truman Memorial Veterans Hospital, Columbia, MO.

Cyclam, ethylene diamine (en) and a linear tetramine (ta) form stable complexes in high yields (> 98%) when pertechnetate is reduced with Sn(II) in basic solutions. Efficient labeling of these three amine ligands were also observed by the transfer of Tc-99m from its complex with DTPA and citrate at room temperature. The labeling yields of all three amine ligands were > 95% following the 30 minute incubation of Tc-99m DTPA with 0.03 M of each amine compound at pH ≥ 11. The transfer efficiency from Tc-99m DTPA to en, ta, or cyclam at pH ≤ 9, however, was less than 10%. Tc-99m citrate, a weak acidic complex, can effectively be used at lower pH to label amines since the transfer of Tc-99m from this complex to en, ta, and cyclam is greater than 90% complete after 30 minutes of incubation at pH ≥ 7. The amount of dissociation of the Tc-99m DTPA and Tc-99m citrate after 30 minutes, forming free pertechnetate and "reduced hydrolyzed Tc-99m", was measured and expressed as a function of pH in buffered aqueous solutions containing no amines. Our results showed that the pH dependence on the Tc-99m complex dissociation varied in a manner that parallels the respective transfer efficiencies of Tc-99m to the amine ligands and indicates that the dissociation of these complexes is the major factor initiating the exchange reactions. We, therefore, conclude that Tc-99m amine ligands can be formed efficiently and in high yields by ligand exchange and that Tc-99m citrate and in all probability other weak Tc-99m chelates can be used as donor ligands at or near physiological pH.

NEW COMPLEXES OF Tc-99 IN THE (+7) OXIDATION STATE. M.J. Abrams, A. Davison, and A.G. Jones. Department of Chemistry, Massachusetts Institute of Technology, Cambridge, MA, and Department of Radiology, Harvard Medical School, Boston, MA.

Two complexes of technetium in the (+7) oxidation state have been isolated and characterized. Both contain aromatic bidentate tertiary amine ligands, and both are readily reduced to the (+5) oxidation state. The treatment of NH_4TcO_4 in ethanolic HCl at room temperature with either 2,2'-bipyridine (bpy) or 1,10-phenanthroline (phen) precipitates the yellow complexes TcO_3ClL (L = bpy, phen). They have been characterized by elemental analysis, UV-VIS and IR spectroscopy. The infra-red spectrum shows metal-oxygen vibrations in the region near 900cm^{-1} (e.g. L = bpy: ν(TcO) = 905, 885 and 865 cm^{-1}), close to the values found in the known rhenium complex originally prepared from ReO_3Cl and 2,2'-bipyridine. These new complexes TcO_3ClL can be reduced to the (+5) state by heating in ethanolic HCl, allowing the isolation of $TcOCl_3L$ as yellow crystals.

The rhenium (+7) complex ReO_3Cl (bpy) can be prepared in a similar way from $NaReO_4$ and 2,2'-bipyridine in ethanolic HCl. It cannot, however, be reduced to the (+5) state without the addition of a more powerful reducing agent. The reaction of $NaReO_4$ in ethanolic HCl containing hypophosphorus acid gives $ReOCl_3$ (bpy) as a green solid.

The technetium (+5) complex $TcOCl_3$ (bpy) can be synthesized independently from $[Bu_4N][TcOCl_4]$ and 2,2'-bipyridine in ethanolic HCl. This and the analogous rhenium complex have been characterized by elemental analysis and IR spectroscopy [e.g. $TcOCl_3$(bpy): ν(TcO) = 980 cm^{-1}].

A SERIES OF OXOTECHNETIUM(+5) CHELATE COMPLEXES CONTAINING A $TcOS_2N_2$ CORE. A. Davison, A.G. Jones, C. Orvig, M. Sohn, M.R. LaTegola, and G. Freeman. Department of Chemistry, Massachusetts Institute of Technology, Cambridge, MA, and Department of Radiology, Harvard Medical School, Boston, MA.

We have previously reported the design and synthesis of the anion oxo[N,N'-ethylenebis(2-mercaptoacetimido)technetate(+5) ($[TcO(ema)]^{-1}$). In vivo, this complex shows rapid renal excretion comparable to that of I-131-iodohippurate sodium. In order to explore other members of this interesting class of tetradentate ligands, we have since synthesized a series of S-benzoyl protected dimercaptodiamides of the type $[PhCOS(CH_2)_nCONH]_2X$ [where n=1, X=$(CH_2)_2$, $(CH_2)_3$, σ-C_6H_4; where n=2, X=$(CH_2)_2$ and $(CH_2)_3$]. By sodium dithionite reduction of TcO_4^- in ethanolic aqueous base, the technetium complexes $\{TcO[S(CH_2)_nCON]_2X\}^-$ [where n=1, X=$(CH_2)_2$, $(CH_2)_3$, σ-C_6H_4; where n=2, X=$(CH_2)_2$] have been prepared and identified.

The conditions of synthesis for this series of chelate complexes is dictated by kinetic rather than equilibrium

control. Therefore it was necessary to determine the optimum ring size in order to maximize the ultimate yield. The complex $[TcO(ema)]^{-1}$, which contains three five-membered rings, was the only one made quantitatively. A complex containing three six-membered rings, using [N,N'-propylene-bis(benzoyl-3-mercaptopropionamide)], was not obtained. These results suggest that the configuration with three five-membered rings is the most stable.

A useful modification to this ligand was the replacement of the benzoyl protecting group by the acetimidomethyl group. This renders the ligand water-soluble, thus obviating the need for an ethanolic reaction medium. It has also been found to be a satisfactory leaving group during the metal chelation step.

THE SUBSTITUTIONAL LABILITY OF BIDENTATE LIGANDS ATTACHED TO AN OXOTECHNETIUM(+5) CORE. B.V. DePamphilis, A.G. Jones and A. Davison. Department of Radiology, Harvard Medical School, Boston, MA, and Department of Chemistry, Massachusetts Institute of Technology, Cambridge, MA.

The oxotechnetium core is known to be common to a number of Tc(+5) species, particularly (but not exclusively) those containing two bis-chelated dithiolate ligands. Noting the high substitutional reactivity of $TcOCl_4^-$ (1) towards 1,2-dithiols, we investigated the relative affinity of the core for bis-chelating ligands with various donor atoms.

Reactions of the pure crystalline compounds $Na[TcO(OCH_2CH_2O)_2]$ (2), $[Ph_4As][TcO(SCH_2CH_2O)]_2$ (3), and $[Ph_4As][TcO(SCH_2CH_2CH_2S)_2]$ (4) with 1,2-ethanedithiol (5) in methanol were monitored spectrophotometrically. The ultimate product in each case was $[TcO(SCH_2CH_2S)]^-$ (6). Sequential addition of substoichiometric amounts of 5 to 2 led instantaneously to 6, with no intermediates being observed. By contrast, 1 reacts via the intermediate $(TcO)_2(SCH_2CH_2S)_3$. Stoichiometric amounts of 5 reacted slowly with 3; with excess 5, the rate increased and there was evidence of an intermediate. No reaction was observed when a 100-fold excess of 5 was added to 4 at room temperature, but addition of a stoichiometric amount of 2N HCl led to 5 within hours.

The synthetic results again emphasize that the oxotechnetium core can be stabilized by ligands other than dithiolates. The reactivity results show that the ligand 5 stabilizes this core best in the thermodynamic sense, and that the kinetic lability of the complexes discussed qualitatively correlate inversely with the total polarizability (or "softness") of the leaving ligand donor set. Also evident is the difference in the specificity of 1 and 2 in reacting with 5, which may be of interest in radiopharmaceutical synthesis.

STRUCTURE-ACTIVITY STUDY OF 11 β-HYDROXYLASE INHIBITORS. S.J. Hays, D.L. Gildersleeve, L.E. Brown, M.C. Tobes, D.M. Wieland, W.H. Beierwaltes. University of Michigan Medical Center, Ann Arbor, MI.

Radiolabeled enzyme inhibitors are gaining increased interest as potential scintigraphic agents. Tissues with high concentrations of unique enzymes, such as 11β-hydroxylase of the adrenal cortex, are suitable targets for this approach. We have extended our structure-activity study of metyrapone analogs to: 1) determine the parent structure with the greatest inhibitory potency and most selective adrenal localization and 2) ascertain an area of bulk tolerance in which to incorporate a gamma label.

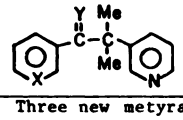

1. metyrapone X = N, Y = O
2. metyrapamine X = N, Y = NH_2H
3. metyrapane X = N, Y = H,H
4. phenylmetyrapone X = C, Y = O
5. metyrapol X = N, Y = OH,H

Three new metyrapone (1) derivatives have been synthesized, metyrapamine (2), metyrapane (3), and phenylmetyrapone (4). Metyrapamine (2) and metyrapane (3) were tritiated by treatment with acetic acid/Pt/tritiated water (25 Ci) at 80°C for 18 hours. Tissue distribution studies with tritiated metyrapamine showed a 3.66% kg dose/gm uptake in the adrenal cortex at 30 minutes. This is in the range of the cortical uptake of metyrapane (3.03%). In contrast, metyrapol's uptake in the adrenal cortex was 6.8% suggesting the structural need for the polar hydroxy functionality at the α-position. Phenylmetyrapone (4) is presently undergoing biological evaluation. Analogs will also be examined in vitro as selective inhibitors of 11β-hydroxylase. Correlation of Ki values with in vivo adrenal cortical uptakes will provide a basis for the evaluation of enzyme inhibitors as potential radiopharmaceuticals.

THE SYNTHESIS OF 1-[C-11]-D-GLUCOSE FOR THE MEASUREMENT OF BRAIN GLUCOSE METABOLISM. C.-Y. Shiue and A. P. Wolf, Brookhaven National Laboratory, Upton, NY.

The glucose analogs, [F-18]-2-deoxy-2-fluoro-D-glucose and 3-deoxy-3-fluoro-D-glucose have been used as tracers for quantitatively mapping the first step of glycolysis in brain and in heart. However, these analogs of glucose require corrections in the tracer model to adjust for differences in transport properties and enzyme affinities. The parent compound, [C-11] randomly labeled glucose has been synthesized by biosynthetic methods. However, there are several problems associated with these methods. We therefore have investigated a synthetic method which overcomes the problems associated with the biosynthetic methods.

The compound 1-[C-11]-D-glucose is synthesized by a modification of the classical Kiliani-Fischer cyanohydrin synthesis. D-Arabinose (*1*) is condensed with [C-11]-sodium cyanide at pH 8.0 to give the aldononitriles (*2*) which are converted to 1-[C-11]-D-glucose (*3*) and 1-[C-11]-D-mannose (*4*) by reduction with Raney alloy in aqueous formic acid solution. The yield and ratio of glucose to mannose depend on the pH of the reaction medium and the ratio of cyanide to arabinose. Compounds *3* and *4* are separated by high pressure liquid chromatography. Current production procedures result in radiochemical yields of 30-40% of *3* and *4* in a synthesis time of 50 minutes from EOB. The same procedures can be used to prepare other [C-11]-labeled carbohydrates.

RAPID CATALYTIC SYNTHESIS OF CARBON-11 LABELED AROMATICS. R.A. Ferrieri*, A.P. Wolf*, M. Speranza†, and F. Cacace‡. *Brookhaven National Laboratory, Upton, NY; †CNR, Montelibretti; and ‡University of Rome, Italy.

[C-11]-benzene derivatives were prepared catalytically by trimerizing [C-11]-acetylene with acetylene and propyne carriers over a silica-alumina support activated by potassium chromate (0.2% by weight). No carrier added [C-11]-acetylene was prepared through recoil labeling (in a 48% radiochemical yield)by bombarding a cyclopropane gas target with a 33 MeV proton beam. The [C-11]-acetylene was mixed with the appropriate alkyne carrier gas and trimerized over the catalyst at 24°C.

In the synthesis of [C-11]-benzene, two studies were performed to ascertain optimum reaction conditions: (i) the time the reactants were exposed to the catalyst was varied; and (ii) the specific activity of the reacting [C-11]-acetylene was reduced. A 10 min exposure time was necessary for optimum reaction. A minimum of 50 μmole of acetylene carrier was necessary before the trimerization proceeded to give an appreciable yield of [C-11]-benzene.

When a mixture of acetylene and propyne was trimerized with [C-11]-acetylene, three [C-11]-aromatic products were generated (benzene, toluene, and xylene). An optimum [C-11]-toluene yield was obtained at an acetylene/propyne mole reaction ratio of .28/.72. This suggests that acetylene is more reactive than propyne. In addition, the observed distribution of [C-11]-xylenes (3.4% ortho, 10.6% meta and 86% para) indicates an apparent regiospecificity in the trimerization. Steric hindrance or electron density effects from the propyne methyl group may account for differences in alkyne reactivity and the regiospecificity.

1:30-3:30 **ROOM E-1**

COMPUTERS AND DATA PROCESSING III: GENERAL

Moderator: Sherman Lee Heller
Co-moderator: Bruce H. Hasegawa

DECONVOLUTION OF THE FIRST PASS PULMONARY TIME-ACTIVITY CURVE FOR A FRAGMENTED BOLUS: A COMPARISON OF METHODS. J.A. Parker and D.A. Chesler, Department of Radiology, Harvard Medical School, Boston, MA.

Prior to calculation of the pulmonary to systemic flow ratio in patients with left-to-right shunts using the gamma variate method, the pulmonary time activity curve can be deconvolved for the time activity curve from the region of the superior vena cava. Three methods of deconvolution analysis were evaluated in this setting: 1) a Fourier transform method with high pass filtering (rectangular or Hanning), 2) a Laplace transform method with filtering based on the signal to noise ratios of the different frequency components and, 3) an iterative method (on each iteration, the values of the system function were corrected successively for each output point in proportion to their contribution to that point). The various methods were compared using artificial data consisting of a gamma variate curve plus systemic recirculation. This system function was convolved with various input functions which represent prolonged or fragmented boluses. Poisson noise was added to the input and output functions prior to deconvolution. The calculated system function was compared with the known system function. The Laplace transform technique with a statistically derived filter gave more accurate and consistent results than the Fourier method. Removal of components with a signal to noise of less than 3 improved the accuracy of the deconvolution. The iterative method allowed accurate calculation of the gamma variate parameters; however, the deconvolved curves were less smooth. Convergence to the final output was essentially complete in 3-5 iterations. The last two methods both produce more accurate results that the high pass filter, Fourier method.

AN IMPROVED DECONVOLUTION TECHNIQUE FOR CALCULATING ORGAN RETENTION FUNCTIONS. A.Kuruc, W.Caldicott and S.Treves. Children's Hospital Medical Center. Harvard Medical School, Boston, MA.

This work was undertaken to develop a deconvolution technique which is conceptually clear, stable to measurement and numerical error, and makes minimal assumptions as to the form of the data.

Previously reported deconvolution techniques have used data smoothing, curve fitting, or frequency domain filtering to reduce the sensitivity of the calculation to measurement error. We feel that a more general method is to place algebraic constraints on the form of the calculated unit impulse response (UIR), which are dictated by physical and physiological considerations, and then use least squares to minimize the reconvolution error. We have developed such a technique for calculating organ retention functions, such as in a renogram, by constraining the calculated UIR to be non-negative and non-increasing when corrected for physical decay.

The system was tested for its ability to estimate UIR's with mathematical curves degraded with Poisson noise to simulate counting statistic error. We defined an error function as the ratio of the euclidean norm of the difference of the true and computed UIR to the euclidean norm of the true UIR. Results on data intended to mimic those obtained from a renogram indicate that the method produces accurate deconvolutions with errors in the range of 1-10%.

We have demonstrated a numerically stable implementation of a constrained least squares deconvolution technique for the special case of organ retension functions. We conclude that it is a practical technique for the analysis of biological data.

QUANTITATION OF GASTRIC EMPTYING. L.S. Graham, R.R. Lake, G.M. Van Deventer, and J.H. Meyer. V.A. Medical Center, Sepulveda, CA and UCLA School of Medicine.

In order to accurately quantitate the amount of radionuclide labeled liquid or solid food in the stomach as a function of time, it is necessary to apply a number of corrections to the raw data. The purpose of this study was to define the corrections that must be made and to incorporate them into patient studies. Four sources of error have been studied: 1) Overestimation of stomach activity due to gut activity overlapping the stomach region-of-interest (ROI); 2) Fluctuations in apparent stomach activity due to variations in the size of operator defined ROIs; 3) Variations in apparent activity due to changes in average depth; 4) Underestimation of stomach activity due to collimator septal penetration and scatter.

Overlap errors and errors due to changes in ROI definition have been minimized by the use of an edge-finding routine within a searching region to consistently and objectively define the stomach ROI. Peak-to-scatter ratios have been used to correct for possible variations in depth for both In-113m and Tc-99m. These ratios were determined using a phantom that could be varied in both size and depth. Correction for collimator septal penetration and scatter has been accomplished through the use of correction factors that are a function of ROI size and depth. These factors were also determined from phantom studies and are best described by power functions. This latter factor has the most significant effect on patient studies. Application of these corrections to clinical studies dramatically improves the quantitative nature of the results of clinical studies.

A METHOD TO DECREASE THE UNCERTAINTY IMPARTED TO STUDIES CORRECTED FOR COUNT RATE LOSSES. M. T. Madsen. Thomas Jefferson University Hospital, Philadelphia, Pa. 19107

In order to accurately determine parameters in computer acquired dynamic studies, it is sometimes necessary to correct for count rate losses. Because the computer-gamma camera temporal resolution is dependent on many variable factors, correction for data losses is best done by monitoring the count rate of a test source positioned at the edge of the field of view. However, the correction factors determined from the test source often impart a significant increase in the statistical uncertainty of the corrected data. The increased uncertainty can be avoided by fitting the test source data.

In this study a paralyzable model was used: $No = N \cdot \exp(-R\,\mu)$, where μ is the paralyzable dead time, N is the initial count rate of the test source, No is the observed count rate of the test source and R is the true counting rate of the entire field of view. R is estimated from the total acquired counting rate. A nonlinear least squares regression finds the best fit by optimizing μ for the minimum chi-square. The fitted data is divided into N to determine the correction factors.

The fitting procedure is easily implemented on the computer. Experimental studies with data losses in excess of 50% have been successfully corrected with no significant increase in the statistical uncertainty.

FULLY AUTOMATED PROCESSING IN GATED BLOOD POOL SCINTIGRAPHY. M.H. Bourguignon, K.H. Douglass, J.M. Links, R.A. Wise, W. Ehrlich, and H.N. Wagner, Jr. The Johns Hopkins Medical Institutions, Baltimore, MD.

A fully automated processing program for gated blood pool studies was developed and evaluated in 5 dogs and 14 consecutive patients. The program first creates a series of edge-enhanced images. A marker point within each ventricle is then identified as that pixel with maximum counts to the patient's right and left of the count center of gravity of a stroke volume image. Regions of interest (ROI) are selected on each frame as the first contour of local maxima of the two-dimensional second derivative which encloses the appropriate marker point, using a method developed by Goris. After shifting the LV end-systolic ROI three pixels to the patient's left, a background ROI is generated as the crescent-shaped area of the shifted ROI not intersected by the ES ROI. The average counts/pixel in this background ROI in the ES frame of the original study are subtracted from each pixel in all frames of the gated study. RV and LV time-activity curves are then obtained by applying each ROI to its corresponding background-subtracted frame, and the ejection fraction and ED, ES, and stroke counts determined for both ventricles. In addition to the automatic EFs, manually drawn ROIs were used to obtain EFs for both ventricles. The manual ROIs were drawn twice, and the average obtained. For the RV, the correlation between auto and average manual EF was 0.88; the correlation between the two manual EFs was 0.52. For the LV, the correlation between auto and average manual EF was 0.96;the correlation between the two manual EFs was 0.91. In the dogs, the correlation with aortic flowmeter measurement of stroke volume was 0.64,a marked improvement over the value of 0.39 with manual analysis of the data.

Automated left ventricular boundary extraction from Tc-99m gated cardiac blood pool scintigrams. J.H.C.Reiber,C.Hoek, S.P.Lie,J.J.Gerbrands,M.L.Simoons. Thoraxcenter,Erasmus University,Rotterdam,Netherlands.

To minimize observer variations in the analysis of Tc-99m blood pool scans,algorithms have been developed for the automated detection of the left ventricular(LV) outline.The procedure only requires the user to indicate the approximate center of the left ventricle in the sum-image of the gated study.The algorithm is based on searching for the minimal cost contour with the cost of a position defined as the inverse of the 2nd-derivative value computed radially from the center.The center position is updated from the detected contour and the procedure repeated for minimal user-dependency (fixed region of interest(ROI)).For the moving ROI-method the contour is detected automatically in each frame;the LV contour in a frame is used to guide the search in the next frame.To compute ejection fraction(EF) a background region is generated in a user-defined direction and has fixed size and distance to the LV boundary.

The fixed ROI-method takes 20 s. on a Dec γ-11 system and the moving ROI-method 3 min.From a set of 25 patient studies with varying cardiac diseases no significant differences in precision in EF were found between the automated fixed-method and the average EF from manually traced outlines by 4 independent observers.Comparing manual tracing and the automated method with same background regions for individual patient studies,intra-observer variations decreased from 1.6 to 0.3% and inter-observer variations from 4.8 to 0.5%. A rate of success in the contour detection of 95% could be assessed from a total of 111 studies.

In conclusion,a routinely useful software package has been developed for the automated detection of the LV activity in gated cardiac blood pool scintigrams.

THEORETICAL BEHAVIOR OF FIXED AND VARYING ROI METHODS FOR CALCULATING EF. S.L.Bacharach, M.V.Green, C.W. Schiepers, C.N. DeGraaf, G.S.Johnston. National Institutes of Health, Bethesda, MD and University of Utrecht, The Netherlands.

We have developed theoretical equations which describe the behavior of the fixed and varying region of interest (ROI) methods for calculating EF. These equations are consistent with previously observed, but poorly understood, experimental observations. It is found from these equations that the ratio EF(v)/EF(f) ≥ 1 (where EF(f,v)=EF by fixed or varying methods), if $\Delta B \geq 0$(where ΔB= the difference between true (unknown) and measured background (B)). In this case EF(v) is always greater than EF(f), in agreement with experimental results previously reported. The two EF's are equal when $\Delta B=0$, thus in principle allowing direct calculation of B without explicit measurement, by equating EF(v)=EF(f). The equations also predict which method (fixed or varying) will give more reproducible and accurate results under given experimental conditions. By taking partial derivities we find that EF(v)is always more reproducible than EF(f) if only B is a source of error. The equations predict that under some circumstances EF(v) will be nearly independent of B, offering some theoretical justification for this previously unexplained phenomenon. The theoretical predictions of reproducibility correlated well with experiment (52 subjects each studied five times: r=.90, slope=.95). If errors in drawing ES ROI are also considered, a more complex equation results. For typical variations in B and number of ES pixels(NESP) resulting from hand drawn ROI's the theory predicts that EF(f) is more reproducible than EF(v) for most experimental conditions. This conclusion is reversed at large ED volumes and high EF's, or if the variance in NESP can be reduced (e.g., by an automated edge detection scheme).